Modulating the senescent and secretory phenotypes of fibroblasts using ultrasound

A thesis presented to the School of Biosciences in the Faculty of Science at theUniversity of Sheffield

In partial fulfilment of the requirements of a degree ofDoctor of Philosophy

By Amani Hamad Alharbi

Registration Number: 180125629

March 2024

I want to thank my mum Munera for setting a beautiful example of a strong, caring woman.

Without her incredible patience and support over the previous few years, I would not have been

able to finish my education.

my brother Dr Ziyad I appreciate your willingness to listen to my complaints, offer advice, and most

of the time, lift my spirits. I wouldn't be able to make it through this road without your faith in me.

In light of what you have done and will continue to provide, I am speechless. You are my lifelong

partner. thank you.

My deep gratitude goes out to my brothers Sami, Yousef, Waleed and sister Manal, especially my

sister in low Dr Abeer, for their unconditional support. Thank you to my nephews and nieces for the

video calls; they never fail to make me smile.

Abstract

Cancer treatment and wound management are two of the biggest problems in healthcare today. Cancer has been referred to as "wounds that do not heal" because it uses the stroma-gathering process to obtain the stroma necessary for growth and survival. Current research has connected replicative senescence in the elderly to chronic wounds and cancer. With aging, a process known as replicative cellular senescence causes the cells to reach a point where they are unable to divide and stop proliferating. Senescence-Associated Secretory Phenotype (SASP), which is manifested in senescent cells, demonstrates a clear change in the profile of secreted proteins, and arises from a restorative programme during aging to a dysregulated cascade that encourages tumorigenesis and chronic inflammation. Low intensity pulsed ultrasound (LIPUS), which is safe and economical in comparison to conventional therapies, has been utilised in several trials to enhance wound healing. In a chronic wound, LIPUS can boost the production of growth factors and proteins while reducing the expression of inflammatory cytokines.

In this study, we investigate whether ultrasound alters fibroblast senescence and SASP in a manner that might be advantageous for the treatment of chronic wounds and other age-related diseases. Using the anti-cancer medication cisplatin to induce senescence in human foreskin fibroblast (HFF), which was then exposed to LIPUS for three days for 20 minutes each day, this was explored. In addition, we investigate the impact of LIPUS on a variety of senescent indicators, including cell shape, senescence-related b-galactosidase activity, foci of DNA damage associated with senescence, and $p21^{WAF1/CIP1}$, a cyclin-dependent kinase inhibitor. As well as screening of senescence associated secretory phenotype (SASP) secreted protein.

Our experiments have produced encouraging results. We observe morphological changes in HFF cells following LIPUS stimulation. In HFF cells treated with cisplatin and stimulated with LIPUS, the b-galactosidase activity was markedly decreased. Cells treated with both cisplatin and LIPUS saw decreased DNA damage, although this effect was not statistically significant. Moreover, in cisplatin-treated cells exposed to LIPUS stimulation, the protein level of p21$^{WAF1/CIP1}$ was similarly significantly downregulated. Regrettably, we were unable to find any effect for SASP released proteins after LIPUS activation on cells treated with cisplatin. It's

interesting that following LIPUS stimulation, we could see a difference in secreted proteins of HFF cells. It might be as a result of the presence of replicative cells in the population of these cells. In conclusion, LIPUS may be a safe, non-invasive therapy for diseases associated with aging. which will enhance senior citizens' quality of life. We observed that this approach had a favourable impact on fibroblast senescence. Which, after more research, might be a viable senescence target therapy or a novel chemotherapy combo to shield normal cells from the harm these medications might otherwise cause.

Table of Contents

List of Tables

List of figures

Declaration

I, the author, confirm that the Thesis is my work. I am aware of the University's Guidance on the Use of Unfair Means (www.sheffield.ac.uk/ssid/unfair-means). This work has not previously been presented for an award at this, or any other, university.

Abbreviations

AP- antagonistic pleiotropy
APP- Amyloid-beta precursor protein
ATM- ataxia-telangiectasia mutant
ATR- ATM- and Rad3-Related
BrdU- Incorporation of bromodeoxyuridine
CAFs- cancer-associated fibroblasts
CamKinaseII- Calcium/calmodulin-dependent protein kinase II CAPZB- F-actin-capping protein subunit beta
CDKIs- cyclin-dependent kinase inhibitors
CLIC4- Chloride intracellular channel protein 4
COL12A1- Collagen Type XII Alpha 1 Chain
COL6A2- Collagen Type VI Alpha 2 Chain
COX-2- cyclo-oxygenase 2
CTGF- connective tissue growth factor (CTGF)
CTSB- Cathepsin B
DDAH1- N(G),N(G)-dimethylarginine dimethylaminohydrolase 1 DDR- DNA damage response
DNA-PKcs- DNA-dependent protein kinase
DSBs- double-stranded DNA breaks
E2F3- Transcription factor3
ECM- extracellular matrix
EGF- epidermal growth factor
ENG- Endoglin
FBN1- Fibrillin-1
FBN2- Fibrillin-2
FBS- Foetal bovine serum
FDR- false discovery rate
FGF- fibroblast growth factor
FGF-2- fibroblast growth factor 2
GM-CSF- macrophage-colony stimulating factor
GNS- N-acetylglucosamine-6-sulfatase
H_2O_2- hydrogen peroxide
HFF- Human foreskin fibroblast
HGF- hepatocyte growth factor
HIFU- high-intensity focused ultrasound
HSCs- Senescent hepatic stellate cells
IGF- insulin-like growth factor
IGFBP7- Insulin-like growth factor-binding protein 7
IGFBPs- IGF-binding proteins
IL1- interleukin-1
IL6- interleukin-6
IL8- interleukin-8
LAMB1- Laminin subunit beta-1
LIPUS- Low-intensity pulsed ultrasound
MIP3- macrophage inflammatory protein 3
MPP- mitochondrial membrane potential
mtDNA- mitochondrial DNA
NaCl- Sodium chloride
NF-κB- nuclear factor kappa light chain enhancer of activated B cells
NO- Nitric oxide
OIS- oncogene-induced senescence

OPG- osteoprotegerin
OXPHOS- oxidative phosphorylation
P13K- platelet-derived growth factor
PAI- plasminogen activator inhibitors
PAI-1- plasminogen activator inhibitor 1
PAI-2- plasminogen activator inhibitor 2
PAPPA- Pappalysin-1
PBS- Phosphate-buffered saline
PDGFA- platelet derived growth factor subunit A
PFA- paraformaldehyde
PIKKs- phosphatidylinositol-3-kinase-like kinases
PLOD3- Multifunctional procollagen lysine hydroxylase and glycosyltransferase LH3 PTX3-
Pentraxin-related protein PTX3
PXDN- Peroxidasin homolog
RAC1- Ras-related C3 botulinum toxin substrate 1
RAF- rapidly accelerated fibrosarcoma
RAS- rat sarcoma
Rb- retinoblastoma protein
RECK- Reversion Inducing Cysteine Rich Protein with Kazal Motifs
ROS- reactive oxygen species
SAHF- senescence-associated heterochromatin foci
SASP- senescence-associated secretory phenotype
SSC5D- Soluble scavenger receptor cysteine-rich domain-containing protein SSC5D
ß-gala- associated beta-galactosidase
ß-galactosidase- associated beta-galactosidase
TGF-beta- transforming growth factor-beta
Tiam 1- T-cell lymphoma invasion and metastasis-inducing factor 1 TIMPs- inhibitors of
metalloprotease
UV- ultraviolet
VEGF- endothelial growth factor

Chapter1
Introduction

1 Introduction

One of the biggest risk factors for the onset of several diseases is age. Most illnesses, including cancer and chronic wounds, have become more prevalent among elderly adults. Numerous cellular processes that act as tumor-suppressing mechanisms throughout life, such as DNA damage responses and cellular senescence, cause degenerative alterations and contribute to the aging phenotype.

1.1 Aging Tissues:

Most biological systems begin to decline as we age, including immune system function decline brought on by inflammation brought on by DNA damage and physical trauma. Fibroblasts and epithelial cells are also involved in the inflammatory process in addition to immune cells (Zhang & Duan, 2018). Fibroblasts, the builders of our tissues, establish the scaffolding of the extracellular matrix in the first act. This is a crucial stage on which the inflammatory drama takes place. Fibroblast cells are primarily responsible for producing the extracellular matrix (ECM) components that provide structural support to tissues. There are several stimuli that can cause inflammation and activate fibroblasts, such as injury, infection, or oxidative stress. Among the pro-inflammatory mediators released by these activated fibroblasts are growth factors, chemokines, and cytokines. (Hinz et al., 2007). By enticing immune cells like neutrophils and macrophages to the site of inflammation, these mediators strengthen the inflammatory response Epithelial cells form a barrier between our tissues and the external environment but also play an active role in the healing process, they also detect and react to inflammatory stimuli. Similar to fibroblasts, activated epithelial cells can release pro-inflammatory mediators that amplify the inflammatory response. Furthermore, during inflammation, epithelial cells may go through a process known as epithelial-mesenchymal transition (EMT), which gives them the ability to migrate and remodel the matrix, leading to fibrosis and tissue damage (Werner & Haller, 2007).

Fibroblasts also play an essential role in tissue repair and regeneration after the initial phase of inflammation is complete. Fibroblasts replenish damaged tissues and return them to normal function

by secreting collagen and other ECM components. However, persistent inflammation may result in excessive ECM deposition and unchecked fibroblast activity, which can cause fibrosis and scarring.Restoring the epithelial barrier after inflammation has subsided requires the presence of epithelial cells. In order to restore tissue integrity, they can spread and migrate to cover exposed areas. Chronic inflammation and tissue dysfunction may result from epithelial cells' diminished ability to repair themselves as they age (Barrientos et al., 2008; Parrish, 2017). Both epithelial cells and fibroblasts undergo functional decline with aging. Anti-inflammatory mediators produced by fibroblasts and epithelial cells aid in reducing inflammation and advancing healing. Tissues become more prone to persistent inflammation as we age because of a decrease in this production. The signalling pathways that control cell function, including those that control inflammation and repair, can become compromised with age. This may cause tissue damage and inflammation to resolve either partially or not at all. Moreover, fibroblasts and epithelial cells may exhibit different patterns of gene expression due to epigenetic changes linked to aging. Their decreased functionality and pro-inflammatory state may be caused by this. Thus, fibroblasts and epithelial cells are involved in inflammation in ways that go beyond their status as immune response targets. Their age-related decline is a major contributor to chronic inflammation and loss of function in various tissues and organs (Ding et al., 2021; Franceschi et al., 2007).

1.2   Chronic Inflammation

Chronic inflammation and loss of function in different tissues and organs are greatly influenced by this age-related decrease in fibroblast and epithelial cell function (Zhang & Duan, 2018). Age-dependent changes in fibroblasts and epithelial cells include cellular senescence, loss of telomeres, oxidative stress, point mutations in extranuclear mitochondrial DNA, chromosomal abnormalities, single-gene mutations and decreased incorporation of sugar into the extracellular matrix. (Naylor et al., 2011). Aging also affects various processes in the gingival tissue, which is the specific soft tissue that forms an essential portion of the oral cavity and surrounds and supports the teeth. Changes in the gingiva include deterioration in cell migration, proliferation, matrix remodelling, myofibroblast differentiation, and wound healing (Caceres et al., 2014). This decrease is made worse by thymic

involution, a defining feature of aging that causes the thymus to gradually shrink in size as a result of the loss of thymic epithelial cells and a decline in thymopoiesis (Cai, 2021). Thymic involution involves a loss of tissue organisation, tissue bulk, and cellularity, with the end result being a decrease in the output of naive T cells. This decrease in naive T cell production is thought to have a significant impact on the features of the peripheral T cell, causing these cells to change in phenotype and function as they age, lose variety, and undergo replicative senescence. Furthermore, it is thought that these age-related alterations in peripheral T lymphocytes have a substantial role in the characteristics of immunosenescence. Demonstrating that thymic activity changes are a major factor in the aging immune system's deterioration (Thomas et al., 2020; Palmer, 2013). According to the antagonistic pleiotropy principle, genes that promote fitness in the early stages of life, such as higher fertility, may have unfavourable effects later in life and accelerate aging (Mitteldorf, 2019). Although thymic atrophy lowers the risk of autoimmune diseases during early life, it ultimately leads to immunosenescence (Turke, 1994; Shanley et al., 2009). According to Whicher et al. (2020), one of the main causes of the increased risk of cancer and chronic wounds in older people is the age-related decline in immune function (Whicher et al., 2020).

Understanding the intricate interactions that occur between fibroblasts, epithelial cells, and inflammation as we age is crucial because it enables us to manage the inflammatory orchestra and preserve the functionality of our aging tissues.

With aging comes an increased risk of chronic wounds and cancer. Older wounds pose a significant clinical burden, are less responsive to contemporary care, and raise annual medical expenses. An estimated £10 billion was spent by the National Health Service each year on treating these wounds and the associated comorbidities (Whicher et al., 2020). Chronic wounds often coexist with conditions such as diabetes and vascular disease, which are more common in the elderly population (Krtolica and Campisi, 2002, Margolis et al., 2002, Gould et al., 2015). Many studies conducted recently have linked cancer and replicative senescence in older adults with chronic wounds. The definition of aging is the progressive loss of reproductivity accompanied by an age-dependent

functional decline, which is influenced by a multitude of genetic and environmental factors. The cells age through a process called replicative cellular senescence until they can no longer divide and multiply. Senescence is defined as the process by which cells stop dividing; more specifically, they stop while still being metabolically active in the G1 phase of the cell cycle (Liu et al., 2019, Dimri and Campisi, 1994, Campisi, 2013, Campisi, 1997, Dvorak, 2015).

1.3 Theories of aging

Aging is just the term used to describe the changes that take place in an organism over its lifetime, although the speed at which these changes happen varies greatly. In short, aging is the result of the interplay between external factors like diet and lifestyle and genotype (Anton et al., 2005). Senescence is the term typically used to distinguish these benign changes from those that raise the risk of illness, disability, or death. Senescence, then, is the gradual breakdown of physiological processes over time; a loss of complexity in many physiological processes and anatomic structures has been linked to normal aging in humans (da Costa et al., 2016, Goldberger et al., 2002).. Multiple processes that combine and interact on multiple levels form the basis of the aging process (Guarente, 2014). These processes occur in tissues and organ systems in addition to at the cellular and molecular levels. There are two primary categories under which theory of aging falls (figure 1.1). Several factors have been linked to aging, including telomere shortening (Kruk et al., 1995), immunological function changes (Effros, 2005), molecular cross-linking (Bjorksten, 1968), free radical-induced damages (Harman, 1992), and the presence of senescence genes in DNA (Lopez-Otin et al., 2013, Lopez-Otin et al., 2023, Archer et al., 2013).

```
                          ┌─────────────────────────┐
                          │     aging theories      │
                          └─────────────────────────┘
                    ┌────────────┴────────────┐
┌───────────────────────────────────┐   ┌───────────────────────────────────┐
│        Program theories           │   │         Damage theories           │
│ According to these ideas, growing │   │ Over time, damage to cells and    │
│ older is an unavoidable process   │   │ tissues is what leads to aging    │
│ that is genetically programmed.   │   │                                   │
└───────────────────────────────────┘   └───────────────────────────────────┘
```

Program theories

Telomere shortening theory The protecting ends of chromosomes are called telomeres. As cells divide, they get shorter, and eventually the cell is unable to divide any longer. Aging and cell death may result from this.

Hormonal theory Hormone shifts related to aging include those in growth hormone, oestrogen, and testosterone. Aging may result from these modifications to how cells perform and repair themselves.

Immunological theory As we age, our immune systems become less efficient. This may increase a person's vulnerability to illnesses and infections, which may hasten the aging process.

Damage theories

Free radical theory Unstable molecules known as free radicals have the ability to harm tissues and cells. Although they are created by regular cellular processes, as people age, their production rises. Aging and cell death can result from free radical damage.

Mutation theory Changes in DNA called mutations can potentially cause cell death or malfunction. The combination of internal and external factors can result in mutations. Aging may be caused by an increase in the amount of mutations in our cells as we age.

Damage accumulation theory According to this theory, damage to cells and tissues accumulates over time and leads to aging. Environmental elements like radiation or pollution exposure, as well as regular biological functions, may all result in this harm.

Figure 1.1 summarising the aging theory

 The two primary categories of getting older theory. First, the aging program theory holds that genetic programming is an inevitable process. Damage theory that aging is caused by cellular and tissue damage over time supplements the program theory (Lopez-Otin et al., 2013, Lopez-Otin et al., 2023, Archer et al., 2013).

1.4   Senescent cells

When Hayflick and Moorhead observed that the cultivated diploid human fibroblast reaches a point where it can no longer proliferate after a finite number of divisions or passages, they made the first discovery of senescence cells. Fibroblast populations consistently exhibit three phases of cell proliferation: phase I, which corresponds to a period of slow proliferation before the first passage, when the culture establishes; phase II, which is marked by rapid cell proliferation; and phase III, during which proliferation gradually comes to an end (Kuilman et al., 2010, Hayflick and Moorhead, 1961) Cellular senescence builds up over time, which is a major characteristic of old organisms .A permanent cell cycle arrest is referred to as senescence. To put it another way, when cells are unable to divide while still being biologically active, they have lost their ability to replicate. Two signs of cellular senescence include the formation of a multi-component senescence-associated secretory phenotype (SASP) and an essentially permanent stop in the cell growth (Maria and Ingrid, 2017, Wiley and Campisi, 2016). The evolutionary purpose of senescence is to protect cells from cell death, meaning that cells become less vulnerable to harm, but at the cost of some of their functionality. As a consequence, senescence is usually seen in response to damage, be that accumulation of damage and mutations due to age or damage by external factors. Other types of cell cycle arrest exist to deal with different challenges. For example, while senescence occurs in response to cell damage, quiescence occurs due to lack of nutrients or growth factor stimulation. Whereas senescence is normally considered to be irreversible, other types of cell cycle arrest, including quiescence, can be reversed as the cell environment changes. It is for this reason that senescence is most commonly considered the pathological form of cell cycle arrest. The gradual decline in the immune system during aging increases the vulnerability of cell through loss of the immune system's capacity to eradicate infections, and also means that the immune system fails to remove senescent cells themselves. As cellular defences deteriorate over time, DNA mutations and protein misfolding eventually become background noise in the division theme. (Campisi, 2016).

The stable cell cycle halt known as cellular senescence can be brought on in healthy cells by a variety of intrinsic and extrinsic stimuli as well as developmental cues. Senescence is thought to be a highly dynamic, multi-step process, during which senescent cells' characteristics continuously change and diversify in a way that depends on the circumstances. It is accompanied by several cellular and molecular abnormalities, different phenotypic modifications, and a persistent proliferative arrest that is insensitive to mitogenic stimuli. Senescent cells exhibit substantial changes in gene expression, altered metabolic activity, and a complicated phenotype known as the senescence-associated secretory phenotype. Cellular senescence can impair tissue regeneration and repair, hastening the aging process(Kumari and Jat, 2021).

1.5　The causes of Senescence

The complicated process of cellular senescence stops the multiplication of cells that could develop into cancerous tumours. Senescence responses are triggered by numerous factors. These include DNA damage, faulty telomeres, the production of specific oncogenes, alterations in the chromatin structure, and potent mitogenic signals as shown in figure 1 (Campisi and d'Adda di Fagagna, 2007).
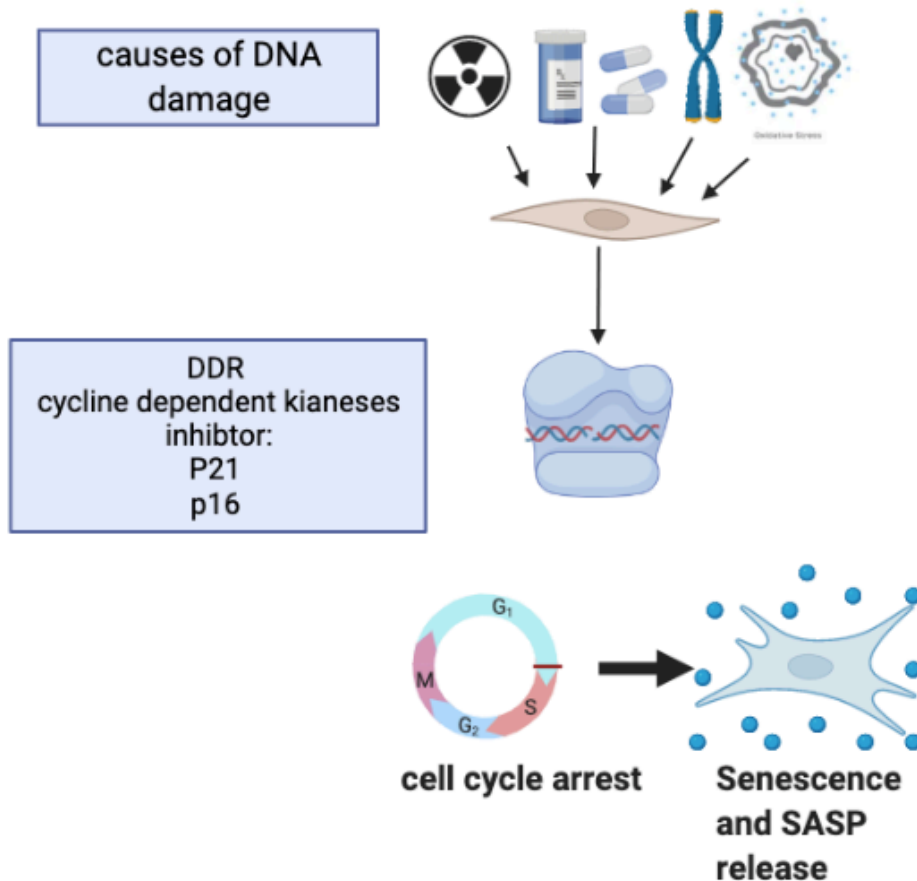
Figure 1.2; The process and causes of cellular senescence

Numerous factors, such as telomere shortening, chemotherapy, and radiation, can damage DNA. These factors can also trigger a response to DNA damage by introducing cyclin-dependent kinases inhibitors, which stop cell cycles and ultimately lead to senescence in cells if DNA damage is not repaired (image generated using BiorRnder website).

1.5.1.1   Telomere shortening

Aging is indicated by cells that are going through cellular senescence as a result of replicative stress brought on by telomere shortening. This condition may influence life expectancy. The telomere consists of extremely repeating clusters 5'-TTAGGG-3' found at the ends of eukaryotic chromosomes (Kaul et al., 2011). Telomeres don't have an antiparallel strand at the 3' end. In humans, the single-strand tail length ranges from 100 to 280 nucleotides. Numerous proteins frequently accompany this single strand, which forms a T-loop. These proteins cap DNA and help prevent fusion or damage to the chromosome ends. A G-quadruplex structure can also be created by this capping structure using two, four, or eight parallel or antiparallel single strands. Every time a cell divides, telomeres get

shorter because of the replication process. Telomeres shorten with each replication due to DNA polymerase's inability to function on the single-stranded 3' ends (Smith et al., 2011). In 1971, Olovnikiov made the initial suggestion for this replication process and related telomere shortening (Olovnikov, 1971, Olovnikov, 1973). However, when telomere shortens to a critical degree, it causes cell cycle arrest, cellular senescence, and apoptosis, which can be seen as a form of defence against the effects of telomere dysfunction illustrated in figure2. (Bernadotte et al., 2016, Matsumoto et al., 2015).
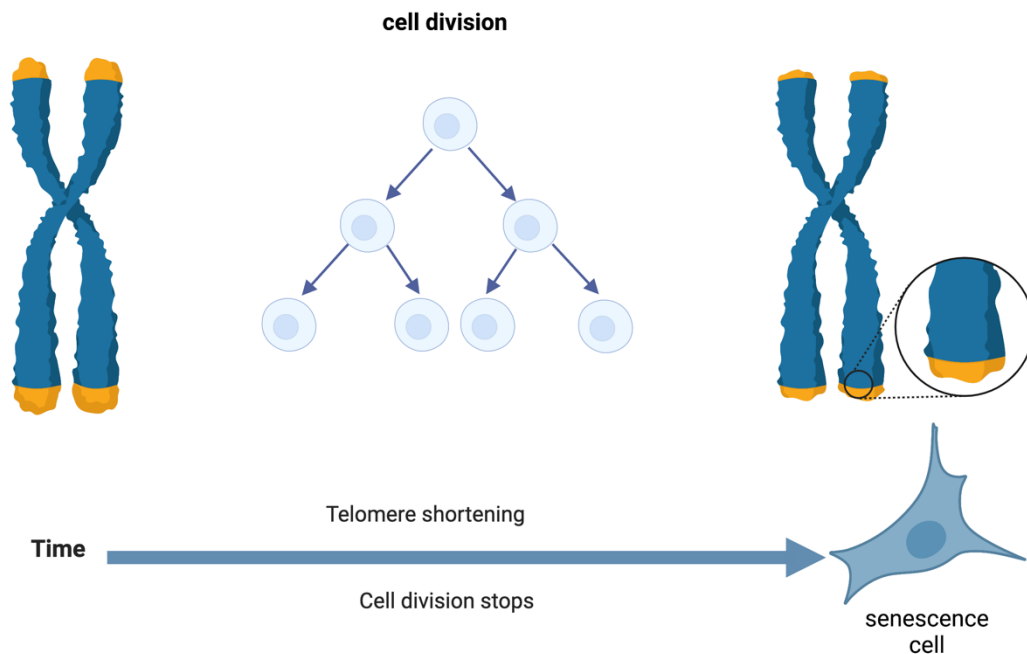
Figure 1.3: Telomere shortening

Cell cycle arrest results from a crucial reduction in telomere size after every division, which can be viewed as a type of defence against the impacts of telomere dysfunction (image generated using BiorRnder website).

1.5.1.2 DNA damage-induced senescence

Aging may be brought on by chemotherapy. Human cancer cells are subject to apoptosis when given high doses of chemotherapy, although senescence can also be brought on by low dosages (Lee and Lee, 2014). There are several types of chemotherapy, each of which uses a distinct strategy to harm cancer cells' DNA. First of all, after the supercoil unwinding process, topoisomerase I and II inhibitors led to the re-linking of dysregulated DNA strands. Senescence is subsequently brought on by significant DNA damage, elevated expression of the tumour suppressor gene (p53), and its downstream targets CDKN1A and PAI1 (Nitiss, 2009). Second, platinum-based chemicals cause substantial DNA damage by DNA cross-linking, which induces senescence (Rottenberg et al., 2021). Additionally, alkylating substances induced DNA crosslinks by interacting with DNA Nucleotides , which led to a DNA damage-mediated senescence response (Hall and Tilby, 1992). The usual microtubule spindle dynamics were disrupted by microtubule inhibitors, preventing cells from entering mitosis and delaying the metaphase-anaphase transition. Additionally, significant DNA damage and the start of the assisted senescence response could result from this cell cycle disruption (Perez, 2009). The chemotherapy have the potential to harm surrounding tissue unintentionally and speed up the aging process.

Radiation therapy can cause DNA damage, which can trigger an irreversible DNA damage response and activate the ATM or ATR and p53-p21 pathway-mediated apoptosis and cellular senescence pathways. Additionally, a rise in the number of senescent cells in the tissue around the tumour may have a variety of local adverse effects, including those that inhibit the immune system (Li et al., 2018, Wang et al., 2022a).

1.5.1.3 Oxidative stress-induced senescence

An imbalance between the generation of reactive oxygen species (ROS) and antioxidant defences leads to an oxidative stress (Moldogazieva et al., 2019). Reactive oxygen species (ROS), which include superoxide radicals, hydrogen peroxide (H_2O_2), hydroxyl radicals, and singlet oxygen, are products of biological systems (Pizzino et al., 2017). oxidative stress can occur due to exposure to ultraviolet (UV)

light and hydrogen peroxide (Mohamad Kamal et al., 2020). Excess ROS to the antioxidant capacity of cells can induce the oxidation of various components, including proteins and lipids, which damages DNA and disrupts cellular function via shortening telomeres, histone deacetylation, and mitochondrial malfunction. As a result, the DNA damage response (DDR) pathway begins, which causes cellular senescence by triggering cell cycle arrests (Terao et al., 2022).

1.5.1.4 Mitochondrial dysfunction-associated senescence

As we age, our mitochondria become more dysfunctional. Both the mitochondrial membrane potential (MPP) and the mitochondrial respiratory level are lowering, which is the reason of this. Increased levels of reactive oxygen species (ROS) as a result of mitochondrial malfunction cause defects in oxidative phosphorylation (OXPHOS), which are linked to senescent cells (Wiley et al., 2016). ROS are understood to be essential for cellular signalling, stress response, and immune system function (Sergiev et al., 2015). However, excessive mitochondrial ROS production and ongoing MMP disruption lead to the development of senescence by damaging mitochondrial DNA (mtDNA). These damages can result in either SSBs or DSBs, which activate DDR signalling pathways and cause the cycle to be paused (Miwa et al., 2022, Correia-Melo and Passos, 2015, Sergiev et al., 2015).

1.5.1.5 Paracrine senescence

The paracrine effect, which causes nearby cells to age prematurely, can be used to induce senescence. Due to the development of a senescence-associated secretory phenotype (SASP), senescent cells are nonetheless metabolically active despite cell cycle arrest. Through the secretion of a variety of substances, such as cytokines and chemokines, growth factors, extracellular matrix (ECM) components, as well as proteases, the SASP mediates the paracrine actions of senescent cells. This causes an inflammatory response, which changes the environment and modifies their niche, hastening the aging process (Chou et al., 2022). Senescent cells need to be eliminated

effectively, and their excessive accumulation in tissues has negative effects that might accelerate the development of cancer and age-related disorders (Gonzalez-Meljem et al., 2018).

1.6   Signalling pathways involved in senescence

Senescence will start when DNA is damaged in one of the many ways listed in section 1.1, which will then trigger the DNA-damage response to repair the damage (DDR). DDR prevents damage from transferring to newly created cells as a result of cell division (Ciccia and Elledge, 2010). DNA-PKcs (DNA-dependent protein kinase), ATM (ataxia-telangiectasia mutant), and ATR (ATM- and Rad3-Related) are the three DDR kinases that are most upstream when DDR is activated by stress sensors Cell development is inhibited by these powerful phosphatidylinositol-3-kinase-like kinases (PIKKs). They belong to the superfamily of serine/threonine kinases (Marechal and Zou, 2013).

The P16^{Ink4a}/Rb (retinoblastoma protein) pathway and the P19^{Arf}/P53/P21^{Cip1} system, both of which are tumour suppressor pathways, are the two principal signalling pathways that contribute to the cell cycle arrest. As p53 and pRB are important transcriptional regulators, they primarily sustain the senescent state by causing extensive alterations in gene expression. P21$^{WAF1/CIP1}$ functions downstream of p53, while P16^{INK4A} acts upstream of pRB. Since they are cyclin-dependent kinase inhibitors (CDKIs) and function as inhibitors of cell cycle progression, they are the essential elements of each pathway. Senescence appears to require a stable stimulus, whereas transitory stimuli appear to trigger a transient growth arrest, allowing the cell to try to repair the damage. The severity and length of the stress stimulus appear to be the determining factors. Senescence can be brought on by prolonged overexpression of any one of these four essential molecules (p53, pRB, p16^{INK4A}, or p21$^{WAF1/CIP1}$) (Chen et al., 2007, Mijit et al., 2020).

1.6.1.1   p53 pathway

When DNA is harmed by a particular stressor, such as oxidative stress, telomere shortening, or oncogenic stress, the p53 pathway is triggered. If the stress is not relieved quickly, p53 initiates post-translational changes in response to these pressures. (Hernandez Borrero and El-Deiry, 2021). Through Chk1-induced p53 phosphorylation at Ser-15, caused by the transcriptional activation of

p21$^{waf1/cip1}$ (the protein encoded by the CDKN1A gene), ATM activates p53 as figure 3 shows (Qian and Chen, 2013). Depending on its degree of expression, p21WAF1/CIP1 has two opposing roles in the advancement of the cell cycle (Low levels of p21$^{WAF1/CIP1}$ function as an assembly factor for the cyclin/CDK4,6 complex and promote its activation, whereas high levels of p21$^{WAF1/CIP1}$ block the kinase activity of cyclin D/CDK4,6 complexes leading to suppression of cell cycle progression. However, because p21$^{WAF1/CIP1}$ is primarily needed for senescence induction, its expression is not maintained in senescent cells (Kumari and Jat, 2021).

1.6.1.2 p16INK4A/pRB Pathway

The persistence of the senescence cell cycle arrest in human cells may be due to the action of pRb, which acts as a second barrier to cellular immortalisation. A series of cyclin-dependent kinases (CDKs), CDK2, CDK4, and CDK6, play a crucial role in the phosphorylation of pRb. The activity of pRb is tightly regulated by various post-translational modifications, including acetylation, ubiquitination, and phosphorylation. It is also believed to impose a block on G1 progression that is alleviated by phosphorylation. When these CDKs phosphorylate pRb, pRb loses its capacity to bind E2F/DP transcription factor complexes, causing the cell cycle to enter S-phase.(Rayess et al., 2012). Senescent cells, on the other hand, exhibit higher levels of the CDK inhibitor p16^{INK4a}, which specifically binds to and inhibits D-type CDKs CDK4 and CDK6. The CDK2-kinase is rendered inactive by the binding of p16^{INK4a} to CDK4/6 and the Cip/Kip family CDK inhibitors, p21$^{Cip1/Waf1}$ and p27^{Kip1}, from cyclin D-CDK4/6 to cyclin E-CDK2 complexes. Thus, to inhibit the phosphorylation of pRb, upregulation of p16^{INK4a} works in conjunction with p21$^{Cip1/Waf1}$, resulting in a permanent G1 arrest in senescent cells (shown figure 4) (Takahashi et al., 2007). It is significant to note that the p16^{INK4a} gene is frequently inactivated in a variety of human malignancies, and as a result, it is known as a tumour suppressor gene. This may also be due to the fact that the p16^{INK4a} gene shares a portion of its coding sequence with the p14^{ARF} gene, a different tumour suppressor gene. Although many of the point mutations in this region only influence p16^{INK4a} activity in human cancer, they do not alter p14^{ARF} activity,

suggesting that the p16^{INK4a}/Rb-pathway also plays important functions in tumour suppression on its own (Kumari and Jat, 2021, Takahashi et al., 2007).
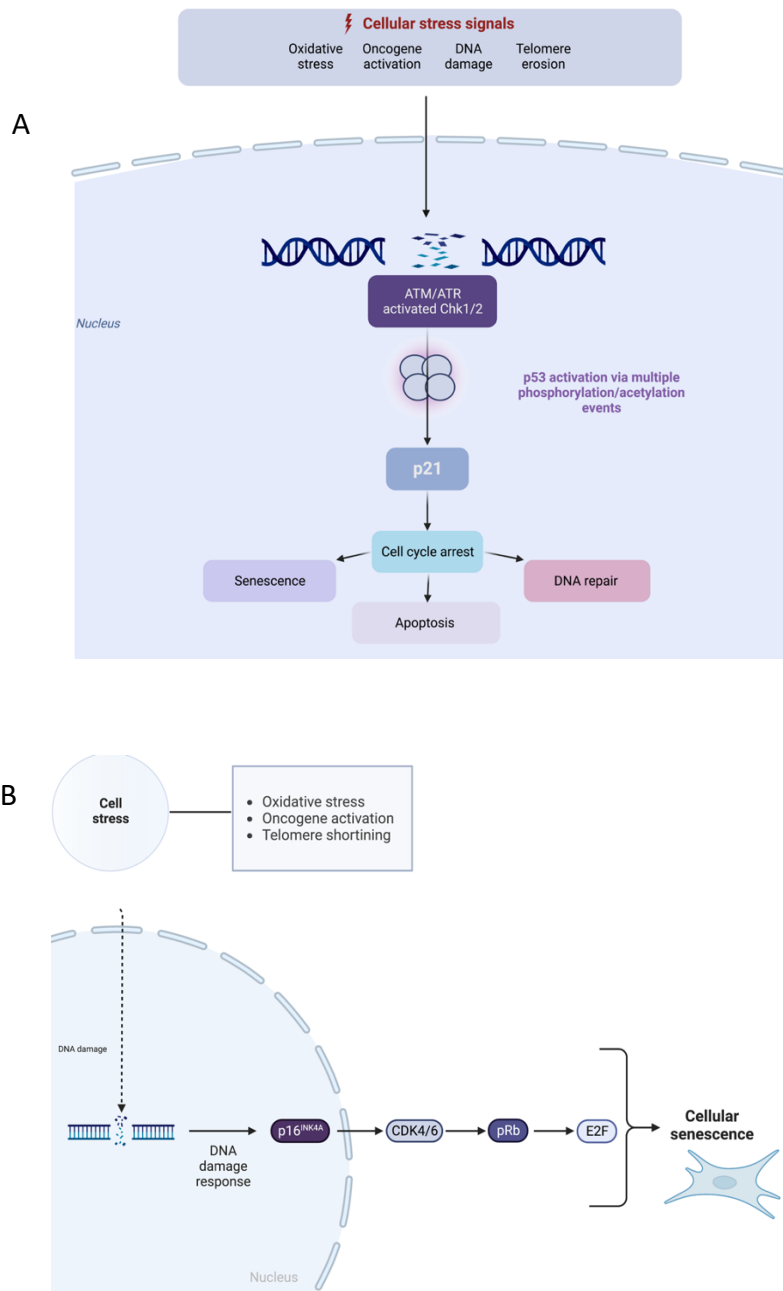
Figure 1.4: senescence signalling pathways

A) the signalling pathway of p53. owing to factors that stress cells and harm DNA. DDR was started as a defensive tactic. ATM activates p53 throughout activating chk1/2 causing p53 phosphorylation at Ser-15, which caused the transcriptional activation of p21$^{waf1/cip1}$ (the protein encoded by the CDKN1A gene) to be activated. **B)** p16^{INK4a}/Rb-pathway; DNA damage was brought on by cellular stress. Higher levels of the CDK inhibitor p16INK4a, which specifically binds to and inhibits D-type CDKs CDK4 and CDK6, are present in senescent cells. Upregulation of p16^{INK4a}, therefore, works in concert with p21$^{Cip1/Waf1}$ to cause a permanent G1 arrest in senescent cells by allowing for the dephosphorylation and stability of the RB-E2F complex (image generated using BiorRnder website).

1.7   Senescence biomarker

Growth arrest prevents a malignant tumour from becoming too large, but it also causes a variety of other illnesses. Senescent cells display a variety of changes while still being metabolically active, such as a rise in associated beta-galactosidase (ß-galactosidase) activity and the expression of cyclins, which control the cell cycle. Additionally, platelet-derived growth factor (PDGF) inhibits the death of intrinsic cells (apoptosis) in addition to the inefficient response to growth factors like the epidermal growth factor (EGF) (Rozengurt, 1992; Yang *et al.*, 2011).

1.7.1   Cell morphology

Senescent cells undergo morphological alteration. compared to their normal state, usually larger, flattened, multinucleated, and vacuolated. Vimentin and other cytoskeletal proteins, as well as proteins that connect cell adhesion to the cytoskeleton, have been related to these morphological alterations (Nishio et al., 2001). Additionally, it is believed that a slowdown in the rate of protein degradation may contribute to an increase in the size of senescent cells (Hwang et al., 2009). ATF6α also seems to be a critical factor in the parallel arrangement of the cells and the loss of fusiform shape. Senescent fibroblasts also secrete specific substances, such as more VEGF than non-senescent fibroblasts, which affects the development of angiogenesis in the majority of clinical diseases. (Shibuya, 2011, Son et al., 2019, Druelle et al., 2016).

1.7.2   Senescence-associated beta-galactosidase (β-galactosidase) activity

Senescence-associated beta-galactosidase (ß-galactosidase) activity is the most common senescence detection marker. It may be seen at pH6 in cultured cells going through replicative or stress-induced senescence as well as in aged tissue in vivo (Dimri et al., 1995).

SA ß-gal activity since it is easy to quantify and can usually be done in situ using a chromogenic substrate like X-gal; therefore, it considers the most common biomarker to detect senescent cells. Numerous research has put forth theories on the origin of beta-galactosidase activity and its function in cellular senescence. The first is that lysosomal-galactosidase activity rises in senescent cells to a

point where it surpasses a cut-off that makes it detectable at a pH of 6.0 (Gerland et al., 2003). A further investigation unequivocally established that the lysosomal -galactosidase 1 (GLB1) gene product is the source of the SABG activity. Enzymatic activity rises concurrently with a considerable increase in this gene's mRNA and protein levels in senescent cells (Lee et al., 2006). Additional to the age-related accumulation of lysosomal -galactosidase in senescent cells, which is likely caused by the increased lysosomal content in the cell, increased cell density may also contribute to the rise in ß-galactosidase levels seen by ß-galactosidase staining at pH 6.0, leading Into false positive results (Shlush et al., 2011, Lee et al., 2006).

1.7.3   Growth arrest

One of the most obvious signs of cellular senescence is the arrest of the cell cycle, which occurs when the cells are in the G1/S phase. As was previously indicated in section 1.1.2, activating the p53/p21^{CIP1} and p16^{INK4a}/Rb tumour suppressor pathways regulates this cell cycle. The p16^{INK4a}, p21$^{waf1/CIP1}$, and p53 protein markers for an arrested cell cycle, as well as a decline in phosphorylated Retinoblastoma protein (pRB). In senescence, following DNA damage, p53 is activated via phosphorylation (p53), which increases temporary expression of the CDKI p21^{CIP1}, which blocks CDK2 activity and enables the dephosphorylation of RB, which sequesters E2F and causes cell cycle arrest. (Gonzalez-Gualda et al., 2021, Althubiti et al., 2014).

The protein p16^{Ink4a}, a cyclin-dependent kinase inhibitor (CDKI) in the p16^{Ink4a}/RB pathway, directly inhibits the CDK4-CyclinD complex, allowing for the dephosphorylation and stability of the RB-E2F complex and, thus, the suppression of the cell cycle (Ben-Porath and Weinberg, 2005, Mohamad Kamal et al., 2020)

However, the p53/p21^{CIP1} pathway is shown in replicative senescence, DNA damage response (DDR), reactive oxygen species (ROS), and oncogene-induced senescence (OIS), and it is believed to be triggered early in the senescence programme (Beausejour et al., 2003). On the other hand, DDR-induced senescence does not result in the activation of the p16^{Ink4a}/RB pathway. It is believed to have

a bigger impact on preserving the chronic senescent state (Dulic et al., 2000, Gonzalez-Gualda et al., 2021). Therefore, it is preferable to use numerous protein markers to identify cell cycle arrest.

1.7.4   Senescence-associated heterochromatin foci (SAHF)

The inhibition of E2F target genes, which are predominantly engaged in boosting cell proliferation and S-phase cell cycle progression, is one of the prerequisites for this irreversible cell cycle exit. During senescence, E2F target gene promoters often develop heterochromatic characteristics. Specialized facultative heterochromatin domains that frequently form in senescent human cells, known as senescence-associated heterochromatin foci (SAHF), are the heterochromatin linked to this process (Narita et al., 2003, Di Micco et al., 2011).

Observing that senescent cells' nuclei contain 30 to 50 colourful, punctate DNA-stained dense foci easily distinguishable from normal cells' chromatin, Narita initially identified SAHF in 2003 (Narita et al., 2003, Aird and Zhang, 2013).

Proliferation-promoting genes, such as E2F target genes like cyclin A, which are necessary for the cell cycle's progression through the S phase, are sequestered by SAHF. Cell transformation can result from the interruption of SAHF formation, suggesting that SAHF play a role in the tumor-suppressive properties of senescence. Recently, there has been evidence to support the idea that SAHF may restrict the amount of DNA-damaging signalling, which may keep senescent cells from going through the apoptosis caused by high DNA damage signalling and retain their viability. Finally, mounting evidence suggests that SAHF may contribute to the in vivo senescence phenotype. Oncogenes, toxic substances and telomere shortening can cause the formation of SAHF in senescent cells; it can also occur in a spontaneous, stochastic, and planned manner (Kreiling et al., 2011, Narita et al., 2006, Aird and Zhang, 2013, Bernadotte et al., 2016)

1.7.5   Senescence-associated DNA-damage foci

Histone γ -H2AX is another typical marker for cellular senescence. The most sensitive indicator of double-stranded DNA breaks (DSBs) and telomere shortening is histone γ-H2AX (Sedelnikova et al., 2004). In most tissues and species, both in vivo and in vitro, injured and senescent cells increase in γ

-H2AX foci (Balajee and Geard, 2004). During all stages of the cell cycle, the very sensitive marker γ -

A2SAX foci identify each DSB. Histone γ -H2AX is a potential indicator of cellular senescence, although

it shouldn't be taken into account as a sole indicator. (Sharma et al., 2012, Sedelnikova et al., 2008).

1.7.6   Senescence Associated Secretory Phenotype (SASP)

Senescence is more than just a cell cycle stop in a growing cell. A senescent cell is a possibly

persistent cell that has experienced extensive alterations in protein expression and secretion, finally

forming the senescence-associated secretory phenotype (SASP) (Coppe et al., 2010). which can

affect the surrounding tissue by soluble and insoluble factors, it can interrupt the signalling

transduction pathways of other cells by activating different cell surface receptors, which leads to the

promotion of different pathologies like cancer. The SASP contains multiple secreted proteins,

including inflammatory cytokines, chemokines, and interleukins that regulate immune responses,

growth factors, secreted proteases, and new secreted extracellular matrix (ECM) components that

can be physiologically active in the surrounding tissue microenvironment (Acosta et al., 2013,

Kuilman et al., 2008).

There have been reports of various SASP factors' functions and behaviours. Senescent cells

themselves operate as autocrine SASP factors, reinforcing cellular senescence. Paracrine

senescence is the paracrine action of SASP proteins such as chemokines like CCL2 and CCL20, as

well as members of the TGF-ß family and vascular endothelial growth factor (VEGF), which results

in the senescence of neighbouring cells (Lujambio et al., 2013, Acosta et al., 2013). Similar to this,

in vitro and may be in vivo, ROS signalling across gap junctions causes bystander senescence

(Nelson et al. 2012). Possible effects of paracrine senescence include amplifying the anti-tumor

response brought on by OIS. The immune cells, including NK cells and macrophages that can

scavenge senescent cells, are apparently affected by the secreted chemokines from senescent cells

as SASP factors (Krizhanovsky et al., 2008). The differentiation of neighbouring cells and the

elimination of unneeded cells are both induced by SASP factors (Munoz-Espin et al., 2013).

Senescent cells secrete SASP factors, which can help cellular plasticity to support tissue repair and reprogramming. Through EGFR signalling, SASP factors can accelerate proliferation and the mesenchymal-epithelial transition, thereby promoting both in vitro and in vivo reprogramming. Effective cell reprogramming in vivo requires senescence induction because senescent cells secrete SASP factors during reprogramming, which facilitates potential reprogramming of cells and allows for tissue repair. SASP factor production also promotes reprogramming of somatic cells.

All things considered, SASP factors have the ability to stimulate cellular plasticity and reprogramming through inducing senescence, facilitating tissue repair, and speeding up proliferation and the mesenchymal-epithelial transition through EGFR signalling (von Joest et al., 2022, Xi et al., 2022).

Whatever its original purpose, the SASP can have both advantageous and negative impacts. Senescence's tumour suppressor properties are mediated by the SASP. Inflammatory cytokines, chemokines, and interleukins that control immune responses, growth factors, secreted proteases, and new secreted extracellular matrix (ECM) components that can be physiologically active in the surrounding tissue microenvironment are among the secreted proteins found in the SASP. The SASP contributes significantly to the control of cellular senescence in tumours. In vitro senescence growth arrest is strengthened by components of the SASP like IL-8, IL-6, plasminogen activator inhibitor 1 (PAI-1), and IGFBP7(Coppé *et al.*, 2010; McHugh and Gil, 2018). The genes for the cytoplasmic proteins RAS and BRAF, which are involved in the transmission of growth factor signals to the intracellular level, are disturbed in cancer cells. IL-6, IL-8, and IGFBP7 are activated by the presence of oncogenic signals from RAS and BRAF to inhibit cell growth. Additionally, elevated RAS in ovarian fibroblasts causes the release of CXCL 1, which inhibits cell proliferation. By turning on the transcription factors NF-κB and C/EBP-β, IL-6 and IL-8 inhibit the development of tumour cells. (Hinds and Pietruska, 2017, Campisi, 2013).

1.7.6.1 Classification of SASP

depending on the type of senescent cell and the senescence inducer, the SASP production varies. Soluble signalling factors make up a significant portion of the SASP in addition to Extracellular Proteases.

1.7.6.1.1 SASP Soluble Signaling Factors

This includes interleukin-6 (IL-6), the most well-known and pleiotropic proinflammatory cytokine of the group. The DNA damage and oncogenic stress-induced senescence of mice and human keratinocytes, melanocytes, monocytes, fibroblasts, and epithelial cells have been linked to IL-6 (Coppe et al., 2008, Lu et al., 2006). IL-1 has been shown to be another interleukin signalling pathway that senescent cells have an increased ability to activate. Senescent endothelium cells, fibroblasts, and chemotherapy-induced senescent epithelial cells all overexpress and produce both IL-1α and -β (Kumar et al., 1992, Lau et al., 2019, Maier et al., 1990, Chang et al., 2002). Through the cell-surface receptors (IL-1 receptor/Toll-like receptor superfamily), which primarily function to activate the nuclear factor kappa B and to activate protein 1 pathways, these cytokines can affect nearby cells (Mantovani et al., 2001). The majority of senescent cells overexpress CXCL-8, CXCL-1, and CXCL-2. CCL-2,8, 7,13, 16, and 26 are further members of the CCL family that are typically increased in senescent cells, in addition to macrophage inflammatory protein (MIP)-3 and -1. (CCL-20, -3). Senescent liver stellate cells, as well as prostate and skin fibroblasts, overexpress MCP-3 (CCL-7) (Sarkar et al., 2004, Bode-Boger et al., 2005, Bavik et al., 2006). The interaction between senescent cells and their surroundings may also be mediated via the insulin-like growth factor (IGF)/IGF receptor network. Almost all IGF-binding proteins (IGFBPs), including IGFBP-2, -3, -4, -5, and -6, are expressed at high levels in senescent endothelium, epithelial, and fibroblast cells. Moreover, IGFBP-7 is secreted when the BRAF oncogene is activated in primary fibroblasts, and this protein then uses autocrine and paracrine mechanisms to cause adjacent cells to age and die (Coppe et al., 2008, Wang et al., 1996, Severino et al., 2013, Mercurio et al., 2020, Wajapeyee et al., 2008). The SASP is connected to other soluble components. Inflammatory cytokines, like granulocyte macrophage-

colony stimulating factor (GM-CSF), are controlled in senescent human fibroblasts by activating NF-B(Lim et al., 2015). Additionally, senescent fibroblasts have large quantities of osteoprotegerin (OPG) in their extracellular milieu (Stojanovic et al., 2020).

1.7.6.1.2 Extracellular Proteases and Extracellular Insoluble Molecules as an Important Subset of the SASP

Biological senescence is one cellular phenomena linked to changes in the expression of ECM components and the secretion of ECM remodelling enzymes. Over evolution, a class of enzymes known as proteases has taken part in a wide range of biological processes (Levi et al., 2020).

MMP-3 and MMP-10, respectively, and collagenase-1 (MMP-1) are the MMP family members that are consistently increased in human and mouse cells going through replicative or stress-induced senescence (Hassona et al., 2014, Ghosh and Capell, 2016, Liu and Hornsby, 2007). In some cases, the MMP-1 and -3 made by senescent cells can also control how much the soluble components of the SASP are active. These MMPs, for instance, are capable of cleaving IL-8, MCP-1, -2, and -4 (Kodali et al., 2006, McQuibban et al., 2002). MMP-9, -2, or -7 can also cleave a range of additional CXCL/CCL family members that make up the SASP. These nearby cells, such as leukocytes or tumour cells, may be the source of these CXCL and CCL cytokines. (Van Den Steen et al., 2003). Serine proteases and plasminogen activation pathway regulators make up a different family of proteases found in the SASP that are implicated in the development of cancer (Martinez et al., 2015). Members of this family include tissue-type plasminogen activators (tPA) and urokinase (uPAR), which are both released by senescent cells in fibroblasts and endothelial cells, respectively cells (Vaughan et al., 2017, Birch and Gil, 2020, Comi et al., 1995, Mu and Higgins, 1995). The CXCR-2 cytokines and PAI-1 appear to support the senescence growth arrest in similar ways (Kortlever et al., 2006).

Fibronectin, a glycoprotein that is present on the surface of cells, plasma, and other bodily fluids, is the insoluble protein released by senescent cells. Both in vivo and in culture, senescent cells expressed fibronectin. Fibronectin stimulates cell adhesion, proliferation, and migration by interacting with the cell's surface receptors, such as the integrins (Cuollo et al., 2020). Senescent cells may have an impact on tissue microenvironments due to the production of molecules other than

proteins as a result of changes in cellular metabolism brought on by senescence. Nitric oxide (NO), reactive oxygen species (ROS), and endothelial nitric oxide synthase are among the substances produced in this group. These elements are the outcome of senescent cells' altered metabolism, which may have an impact on nearby cells (Coppe et al., 2010, Dasgupta et al., 2010). These reactive substances are well-known for altering cellular phenotypes, such as monocyte differentiation. These chemicals can also make cancer cells more aggressive and speed up aging and age-related deterioration(Finkel et al., 2007).

1.7.6.2   Classification of SASP based on the mechanism of action

As is well known, SASP consists of a variety of inflammatory proteins, each of which has a unique mode of action (figure 1.5)

1.7.6.2.1   Receptor requiring SASP

Interleukins, chemokines, and growth factors are examples of soluble signalling factors that belong to this category. These signalling molecules attach to their receptors and subsequently initiate intracellular signal transduction pathways. (Kuilman et al., 2008). It demonstrates how an essential part of cellular senescence is played by the autocrine activity of the expression of the secreted SASP components. The signalling mechanism is also activated by the binding of chemokines and growth factors to their receptors, including hepatocyte growth factor, fibroblast growth factor (FGF), transforming growth factor ß1, and granulocyte-macrophage colony-stimulating factor. The SASP components have as their targets all cells that express those receptors. Consequently, senescent cells that release SASP may also be targets for actions that could worsen or prevent the development of senescence in cells (Borodkina et al., 2018, Byun et al., 2015).

1.7.6.2.2   Direct acting SASP

The majority of the SASP elements in this group are MMPs and serine proteases. By degrading cell membrane proteins and extracellular matrix (ECM) through their proteolytic activity, these substances alter the environment around senescent cells. The molecules that carry the signal are

harmed by it. Non-protein components like ROS and NO are also included in this group (Byun et al., 2015).

1.7.6.2.3 SASP regulatory factors

Tissue inhibitors of metalloprotease (TIMPs), plasminogen activator inhibitors (PAI), and insulin-like growth factor-binding proteins are a few examples of SASP regulatory factors. TIMP is strongly activated by a number of cytokines and hormones (Reichenstein et al., 2004). By preventing MMP activity, PAI-1 also prevents cancerous cells from encroaching on healthy tissue. IGFBP is a protein that transports IGF to target cells and modulates illnesses associated with aging (Cesari et al., 2010, Rajpathak et al., 2009, Borodkina et al., 2018).

As a result, a variety of indicators can be utilised to identify cellular senescence. Senescence-associated -galactosidase activity, a straightforward experiment to identify metabolic alterations, is the most typical marker. Directly measuring the proliferation rate or analysing the expression of p16^{Ink4} and p21$^{Waf1/CIP1}$ can be used to identify changes in proliferation. It is also possible to use changes in cell shape, but these are more difficult to quantify. Finally, it is possible to look at SASP adjustments. It is crucial to keep in mind that numerous assays are preferred because senescence is produced by a variety of causes, each of which may influence the markers differently.

```
                    ┌─────────────────────────┐
                    │   Classification of SASP │
                    └─────────────────────────┘
                       │                    │
          ┌────────────────┐      ┌──────────────────────┐
          │     Soluble    │      │    Extracellular     │
          │ Signaling SASP │      │   Proteases and      │
          │     factors    │      │    Extracellular     │
          └────────────────┘      │  Insoluble Molecules │
                 │                └──────────────────────┘
                 │                     │              │
          ┌────────────┐      ┌──────────────┐  ┌──────────────┐
          │   requir   │      │ Direct acting│  │     SASP     │
          │  Receptor  │      │    SASP      │  │  regulatory  │
          └────────────┘      └──────────────┘  │   factors    │
                 │                   │           └──────────────┘
                                                        │
   ┌───────────────────────┐  ┌────────────────┐  ┌──────────────────┐
   │ These signalling      │  │ Act directly by│  │ Required cytokines│
   │ molecules required    │  │ altering the   │  │ and hormones to   │
   │ receptors start       │  │ environment    │  │ regulate SASP     │
   │ intracellular signal  │  │ around         │  │ factor            │
   │ transduction          │  │ senescent cells│  └──────────────────┘
   └───────────────────────┘  └────────────────┘
```

Figure1.5; different classification of SASP depending on SASP production and mechanism of action

1.8   Role of Cellular senescence

1.8.1   Cellular Senescence in Health

It's common knowledge that circumstances imposing cellular stress cause cellular senescence, which is thought to be a protective mechanism. Even though growth arrest causes a variety of illnesses, it is crucial to avoid the overgrowth of a malignant tumour. This reaction includes a proinflammatory phenotype known as the senescence-associated secretory phenotype (SASP) together with a typical persistent cell cycle halt. Additionally to the well-known disruption of aging processes. Cellular senescence in tumours is significantly suppressed due in large part to the SASP. Due to the production of fresh granulation tissue and the introduction of myofibroblasts, it also aids in the wound healing process and contraction during the epithelization phase (Baz-Martinez et al., 2016).

1.8.2   The normal wound healing process

1.8.2.1   *Coagulation/inflammation phases*

A couple of the initial stages of wound healing are coagulation and inflammation. They are necessary to halt bleeding, clear away debris and injured tissue, and encourage healing. Wound healing may be

slowed down or compromised if coagulation or inflammation are compromised (illustrated figure 1.6) .

We refer to the process of clotting blood as coagulation. It is caused by damage to blood vessels, which releases platelets and other clotting factors into the air. These clotting factors work together to form a clot that stops the bleeding and closes the injured vessel.

There are three phases of coagulation involved:

Primary hemostasis. In this initial phase of coagulation, platelets serve as the mediators. When platelets are activated by air, they adhere to the damaged vessel wall. Coagulation takes place to halt further bleeding. Thrombocytes and platelets coagulate within a fibrin network to reestablish homeostasis. They also release chemicals that attract more platelets and clotting factors to the site of the wound. Hemostasis secondary. A fibrin clot forms as a result of a cascade of clotting factors during this stage of coagulation. A protein called fibrin creates a robust net that ensnares platelets and other blood cells, creating a clot that shuts off the injured blood vessel.

Retraction of clots and fibrinolysis. After the bleeding stops, the clot starts to shrink and retract. Platelets and other cells that compress the fibrin mesh accomplish this. Another method that gradually dissolves the clot is fibrinolysis. The body's reaction to an injury or infection is inflammation. Pain, swelling, heat, and redness are its defining characteristics

(Demidova-Rice et al., 2012b, Gonzalez et al., 2016).

Wound healing requires inflammation because it aids in the removal of damaged tissue and debris as well as the fight against infection. There are four phases to inflammation:

dilation of the vaso. The first stage of inflammation is marked by the enlargement of blood vessels. By increasing blood flow to the damaged area, this helps the healing cells by supplying them with nutrients and oxygen.

increased permeability of the arteries. There is more fluid leaking from blood vessels into the surrounding tissues during this stage of inflammation. This results in swelling and aids in the removal of debris and poisons from the injury site.

infiltration of neutrophils. White blood cells called neutrophils are essential in the fight against infection. Chemicals released by injured cells and other immune cells draw them to the site of injury. Bacteria and other alien invaders are engulfed and destroyed by neutrophils. invasion by macrophages. Another subset of white blood cells involved in wound healing are macrophages. Chemicals released by neutrophils and other cells draw them to the site of injury. Macrophages aid in the initial stages of tissue repair by eliminating debris and damaged tissue.

Usually, the inflammatory stage of wound healing lasts three to five days. The repair phase then starts.

Inflammation and coagulation are crucial for the healing of wounds. Coagulation aids in halting bleeding and guards against infection of the wound. Inflammation facilitates repair by assisting in the removal of debris and damaged tissue.Wound healing may not occur at all or may occur more slowly if coagulation or inflammation is compromised. For instance, bleeding disorders make it difficult for blood to clot, which can result in excessive bleeding and a protracted healing process for wounds. Impaired inflammation can cause a delay in wound healing in people with inflammatory diseases like diabetes or arthritis (Broughton et al., 2006, Sorg et al., 2017, Wang et al., 2022b)

1.8.2.2   Proliferative Phase

Re-epithelialization begins to replace the tissue that has been lost as a result of the damage after the inflammatory phase, and it is this process that causes the wound to close. In order to maintain cell proliferation and start keratinocyte migration, which is crucial for granulation development, numerous growth factors are secreted by various cells in this phase, including the residual inflammatory cells and dermal and epidermal cells. As additional cells are produced to cover the wound, the remaining keratinocytes at the wound edge and epithelial stem cells from surrounding hair follicles begin to move toward the wound site (Landen et al., 2016). The development of angiogenesis, which joins broken blood vessels with new ones to organise the microvascular blood network throughout the newly formed granulation tissue, is also part of this stage. The neovascularisation is regulated by vascular endothelial growth factor, angiopoietin, fibroblast growth

factor 2 (FGF-2), and PDGF (Demidova-Rice et al., 2012a). In the proliferation phase, granulation tissue that is made up of various cell types, such as fibroblasts, granulocytes, macrophages, and blood vessels with collagen bundles, replaces the temporary wound matrix that was created during the homeostasis phase to restore the texture and function of the injured area. The fibroblast in granulation tissue is crucial for the healing of wounds. The fibroblasts begin to move from the adjacent dermis and from fibrocytes to the injured area in response to growth factors like PDGF, TGF, and EGF. To fill in the area of the wound, the fibroblasts begin to multiply, generate proteinases, and deposit collagen and other extracellular matrix (ECM) components (Landen et al., 2016).

1.8.2.3   Maturation Phase

In order to restore tissue structure and function, a critical step in the healing process of wounds is matrix remodelling, which involves the degradation, reorganisation, and rebuilding of the damaged extracellular matrix (ECM). Enzymes, ECM components, and various cell types interact intricately in this process. Matrix metalloproteinases (MMPs), which degrade damaged ECM components like collagen, fibronectin, and proteoglycans, are responsible for the ECM remodelling degradation process. This makes room for the synthesis of fresh matrix proteins. Growth factors and cytokines released by different cells, such as fibroblasts, macrophages, and platelets, in addition to controlling cell migration and proliferation, also promote the migration and proliferation of new cells into the wound site. at last producing new extracellular matrix (ECM) proteins, such as collagen, hyaluronic acid, and elastin. The main cells involved in this process are called fibroblasts. Following their deposition, the proteins create a fresh, well-organized matrix in the wound bed. Stabilisation and cross-linking: The newly deposited collagen fibres are cross-linked by enzymes such as lysyl oxidase (LOX), giving the developing tissue strength and stability (Keane et al., 2018, Gurtner et al., 2008).

Depending on the type of tissue and the extent of the injury, the precise profile of remodelled matrix proteins varies. Here are some examples. Collagen, the most prevalent protein in the

extracellular matrix, offers tensile strength and structural support. Collagen type III is first deposited during healing, and for long-term stability, it is replaced by stronger collagen type I.Fibronectin facilitates migration, proliferation, and adhesion of cells. Water is drawn to and lubricated by hyaluronic acid, which promotes cell migration and produces an environment that is hydrated for healing. Tissues can stretch and contract back to their original shape thanks to elastin. Proteoglycans contribute to the structural integrity and organisation of the extracellular matrix (ECM) by binding to water and collagen. They also control the activity of growth factors and cell signalling (Landen et al., 2016, Tracy et al., 2016, Klingberg et al., 2013).
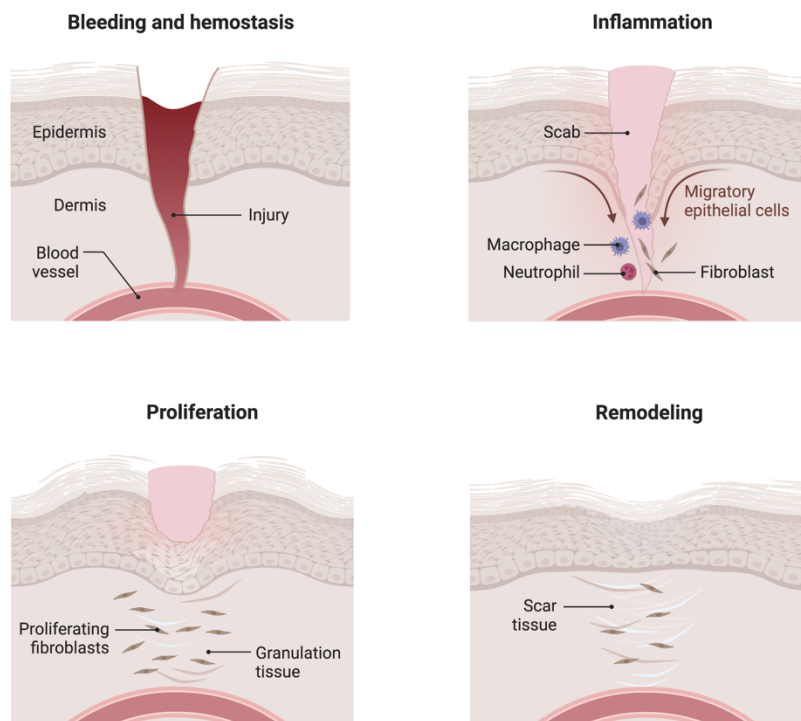
Figure 1.6: stages of wound healing.

!)The coagulation phase, which is the body's initial response to injury and occurs to stop any bleeding. 2) inflammatory Phase, during this time, neutrophils enter the site to eradicate bacteria and clear out debris. Additionally, to aid in tissue regeneration, these cells produce proteins and growth factors that entice immune system cells (macrophages)to the wound. 3) proliferation phase New blood vessels are created as granulation tissue from the proliferative phase fills the wound bed with connective tissue. The wound margins shrink and pull toward the centre of the wound as it contracts. 4) Maturation Phase The last stages of wound healing include scar formation and matrix remodelling (image generated using BiorRnder website).

.

1.8.3   Wound Healing

The process of wound healing benefits from cellular senescence in young persons. Senescent myofibroblasts gather as a natural element of the healing process for wounds. Myofibroblasts, which had initially multiplied in response to the damaging stimulation, were recognised as senescent cells. Through its cell surface receptors, DNA damage response, and p53 activation, the secreted ECM-associated signalling protein CCN1 can cause fibroblast senescence, which activates the p16^{INK4a}/pRb pathway in a reactive oxygen species (ROS)-dependent manner. CCN1 is highly expressed at sites of wound repair. Further research revealed that CCN1 may have therapeutic value in treating specific kinds of non-healing wounds by hastening neutrophil clearance(Jun et al., 2015). The prevalence of α -SMA in the senescent fibroblasts led to their identification as myofibroblasts. They were found to collect in the granulation tissue of healing wounds, where they produced antifibrotic genes. Importantly, CCN1 abnormalities cause fibrosis to worsen even in the absence of senescent cells. (Jun and Lau, 2010).

Due to the creation of new granulation tissue and the introduction of myofibroblasts, SASP also plays a significant physiological function in the repair of injured tissues and the contraction of wounds during the epithelization phase. the temporary appearance of senescent cells with the SASP in subcutaneous fibroblasts, where the SASP contributed to the tissue healing of injured skin. Fibroblasts in injured tissues produce SASP factors that attract immune cells that help remove the damaged tissues. In order to make new skin, senescent fibroblasts simultaneously release growth factors known as SASP factors and encourage the division of skin progenitor cells. Immune cells sourced from the fresh skin gradually eliminate senescent fibroblasts (Demaria et al., 2014). In the case of liver damage, hepatic stellate cells go through cellular senescence in order to produce SASP factors and draw in immune cells. Senescent hepatic stellate cells (HSCs) are removed by immune cells in order to reduce the creation of too much collagen and stop fibrosis (Yoshimoto et al., 2013). With aging, senescent cells start to accumulate in the aged tissue due to the failure of the immune system to properly clear the senescent cells. This leads to an increase in the secretion of inflammatory

cytokines. Clarifying the mechanism of SASP persistence is crucial for managing SASP because the pathogenic form of SASP tends not to be transient but to persist, causing undesired effects like cancer progression or chronic inflammation (Ohtani, 2022). It is important to take into account the type of cells going through senescence and SASP, such as whether they are stromal cells or precancerous epithelial cells, while analysing the role of SASP in tumour growth Determining whether the cancer is in an early or late stage is also crucial since SASP in precancerous epithelial cells prevents carcinogenesis whereas SASP in stromal fibroblasts in advanced cancers promotes tumour growth (Ohtani, 2022). SASP components increased cell proliferation, particularly in premalignant and malignant cells. Different cells have increased tumorigenicity due to MMPs, connective tissue growth factor (CTGF), or IGFB-rP2 released by senescent fibroblasts, which also accelerates the angiogenesis process (Liu and Hornsby, 2007, Kim et al., 2004, Yang et al., 2005, Tonini et al., 2003) Additionally, chemokine components in SASP that are released by senescent cells stimulate cell migration and invasion. Senescent cells release FGF, IL-6, IL-8, MMP-2, and MMP-3, which encourage the invasion of cancer cells. Proteases like uPA and PAI1, which act as uPA regulators, are also involved in the invasion of cancer cells (Coppe et al., 2008, Parrinello et al., 2005)Additionally, the temporary build-up of senescent fibroblasts and endothelial cells at the wound site triggers the development of myofibroblasts by secreting platelet-derived growth factor AA (PDGF-AA). When PDGF-AA was administered, the delay in wound closure was reversed. At the same time, the amounts of fibrotic tissue were maintained, indicating that other SASP factors—likely MMPs—are involved in the healing process. (Paramos-de-Carvalho et al., 2021, Demaria et al., 2014). Senescent cell removal decreased the number of myofibroblasts, slowed wound healing, and increased fibrosis, all of which could be avoided by ectopic PDGF-AA injection. Senescent cells contribute significantly to tissue repair by cell-autonomous pathways, such as the release of PDGF-AA in the skin and Mmp9, Mmp13, and IL-6 in the regenerating liver. Senescent cells may thereby prevent unchecked cell growth by limiting tissue regeneration. On the other hand, chronic wounds are caused by the extended presence of senescent cells in the elderly, which hinders re-epithelialization and wound closure (Jun and Lau, 2010, Demaria

et al., 2014). One promising method for preventing cancer and promoting tissue repair is pharmacological Nrf2 activation. Nrf2 is a crucial regulator of the antioxidant defence system. On the other hand, fibroblasts' Nrf2 activation causes cellular senescence. A senescence-promoting matrix is deposited by fibroblasts with activated Nrf2, and plasminogen activator inhibitor-1 is a major inducer of the senescence programme. Skin tumorigenesis as well as the re-epithelialization of skin wounds were encouraged by Nrf2 activation in fibroblasts(Hiebert et al., 2018).

1.8.4   Tumor Suppression

Senescence has a significant impact on the suppression of pre-malignant to malignant disease progression and the suppression of cancer cell proliferation. Senescence induction is linked to the production of several important oncogenes, including ras, cyclin E, raf, and E2F3, which may have a tumor-suppressive effect (Sarkisian et al., 2007, Althubiti et al., 2014). This might be accomplished by preventing the growth of cancerous cells. Additionally, senescence can prevent the spread of cancer since premalignant tumours with more senescence may have lower invasion levels (Collado et al., 2005). Senescence is frequently triggered by major oncogene alterations to eliminate premalignant cells before they get more mutations and spread (Haferkamp et al., 2009, Wyld et al., 2020).

1.9   Cellular senescence and cellular age
1.9.1   Age-related disease and senescence

Senescent cells fail to be effectively cleared by the immune system as we age, and they begin to accumulate in the old tissue. This causes inflammatory cytokines to be secreted more frequently, which encourages chronic inflammation and speeds up the progression of age-related illnesses, including chronic wounds. Additionally, it increases p16^{Ink4a}, which encourages tumour growth.

1.9.2   Chronic wound

One of the age-related illnesses that is spread all over the world is chronic wounds. Chronic wounds are those that don't heal after receiving several treatments, exhibit loss of skin quality due to

underlying anatomical structure, take longer than three weeks to heal and are resistant to treatment (Makrantonaki et al., 2017).

1.9.2.1   Causes of chronic wound

Disruption of the natural biological process of healing a wound causes the wound to fail to heal and turn into a chronic wound. Chronic age-related wounds may develop as a result of aging stromal tissues and cellular responses that are ineffective. In fact, there has been a steady rise in the number of chronic wounds among people over 65, including chronic venous leg ulcers, pressure ulcers, and diabetic ulcers. Chronic illness, vascular insufficiency, diabetes, malnutrition, aging, and local variables, including pressure, infection, and oedema, are only a few of the causes of wound healing delays (Wall et al., 2008, Zhao et al., 2016)

The three main types of chronic wounds are vascular ulcers, pressure ulcers, and diabetic ulcers. All of these classifications share several characteristics, such as a protracted inflammatory phase, persistent infection, medication resistance in the wound, and the inability of dermal and/or epidermal cells to react to stimuli that promote healing. The wound-healing process fails as a result of these occurrences (figure 7) (Demidova-Rice et al., 2012b).
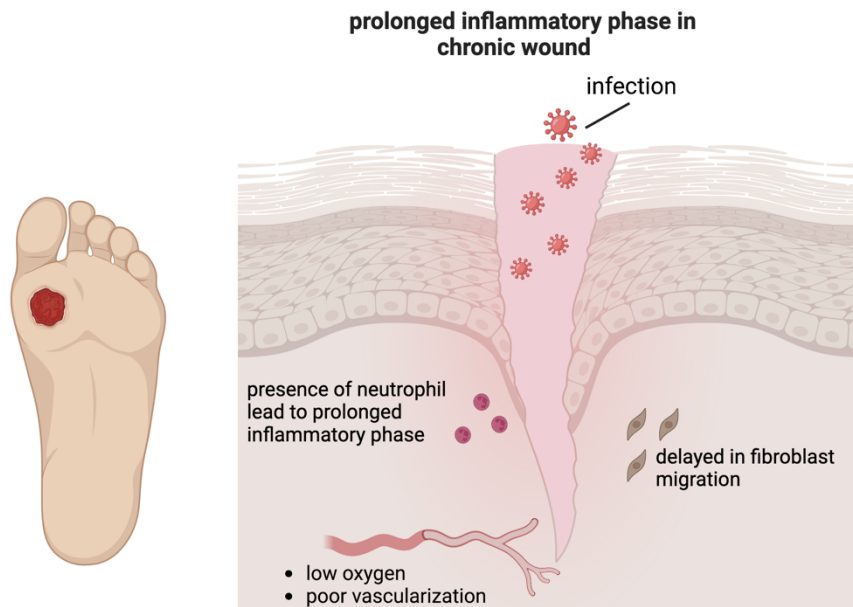
Figure 1.7: chronic wound

In a chronic wound the immune system was compromised by the bacteria in the wound, the inflammatory phases of the wound's healing were delayed, and fibroblast migration was unsuccessful. The process of covering the wound bed with new epithelium is known as re-epithelialization, but it is delayed in chronic wounds due to keratinocytes' reduced proliferative capacity. There are several reasons for this reduced proliferation, such as: Modified growth factor signalling, an inflammatory milieu, Increased oxidative stress, which can harm cellular components and hinder keratinocyte proliferation, is a characteristic of chronic wounds. Lastly, senescent cells are accumulated by keratinocytes in chronic wounds. Neighbouring keratinocytes' normal proliferation may be interfered with by these senescent cells. image generated using BiorRnder website.

1.9.2.1.1 Wound duration

One of the elements that influences the chance of wound healing is the length of the wound. It is less likely for the wound to heal because it takes so long. There are clear distinctions in the microenvironments of acute and chronic wounds. The chronic wound exhibits a protracted inflammatory phase and a decline in antibiotics medications, both of which prevent it from progressing to the final stage of the wound healing process (Bosanquet and Harding, 2014). For the following reasons, systemic antibiotics are not always beneficial in treating chronic wounds:

Antibiotic resistance: If bacteria are exposed to the same antibiotic repeatedly, they may eventually

become resistant to it. Given that bacteria in chronic wounds can live for months or even years, this is a serious issue.

Antibiotics may have trouble getting to the infection site in chronic wounds because of their frequently poor blood flow. In addition to, Biofilms: Communities of bacteria embedded in a sticky matrix are known as biofilms, and they are frequently formed by bacteria in chronic wounds. Antibiotics have a hard time penetrating biofilms, and they can shield bacteria from the immune system. Lastly, Diabetes and peripheral vascular disease are two examples of underlying medical disorders that are frequently linked to chronic wounds. These ailments may hinder the body's natural healing process and increase the risk of infection(Uddin et al., 2022, Falcone et al., 2021)

1.9.2.1.2 Wound infection

One of the most frequent issues in a chronic wound is wound infection. Colonization causes all wounds to pick up bacteria from the patient's surroundings or the skin around them. Large-scale bacterial colonisation of the injured tissue is thought to slow the healing process. The patient's immune system's health and the variety and quantity of bacterial species found in the wound, however, may have an impact on the severity of the infection. When the patient's immune reaction is beaten back by bacterial proliferation, the wound becomes infected. The immune system's effectiveness is altered by diabetes, age-related illnesses, and obesity, which raises the risk of infection (Siddiqui and Bernstein, 2010).

1.9.2.1.3 persistent inflammation

Chronic wounds are characterised by ongoing inflammation. There is an increase in inflammatory cells such neutrophils, lymphocytes, and macrophages in the microenvironment of chronic wounds. Furthermore, increased neutrophil infiltration is thought to be a sign for chronic wounds and appears to be the cause of persistent inflammation. The overproduction of reactive oxygen species (ROS), which harms the ECM, cell membrane, and causes premature fibroblast senescence, is brought on by an accumulation of neutrophils. Growth factor production is increasing while their bioavailability is decreasing, and neutrophils and activated macrophages are releasing pro-inflammatory cytokines

like IL-1 and TNF-, which leads to the degradation of the extracellular matrix (ECM), hinders cell migration, and lowers fibroblast proliferation and collagen synthesis. Inflammation rises as a result of ECM degradation (Zhao et al., 2016).

1.9.2.1.4 Chronic age-related wound

Chronic age-related wounds may develop as a result of aging stromal tissues and cellular responses that are ineffective. The tissue function starts to decline as we become older. Age-related ECM dysregulation and fibroblast function result in an inability to reduce inflammation (Wall et al., 2008). Fibroblasts are important players in the process of normal wound healing, as was previously mentioned. This type of fibroblast failure has been associated with a significant number of cells experiencing an irreversible cell cycle arrest, also known as replicative senescence with aging.

Additionally, the environment around a chronic wound produces significant levels of oxidative stress and pro-inflammatory cytokines, which speed up telomere shortening and cause premature senescence in fibroblast cells. These are indicators of cellular senescence when the production of cyclin D1 decreases and the level of p21 is altered. this can impact the overall rate of wound healing (Telgenhoff and Shroot, 2005, Henderson, 2006).

1.9.2.2 Role of Senescence in the development of chronic wound

It is well known that, partly due to cellular senescence, older skin is more prone to developing chronic wounds than younger skin. The primary mechanisms by which senescent cells obstruct the healing of chronic wounds (including SASP, ROS, immune system malfunction, and stem cell dysfunction) (Wei et al., 2022). The SASP causes differential gene expression of bioactive mediators such as inflammatory cytokines, growth factors, and ROS in fibroblast senescence, which is still metabolically active. It has been demonstrated that the production of these factors by senescent fibroblasts might encourage the growth of preneoplastic and neoplastic epithelial cells. (Krtolica et al., 2001). Numerous investigations discovered that the transcription of various inflammatory mediators had been upregulated. An immune response is triggered by inflammatory signals, which result in the elimination of defective cells. However, these clearance procedures are harmed in aging tissues,

resulting in strong immune response and sterile inflammation, which in turn causes numerous protracted disease processes (Prattichizzo et al., 2016).

Additionally, through controlling the nearby microenvironment, senescent fibroblasts produce a group of SASPs that have an impact on various aspects of wound healing, including matrix remodelling, angiogenesis, and cell proliferation (Coppe et al., 2008, Acosta et al., 2008).

of the skin, which leads to deregulation in the chronic wound environment.

Pro-inflammatory cytokines (IL1, IL6, and IL8), growth factors, tissue transglutaminase, collagen III, and fibronectin are among the extracellular matrix-related enzymes in SASP. In addition to the high expression of the plasminogen activator inhibitor (PAI-2). These substances affect wound healing by concentrating on NF-κB. SASP generally causes matrix proteolysis and rising inflammation, which are the primary characteristics of aging and diabetes (Wilkinson et al., 2019). It downregulates collagen I, one of the primary structural components of the skin, which causes specific healing anomalies, including keloid formation, hypertrophic scarring, and dysregulation in the chronic wound environment (Wall et al., 2008, Simone et al., 2014).

Fibroblasts play a crucial part in wound healing from the time that inflammation has subsided until the proliferative phase has fully developed the epithelium. They play a vital role in a variety of processes, including the production of various matrix metalloproteinases that break down fibrin clots and the production of a new ECM that contains components like collagen structures, glycoproteins, hyaluronic acid, and heparan sulphate to support other cells involved in wound healing and wound contraction (Bainbridge, 2013).

A damaged ECM is unable to promote keratinocyte migration in chronic wounds. This results in keratin mutations, fibroblast dysfunction, and impaired capillary function, which raises reactive oxygen species levels, damages DNA, arrests the cell cycle, and ultimately results in inadequate epithelization and healing (Harding et al., 2005, Telgenhoff and Shroot, 2005). However, with aging, the ECM is dysregulated, and fibroblast function changes, leading to a failure to resolve inflammation (Wall *et al.*, 2008).

1.9.2.3   Role of Senescence in the Development of Cancer

Overexpression or overactivation of oncogenic proteins result in excessive cell division, which causes cancer. Normal cells release p53 to control the cell cycle in order to prevent excessive proliferation by going through the apoptosis phase or succumbing to senescence (Dimri, 2005). The SASP factors support senescent growth arrest and/or immune surveillance, which together help to reduce cancer (Faget et al., 2019). Proteins like MMP-3, which are secreted by senescent cells, can encourage tumour invasion and metastasis (Parrinello et al., 2005, Zeng et al., 2018).

Additionally, senescent cells release IL-1, an essential SASP initiator and regulator. Through the activation of NF-κB,, IL-1 causes an autocrine inflammatory response that results in the production of IL-6 and IL-8 (Orjalo et al., 2009). These inflammatory cytokines then support the halt of senescence-related proliferation by increasing the formation of reactive oxygen species and maintaining the response to DNA damage (Acosta et al., 2008). Additionally, IL-1 causes paracrine senescence in nearby cells to slow the growth of tumours (Coppe et al., 2010, Jochems et al., 2021). Throughout the various stages of cancer growth, the context, cell type, and other factors have a significant impact on the SASP's effectiveness (Coppe et al., 2010, Jochems et al., 2021).

The parenchyma, the epithelium in healthy tissue, the malignant cells in tumours, and the stroma, a collection of various tissue cells including fibroblasts, inflammatory cells, blood vessels, and matrix proteins like collagen and fibronectin, are all present in tumours. The purpose of the stroma is to support the parenchyma and supply it with nutrients and oxygen (Dvorak, 2015). A change in the stroma in cancer will cause the tumour to invade and spread. To stop the growth, invasion, and metastasis of cancer, therapeutic targeting of the tumour stroma can be made possible by being aware of these alterations (Bremnes et al., 2011, Valkenburg et al., 2018).

Different cell types, including cancer-associated fibroblasts (CAFs), which could be characterised as any fibroblast with carcinogenic potential, are activated in the tumour stroma. By generating cytokines and chemokines, changing the ECM, and otherwise influencing the behaviour of cancer

cells, CAFs play a vital role in the tumour microenvironment (Krtolica and Campisi, 2002, Shiga et al., 2015, Gascard and Tlsty, 2016). Senescence can therefore have either good or negative impacts on the growth of tumours. By halting the growth of the tumour cell, senescence in young people stops the spread of cancer. The replicative senescence of CAFs in older adults creates a milieu that is tumorigenic. Senescence cells are metabolically active, and the SASP affects nearby cells by destroying their ECM, which encourages the growth of cancer. (Schosserer et al., 2017).

Cancer therapy is another reason that could hasten senescence because, as explained in Section 1.1.1.2, senescence is triggered by stress. In both normal and tumour cells, chemotherapy and radiotherapy cause the double strands of DNA to break, which starts a DDR and causes a senescence (Campisi, 2013). Additionally, chemotherapy causes DNA damage that results in SASP release, which prevents neighbouring cells from responding to p53's tumour suppression (Coppe et al., 2008). Senescence, which prevents cancerous cells from proliferating, can help combat cancer, but it can also be harmful to older individuals because it affects the cells around them.

1.10 Therapeutic ultrasound

Ultrasound is simply sound waves which are too high for the human ear to hear. widely used in imaging medicine for medical diagnosis. In 1927, ultrasound was first recognized to produce lasting changes in biological systems. Low-intensity pulsed ultrasound (LIPUS) is a form of ultrasound that is delivered at a much lower intensity (<3 W/cm2) than traditional ultrasound energy and output in the mode of the pulse wave, and it is typically used for therapeutic purposes (Xin et al., 2016). LIPUS can be found to have a rage of biological effects on tissues, including promoting bone-fracture healing (Erdogan et al., 2006, Urita et al., 2013), accelerating soft-tissue regeneration (Zhou et al., 2004, Ikai et al., 2008) and inhibiting inflammatory responses (Nakao et al., 2014).

1.10.1 The physical mechanism of the ultrasound

A sound wave is produced by a source oscillating sinusoidally with time and back and forth in space around its initial position. Ultrasound is the term used to describe sound waves that vibrate at frequencies higher than those typically heard by humans. (Wu and Nyborg, 2008).

Frequency which The number of cycles a particle uses to compress and rarefy in one second is one of important variable could affect the LIPUS stimulation (Xin et al., 2016, Abu-Zidan et al., 2011). Additionally, the ultrasonic wave has the power to vibrate various particles found in extracellular fluids, intracellular fluids, and cell membranes. The ultrasonic beam is yet another ultrasound-related concept. The geographical dispersion of the beam contains both bigger and smaller concentrations of energy (Schortinghuis et al., 2003, Xin et al., 2016)

1.10.2 Low-intensity pulsed ultrasound (LIPU)

LIPUS is a medium-frequency ultrasound (0.7-3 MHz) that emits in the pulse wave mode (100 and 1,000 Hz). It is provided at a significantly lower intensity (30 mW/cm2) than conventional ultrasound energy (figure 8) (Watson, 2008). Nearly all LIPUS researchers conducted their studies using sound waves with an intensity of 30 mW/cm2, a pulse ratio of 1:4, and a frequency of 1.5 MHz. But these variables change based on the tissue being treated (Pounder and Harrison, 2008). For therapeutic purposes, the Pulse frequency is the number of times the devices give the ultrasonic pulses in one second, (Xin et al., 2016).
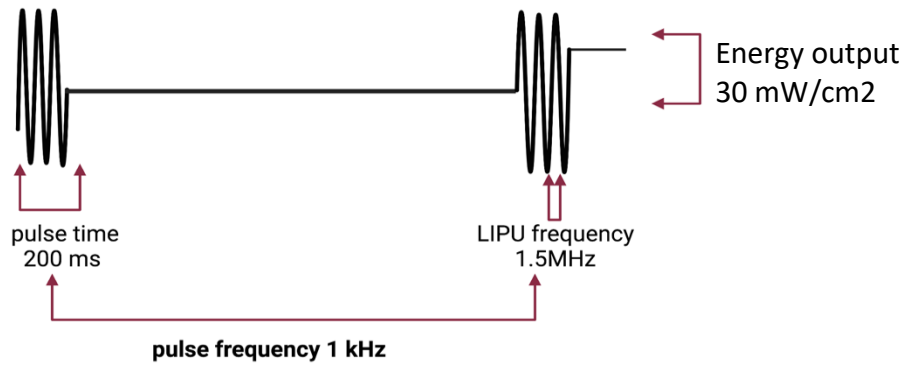
Figure1. 8: low intensity pulsed ultrasound parameter

The LIPU parameters include sound waves that have a frequency of 1.5 MHz, an intensity of 30 mW/cm2, and a pulse ratio of 1:4.

1.10.3 Biophysical effect of therapeutic ultrasound

As the ultrasound waves penetrate the tissues, it causes vibrations in cell membranes and

intracellular and extracellular fluids, which results in the movement of particles in the tissues. When

an ultrasound wave traverses through tissue, the wave energy is absorbed and can result in heating.

This process of energy loss (attenuation) is related to the density of the tissue (Schortinghuis et al.,

2003). Another concept of ultrasound is the Ultrasound beam. The energy within the beam is not

equal in space; it has areas of higher and areas of lower intensity.

The thermal and non-thermal effects are the two main categories of the acoustic vibrations (Baker

et al., 2001). The LIPU has minimal thermal effects because it operates in a low-intensity, pulsed

output mode. As an ultrasonic beam passes through tissues, its energy is reduced, and any scattered

energy from the beam may be absorbed by the tissue. As it passes through the tissues, the energy of

the sound wave causes the particles to vibrate. Due to the increase in molecular vibration, the tissue

may produce greater heat, and the ultrasound may subsequently result in thermal changes in the

tissue (Watson, 2008).. How quickly the temperature rises depends on the density, heat capacity,

and intensity attenuation of the tissue (ter Haar, 1999).

It is believed that therapeutic ultrasound offers non-thermal effects that combine cavitation, acoustic streaming, and micromassage. This different biophysical impact can be considered in conjunction with tissue vibration (ter Haar, 2007). The term "acoustic streaming" refers to the way that sound waves physically affect ions and small molecules. The mechanical pressure of the wave causes fluid to travel only in one direction around and along cell membranes (Nyborg, 1982). Cavitation, in which a sound wave physically influences a small gas present in the fluid, is another component that affects the tissue fluid. The tiny gas bubbles contract and expand as the sound wave travels through the tissue. The cell may suffer damage as a result of this abrupt pressure change. The pulsing of gas bubbles, however, might disrupt cellular activity and alter how the cell works (Johns, 2002). Together, these findings may imply that ultrasonic "injures" the cell, causing growth retardation, and then triggers a cellular recovery response that is characterised by an increase in protein production, as reported by a different study (Webster et al., 1978, Su and Cavaco-Paulo, 2021, Pathak et al., 2022).

1.10.4 LIPU therapy for chronic wound

Due to its capacities for deep penetration to reach deeply seated tissues, the concentration at the site of injury, and low scattering, ultrasound mechanical waves have been created for the treatment of a variety of diseases, including injured skin, malignancies, and bone fractures (Alkahtani et al., 2017).

The LIPU has been successful in treating fracture-related conditions. The LIPUS signal travels through the tissue to the bone, where cells use integrin mechano-receptors to convert this mechanical signal into a metabolic reaction. The cells increase cyclo-oxygenase 2 (COX-2) production, which prompts molecules to improve fracture repair and has demonstrated an increase in healing rate by accelerating mineralisation and bone regeneration (Harrison et al., 2016, Pounder and Harrison, 2008)

In order to treat wound healing, low-intensity pulsed ultrasound (LIPU) is currently being researched. Tissue debridement, inflammation control, moisture balance, and epithelialization of wound margins have all been used to guide the care of chronic wounds (Alkahtani et al., 2017). Because LIPUs are

safer and more economical than conventional treatments, they have been utilised in numerous studies to treat various illnesses. According to many research, LIPU regulates cellular activity, the calcium/CamKinaseII/Tiam1/Rac1 pathways that encourage fibroblast migration (Roper et al., 2015). In addition, it increases growth factors and protein synthesis and decreases the expression of inflammatory cytokines (Alkahtani *et al.*, 2017).

Animal studies have also shown that ultrasound can promote several other activities, including as angiogenesis, collagen deposition, and histamine release. These studies also showed that ultrasound could reduce wound size, hasten wound healing, and speed up in vitro cellular proliferation (Chang, Perry and Cross, 2017).

Therapeutic ultrasound has been linked to a variety of biological effects, both in vitro and in vivo (Johns, 2002). Maxwell et al. (1994) demonstrated that therapeutic ultrasound could affect cell membrane characteristics such as cellular adhesion, membrane permeability, and calcium ion flux (Maxwell et al., 1994, Mortimer and Dyson, 1988). In addition, ultrasound could raise cell proliferation, protein synthesis, and cytokine production, as well as levels of growth proteins (Reher et al., 1999, Doan et al., 1999). These biological changes support the idea that therapeutic ultrasound may improve fibroblast performance, resulting in improved collagen synthesis and matrix repair. Consequently, improve wound health.

According to the results of the randomised controlled clinical trial, LIPU had no discernible impact on pressure ulcer patients (ter Riet et al., 1995). The treatment administered at various stages of the chronic wound may be the cause of the discrepancy in this instance. Smoking and the patient's overall health are two common risk factors associated with chronic wounds that reduce the effectiveness of treatment. When using LIPU as a treatment, these should be taken into account (Reddy et al., 2008).

1.10.5 LIPU therapy for cancer

It is not a novel idea to use ultrasound to treat tumours. Since a long time ago, high frequencies running between 500 kHz and about 3 MHz have been utilised to target tumours with high-intensity

focused ultrasound (HIFU), which uses cavitation to turn mechanical energy into heat and kill tumour cells. This technique's benefit is that it enables real-time visualisation of gas bubbles produced by cavitation and boiling of the targeted soft tissue without damaging the nearby normal cells (Maloney and Hwang, 2015, Kennedy, 2005, Serup et al., 2020).

Sonodynamic treatment, which uses low-intensity ultrasound to generate cavitation formation that facilitates the creation of free radicals that quickly kill cancer cells, has been utilised in several cancer therapy procedures to stimulate cells or affect cell behaviour. which makes some medications that target cancer cells more harmful (Wood and Sehgal, 2015). Using ultrasound to deliver therapeutic materials is known as ultrasound-mediated targeted delivery, which is another way that ultrasound is used to treat cancer. The advantages of utilising such a strategy are taking advantage of ultrasound's therapeutic capabilities and its employment as a courier for medical supplies and using contrast agent such as microbubbles. As ultrasound causes microbubbles to break and accurately release large amounts of loaded pharmaceuticals to tumour locations, maximising treatment efficacy while concurrently minimising drug toxicity, microbubbles are thought to be one of the ideal messengers for therapeutic materials to be employed with ultrasound. The cell membrane is breached during cavitation, which also results in the ultrasonic effect, creating a reversible pore with a diameter of hundreds of nanometers. The outcome may result from the wave pressure that could alter the shape of the cell membrane and encourages substances to enter cells through the endocytosis (Tian et al., 2020, Wang and Zheng, 2019, de Maar et al., 2021). Using ultrasonic contrast agents, microbubbles, and ultrasound-mediated gene transfer are further methods. Small gas bubbles in a fluid grow, oscillate, and then collapse as a result of the ultrasonic waves' cavitation. Cavitation causes cell membranes to become more permeable, allowing nucleic acids to flow passively into the cytoplasm through pores created by cavitation. Ultrasound-induced cavitation effects boost the effectiveness of DNA absorption through cavitation-induced pores when combined with microbubbles. Due to this, gene therapy can be incorporated into cells' nuclei without damaging nearby healthy cells (Krut et al., 2022, Feril, 2009, Wood and Sehgal, 2015).

1.11 inhibition of cellular senescence

The extensive biological impacts of senescence in tissue-aging pathologies make therapy that targets senescence a potential treatment option for many age-related disorders. Many effective methods are being developed to eliminate senescent cells or lessen their negative effects. (Wei et al., 2022). There is different approaches have been developed for targeting senescent cells, either by inducing apoptosis to senescence or by targeting the SASP to prevent it from affecting the surrounding tissue.

1.11.1 Induce apoptosis in senescence cells using drugs (senolytics drugs)

Senescent cells have extremely diverse molecular biology and physiological function; therefore, targeted techniques are needed that, ideally, maintain senescent cells under beneficial conditions while eradicating negative effects. A senolytic medication that can target senescence cell anti-apoptotic pathway, the SRC/tyrosine kinase inhibitor dasatinib (D+Q) and, subsequently, BCL-2 family inhibitors were used in the study to demonstrate the removal of senescent cells. First-generation medications often function by briefly blocking the senescence anti-apoptotic pathway, which causes senescent cells to self-destruct with tissue damaging SASPs. The majority of medications can be administered irregularly using intermittent dosing techniques. Given that senescent cells take many days to aggregate and produce a SASP, the success of this interval dosing strategy is anticipated (Lee et al., 2021, Gasek et al., 2021).

Second-generation senolytics that make use of senescence-related information. Senescent lysosomal cells are the focus. Senescent cells have been demonstrated to increase ß-galactosidase activity and lysosomal mass, therefore they used galacto-oligosaccharide-coated nanoparticles and -galactosidase-activated prodrugs in this method to at least partially eradicate senescent cells (Munoz-Espin et al., 2018). Another strategy is based on the fact that some senescent cells have high levels of lysosomal activity, making them vulnerable to lysosomal ATPase inhibitors. At least some senescent cells rely on glutamine metabolism as a pH-buffering system because of ruptured lysosomal membranes; their susceptibility to apoptosis is increased when this metabolism is inhibited. (Johmura et al., 2021)

1.11.2 Clearance of senescence from tissue (senescence immunotherapy)

Senescence cells can build up in unhealthy tissues with aging and in many chronic diseases, impairing innate and adaptive immune responses. Whether immune system dysfunction fosters senescence accumulation or, conversely, whether immunological dysfunction promotes immune system loss of ability to clear senescence, Other approaches include modifying immunological clearance of senescent cells to reduce the load of senescent cells associated with aging and pathologic diseases (Prata et al., 2018). Senescent cells tend to express specific cell surface proteins more intensely than most other cell types, which led to the development of CAR T cells, vaccinations, and antibody-drug conjugates targeting these cell surface markers. Each method destroys senescent cells, albeit occasionally, they may also harm active macrophages and other non-senescent cell types. Whether these methods preferentially destroy senescent cells with a proapoptotic, inflammatory, tissue-destructive SASP, those with a largely growth-promoting SASP, or both types of senescent cells, is not yet known (Amor et al., 2020, Yoshida et al., 2020).

1.11.3 SASP inhibitors (Prevent SASP from affecting the surrounding tissue)

Suppressing the SASP without eliminating senescent cells is an alternative therapeutic approach for alleviating cellular senescence-related phenotypes or diseases and preventing the SASP from affecting surrounding tissue. SASP inhibitors (senomorphics) can directly or indirectly attenuate the SASP of senescent cells by inhibiting transcription factor nuclear factor (NF)-κB, the JAK–STAT signal transduction pathway, the serine/threonine protein kinase mTOR, mitochondrial complex-1-related or 4-related targets, or other pathways involved in the induction and maintenance of the SASP (Tilstra et al., 2012, Moiseeva et al., 2013).

SASP cytokines and chemokines that promote inflammation can be decreased by NF-B inhibitors, which mediate the cell response to inflammation. Targeting alternative splicing in senescent cells may be a workable strategy for suppressing the SASP, according to an RNA-mediated interference screen. Rapamycin appears to increase the health span of mice by inhibiting mTOR and suppressing the SASP (Georgilis et al., 2018).

SASP inhibitors have the potential to suppress both the proapoptotic, inflammatory, and tissue-destructive sets of SASP factors, as well as the growth-promoting set of SASP factors. However, most SASP inhibitors require ongoing administration to maintain suppression of the SASP, though some can have lasting effects after only a short course of administration (Mannick et al., 2018, Chaib et al., 2022).

1.12 Importance of topic in the search field

Numerous chronic disorders, such as myocardial infarction, Alzheimer's, strokes, increased cancer, and lung and bone dysfunctions, have been related to aging and cellular senescence. Additionally, it is the cause of several age-related disorders, such as frailty, which increases the likelihood of developing dementia, sarcopenia (loss of muscle mass), urinary incontinence, and difficulties with memory and concentration (cognitive impairment). Finding a method to either lessen or eliminate the burden of senescence is necessary to avoid aging-related illnesses, extend life, and improve quality of life as one age because senescence leads to numerous age-related pathologies. As was mentioned in section 1.5, senotherapy helps to either reverse senescence or inhibit SASP, protecting the surrounding tissue from the pro-inflammatory damage induced by SASP. As studies have performed on ability of LIPU in treating chronic wound as mentioned in section 1.6.4 therefore the subject of how LIPU influences fibroblast senescence is brought up by focusing on the function of senescence in the development of chronic wounds and the benefits of LIPU in treating such circumstances due to its biophysical action. Using a procedure like this is a simple, safe, and affordable choice. It will be more likely that this method will be employed to treat chronic wounds if LIPU has a good impact on fibroblast senescence in those tissues. SASP and fibroblast senescence are characteristics that both cancer and chronic wounds share. CAF senescence might benefit by the use of this low-intensity ultrasound technique. Any beneficial effect on secreted SASP can protect the surrounding tissue from DNA damage caused by chemotherapy, which will enable for innovative combination therapy. As the SASP can induce senescence in surrounding tissue in addition to the negative effect of these secreted proteins in developing cancer.

1.13 hypothesis

I hypothesise that low-intensity ultrasound will modulate senescence and may prove beneficial for

treating chronic wounds. Therefore, this project aims:

1.13.1 Aim

1- To test whether LIPU has any effect on senescence markers in skin fibroblasts and alters the

   secretory phenotype (SASP).

2- To ascertain whether LIPU shields healthy cells from the senescent damage brought on by

   chemotherapy, which would enable the development of novel combination therapies.

Chapter2
Materials and Methods

2 Materials and Methods

2.1 Cell culture

Non-transformed (primary) human foreskin fibroblasts (HFF's) were used for the study as they undergo replicative senescence which is essential for this study. HFF's were purchased from ATCC the consent for which is detailed in Amit et al 2003 (Amit et al., 2003) . The HFF cells (passage numbers 22–28) were cultured at 37° with 5% CO_2. They maintained in their media (DMEM D5796 from sigma) supplemented with 10% Foetal bovine serum (FBS) Gibco by Life Technologies 10347-028 and 20mM L- glutamine, 10 mM HEPES purchased from Sigma-Aldrich (RNBJ9567) and 20 µg/ml gentamycin. The confluent cells were washed with Dulbecco PBS (without $MgCl_2$ and $CaCl_2$) (PBS) purchased from Sigma-Aldrich (#B8537). They were then incubated with 5ml Trypsin-EDTA (0.05%) Gibco by Life Technologies 25300-062 for 5 minutes until the cell detached for flask service. The detached cells were collected in falcon tubes then centrifuged at 1500 rpm for 5 minutes. Cell pellets were resuspended in their media and split into culture flasks containing fresh culture media at 1:2 or 1:4 ratio every three days.

2.2 Effect of LIPU stimulation on senescent cell

2.2.1 Senescence induction

HFF were seeded in 24-well plates at 5×10^4 per well for senescence induction or 2×10^4 for treatment comparison. Senescence was induced using H_2O_2 or cisplatin at concentrations and for durations summarised in Table 2-1.

	Concentration	Treatment time with senescence inducer	Supplier	Catalogue number	LIPUS treatment time
Cisplatin	2μM	24 H	Sigma	PHR1624-200MG	Start after washing the treatment used to induce senescence in HFF cells for 3 Days 20 minutes each day
	5μM	24 H			
	10μM	24 H			
	50μM	24 H			
H$_2$O$_2$	100μM	1 H- 2H	Sigma	SZBF1960V	
	200μM	1 H- 2H			
	500μM	1 H- 2H			
	700μM	1 H- 2H			

Table 2-1 treatment time and concentration for senescence inducer in HFF cells.

HFF cells have been exposed to Cisplatin and H$_2$O$_2$ at varying concentrations and treatments to cause senescence.

.

2.2.2 Low-intensity pulsed ultrasound (LIPU) stimulation

The water-based gel was used to connect cells in culture to a 2.5-cm diameter ultrasound transducer (Smith & Nephew). The transducer produced 30mW/cm2 (spatial average, temporal average) pulsed ultrasound with a 1.5-MHz wave frequency, pulsed at 1 kHz, 20% duty cycle, for 20 minutes during three days of stimulation experiments as mentioned in. The plates containing the treated and untreated cells were subjected to LIPU separately at following order plate, gel, LIPU. Control and stimulated samples were kept on different plates to minimise crosstalk and prevent indirect stimulation through sound transmission. Notably, to reduce the possibility of confounding variables, control plates were handled in exactly the same way as stimulated samples—the LIPU stimulus was not present. (Roper et al., 2015) (illustrated figure 2.1).
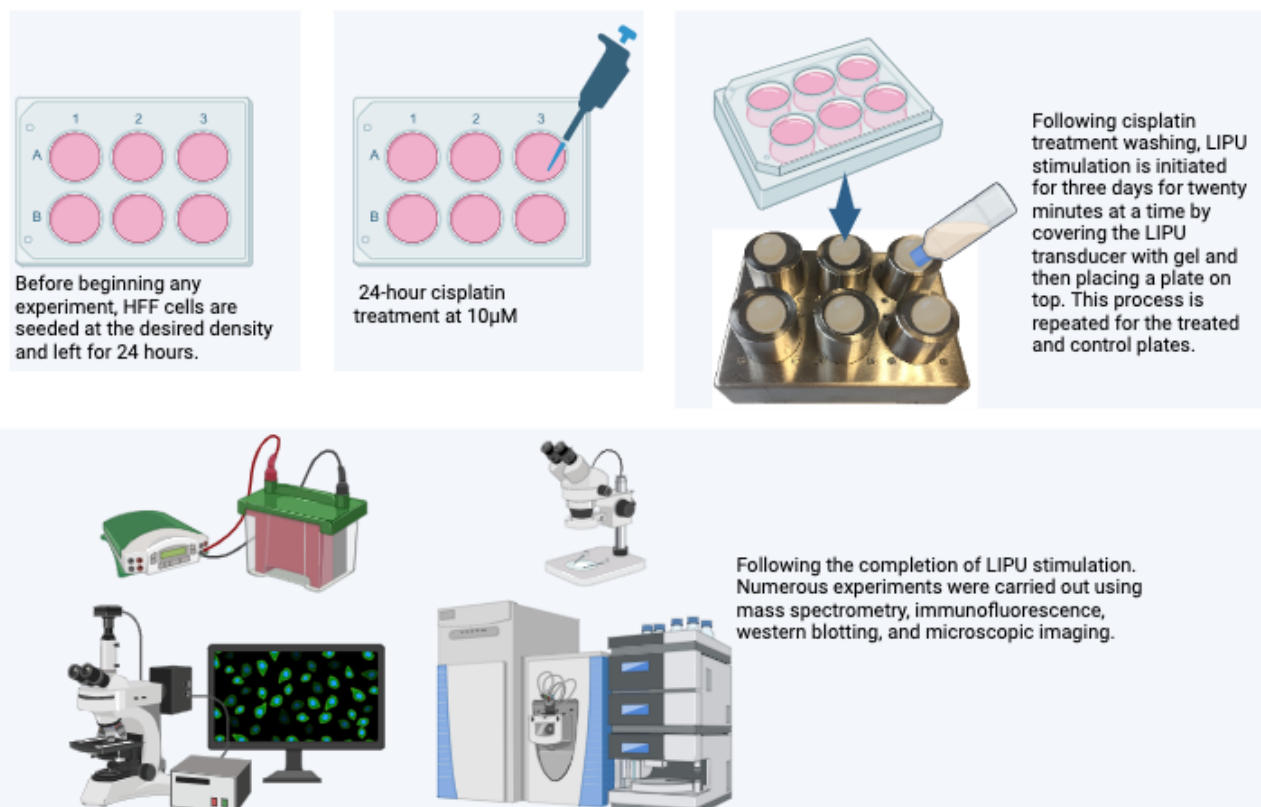
Figure 2.1 LIPU experimental method

The following timeline is followed when creating the experiments: After the cells are seeded for 24 hours, the cells are treated with cisplatin for another 24 hours. Next, after washing the cells. both treated plate with cisplatin and untreated plate undergo LIPU stimulation, which lasts for 20 minutes for three days, following which the desired experiment is conducted. image generated using BiorRnder website.

2.3   Senescent cells detection

2.3.1   Beta- galactosidase assay

A beta-galactosidase assay was first used to detect and identify the senescence cells, which detects

senescence-associated beta-galactosidase (b- gal) activity at PH 5-6, as it is the standard marker for

identifying senescence cells. This experiment was conducted using six well plates and the number of

cells was 8 x 10^4 cells per well for untreated HFF and for US treated HFF and 1.5 x10^5 for cisplatin-

treated and cisplatin with US samples. The LIPU stimulation was performed 20 minutes daily for three days. The cells were washed twice in PBS-, Then, fixed with 4% paraformaldehyde for 5 min at room temperature. They were washed three times in PBS-. Each time 20ml of b- galactosidase staining solution was made freshly according to (Wang et al., 2013) by mixing 4 mL of Citric acid/sodium phosphate buffer at pH 5.0 or 6.0: by mixing 0.1 M citric acid solution to 50 mL of 0.2 M sodium phosphate solution until the pH reaches 6. Then add 100 µl of 200 mg/mL X-gal solution. And add 1ml 100 mM potassium ferrocyanide and 1ml 100 mM potassium ferricyanide. Next, add 600 µl of 5M NaCl, 40 µl 1 M magnesium chloride and 13.26 mL distilled deionized water see table 2-2 for the prepared solution. Add 2 mL of staining solution to each well on the six-well plate and incubate at 37°C without co2 to avoid crystallisation overnight. The image was captured using a Dino-Lite camera.

Table 2-2 the solutions used to make up the beta-β galactosidase staining solution

List of buffer and solution method of preparing ß galactosidase staining

Buffer/solution	Chemical composition	Catalogue number
4% PFA	4g of paraformaldehyde with 100ml of PBS- and 4 drops 2.5 M NaOH heat and stir until it dissolves	GPR 294474L
Citric acid	2.1 g citric acid monohydrate in 100 mL distilled deionized water.	Sigma SLBM6080V
Add sodium phosphate	2.84 g/100 mL sodium phosphate dibasic	Afa-Aesar 10186427
200 mg/mL X-gal solution	100 mg X-gal powder in 0.5 mL dimethyl-formamide (DMF)	Cambridge Bioscience # 2671-1G
100mM potassium ferrocyanide	2.12 g in 50 mL distilled deionized water.	Sigma 2033832
100 mM potassium ferricyanide	1.65 g in 50 mL distilled deionized water.	Sigma # 244023-5G
5M NaCl	14.61g in 50 mL distilled deionized water.	Fisher chemical 2033832
1 M magnesium chloride	10.17 g in 50 mL distilled deionized water.	Fisher chemical S271-500

2.4 Immunofluorescence Analyses for DNA Damage

2.4.1   2.4.1 ɣ-H2AX staining

To understand the severity of DNA damage caused by using chemotherapy and ultrasound effect on the DNA damage caused by chemotherapy, Ɣ -H2AX staining was performed. Cells were seeded in 24 well plates on coverslips, at 3×10^4 cells per well for treatment with 10µM of cisplatin or 1×10^4 cells for untreated well. Cells were stimulated with LIPU as described in section 2.2. The staining was performed as explained in (Wang et al., 2013). Briefly, cells on the coverslips were washed once with TBS, before fixing for 10 minutes at room temperature with 4% paraformaldehyde. Wash with PBS- then permeabilize cells on coverslips for 5 minutes at room temperature with 0.2% Triton X-100. Coverslips were washed three times

with TBS at room temperature for five minutes each time. Coverslips should be incubated in a blocking buffer (5% bovine serum albumin (FBS) in PBS-) for 2 hours at room temperature. Dilute the main antibody Ɣ-H2AX in 5% FBS 1:1000 overnight in 4°Wash all coverslips six times for five minutes each time. Incubate coverslips for 45 minutes at room temperature in the dark with suitable dilutions of fluorescence-labelled (DAPI) as secondary antibody 1:15000 in PBS-. After that, the coverslips were washed twice with PBS- and then cleaned with distilled water before being mounted with ProLongTM Gold Antifade mounting media with DAPI (Thermo Fisher #P36931) (tables 2-3 & 2-4). Then, inspected with Widefield microscope (Camera-based microscopy systems). The image analyses were performed using cell profiler 4.2.0 software (Speckle Counting pipeline).

Table 2-3 the solutions used in Ɣ-H2AX	
Method of solution used to prepare γ-H2AX staining	
Buffer/ solution	Chemical composition
Permeabilization buffer	10X PBS- Distalled water Triton 100X
Blocking buffer	5% FBS PBS-

Table 2-4 List of the antibodies used in staining				
The antibodies used for γ-H2AX assay				
Antibodies	Antibody source	Concentration	Supplier	Catalogue number
Ⴤ-H2AX	Rabbit	1:1000	Cell Signaling	9719S
DAPI	fluorescent dye	1:1000	Boster Bio	AR1176

2.5   Immunoblotting (Western blotting)

In a clean microcentrifuge tube with an equal volume of SDS-PAGE protein loading buffer, 10 to 20 µl of the supernatant from the samples was transferred after they had been briefly spun down. Before loading, each sample was heated for 10 minutes at 850C. Before loading with 1X BoltTM MES SDS running buffer onto NuPAGE® 4-12% Bis-Tris protein gels (12 wells). The Page Ruler TM Plus Prestained Protein Ladder was employed as a molecular weight standard. The gel was operated for 22 minutes at 200 volts. Following SDS-PAGE separation, materials were transferred from the gel to a 0.45 m Nitrocellulose membrane using a micro blot module for 90 minutes at 30 volts. Following protein transfer, the nitrocellulose membrane was blocked for 60 minutes on a rocker at room temperature with 1X casein diluted in 1% TBS- Tween-20. The blocked membrane was incubated overnight at 4°C on a rocker with a suitable primary antibody diluted with the same blocking solution see table 2-5. The membrane containing the primary antibody was washed for 15 minutes with TBS-Tween-20 (3 times with 5 minutes/wash) and incubated for 30 minutes at room temperature on a rocker away from light with fluorophore-conjugated secondary antibodies diluted in 1X casein containing 1% TBS-Tween-20 (table 2-6). The immunoblotted proteins were detected using the Odyssey infrared imaging system (700 nm and 800 nm channels, 100 um resolution) after being washed 3 times with TBS-Tween. Digital-densitometric analysis was used to determine band intensity using a free edition of LI-COR Image StudioTM then to analyse the Image StudioTM Lite was used. A housekeeping protein standardisation was used to correct for loading within an experiment and fold

changes were normalised to the average of datasets with similar treatments between experiments

to guarantee reliable comparisons between different experiments. An Excel software was used to

scaled the finding intensity throughout the entire gel and adjusted to the loading control (GAPDH).

Table 2-5 list of solutions used in immunoblotting.
The methods of solution used in western blotting (All solutions were made up in distilled water unless otherwise specified)

Buffer/solution	Chemical composition
Tris-buffered saline (TBS) pH 7.4 using HCl	100mM Tris-Base 140mM NaCl
TBS-Tween	1X TBS + 0.1% (v/v) Tween-20
1X Low molecular weight protein transfer buffer pH 8.0	192mM Glycine 25mM Tris-Base 10% Methanol
Western blot lysis buffer	10% Glycerol 20mM HEPES 140M NaCl 1% NP40 0.5% Sodium Deoxycholate 4mM EGTA 4mM EDTA 0.1% SDS 1X complete protease inhibitor (purchased from Roche #11697498001) 10X Phosphostop inhibitor (purchased from Sigma #4906837001)
SDS-PAGE protein loading buffer	0.1M Tris-HCl, pH 6.8 15% Glycerol 2% SDS

	0.01 Bromophenol Blue

Table 2-6 list of antibodies used as primary in immunoblotting				
List of primary and secondary antibodies used in immunoblotting				
Primary Antibodies	Antibody source	Dilution	Supplier	Catalogue number
P21 waf1/cip1	Rabbit	1:2000	Cell Signaling	2947S
P16 ink4a	Goat	1:1000	R&D	AF5779
CLIC4	Rabbit	1:1000	Cell Signaling	D2A7D
GAPDH	Rabbit	1:5000	Cell Signaling	2118S
Secondary antibodies				
goat anti-rabbit 800	Goat	1:1000	Abcam	ab205718
Donkey Anti Rabbit	Donkey	1:1000	Abcam	ab205722

2.6 The ultrasound effect on the secretory phenotype of senescent cells (SASP)

2.6.1 Paracrine effect

As a result of the paracrine impact, SASP affects neighbouring cells by enforcing cell senescence.

Following the treatment of the cells as indicated previously, the medium from various conditions was

taken and centrifuged for 5 minutes at 1500 rpm before being filtered through a 0.2 filter. Then, at a

density of $1x10^5$, new cells were plated 1:1 of harvest media, and a new medium was added to the

cells, which was left for 5 to 6 days. Then, using p21 as the primary antibody, immunoblotting was

conducted.

2.6.2 Interleukin 6 ELISA

An IL6 Assay was done by plating 1.5 $x10^5$ cells per well to assess the level of IL6 after treatment with

the senescence inducer. After preparing the samples as indicated earlier, the samples' medium was

collected and analysed using the Bio-Techne D6050 Human IL-6 Quantikine ELISA Kit. According to

the kit protocol, 100µ of the sample was mixed with 100µl of the diluent assay RD1W and incubated for 2 hours at room temperature in the 96 well plates included with the kit. After that, wash it three times with washing buffer. After that, each well-received 200µl of human IL6 conjugate was incubated for 2 hours. In addition, the wells were washed four times with a washing buffer. A substrate solution is added and incubated at room temperature for 20 minutes in the dark. The stop solution was then added. The plate was scanned with a plate reader at 450nm and 540nm for correction.

2.6.3 Mass spectrometry

2.6.3.1 Sample preparation

We prepared the sample by seeding confluent cells for all condition in rich media as indicated in Section 2.2 (DMEM# 596) (figure 2-2). Conditioned media was harvested and a protease cocktail 1:200 was added as soon as harvested (Sigma #109M4068V). Samples were stored at

-80°C until S-trap digestion. The samples were concentrated by centrifuging through amicon filters with a 3 KDa cut-off (Merck #ufc900324) down to 250µl at 4000g. The flow-through was stored at -20°C for future use.
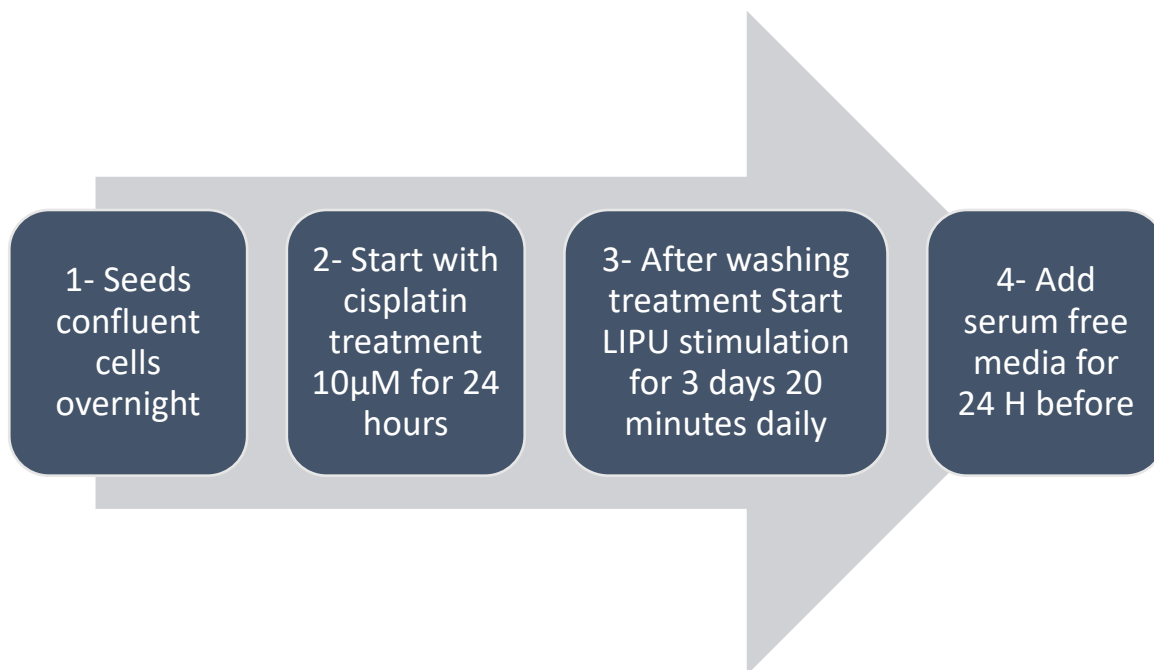
Figure 2.2 timeline of preparing the sample

The following timeline is followed when creating the experiments: After the cells are seeded for 24 hours, the cells are treated with cisplatin for another 24 hours. Next, after washing the cells they undergo LIPU stimulation, which lasts for 20 minutes for three days, then incubate the cells with serum free media for 24 hours and conduct the mass spectrometry

After that, the samples were normalised by volume, and S-trap digestion was performed using volume 25µl/µg of the concentrated media (our samples). The samples were mixed with an equal volume of S-trap lysis buffer containing 20% SDS (Sigma-Aldrich, 05030), 50mM M of Triethylammonium bicarbonate (TEAB), pH 7.55 (Thermo fisher, 90114). And centrifuge for 8 minutes at 13000 g.

1mM of TCEP was added to the samples (Merck, 646547). The samples were heated in a at 70°C for 15 minutes. Then incubated in the dark for 30 minutes at 37°C after being alkylated with 0.5 M of iodoacetamide ((IAA) Merck, I6125) to a final concentration of 5 mM.

After that, the samples were acidified with phosphoric acid at a concentration of 1.2%.

S-trap binding buffer (90% MeOH, 100 mM TEAB, pH 7.1) was added to the acidified lysate. After loading 165µl of sample into the S-trap columns (Protifi, C02), the samples were centrifuged at 4000 x g for 30 seconds to pass through the S-trap. After that, the S-trap was washed three times with 150 µl of binding buffer before being transferred to a clean 2 ml Eppendorf tube. At ratio 1:10, the MS grade trypsin (90058) diluted in 50 mM TEAB buffer. Air bubbles were avoided by gently adding 50µl

of trypsin in TEAB buffer to the samples. Parafilm was used to seal the S-trap then incubated for 1 hour at 47°C without shaking. The peptides were then eluted by passing 40μl of 50 mM TEAB, 40μl of 0.2% of aqueous formic acid (Fisher Chemical, A117-50), and 40μl of 50% acetonitrile containing 0.2% aqueous formic acid through the s-trap, then centrifuge at 4000 g for 30 seconds before adding the next buffer. Dry down the peptides by centrifuging in an Eppendorf SpeedVac for 60-90 minutes at 45°C with the Eppendorf tube lids open to allow for evaporation. After drying the samples, the peptides were resuspended in 0.5% formic acid and vortex mixed for 10 minutes at the lowest speed. The orbitrap was then used to inject the samples into labelled polypropylene vials (Thermo Scientific #160134) and perform the LC-MS/MS analysis.

2.6.3.2   LC-MS/MS analysis
This analysis done by mass spectrometry department at the university of Sheffield.

An Orbitrap Elite (Thermo Fisher) hybrid mass spectrometer equipped with an easy spray source, connected to an Ultimate RSLCnano LC System, was used to analyse 18μl of each sample utilising nanoflow LC-MS/MS (Dionex). The Orbitrap Elite was run with one MS (in the Orbitrap) acquired at a resolution of 60,000 at m/z 400, with the top 20 most prevalent multiply charged (2+ and higher) ions in each chromatographic window subjected to MS/MS fragmentation in the linear ion trap.

2.6.3.3   Mass spectrometry data analysis (MaxQuant)
MaxQuant version 1.6.10.43 was used to analyse all raw mass spectrometry data also done by mass spectrometry department the university of Sheffield. The following search parameters were used to cross-reference the data against a human UniProt sequence database (June 2015): Trypsin/P digestion with a maximum of 2 missed cleavages, variable methionine oxidation and N-terminal protein acetylation, fixed cysteine carbamidomethylation, a match between runs enabled with a match time window of 0.7 min and a 20-min alignment time window, label-free quantification allowed with a minimum ratio count of 2, a minimum number of neighbours of 3 and an average number of neighbours of 6. For FTMS scans, a 20ppm initial search precursor tolerance and a 4.5ppm main search precursor tolerance were employed, while ITMS scans had a 0.5 Da tolerance. Identification level cut-offs were set at a protein FDR of 0.05 and a peptide FDR of 0.05.

2.6.3.4 Bioinformatic Analysis (Perseus)

All LFQ intensities were set as primary columns in Perseus version 1.5.6.0 after loading the MaxQuant output. The matrix was filtered to exclude all potentially contaminating proteins, which were only recognised by their site and reverse sequences. The log2(x) default function was used to modify the LFQ intensities. Rows were systematically annotated with their condition names to categorise experimental conditions. Filtering rows based on valid values in at least one group with a minimum of 4 repeats for statistical analysis removed rows with no LFQ intensities in all categorised categories. Outliers were removed after the data was shown using multi-scatter plots and Pearson's correlation analysis. The missing values were randomly imputed with a width of 0.3, and a downshift of 1.8 from the standard deviation after the data were normalised by subtracting column medians. Two-sided Student's t-tests with a permutation-based FDR calculation (FDR = 0.05) with an (S0) =0 were used to identify

quantitatively enriched proteins between groups. The data was then saved to an excel file, then imported into GraphPad Prism to construct the figures and graphs shown.

2.7 Cell number variation

We decided to vary the seeding density of cells in each experiment for a number of reasons. First of all, we needed to reach the endpoint of the experiment with the same amount of cells. Chemotherapy has been shown to slow and ultimately arrest the cell cycle (Wahba et al., 2018), therefore to achieve similar numbers at the endpoint, different numbers were needed at the start. Second, contact inhibition brought on by the cell confluency may have an impact on the degree of the p21 expression, so it was necessary to avoid cells becoming confluent at any point in the experiment (Leontieva and Blagosklonny, 2014, Siavoshian et al., 1997). Additionally, the confluent cells influence the SA—Gal staining by producing misleading positive results (Cazin et al., 2017). The HFF may experience some replicative senescence, as the passage number we employed may be high for primary cells. We observed an elevation in the senescence markers we evaluated in the untreated HFF (Magalhaes et al., 2022, Guerrero et al., 2021)

2.8 Statistical analysis

GraphPad Prism 8 software was used to perform statistical analysis on the data. When applicable, the student's t- test was used to compare two samples with uneven variance. To reach the mean of more than two samples within the same experiment, a one-way analysis of variance (ANOVA) and two way analysis of variance were used, along with Tukey's multiple comparisons test for post hoc comparisons. Significant was defined as a P value of less than 0.05. In all instances, error bars indicate standard deviation.

Chapter 3

The ultrasound effect on the

fibroblast senescent

3 The ultrasound effect on the fibroblast senescent

3.1 Introduction

As previously stated, cellular senescence involves not only irreversible growth arrest but also a wide range of other cellular processes, such as the activation of anti-proliferative molecules, modifications to the cell's secretome, changes to chromatin and chromosome instability, control of tumor progression, telomere shortening, as well as a wide range of biological processes, such as tissue repair, wound healing, embryonic development, organismal aging, and age-associated dysfunction (Resnik, 2020). Senescence affects old tissue because it is metabolically active, which promotes many diseases like persistent wounds and tumor invasion.

The chronic wound is typically accompanied by changes at several stages, such as prolonged inflammation and reduced immune cell function/signalling, increased cellular senescence, as well as postponed re-epithelialization, re-vascularization, granulation tissue creation, and wound closure (Vu et al., 2022, Bonham et al., 2020).

Low intensity pulsed ultrasound (LIPU) has been utilised in numerous studies to treat issues related to wound healing. According to LIPU, controlling cellular activity, the calcium/CamKinaseII/Tiam1/Rac1 pathways that encourage fibroblast migration, increasing growth factors and protein synthesis, and lowering inflammatory cytokine expression can all help improve wound healing (Alkahtani et al., 2017, Roper et al., 2015). Since fibroblast senescence is a factor in the development of chronic wounds and LIPU has been found to be effective in treating them, this chapter's investigation will be on how LIPU affects fibroblast senescence.

3.2 Aim

Using LIPU, it will be tested whether senescent skin fibroblasts' proliferation can be recovered. as well as to ascertain whether the use of LIPU shields healthy cells from the senescent damage brought on by chemotherapy, which would enable the development of new combination therapies.

3.3 Senescence induction

Creating a reliable senescence test is the first stage of project design. First, select an inducer of premature senescence in cultured HFF (human foreskin fibroblast). Because they originated from

primary human fibroblast cells, this cell line was chosen. We've decided on The HFF that has been subjected to oxidative stress brought on by exposure to hydrogen peroxide (H_2O_2) and chemotherapeutic medication cisplatin.

In order to induce senescence in the HFF cells while preventing cell apoptosis, the ideal dose concentration and treatment duration must be chosen as the initial stage in developing the experiments for this project. The ideal experimental conditions were found by culturing 1.0×10^5 cells in a six-well plate and subjecting them to various cisplatin concentrations for a range of treatment periods. The ideal treatment regimen is illustrated in figure 3.1.

The 'gal assay' was used to find the 'galactosidase' linked to senescence in order to identify senescent cells. A 48-hour incubation period was spent utilising the gal staining solution made as described in (Wang et al., 2013) at PH 6.. A Dino-Lite Microscope Camera captured the image, and the senescent cells were manually counted. The percentage was determined by dividing the number of stained cells by the total number of cells and multiplying the result by 100. The dose and treatment duration we employed to induce senescence are displayed in Table 1.3. After experimenting with various timeframes and doses, we have found that cisplatin dose 10μM causes senescence in 71% of HFF cells after 24 hours. Also, we detected a change in cell morphology (the cells enlarge and become flattered). In addition, 17% of HHF cells were found to be senescent and untreated. Due to the cells' age and passage number, which may have caused some replicative senescence, this percentage was slightly higher than anticipated. which is believed to be brought on by the telomere, the protective caps on the ends of chromosomes, shortening, according to Hayflick's limit. Every cell division causes the telomeres to get shorter; when this happens, the cell can no longer divide and enters senescence (Hayflick and Moorhead, 1961). The outcome is in line with the existing literature in section 1.1.1.2 demonstrating how chemotherapy drugs like cisplatin can harm DNA and accelerate aging (Yip et al., 2006, Lee et al., 2006).

Another putative senescence inducer was investigated at a 33% concentration of H_2O_2. Again,

different concentrations and various treatment durations were looked at to determine the ideal treatment duration (figure3.2). The findings suggested that H_2O_2 is more deadly to cells than cisplatin. H_2O_2 was thus removed, and in the experiment that followed, cisplatin 10μM for 24 h was used as the senescence inducer. This dose was utilized in order to shorten experiment times.

2μM cisplatin

5μM cisplatin

10μM cisplatin

50μM cisplatin
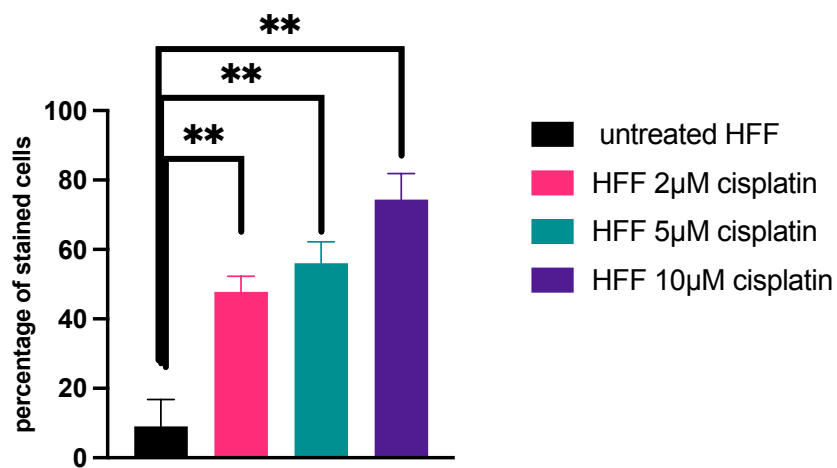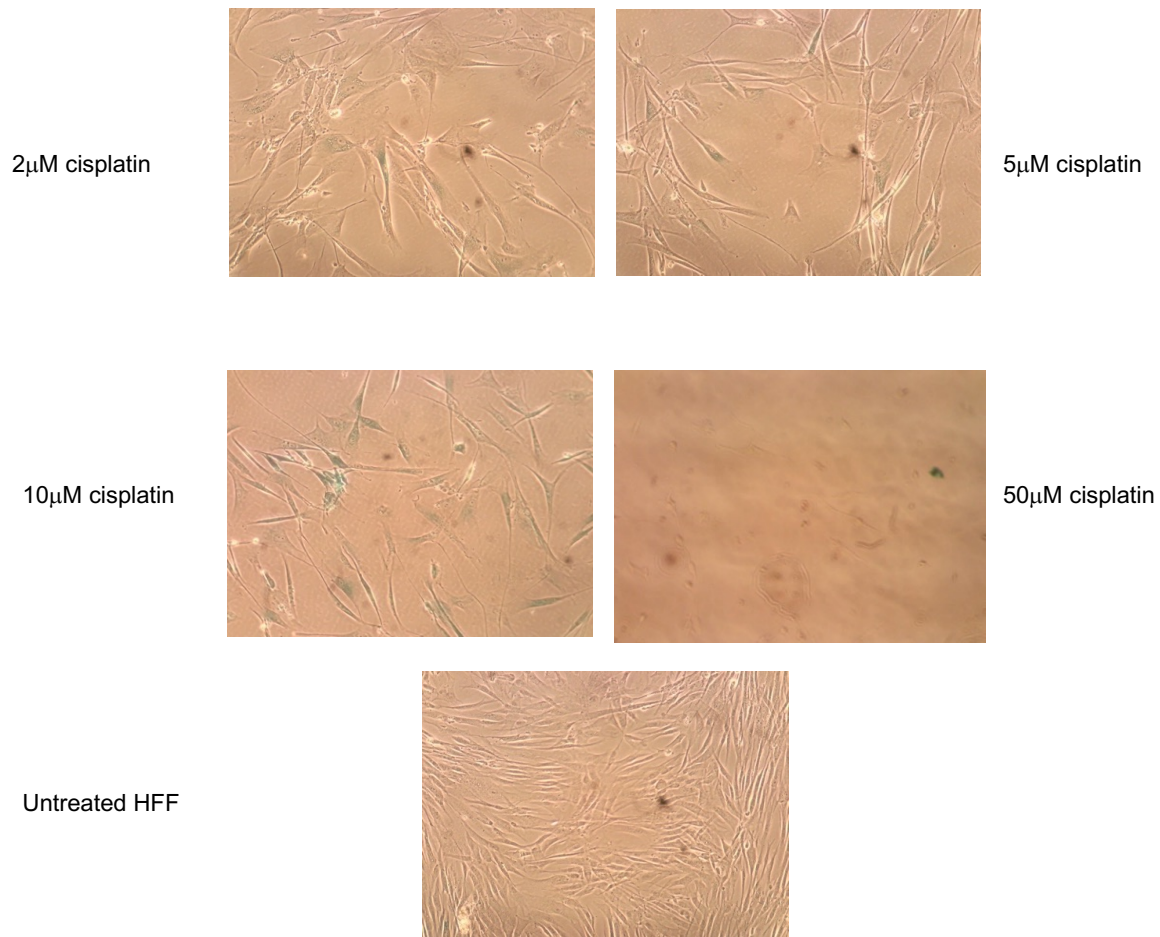
Untreated HFF

Figure 3.1: images showing cisplatin inducing HFF senescent at different concentration after 24H of treatment.

Comparing to untreated HFF 2μM of cisplatin seems to induce senescent in 52% of HFF cells (pink), while the 5μM induce senescent in 63% of HFF cells (green), and finally 10 μM seems to induce senescent in 89% of HFF cells (purple). 50 μM cisplatin was tested but was toxic to the cells. The senescent cells were manually counted, and percentage obtained by dividing stained cells over total number of cells multiply by 100 (n=3 across independent experiments) ($P < 0.05$).

A)
1H treatment

100μM H₂O₂ ... 200μM H₂O₂

500μM H₂O₂ ... 700μM H₂O₂

Untreated HFF

B)
2H treatment

100μM H₂O₂ ... 200μM H₂O₂

500μM H₂O₂ ... 700μM H₂O₂

Untreated HFF
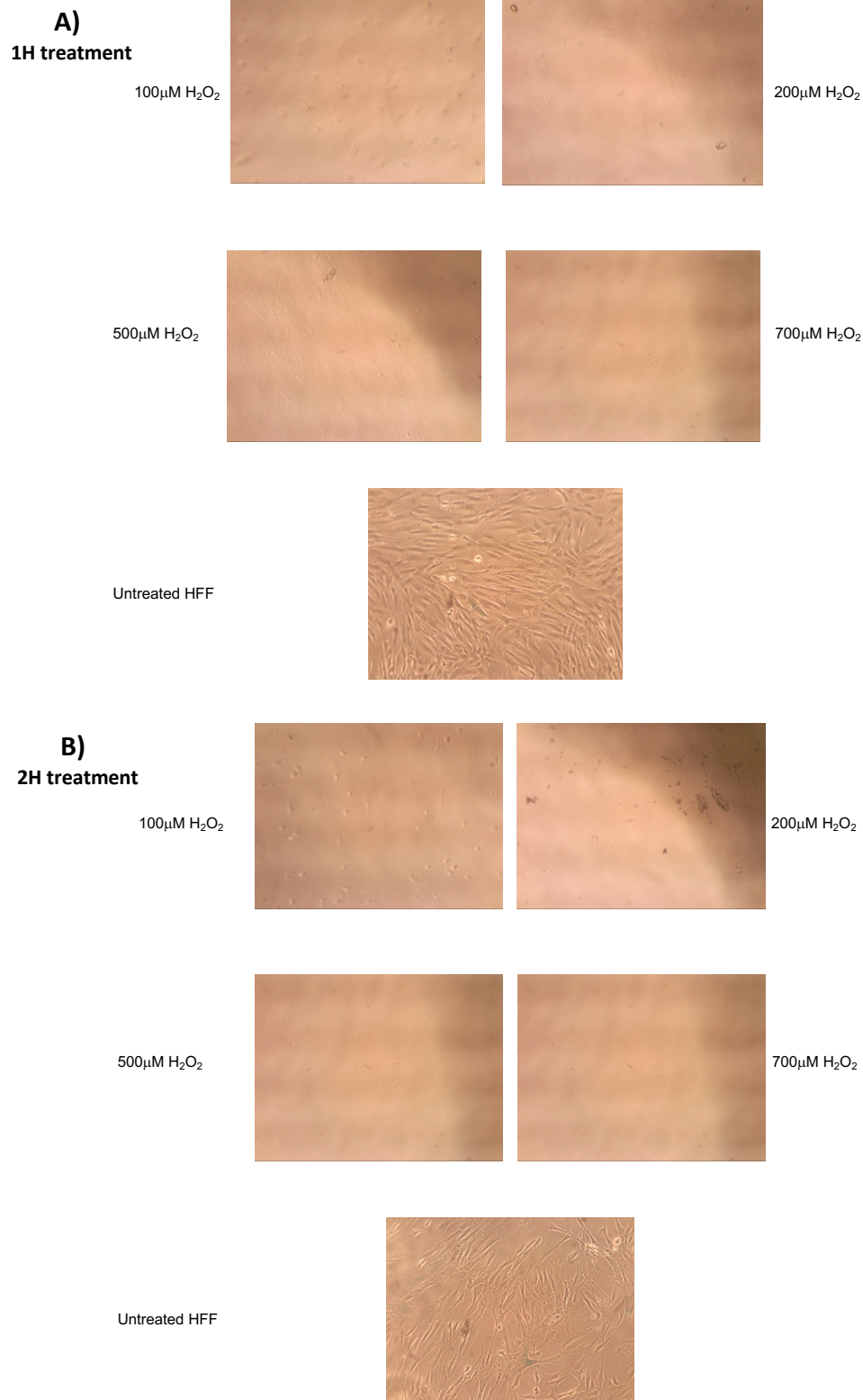
Figure 3.2: H₂O₂ treatment for inducing senescent in HFF cells.

A) showing the different concentration of H_2O_2 (100,200,500 and 700 μM) for 1 hour. B) showing the different concentration of H_2O_2 (100,200,500 and 700 μM) for 2 hours. Owing to H_2O_2's intrinsic cytotoxicity, cells die before a discernible BGal signal is seen. (n=3 across independent experiments).

3.4 Low Intensity pulsed Ultrasound stimulation (LIPU)

With the use of a specially designed device made by Smith & Nephew, we were able to perform LIPU stimulation over six-well plates. The system consists of six emitters that generate ultrasonic waves with the following characteristics: a total output of 30 mW/cm, a frequency of 1.5 MHz, an amplitude of 150 mVpp, and a pulse repetition rate of 1 kHz with a 20% duty cycle. Which Nearly all LIPUS researchers conducted their studies using same parameters (Pounder and Harrison, 2008, Erdogan et al., 2006, Katano et al., 2011, Urita et al., 2013, Jang et al., 2014, Nakao et al., 2014) The gel was utilized as a connector to help the sound wave travel and get to the plates. Each experiment was conducted on two plates, one of which had a row that had been exposed to 10 µM cisplatin for 24 hours, and the other did not. To ensure that the treatment had an immediate impact on the treated cells, one plate underwent LIPU stimulation right after washing the cisplatin treatment, while the other served as a negative control plate. To investigate the LIPU effect and determine the ideal treatment period, we used the P21$^{wafa1/cip1}$ protein level as a senescent marker by using western blot as stated in section 2.5. According to figure 3.3, we discovered that at day 3, the elevated P21 expression induced by cisplatin was reduced by LIPU. Moreover, the literature also indicates that LIPU exhibits peak effect on wound healing after three days of treatment, suggesting this this stimulation period has physiological relevance (Roper et al., 2015). These result led us to choose a three-day therapy period. The question that remains after senescent inducer and treatment time optimization is how LIPU stimulation will impact HFF senescence.
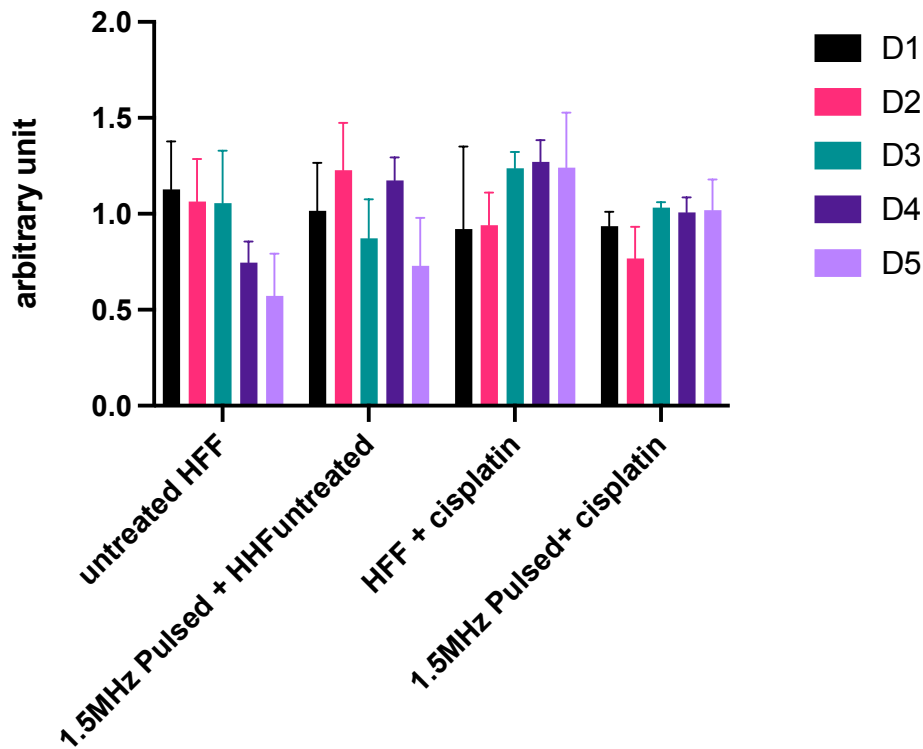
Figure 3-3 p21$^{waf1/cip1}$ level at different days of LIPUS stimulation.

P21 expression was measured by Western blot. The LIPUS effect seems Affected after third day of the treatment (green)(n=3) Statistical analysis was calculated using two-way ANOVA (n=3 across independent experiments).

3.5 BrdU assay

The BrdU assay was carried out to test whether cisplatin was reducing cell proliferation and could therefore be considered to have induced senescence. This assay conducted using the BrdU Elisa kit from Roche to test cell proliferation by determining levels of BrdU incorporation into the newly synthesised DNA of actively proliferating cells, before and after the cisplatin treatment, in order to confirm that cisplatin with concentration 10µM is arresting the cell cycle of HFF cells. After incubation with BrdU and anti-BrdU, the plate was scanned by a plate reader at a wavelength of 450 nm. The result is consistent with the literature, which demonstrates that this specific treatment arrests the cell cycle, and reveals that cisplatin doses of 10µM for 24H are halting the cell cycle in HFF cells compared to untreated cells (figure 3.4).
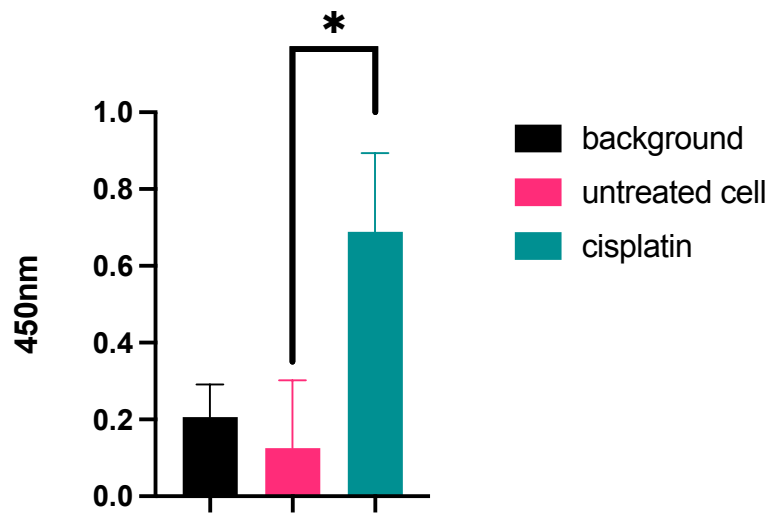
Figure3.4; BrdU assay

HFF cells treated with cisplatin (green bar) exhibited significant reduced cell cycle compared to HFF (pink bar). The black bar represents BrdU measurements in the absence of cells, showing that cisplatin effectively stopped proliferation entirely. (P=<0.05). (n=4 across independent experiments). Error bars represent SD. Statistical significance was calculated using a t-test and one-way ANOVA with Tukey's post hoc test (n=3 across independent experiments).

3.6 Senescence markers assay

3.6.1 The LIPU effect on SA-β-galactosidase activity (β-galactosidase assay)

The expanded and flat cell shape of senescent cells, as well as the presence of ß-galactosidase activity at pH 6.0, are important characteristics. Even while growing cells lack ß-galactosidase, induced senescence has enhanced activity. X-gal was used to quantify senescent levels following cisplatin and LIPU treatment, as previously mentioned in section 1.3, since A ß—gal activity is generally measured by in situ staining using a chromogenic substrate (Lee et al., 2006). throughout this experiment. In order to prevent false positive staining in the case of prolonged incubation at high density which can be reason for Cultures with high densities have the capacity to produce stress in cells, which can trigger the lysosomal stress response pathway(Kurz et al., 2000). Moreover, to guarantee that the same number of cells were counted at the conclusion of the experiment, the number of cells used for this assay was 8×10^4 cells per well for HFF and 10×10^5 cells for the HFF + cisplatin. then applying LIPU stimulation 20 minutes daily for three days. After the treatment, the cells were fixed using 4% paraformaldehyde. Then stained with ß-gal solution at PH6 and the cells were counted manually following the method mentioned in section 3.1. The results indicated that senescent cells' beta-galactosidase activity was significantly reduced (P value 0.0090) after ultrasonic stimulation,

84

indicating that ultrasound may diminish the amount of senescent induced in this cell line (figure 3.5(A&B)). There is ß- galactosidase activity present in the HFF may be a result of the assay's usage of high cell passage number. Any primary cells with a high passage number are susceptible to replicative senescence. The LIPU, however, has no impact on the beta-galactosidase activity for primary HFF (figure 3.5(A)). As the stain was bright and we manually counted the cells, the biggest difficulty we encountered in this assay was difficulty counting the senescent cells. Finding a different method to enable us to measure labelled cells quantitatively was the answer.
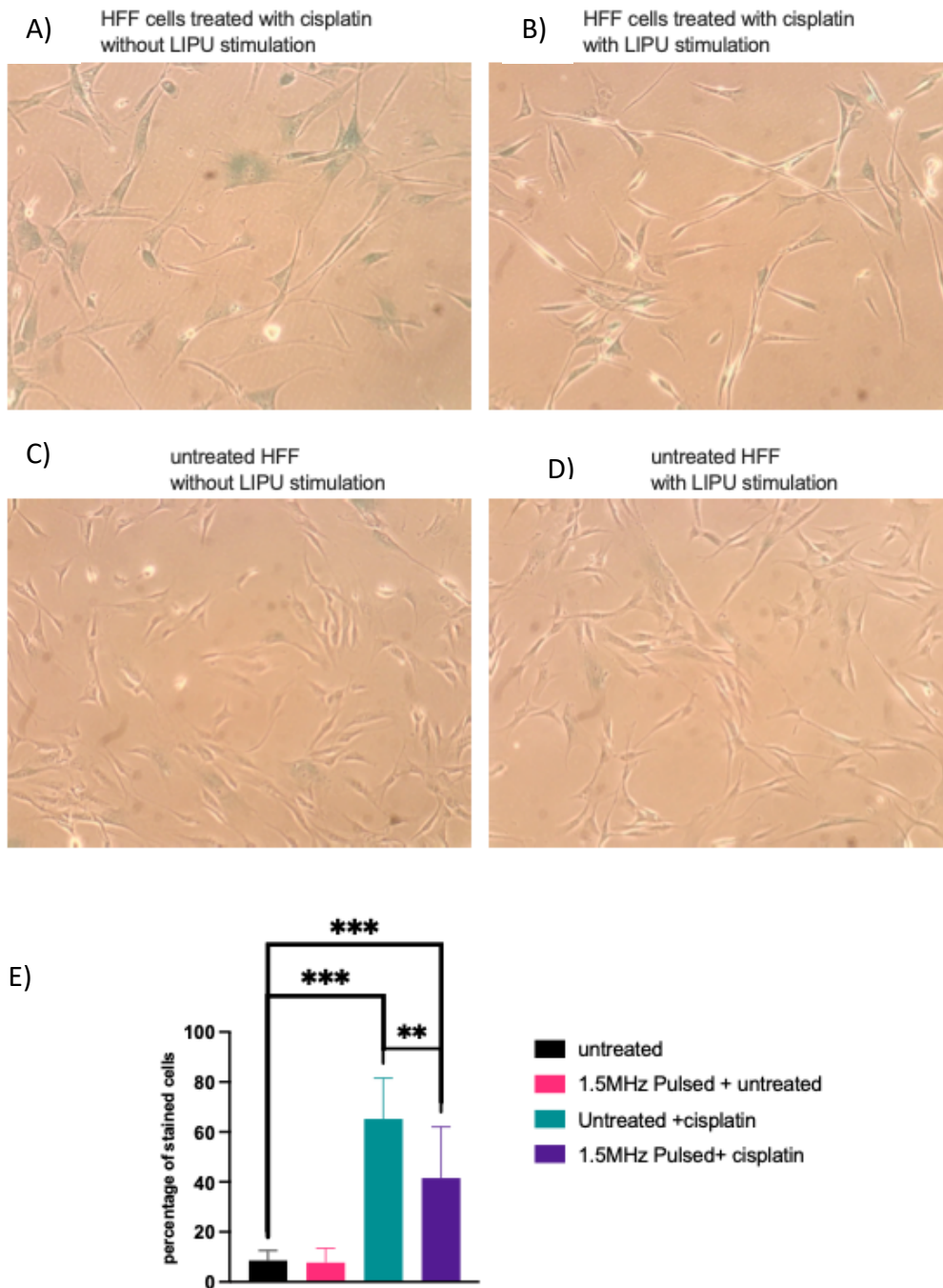
Figure 3.5 β- gal assay with LIPUS treatment

A) shows the HFF cells treated with 10µM of cisplatin to induce the senescence in HFF and stained by β-GalAssay to detect the senescence-associated-β-galactosidase activity; 75% of cells became senescent. **B)** shows the HFF cells + cisplatin after three days of LIPUS stimulation and the number of senescent cells dropped to 48%. **C)** shows the HFF cells has 7% of cells stained. **D)** shows the HFF cells + LIPUS has 5% of cells stained. E)shows the statistical analysis of senescence-associated-β-galactosidase activity and show significant reduction in β-galactosidase activity after LIPUS stimulation (purple) compared to HFF +cisplatin (green) $p=<0.05$. While HFF cells and HFF has no difference in β-galactosidase activity (black & pink respectively) (n=6 across independent experiments). Error bars represent SEM. Statistical significance was calculated using a t-test andone-way ANOVA with Tukey's post hoc test.

3.6.2 The LIPU effect on cell DNA damage (Ɣ-H2AX staining)

One of the medications based on platinum is cisplatin. a powerful cytotoxic agent that damages DNA. Cisplatin has the ability to directly bind double-stranded DNA in the nucleus and create intra- or interstrand cross-links that prevent DNA replication and RNA transcription (Woods and Turchi, 2013, Huang et al., 2022). in order to comprehend the extent of DNA damage brought on by cisplatin and determine whether LIPU stimulation can influence the cell nucleus and reduce or reverse DNA damage. DNA damage was examined using the Ɣ -H2AX staining method. The cells were planted in 24 well plates on coverslips at various densities—3×10^4 cells per well for the sample treated with 10 µM cisplatin and 1×10^4 cells for the untreated well—and underwent US stimulation for three days for 20 minutes each time. The fluctuation in cell density will enable the cells to have the same number of cells at the conclusion of the experiment. After LIPU stimulation, all samples were fixed with 2% PFA, incubated with Ɣ -H2AX antibody (1:1000) overnight, washed with PBS - (5 times for 30 minutes), stained with DAPI (1:15,000), and imaged using a wide-field microscope at The Wolfson Light Microscopy Facility at the University of Sheffield. This system is outfitted with the most recent sCMOS and EMCCD cameras capable of detecting the faintest of signals extremely fast. CellProfiler version 4.2.4 cell image analysis software was used for the image analysis. By computing the integrated density in Ɣ -H2AX pictures, the Speckle Counting pipeline enables us to recognise the foci within the nuclei and displays the number of foci per nucleus. Additionally, it demonstrates the connection between the two labelled nuclei (Ɣ -H2AX and DAPI).

According to the results (Fig 3.6 & 3.7), the sample that was exposed to 10µM cisplatin had the most DNA damage when compared to other conditions. It is obvious that the severity of DNA damage is increased with the use of cisplatin. The DNA damage does, however, seem to be less severe with ultrasound stimulation figures 3.6 & 3.7 (A). the sample with cisplatin has nearly the same number of cells so it is unlikely that LIPU reduced the number the cells (figure 3.7 (B).As expected, the least amount of DNA damage was found in the HFF cells samples. Telomere shortening may be the cause

of DNA damage in samples that have not been treated. Replicative senescence may result from increased cell passage numbers, as was already indicated figures 3.6 & 3.7 (A) . However, these results raise questions about the role ultrasound plays in DNA damage repair. Our results suggest that the LIPU mechanism may mitigate the DNA damage brought on by chemotherapy.
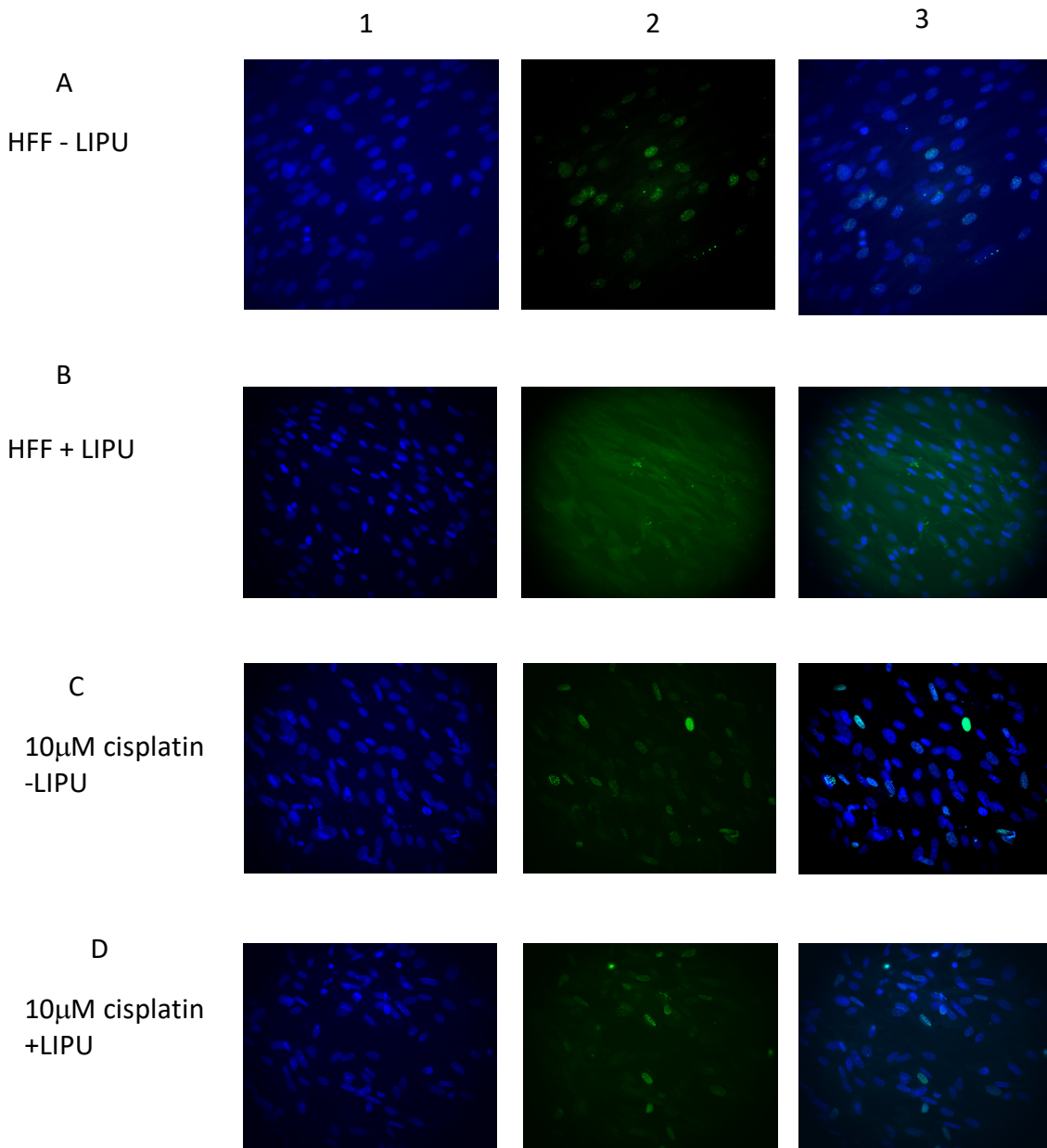
Figure 3.6; immunoflurocent; γH2AX staining of DNA damage

1- represent DAPI staining. 2- represent gamma h2ax staining. 3- merge of 1&2 staining A) represent the HFF. B) represent HFF +LIPU. D) represent the HFF + cisplatin Here the dna damage severe compared to other conditions. C)represent HFF cells +cisplatin +LIPU where the DNA damage lower than the one +cisplatin.. Both A&B showing lower amount of DNA damage

A

B
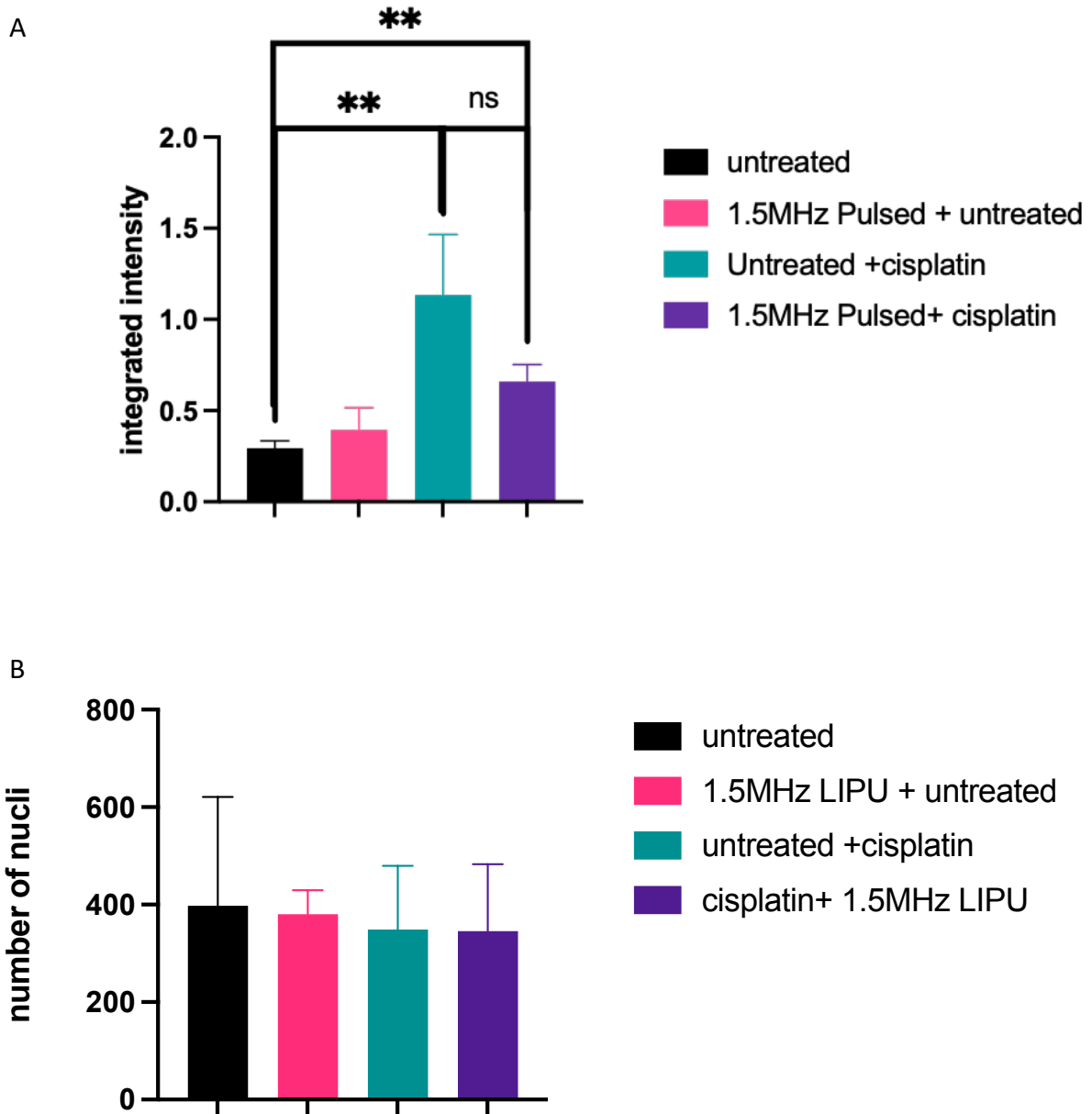
Figure 3.7: statistical analysis of immunofluorescence

A) represent the statistical analysis of integrated intensity the green represent HFF +cisplatin which has high amount of DNA damage, The purple represent HFF + cisplatin +LIPU shows non-significant reduction in DNA damage amount, black represent HFF and pink represent HFF +LIPU. Both HFF and HFF +LIPU has the lowest amount of DNA damage. (n=3 across independent experiments). Error bars represent SD. Statistical significance was calculated using a t-test and one-way ANOVA with Tukey's post hoc test. Significant <0.05
B) showing total number of cells in each condition by counting total DAPI staining

3.6.3 The LIPU effect on the protein level of p21^{waf1}/cip1 and p16^{INK4a} (western blot)

Cyclin-dependent kinase inhibitors (CKIs) are essential in regulating the cell cycle in non-transformed

cells. They are associated with the reduction of cell proliferation when cells are subjected to stress

conditions such as DNA damage. The expression of p16^{Ink4a} and p21$^{waf1/cip1}$ both increases. They,

therefore, recognise it as one of the senescence markers (Romanov et al., 2012). As a first step, we seed 3 x 10^5 cells per well for the sample treated with 10µM cisplatin and 1 x 10^5 cells per well for the untreated HFF in order to assess the protein level of p21 $^{waf1/cip1}$. First, we perform 20-minute LIPU stimulation over the course of three days. After that, we ran a western blot as describe in section 2.5

Using the axel programme (see Methods section 2.5), all findings were scaled to the intensity throughout the entire gel and adjusted to the loading control (GAPDH). Following exposure to LIPU stimulation, the results demonstrate a substantial decrease in P21 levels in the cells treated with cisplatin. This outcome is in line with the other senescence markers we looked at. The passage number utilised to carry out this experiment was above 20. Thus, some of the cells may experience replicative senescence, but like in prior work, we found a rise in the p21 level in untreated HFF, illustrated figure3.8. This finding prompts the question of whether the cell cycle halt caused by the cisplatin is transitory or permanent.
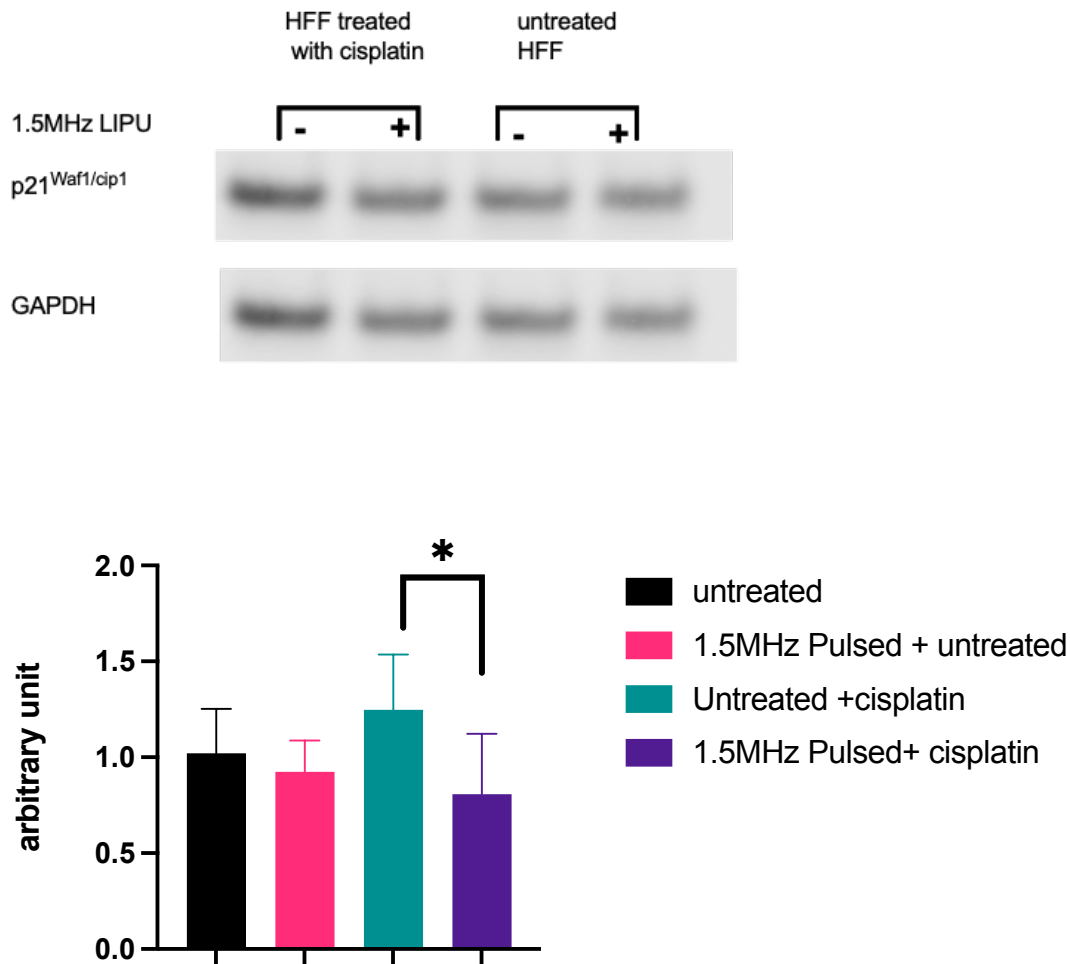
Figure 3.8 p21^waf1/Cip1 levels

p21$^{waf1/Cip1}$ levels were assessed in cell lysates using western blot from cells treated with various conditions p21$^{waf1/Cip1}$ level is overexpressed in HFF cells with cisplatin (green) compared to HFF cells +cisplatin +LIPU (purple), the LIPU seems to significantly downregulate the p21waf1/Cip1 according to a Western blot lysate ($P<0.05$). HFF show increase in even the HFF p21waf1/Cip1 (black) and HFF cells +LIPU show a reduction (pink), but it is not significant. (n=4 replication). Error bars represent SD. Statistical significance was calculated using a t-test and one-way ANOVA with Tukey's post hoc test.

After washing the therapy off, we chose to give the cell some downtime in order to demonstrate that the cisplatin treatment permanently stopped the cell cycle. To accomplish this, we incubate the sample for three days before the LIPU stimulation. We started the LIPU after the giving time and ran it for 20 minutes for three days. The western blot performed as indicated in section 2.5. The outcome followed the same trend as our earlier observations, with samples treated with cisplatin showing a significant decrease in p21 levels in senescent cells following ultrasound stimulation. It's interesting to note that untreated samples exhibit a similar pattern and a decrease in the p21 level (see figure3.9). These findings suggested that the therapy might influence senescent cells by lowering p21 expression.
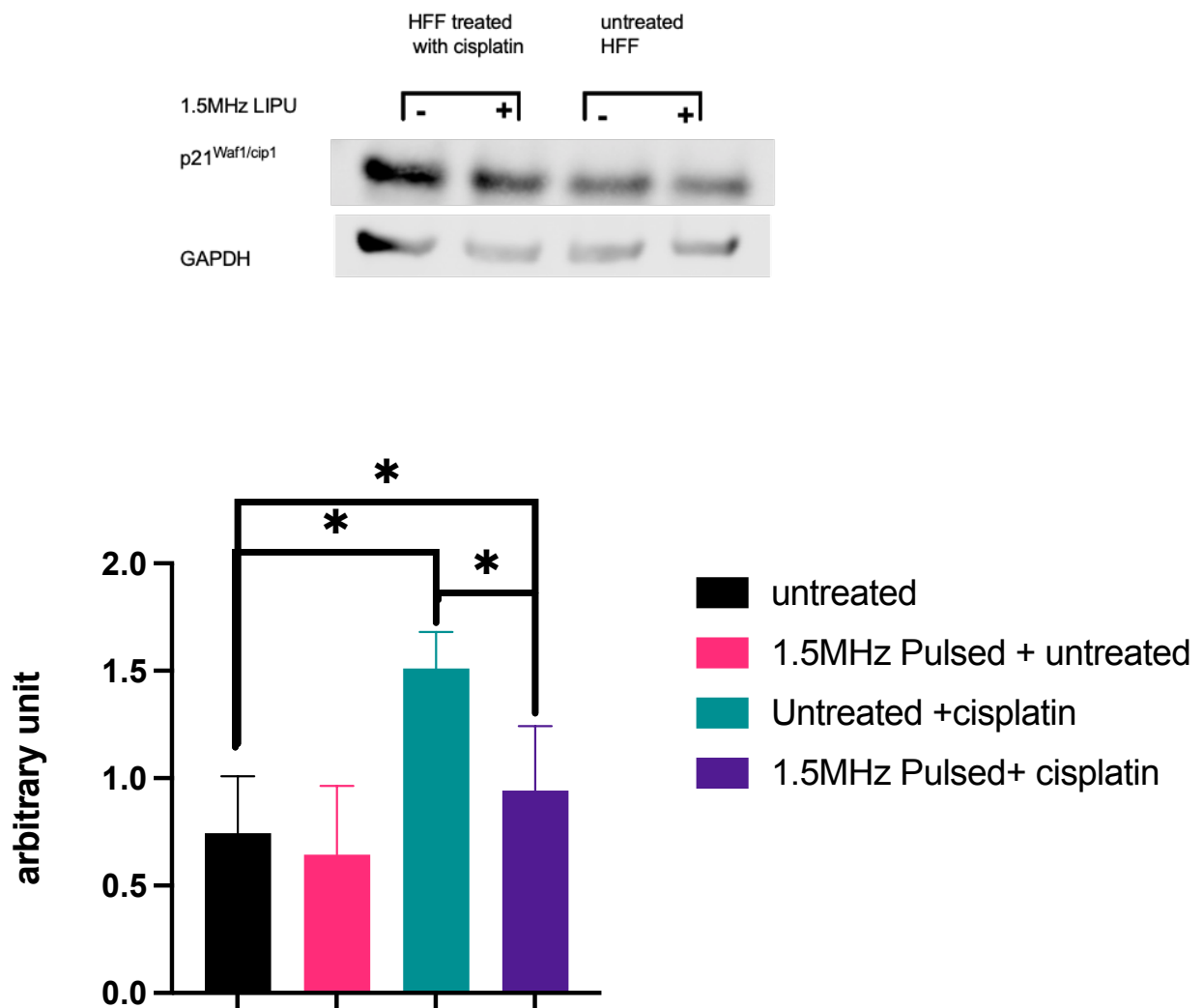
Figure 3.9 p21$^{waf1/Cip1}$ levels 3 Days after cisplatin treatment

 p21$^{waf1/Cip1}$ levels 3 Days after cisplatin treatment washed and LIPU stimulation in day 5 after seeding the cells were assessed in cell lysates using western blot from cells treated with various conditions p21$^{waf1/Cip1}$ level is overexpressed in HFF cells with cisplatin (green) compared to HFF cells +cisplatin +LIPU (pink), the LIPU seems to significantly downregulate the p21$^{waf1/Cip1}$ according to a Western blot lysate (P<0.05). HFF show increase in even the HFF p21$^{waf1/Cip1}$ (black) and HFF cells +LIPU show a reduction (pink), but it is not significant. (n=4 replication). Error bars represent SEM. Statistical significance was calculated using a t-test and one-way ANOVA with Tukey's post hoc test.

Additionally, we used a western blot to evaluate the level of p16inka4 protein as in section 2.5. Sadly,

we were unable to identify any protein levels in the membrane (see appendix). This finding motivates

us to experiment with an alternative approach to research the LIPU influence on p21 and p16. Therefore, the solution is to research how LIPU affects the expression of the p21 and p16 genes.

3.7   discussion
3.7.1   Cisplatin effect on skin fibroblast

Cisplatin, also known as cis-diamminedichloroplatinum(II), is a square-planar coordination compound of platinum. It barely dissolves in water. Cisplatin has a melting point of 270° C, a density of 3.74 g/cm3, and a molecular weight of 301.1 gm/mol (Dasari and Tchounwou, 2014). is a form of anti-cancer that is used to treat several cancers, including breast cancer, head and neck squamous cell carcinoma, ovarian cancer, and small cell lung cancer. (Pignon et al., 2008, Dhar et al., 2011, Lynch et al., 2009, Matsuki et al., 2013).

3.7.1.1   Mechanism of Action

Because cisplatin uptake was linear, nonsaturable, and unaffected by platinum analogs, it was first believed that cisplatin and its analogues entered cells through passive diffusion. (Sedletska et al., 2005).

The interaction of cisplatin with DNA, which results in DNA adducts, mediates the effect of cisplatin. DNA transcription and replication are hampered by the formation of cisplatin-DNA adducts. The mode of action entails causing DNA adducts, such as intrastrand and interstrand cisplatin DNA cross-links, to develop in cancer cells, which then causes the DNA structure to be disrupted, causing cytotoxicity. Cellular proteins are able to recognize this change in structure and use it to repair DNA damage caused by cisplatin, which requires stopping the cell cycle at S, G1, or G2-M. Cells activate pathways linked to apoptosis or senescence if the damage is greater than their ability to heal it (Siddik, 2003, Singh et al., 2018, Basu and Krishnamurthy, 2010).

3.7.2   Cisplatin as an inducer of premature senescence in HFF
One of the main chemotherapy medications used to treat cancer is cisplatin. Low concentrations of DNA-damaging drugs such as cisplatin tend to cause senescence rather than apoptosis in exposed cells (Li et al., 2014). Cisplatin can bind to DNA to form intrastrand and interstrand cross-links

between purine bases and induces apoptosis by inhibiting DNA replication and transcription. Which leads to activating DDR and cell cycle arrest. In addition, cisplatin causes mitochondrial damage, which increases the production of reactive oxygen species (ROS) and lipid peroxidation (Olszewska et al., 2021, Qu et al., 2013, Yu et al., 2017). As shown in Figures 3-1& 3-4, we discovered that 10µM of cisplatin for 24 hours could arrest the cell cycle. A 2004 study that used the same dosage and treatment duration also discovered that cisplatin could stop the cell cycle in fibroblasts (Zhao et al., 2004).

DNA damage signalling plays an essential role in cell senescence. Following DNA double-strand breaks, the activation of ataxia-telangiectasia mutated (ATM) is induced and subsequently becomes recruited as an inactive dimmer to the DNA lesion by the Mre11-Rad50-Nbs1 (MRN) complex formation field (Lee and Paull, 2005). The MRN complex and ATM bind with each other through multiple protein-protein interactions and are located at the damaged DNA foci marked by phosphorylated histone (Ɣ -H2AX) to regulate numerous downstream mediators for coordinating the DNA damage response Field (Kinner et al., 2008;(Kinner et al., 2008, Zhang et al., 2015). in the figures 3.6 & 3.7 , in the gamma-H2AX assay, we used a Ɣ -H2AX antibody to detect a histone formed by phosphorylation at sites of the double-strand break. This assay confirms the accumulation of senescence-associated Ɣ -H2AX foci caused by administrating of cisplatin which is known as the senescence marker (Siddiqui et al., 2015, Merz et al., 2019)

That cisplatin accelerates the aging of HFF cells is something we can confirm. First, we count the number of senescent cells by searching for a recognised senescent marker, which indicates the existence of SA ß-galactosidase activity and a change in cell shape (flattened and expanded cellular shape) during senescence brought on by the cisplatin treatment (Klement and Goodarzi, 2014). Another senescence marker we used to confirm that cisplatin has induced premature senescence in HFF cells by quantifying cyclin-dependent kinase (Cdk) inhibitors p21$^{CIP1/WAF1}$. The figure 3.8 shows p21 level is upregulating, which indicates an induced cell cycle arrest, and it is another senescence marker (Wagner and Wagner, 2022).

3.7.3 Effect of LIPU stimulation on different senescent markers

In connective tissue, fibroblasts make up the majority of cells and play a crucial role in tissue repair and remodelling after injury. The extracellular matrix is degraded by fibroblasts that are senescent, which increases the chronicity of wounds. According to one theory, the barrier beyond which wounds become difficult to heal is reached by an accumulation of senescent fibroblasts (Harding et al., 2005). As a result, primary skin fibroblasts are an effective model to comprehend how the US promotes tissue regeneration and how this influences fibroblast senescence.

It is possible to think about acoustic pulsed energy as a type of mechanical energy that does not directly exert mechanical stress on cultured cells (Zhou et al., 2004). In order to produce a sinusoidal signal with a 1.5 MHz frequency, 20% duty cycle, 1.0 kHz repetition frequency, and 30 mW/cm2 SATA intensity, the LIPU stimulation parameter was selected in accordance with the customised device offered by Smith & Nephew. De Avila Santana employed it in 2013; Roper did so in 2012 and 2015; both utilised the same parameter (de Avila Santana et al., 2013, Roper et al., 2012, Roper et al., 2015). many research projects on the LIPU method of healing chronic wounds. They discovered that by affecting the inflammatory phase, low-intensity ultrasound speeds up the healing of chronic venous ulcers. Additionally, it stimulates the development of new tissue, as evidenced by an expansion of the region of granulation tissue, a propensity for higher VEGF expression, and thicker collagen fibres (de Avila Santana et al., 2013). Additionally, it appears that LIPUS stimulation causes enhanced cell migration, which is a well-described response (Jang et al., 2014, Katano et al., 2011, Atherton et al., 2017).

Given that integrins used to detect extracellular signals are stimulated by mechanical waves, it is feasible that the LIPU can encourage fibroblast proliferation. The activation of the integrin receptor, suppression of Rho-associated coiled-coil protein kinase (ROCK), and promotion of extracellular signal-regulated kinase (ERK) by low-intensity US have all been demonstrated to be necessary for fibroblast proliferation (de Avila Santana et al., 2013). The results of a different study indicate that LIPUS increases fibroplasia, with fibroblast proliferation enhancing the extracellular matrix and supporting new tissue. This stimulation results in increased amounts of hypertrophic collagen fibres.

Our results lend credence to the idea that LIPU stimulation influences chronic wounds and aids in their treatment by influencing fibroblast senescence, which has been linked to the development of chronic wounds (Wei et al., 2022). We discovered that the senescence-related -galactosidase activity appears to be decreased by the LIPU. This is the most widely utilised indicator for senescent or old cells. The D-galactose residues in the D-galactosides are broken down by the lysosomal -GAL (de Mera-Rodriguez et al., 2021). Additionally, as shown in figure 3.5, the cell morphology of HFF treated with cisplatin after LIPU stimulation was different from HFF treated with cisplatin that had not been exposed to LIPU. But there are certain drawbacks to using the beta-gal assay as a senescence marker. For example, SA-β-gal expression can differ even within the same cell population. The interpretation of SA-β-gal staining results may pose a challenge due to the sensitivity of SA-β-gal activity to assay conditions, including pH, temperature, and fixation method. This can make comparing the findings of various studies challenging (de Mera-Rodriguez et al., 2021).

The p21 protein, which has been identified as a cell cycle inhibitor, is another senescence marker we have evaluated (Wagner and Wagner, 2022). In the image 3.8, we show that in cells treated with cisplatin, LIPU may reduce the P21 level by a 0.5-fold change. Since there are several stages of senescence and heterogeneous aging in this cell type. Moreover, The transcription factor E2F1 is in charge of p16 expression in HFFs. But in HFFs, the binding of the Rb tumour suppressor protein inhibits E2F1 activity (Narita et al., 2003). we were unable to detect the expression of p16[Inka4] using a western blot (Wagner and Wagner, 2022).

It's interesting to note that one of our findings suggests LIPU may be able to lessen the DNA damage brought on by cisplatin as in figure 3.6. It is possible for the mechanical stimuli from ultrasonic exposure to be transduced and to activate the proper effector mechanisms, which in turn modify gene expression and cause some of the biochemical events that result in cell recovery and alternation (Przystupski and Ussowicz, 2022). According to research done by Amaya in 2021, paclitaxel's cytotoxic effects on cultured cells can be countered by low-intensity ultrasound therapy. As a result, they hypothesise that ultrasound causes the paclitaxel-induced stiff microtubule cytoskeleton to be

disrupted, leading to the formation of paclitaxel-bound fragments that degrade. Tubulins that are unbound by paclitaxel organise into a new microtubule network. The effect of paclitaxel on microtubules can therefore be eliminated by ultrasound shock waves (Amaya et al., 2021). However, more research is required to determine how LIPU might impact the cell cycle and whether it might repair DNA damage brought on by cisplatin. This enables cutting-edge combo therapy that shields healthy cells from chemotherapy.

.

CHAPTER 4

The ultrasound effect on the secretory phenotype of
senescent cells (SASP)

4 The ultrasound effect on the secretory phenotype of senescent cells (SASP)

4.1 Introduction

Senescent cells are metabolically active. As a secretory phenotype of senescent cells, it secretes several pro-inflammatory secretomes (SASP). Interleukins (IL-1 family, IL-6), chemokines (e.g., IL8, CCL2), and growth factors (e.g., essential fibroblast growth factor [bFGF], hepatocyte growth factor [HGF/SF]) are all strongly upregulating in these cells. The production of proteases, including matrix metalloproteinases (MMPs), and alterations in insoluble protein/extracellular matrix (ECM) components, particularly a decrease in numerous collagens and proteoglycans, are additional hallmarks of the SASP (Malaquin et al., 2016).

4.2 Aim

Understand the LIPU effect on the secretory phenotype of fibroblast senescence.

4.3 Result

4.3.1 The impact of LIPU stimulation on paracrine senescence

Some SASP components, such as plasminogen activator inhibitor-1 (PAI-1), IL-8, VEGF, IL-1, and others, may cause the onset of senescence in one cell to induce senescence in neighbouring cells, resulting in an exponential effect over time (Nelson et al., 2012, Parikh et al., 2019). Paracrine senescence is the term for this. This type of senescence, also known as transmissible senescence, is caused by the secretions of senescent cells, known as SASP. It's usually less intense than primary induced senescence, but it can have positive effect by encourage the elimination of pre-cancerous cells by enhancing immune surveillance and negative consequences as many pro-tumorigenic effects, including the enhancement of malignant phenotypes and the promotion of tumour start, can be

mediated by SASP paracrine signalling. (Acosta et al., 2013, Hernandez-Segura et al., 2018, Lujambio, 2016, Gonzalez-Meljem et al., 2018).

The medium from cells treated with cisplatin and untreated cells was harvested and applied in a 1:1 ratio to new HFF cells for seven days to see if the SASP could produce a paracrine effect (Fig. 1.4A). Expression of the cyclin-dependent inhibitor p21$^{waf1/Cip1}$ was measured to assess the paracrine effect on young HFF cells as one of the senescence markers. As indicated in figure 1.4B, when compared to cells treated with untreated media, cells treated with SASP media conditioned by senescent cells. appear to have significantly higher levels of the p21$^{waf1/Cip1}$ protein, according to a western blot. However, without cisplatin, cells will condition the media and that there will be some replicative senescent cells in the population. Therefore, we have noticed that p21$^{waf1/Cip1}$ is upregulated.

In cells treated with conditioned media from senescent cells , the p21$^{waf1/Cip1}$ protein level has increased by 40% (Fig. 1.4B). We decided to collect media from various cell conditions. To test whether the ultrasound treatment affects the treated cells with harvested media (media from cells +cisplatin, untreated cells, cells +cisplatin + LIPU treatment, and cells+ LIPU treatment). p21$^{waf1/Cip1}$ level in cells treated with both media harvested from cells with cisplatin-induced SASP and LIPU might be slightly lower p21$^{waf1/Cip1}$ level than others, as figure 1.4 (c) indicates. However, the change was not significant. After that, when we used a western blot to detect p21waf1/Cip1 in paracrine senescence, we were unable to determine the impact of LIPU stimulation on senescent cells. Finding out whether the LIPU has an impact on interleukin 6 (IL6), a protein known to be generated by SASP, is the next step.
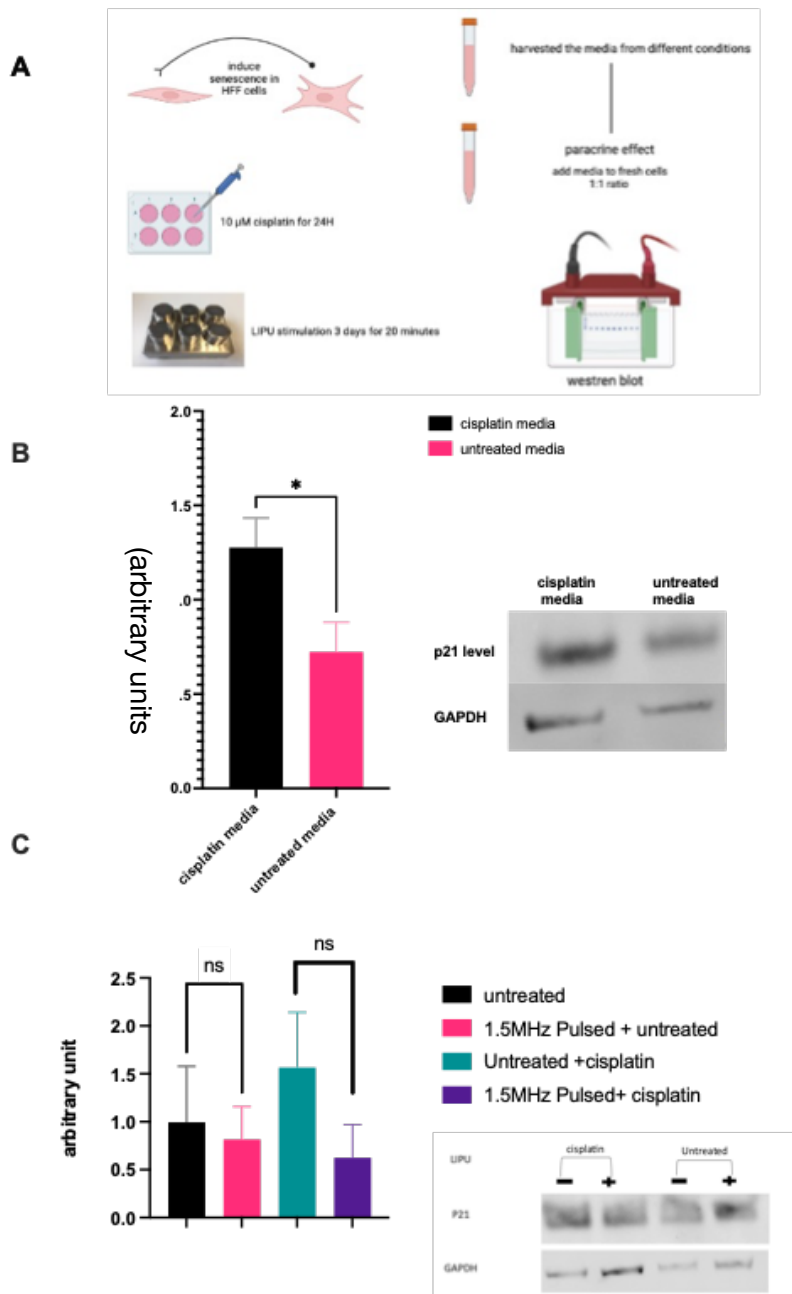
Figure 4.1: paracrine senescence.

p21waf1/Cip1 levels were assessed in cell lysates using western blot from cells treated with various conditions medium; new cells were treated with a 1:1 ratio of harvested media and left for seven days. (A) Representative of the method used to conduct this experiment (B) p21$^{waf1/Cip1}$ level is significantly overexpressed in cells treated with medium from cells treated with cisplatin (black) compared to untreated cells (pink), according to a Western blot lysate (P< 0.05). (C) graph representing the measurement of p21$^{waf1/Cip1}$ levels under various LIPU stimulation conditions. After LIPU stimulation, non-significant decrease in p21$^{waf1/Cip1}$ levels in cells treated with cisplatin medium (purple), even the untreated cells show a reduction after adding media from cell treated with LIPU (pink), but it is not significant. (n=4 replication). Error bars represent SD. Statistical significance was calculated using a t-test and one-way ANOVA with Tukey's post hoc test.

4.3.2 Ultrasound stimulation and its effect on Interleukin 6 Elisa assay

Senescent cells accumulate in damaged or aged tissues and impact surrounding cells via SASP factors, yet the pro-inflammatory microenvironment is maintained.

As a result, sterile inflammation develops, leading to age-

related illnesses such as cancer (Lasry and Ben-Neriah, 2015, Acosta et al., 2013).

Furthermore, the SASP secretion differs depending on the senescent cell type and the senescence inducer (Watanabe et al., 2017). One of the SASP-produced soluble proteins is interleukin 6 (IL6). and it has been highlighted in the literature as one of the pro-inflammatory proteins secreted by SASP. As a result, we chose to use the IL6 human Elisa kit to measure the IL6 level in media obtained from various conditions (HFF cells treated with cisplatin without LIPU, HFF cells treated with cisplatin and LIPU, untreated HFF cells without LIPU and untreated HFF cells with LIPU stimulation). The abundance of IL6 in media measured by ELISA. When the stain was still developing, its wavelength measured between 450 and 540 nanometres. As figure 2.4 shows, due to variation between replicates, a statistically significant result was not obtained. The result here shows the average of three repeats; each one gave a different reading each time. although IL6 was a sensible candidate, a clear effect of US on IL6 secretion was not obtained. Therefore, we moved away from a candidate-based approach to screen for changes in the secretive using mass spectrometry.
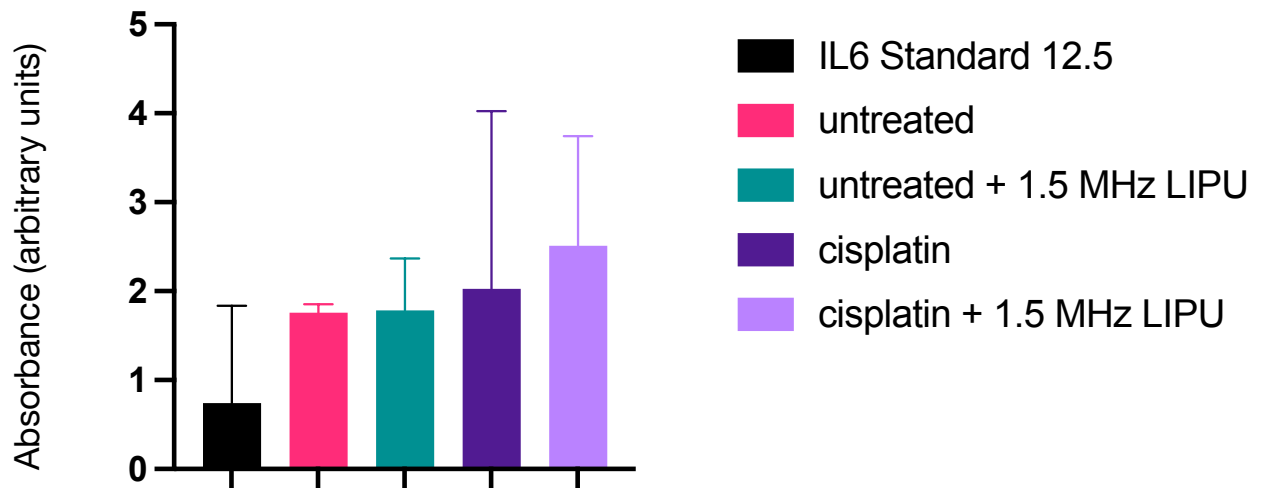
Figure 4.2: LIPU stimulation effect on IL6 level in different media conditions.

Measurements of IL-6 had difficulty with reproducibility, making the effects of LIPU on IL-6 difficult to determine. (n=3 across independent experiments)

4.3.3   Pilot mass spectrometry for HFF Secretome

The proteins secreted by cells are often identified and analyzed using techniques including ELISA assays, western blotting, or pre-selected antibodies of cultured media (Coppe et al., 2008, Quijano et al., 2012). All these techniques, while offering objective results, rely on a candidate-based approach and are unable to do a complete examination of the host secretome. We chose label-free quantification mass spectrometry as a quantitive strategy to investigate the conditioned medium and identify the host secretome thoroughly.

Less abundant proteins will be hidden by the presence of foetal bovine serum (FBS) in the culture medium. So, for this experiment, we decided to use a serum-free medium. The label-free quantification (LFQ) technique was used in this investigation employing s-trap columns. Label-free quantification intensity, or LFQ intensity, is a metric used to express how abundant a protein is in a given sample. It is dependent on the strength of the signal produced when a protein is mass spectrometer-detected after being labelled with a fluorescent tag. The protein is more prevalent in the sample the higher the LFQ intensity (Bai et al., 2023).

Before applying the optimized methodology to all media conditions, one test experiment was conducted utilizing S-trap midi columns (≥ 300 μg) to optimize the approach with untreated media with and without ultrasound stimulation. The conditioned media containing soluble proteins and exosomes were collected. After 25ug of a protein digest was analyzed using a Top20 LC-MS/MS method for two hours, the results were reasonable. By calculating LFQ intensity seems to reduce after applying LIPU stimulation (figure 3.4 (A)). Moreover, we were able to identify total 402 proteins and 190 of them were also identified in SASP atlas shown on the first try illustrated figure 3.4 (B)(Basisty et al., 2020). (Appendix show table of LFQ intensity)
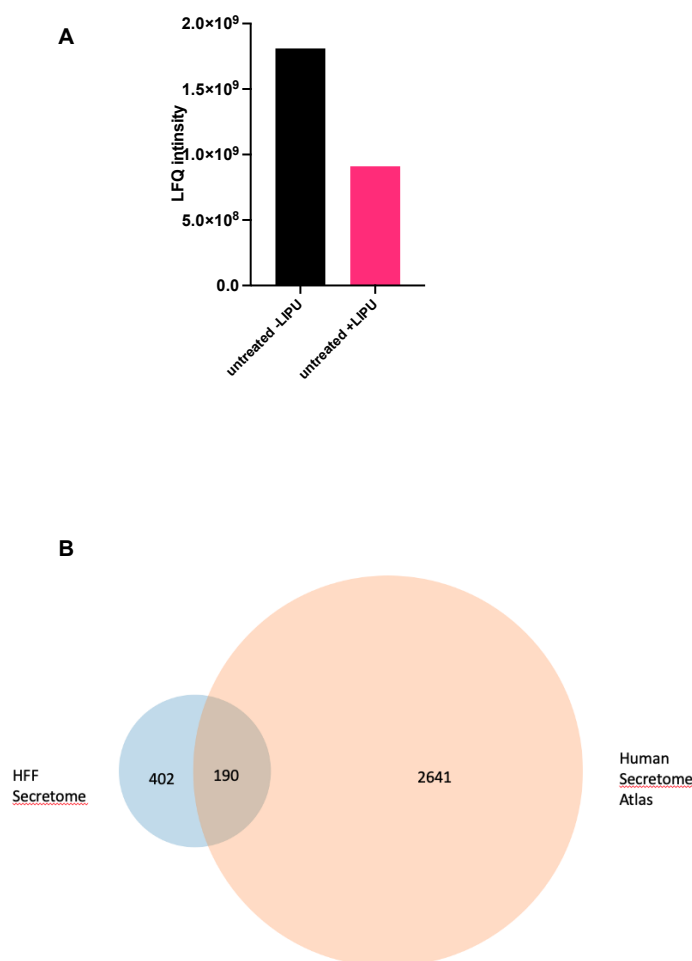
Figure 4.3 Optimization of protein extraction from HFF cells samples for S-trap digestion.

A) Bar chart represents a comparison of total label-free quantification (LFQ) intensity of proteins (black) extracted from untreated HFF cells without LIPU stimulation and total (LFQ) intensity of proteins (pink) extracted from untreated HFF cells with LIPU stimulation, of proteins extracted with buffers containing either 5% SDS or 1% Doc, from HFF cells secretome was optimized using S-trap digestion methods. B) Venn diagram of secreted proteins (402) and proteins that were identified in the Human Secretome Atlas dataset (2641), 190 proteins were identified in two datasets.

4.3.4   mass spectrometry for HFF Secretome (label-free quantification)

following assay optimization. Four different sets of conditioned media were used in the experiment

show in table 4.1. Utilizing the same procedure as in section 1.3.3, with four repetitions of each

condition. Utilizing MaxQuant, data were processed and quantified(Cox and Mann, 2008). 1174

proteins were identified from 25 μg of protein digest that was analyzed using a 2-hour Top 20 LC-

MS/MS method with a 1% FDR. Of these proteins. 780 proteins were quantified in at least three

replicate samples in one group using Perseus statistical analysis on four replicates of each condition.

The data was regularly distributed, as shown by histogram plots of the intensities of each duplicate

after being transformed by Log2 (Figure 4.4). The distributions are reproducible, but not normal

disruptions occurred in the intensity distribution of the rest of the repeats of the different media

conditions. Except for the first replicate of the untreated sample without LIPU, which was eliminated

because there was no correlation with the other groups, the multi-Scatter plot in Table 4.2 indicates

the quality of the tests we conducted and demonstrates a reproducible finding overall.

Table 4.1 Different media conditions used to perform mass spectrometry
The different media conditions used in mass spectrometry experiment
HFF cells treated with cisplatin without LIPU
HFF cells treated with cisplatin with LIPU
HFF cells without LIPU
HFF cells with LIPU
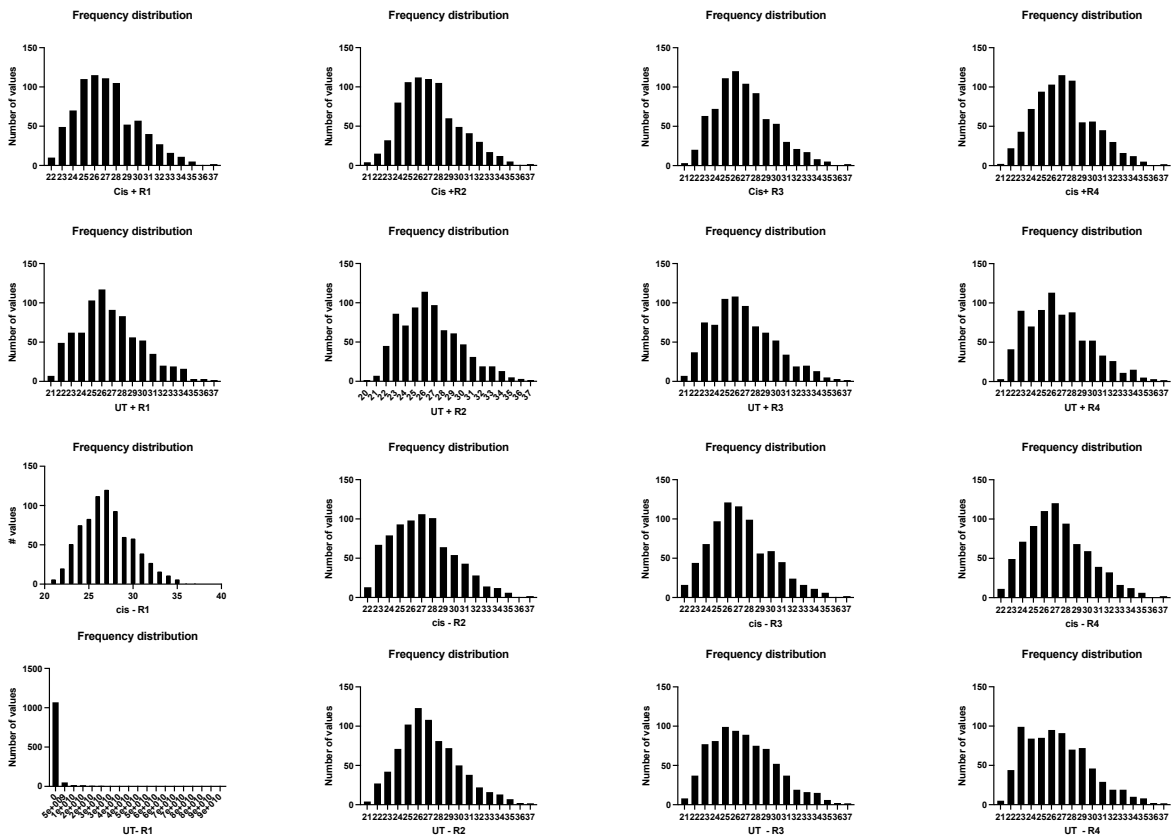
Figure 4.4 Histogram of LFQ intensity values for four replicates of different media conditions.

They showed a normally distributed intensity except for the first repeat of the untreated sample without LIPU that was excluded—normalized with imputed intensity values for statistical analysis.

Table 4.2 The table represents the Pearson correlation of the biological replicates

high (red), middle (yellow), and low (green). Correlation in the same group was highest at 0.98; in between groups, the lowest was 0.86. These show that biological replicates inside the same groups were reproducible.

LFQ intensity AA_+Cis_R1	LFQ intensity AA_+Cis_R2	LFQ intensity AA_+Cis_R3	LFQ intensity AA_+Cis_R4	LFQ intensity AA_+UT_R1	LFQ intensity AA_+UT_R2	LFQ intensity AA_+UT_R3	LFQ intensity AA_+UT_R4	LFQ intensity AA_-Cis_R1	LFQ intensity AA_-Cis_R2	LFQ intensity AA_-Cis_R3	LFQ intensity AA_-Cis_R4	LFQ intensity AA_-UT_R1	LFQ intensity AA_-UT_R2	LFQ intensity AA_-UT_R3	LFQ intensity AA_-UT_R4	Name	
NaN	0.982578	0.985171	0.981755	0.941041	0.925273	0.932514	0.931804	0.982121	0.975406	0.983937	0.981664	0.924829	0.938869	0.911588	0.902024	LFQ intensity AA_+Cis_R1	
0.982578	NaN	0.982337	0.980627	0.942765	0.933065	0.934059	0.934984	0.983587	0.965539	0.974835	0.98221	0.924718	0.940035	0.912972	0.911427	LFQ intensity AA_+Cis_R2	
0.985171	0.982337	NaN	0.976315	0.941761	0.931961	0.932881	0.93465	0.979519	0.969329	0.977302	0.976745	0.922089	0.941274	0.914347	0.911129	LFQ intensity AA_+Cis_R3	
0.981755	0.980627	0.976315	NaN	0.926052	0.906982	0.915318	0.915489	0.978204	0.970466	0.980764	0.978777	0.929272	0.929777	0.898156	0.884973	LFQ intensity AA_+Cis_R4	
0.941041	0.942765	0.941761	0.926052	NaN	0.989021	0.991794	0.989508	0.944149	0.935466	0.931322	0.927796	0.888866	0.975663	0.977405	0.976677	LFQ intensity AA_+UT_R1	
0.925273	0.933065	0.931961	0.906982	0.989021	NaN	0.991649	0.987347	0.931213	0.923368	0.917641	0.913269	0.873578	0.972366	0.976367	0.984008	LFQ intensity AA_+UT_R2	
0.932514	0.934059	0.932881	0.915318	0.991794	0.991649	NaN	0.989127	0.934629	0.927254	0.921406	0.916188	0.8761	0.972662	0.977768	0.980221	LFQ intensity AA_+UT_R3	
0.931804	0.934984	0.93465	0.915489	0.989508	0.987347	0.989127	NaN	0.932251	0.924935	0.921554	0.914814	0.87572	0.970132	0.974792	0.977531	LFQ intensity AA_+UT_R4	
0.982121	0.983587	0.979519	0.978204	0.944149	0.931213	0.934629	0.932251	NaN	0.972721	0.980925	0.987939	0.922074	0.942517	0.91789	0.910664	LFQ intensity AA_-Cis_R1	
0.975406	0.965539	0.969329	0.970466	0.935466	0.923368	0.927254	0.924935	0.972721	NaN	0.982498	0.970758	0.921526	0.945037	0.922941	0.914798	LFQ intensity AA_-Cis_R2	
0.983937	0.974835	0.977302	0.980764	0.931322	0.917641	0.921406	0.921554	0.980925	0.982498	NaN	0.981683	0.931066	0.938158	0.910514	0.896207	LFQ intensity AA_-Cis_R3	
0.981664	0.98221	0.976745	0.978777	0.927796	0.913269	0.916188	0.914814	0.987939	0.970758	0.981683	NaN	0.933386	0.93159	0.89597	0.889062	LFQ intensity AA_-Cis_R4	
0.924829	0.924718	0.922089	0.929272	0.888866	0.873578	0.8761	0.87572	0.922074	0.921526	0.931066	0.933386	NaN	0.927727	0.871652	0.860519	LFQ intensity AA_-UT_R1	outlier
0.938869	0.940035	0.941274	0.929777	0.975663	0.972366	0.972662	0.970132	0.942517	0.945037	0.938158	0.93159	0.927727	NaN	0.974735	0.974574	LFQ intensity AA_-UT_R2	
0.911588	0.912972	0.914347	0.898156	0.977405	0.976367	0.977768	0.974792	0.91789	0.922941	0.910514	0.89597	0.871652	0.974735	NaN	0.985518	LFQ intensity AA_-UT_R3	
0.902024	0.911427	0.911129	0.884973	0.976677	0.984008	0.980221	0.977531	0.910664	0.914798	0.896207	0.889062	0.860519	0.974574	0.985518	NaN	LFQ intensity AA_-UT_R4	
												outlier					

We next used the UniProt database to conduct a bioinformatics analysis to detect and identify the proteins detected by mass spectrometry. Additionally, we compared The Human Secretome Atlas with our HFF Secretome (Basisty et al., 2020) We were proteomics data analyses for the existence of a secretion signal peptide in various fibroblast cells. Multiple kinds of senescence inducers led to the

creation of the Human Secretome Atlas, a database containing 2641 proteins. We could discover

total 1146 Secretome proteins in our sample , The Human Secretome Atlas showed 464 of them.

(Appendix show table of LFQ intensity and the identified protein)
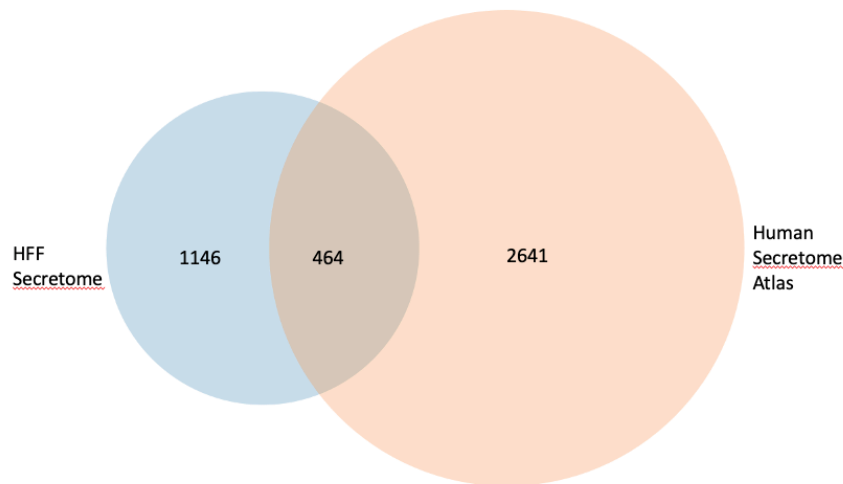
Figure 4.5Venn diagram of secreted proteins

Venn diagram of secreted proteins from all media conditions (1146) and proteins identified in the Human Secretome Atlas dataset (2641). 464 proteins were identified in two datasets.

4.3.4.1   Characterization of HFF Secretome changes in the HFF senescence induced by cisplatin

The next step is to determine whether cisplatin impacts HFF cells. Using Perseus, we quantified the

difference in protein levels between HFF cells treated with cisplatin and untreated HFF cells (Tyanova

et al., 2016). Contaminate and reverse were eliminated, and the data were restricted to proteins that

were only discovered in at least three replicates of each group. Additionally, data were normalized

by subtracting the distribution's median, missing values were imputed from each sample's data

distribution using a downshift of (1.8 and a width of 0.3), and a t-test with a permutation-based FDR

of 5% was then run (Tyanova et al., 2016).

With this test's help, we could identify 366 proteins that were significantly up-or down-regulated in

cisplatin-treated HFF cells compared to untreated HFF. The secretome peptide distribution between

the two groups is visualized in Figure 6.4 by a volcano plot; the peptides on the right side correspond

to proteins significantly upregulated in response to cisplatin treatment for the HFF. After cisplatin

exposure, 235 out of 366 are upregulated, and 130 are downregulated. proteins were also present in the Human Secretome Atlas (Basisty et al., 2020). Once we have identified the impact of cisplatin on the HFF Secretome, the fundamental query at this point is: Can the HFF Secretome be affected by LIPU stimulation following cisplatin treatment?
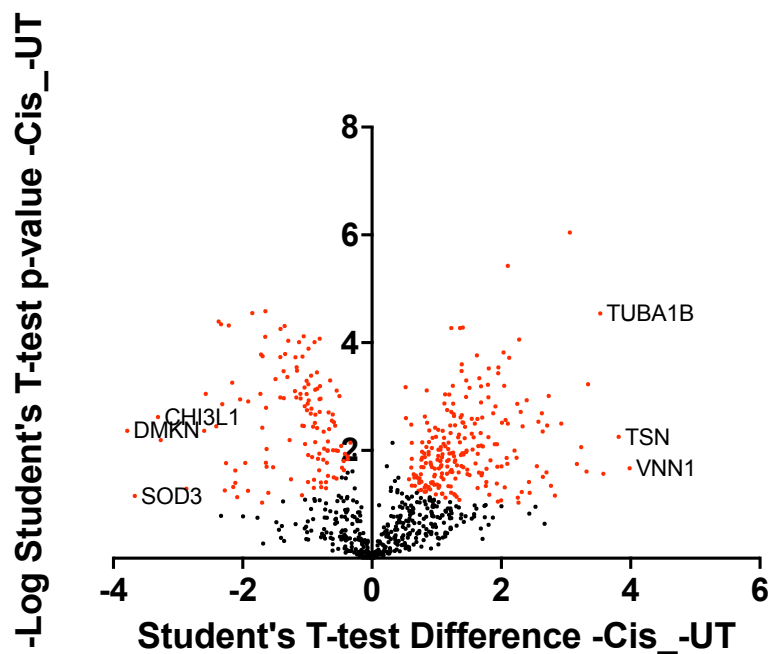
Figure 4.6 Volcano plot showing significantly proteins regulated by cisplatin treatment.

 Data from analyzing four replicates of media of HFF cells treated with cisplatin and three replicates of media of untreated HFF cells were filtered to retain proteins quantified in at least three replicates of one group (366). The data were normalized by subtracting the median intensity value of each sample, and statistical analysis was performed using t-testing with a permutation-based FDR of 5% and S0 of 0.1. red dots on the right represent proteins significantly upregulated with cisplatin treatment, and red dots on the left represent proteins significantly downregulated with cisplatin treatment.

4.3.4.2   *Characterization of HFF Secretome changes after LIPU stimulation in the HFF senescence induced by cisplatin*

Through analysis of the HFF secretome, the effects of cisplatin on HFF cells were ascertained. The same procedure used in section 1.3.4.1 was applied to evaluate the impact of LIPU stimulation on cisplatin-induced HFF senescence. A t-test was run with a 5% permutation-based false positive rate. The distribution of senescent secretome peptides in the two groups of cisplatin-treated HFF cells with

and without LIPU stimulation is shown in Figure 7.4 as a volcano plot. We found that LIPU stimulation has no effect on the HFF senescent secretome, despite the stimulating effect that we describe in chapter 3. The t-test indicates that no peptides are visible following LIPU stimulation. The impact of LIPU on senescent cells is not enough to counteract the cisplatin-induced SASP induction, according to the results. To ascertain whether the LIPU stimulation affects HFF cells in the absence of cisplatin, we then employed mass spectrometry.
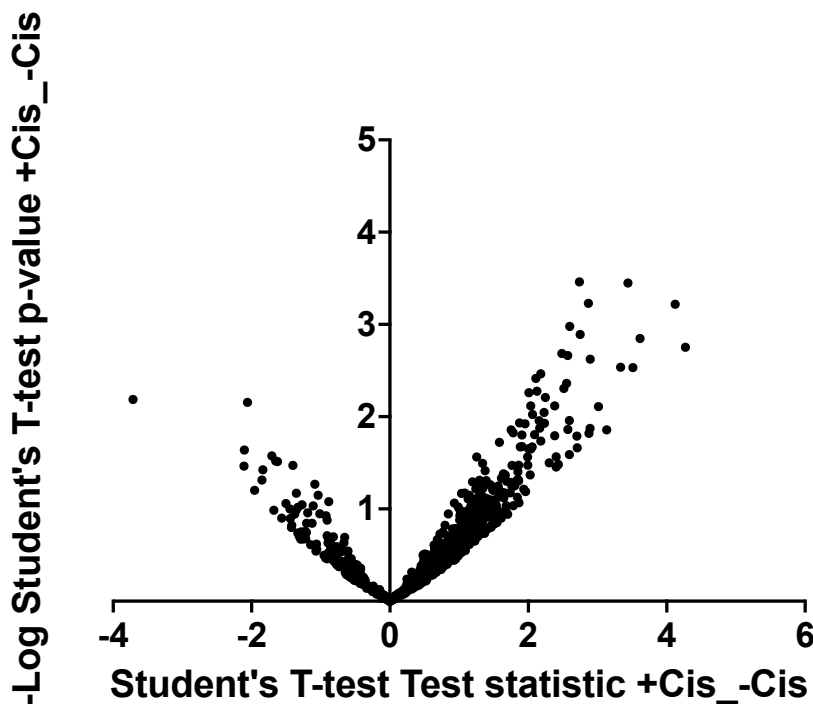
Figure 4.7 Volcano plot showing significantly proteins regulated by cisplatin treatment.

Data from the analysis of 4 replicates of media of HFF cells treated with cisplatin without LIPU stimulation and four replicates of media of HFF cells treated with cisplatin with LIPU stimulation was filtered to retain proteins quantified in at least three replicates of one group. The data were normalized by subtracting the median intensity value of each sample, and statistical analysis was performed using t-testing with a permutation-based FDR of 5% and S0 of 0.1. the data shows no significance after applying LIPU stimulation with cisplatin treatment.

4.3.4.3   Characterization of HFF Secretome changes after LIPU stimulation in the HFF cells

Given that the experiment's passage number is 26, to tested whether the secretive of p26 HFF's was affected by LIPU. As a result, at this passage number, it does not have a high proliferation rate; which may be caused by some cells entering the replicative senescence (Zhao et al., 2004). We used the t-

test on HFF. The t-test had a permutation-based FDR of 5%. The distribution of secretome peptides in the two groups of untreated HFF cells with and without LIPU stimulation is shown as a volcano plot in Figure 8.4 (A). When compared to untreated HFF cells without LIPU, we were able to identify 19 proteins that had significantly higher or lower levels in the untreated HFF cells with LIPU. The abundance of nineteen proteins exhibited significant difference between HFF with and without LIPU stimulation (both in the absence of cisplatin), as shown by the heat map in Figure 8.3 (B). After exposure to LIPU, we discovered that 14 of these proteins were upregulated, whereas five were downregulated.
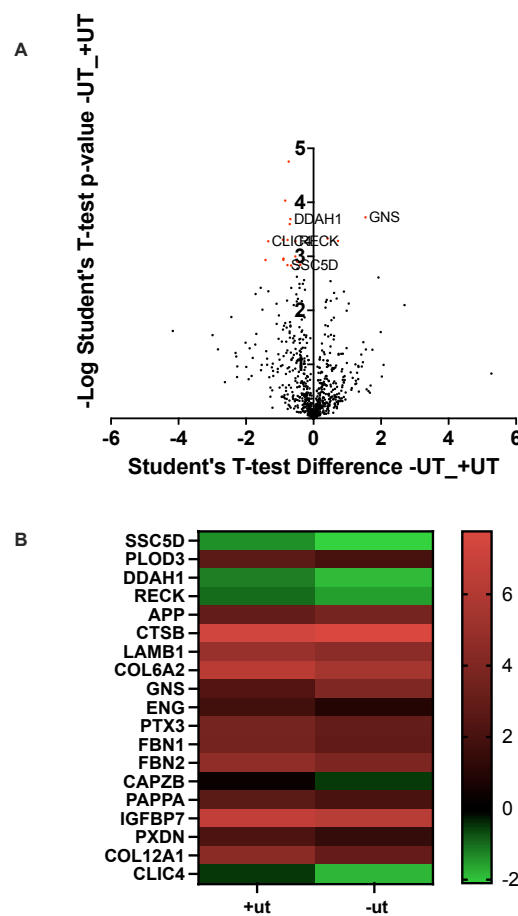
Figure 4.8 Volcano plot showing significantly proteins regulated by LIPU treatment.

A) Data from the analysis of 4 replicates of media of HFF cells untreated with LIPU stimulation and three replicates of media of untreated HFF cells without LIPU stimulation was filtered to retain proteins quantified in at least three replicates of one group (19). The data were normalized by subtracting the median intensity value of each sample, and statistical analysis was performed using t-testing with a permutation-based FDR of 5% and S0 of 0.1. The red dots on the right represent two proteins significantly upregulated after LIPU stimulation, and the red dots on the left represent 17 proteins significantly downregulated after LIPU stimulation. **B)** heatmap represents LFQ intensity of proteins that upregulated and downregulated after LIPU stimulation

We calculated the fold change for each protein to help us focus the data, and we identified five genes whose fold change is greater than 1.5, as shown in figure 9.3 (A). After LIPU stimulation, we discovered that the GNS protein was upregulated. SSC5D, DDAH1, RECK and CLIC4 were downregulated (see figure 9.4(B)). The function, location and protein expression of these five proteins was determined using the bioinformatics database UniProt. This result would enable us to comprehend better the role LIPU stimulation plays in treating age-related diseases brought on by replicative senescence, such as chronic wounds. (Tables 4.3and 4.5)
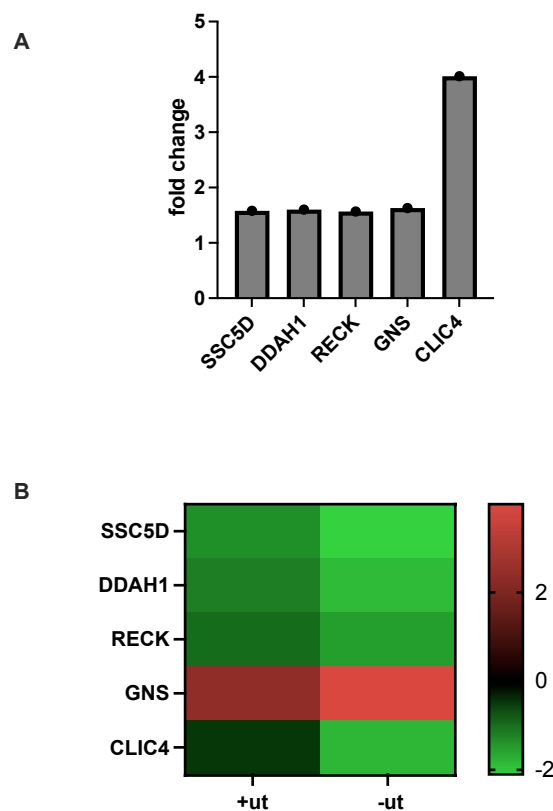
Figure 4.9 proteins significantly regulated by LIPU treatment.

A) bar chart represents proteins that have a more considerable log2 fold change (above 1.5). B) heatmap represents LFQ intensity of proteins that upregulated and downregulated after LIPU stimulation

Table 4.3 The function of proteins with substantial fold changes
The biological function of different proteins showing fold change in mass spectrometry

Gene	Function
SSC5D	binds to proteins in the extracellular matrix. Acts as a pattern recognition receptor by binding to pathogen-associated molecular patterns (PAMPs) found on Gram-positive, and Gram-negative bacteria and fungi (PRR) cell walls. It causes bacterial and fungal aggregation, preventing the release of cytokines induced by PAMP. and has no inherent bactericidal action. This may influence some epithelium surfaces' natural defence and homeostasis.
DDAH1	plays a part in regulating the production of nitric oxide.
GNS	N-acetylglucosamine-6-sulfatase is a gene that contains instructions for generating the enzyme. This enzyme is found in lysosomes and cell compartments that degrade and recycle many kinds of chemicals. Glycosaminoglycans are enormous molecules that are broken down step by step by an enzyme called N-acetylglucosamine-6-sulfatase (GAGs). The buildup of GAGs disrupts normal cellular processes and causes other lysosomal proteins to perform ineffectively.
RECK	performance as a serine protease inhibitor, inhibiting the enzymatic activity of matrix metalloproteinase-9 (MMP9) and decreasing its production. also prevents MMP2 and MMP14 metalloproteinase activity (MT1-MMP)
CLIC4	promote endothelial cell proliferation and regulate endothelial morphogenesis (tubulogenesis). is a p53 and TGF-β regulated

Table 4.3 the distribution of proteins regulated by LIPU stimulation		
The expression cite and location of proteins regulated by LIPU		
Gene	Location	Protein expression
SSC5D	Intracellular, Secreted (different isoforms) Located in Nucleoplasm, Cytosol	Cytoplasmic expression in most tissues.
DDAH1	Intracellular Located in Nucleoli, Plasma membrane, Cytosol	Cytoplasmic expression
RECK	Membrane Located in Plasma membrane	Distinct positivity in extracellular matrix with additional cytoplasmic expression
GNS	Intracellular	Cytoplasmic expression with a granular pattern in all tissues.
CLIC4	Intracellular Located in the Plasma membrane, Centrosome	Cytoplasmic and membranous expression

4.3.5 CLIC4 and RECK protein level assessed by western level

Time constraints prevented us from confirming every protein found in the mass spectrometry results. As a result, we decided to use western blot to confirm the results for one candidate. Expression of the CLIC4 was evaluated by quantifying the protein level. According to figure 4-10, which compares HFF cells with HFF cells +LIPUS, it appears that LIPUS has dramatically upregulated levels of the CLIC4 protein. There will, however, be some replicative senescent cells in the population because the passage number utilized to do this experiment was close to 26.
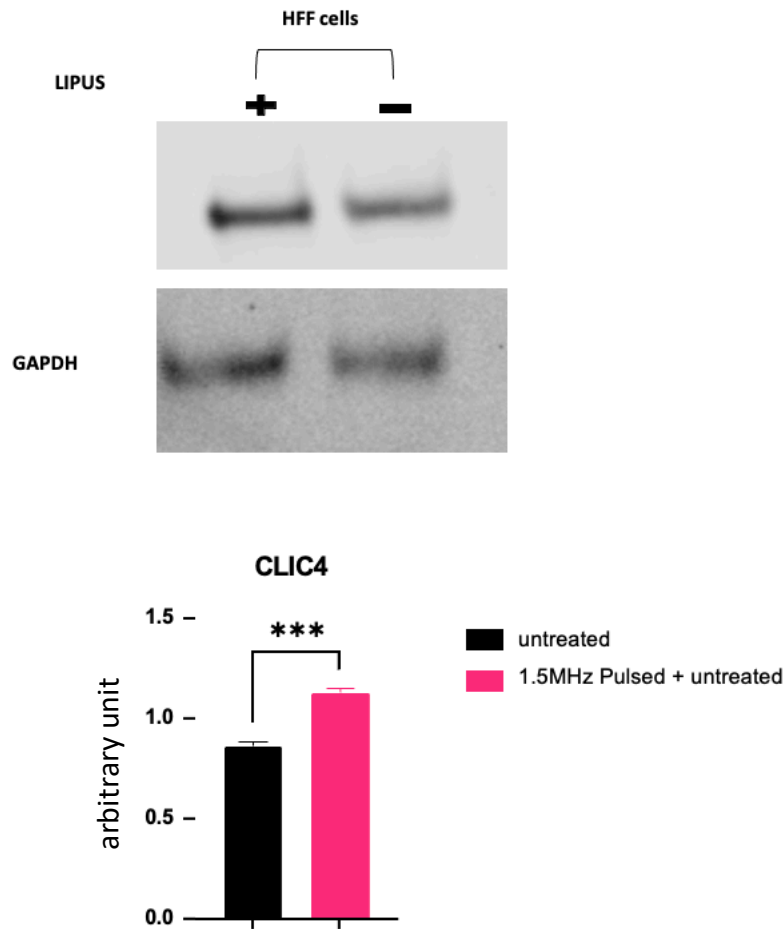
Figure 4.10 clic4 protein level

Clic4 level is significantly overexpressed in HFF cells +LIPUS (pink) compared to HFF cells (black), according to a Western blot lysate (P<0.01). (n=3 replication). Error bars represent SD. Statistical significance was calculated using a t-test.

4.4   Discussion

4.4.1   Paracrine effect

This chapter's first section was dedicated to the investigation of the SASP, or senescence-associated secretory phenotype, which was caused by the drug cisplatin. In order to examine the paracrine impact on normal HFF cells, we selected to examine the P21$^{WAF1/CIP1}$ level as a senescence marker. When cisplatin SASP medium was applied to HFF cells, which was to study the effect of SASP on normal cells. we discovered that P21$^{WAF1/CIP1}$ levels were upregulated relative to cells that

had received unconditioned media, showing that senescence may be transmitted via reinforcing senescence in HFF cells. This experiment revealed that the paracrine senescence arrest depends on the activation of P21$^{WAF1/CIP1}$ as suggested in figure 4-1 (B)(Acosta et al., 2013, Capparelli et al., 2012, Mosteiro et al., 2018). We couldn't find any appreciable change in the level of P21$^{WAF1/CIP1}$ protein when we added media from other conditions that had been treated with LIPUS, though. According to this finding, the LIPUS treatment's duration or other parameters were insufficient to have an impact on the SASP that was secreted. Because we used primary HFF cells and a passage number that is considered high for primary cells, the P21$^{WAF1/CIP1}$ level in the unconditioned medium was increased in both experiments (Crochemore et al., 2019, Morisaki et al., 1999, Kim et al., 2014, Zhao et al., 2004). . Given this, telomere shortening-induced replicative senescence could be the reason. Different experiments, like Southern Blotting and Terminal Restriction Fragment Analysis, can be used to confirm this.Ultrasound stimulation and its effect on senescent SASP. However, The Conditioned Media Experiment Has Its Limits A complex mixture of secreted components, including proteins, metabolites, exosomes, and other substances, may be found in conditioned media, albeit in varying concentrations. These factors may be difficult to identify or investigate separately due to their dilution (Duval et al., 2017). Furthermore, Experiments using conditioned media fall short of accurately simulating the complex in vivo milieu in which continuous perfusion, extracellular matrix, and cell-to-cell interactions are essential., Experiments with conditioned media typically expose recipient cells to secreted factors for a brief amount of time, which may cause them to miss long-term downstream effects (Sivagnanam and Gijs, 2013). Lastly , Non-specific effects: It can be challenging to discern the precise effects of cisplatin-induced cellular communication due to substances secreted by donor cells that are stressed or dying.

In order to evaluate the impact of LIPUS on senescent-secreted SASP, we first chose one of the proteins that SASP secretes, Interleukin 6. According to the research, IL6 is one of the SASP-released

proteins and is also known to be increased in senescent cells (Coppe et al., 2010). ELISA was used to analyse the level of IL6 protein. Even after utilising the free serum media, we anticipated could interfere with ELISA reading, the data were not reproducible using this assay's troubleshooting methods see figure 4.2. According to the cell and tissue of origin, as well as the triggers involved, SASP composition differs. Thus, our approach might not be the best choice for this application (Ortiz-Montero et al., 2017, Collado et al., 2007). If we were just looking at one candidate, this could be accomplished by using real-time PCR to investigate the IL6 gene. Consequently, a thorough examination of the senescent secretome was required. The best strategy to use was label-free quantitation using mass spectrometry. Our study of the data revealed that the cisplatin treatment affects HFF cells, supporting the conclusion from chapter 3 and demonstrating that the cells undergo a considerable change by significantly up- and down- regulating several of the secreted proteins. In addition, we discovered that 366 proteins in our results were also found in the SASP atlas (Basisty et al., 2020). Moreover, to obtain functional information from the analysis of differentially expressed peptides, one could employ pathway analysis, gene ontology (GO) enrichment analysis, and protein-protein interaction analysis.

Sadly, unlike what we saw in chapter 3 that LIPUS impacts the HFF senescent produced by cisplatin, we could not see any appreciable changes in secreted SASP following. This make it evident that while the effect of LIPUS may be restricted to cell metabolism, SASP production is unaffected. Indeed cisplatin causing the cells to enter irreversible cell cycle arrest (Sriratanasak et al., 2022). The question was whether the treatment time and dose caused greater harm than planned, which could be resolved by testing another chemotherapy-induced senescence or by attempting to lessen the cisplatin dose. Furthermore, because the mechanisms underlying chemotherapy-induced senescence are still unknown, the LIPUS was unable to reverse the SASP effect. However, by altering the LIPUS parameters, such as using continuous ultrasound instead of pulsed ultrasound or lengthening the treatment time and ultrasound amplitude, we may be able to see better results. So,

until we used alternative methods to assess the SASP, we can't say that LIPUS therapy is insufficient in this case.

4.4.2 Ultrasound stimulation and its effect on untreated HFF cells

As primary HFF cells are used, they might experience some replicative senescence with increasing the passage number. When we apply LIPUS stimulation interestingly, we notice a significant change in secreted proteins. The CLIC4 was found to be the most secreted protein that has been affected by LIPUS stimulation. The LIPUS has increased the secreted protein by a four-fold change. The CLIC family of proteins, which were initially recognized as chloride channels of intracellular membranes, includes CLIC4. based on peptide sequence it was predicted to be a channel and has been found to form a channel in in-vitro systems, but that channel function has not been demonstrated in cells. The CLIC4 typically acts as an apoptotic regulator. When DNA damage occurs, CLIC4 overexpression triggers apoptosis mediated by p53. It was interestingly discovered that CLIC4 is upregulated after LIPUS stimulation as figure 4-9 (B), suggesting a potential anti-senescent target therapy (Suh et al., 2005, Suh et al., 2007). CLIC4 is nuclear in the epidermis and upregulated in wounded skin.

The presence of Clic4 in the wound process is to enhance the ability of keratinocytes to reepithelialize the wound site (Padmakumar et al., 2012). Sphingosine 1-phosphate (S1P) causes CLIC4 to temporarily move to the plasma membrane in endothelial cells, where it mediates S1P-induced activation of Rac1 (rather than RhoA) downstream of S1P receptor 1. (S1PR1). When Hela cells are stimulated by serum or LPA, CLIC4 quickly and transiently moves from the cytosol to B1-integrin on the plasma membrane (Mao et al., 2021). When TGF-beta 1 was applied to fibroblasts, CLIC4 was elevated, which helped the fibroblasts become myofibroblasts. By boosting TGF-beta signaling in a positive feedback loop, CLIC4 plays a crucial role in the formation of a supportive tumour microenvironment. To counteract some of the tumor-enhancing effects of the cancer stroma, targeting CLIC4 in the tumour stroma should be taken into consideration (Shukla et al., 2014).

As a result of cellular stress factors such DNA damage and senescence, cytoplasmic CLIC4 moved to the nucleus. Nuclear translocation is additionally linked to apoptosis or growth stop (Suh et al., 2004). Nonetheless, we were able to identify Clic4 in the plasma membrane in our results. Hence, it is hypothesised that LIPUS treatment affects Clic4 localisation.

CHAPTER 5
Discussion & conclusion

5 Discussion

5.1 Cisplatin effect and premature senescence

Cancer cells experience apoptosis or premature senescence in response to the stress brought onby therapy. Similarly in a study done on nasopharyngeal cancer cells, the cells show signs of cellular senescence after being treated with cisplatin. At low dosages, cisplatin therapy produces cellular senescence; at large doses, it induces apoptosis (Wang et al., 1998, Demaria et al., 2017, Seluanov et al., 2001). By telomere shortening and genomic instability, cytotoxic therapy causes cellular senescence and may contribute to the early aging phenotype. Although aging is characterised by a number of loss-of-function diseases and is defined as the time-dependent functional decrease that affects most living organisms (Ness et al., 2018, Lubberts et al., 2020).

When cisplatin damages DNA, the DNA damage response (DDR) mechanism is activated, which stops the cell cycle. The DDR pathway begins with the recruitment of Rad3-Related (ATR) and Ataxia Telangiectasia Mutated (ATM) kinases to the sites harbouring DSBs. As seen in figures 3-6& 3-7, which demonstrates a rise in histone H2AX at Ser139 (-H2AX) in cells treated with cisplatin, this recruitment results in the phosphorylation of hundreds of proteins, including γ-H2AX (Mikula-Pietrasik et al., 2020). Figure 3-8 shows that following cisplatin therapy, there is an increase in p21 $^{WAF1/CIP1}$. Another cell cycle inhibitor, p21^{Cip1}, whose transcriptional activity is controlled by p53 and functions as a downstream effector of p53, is upregulated and prevents the reinitiating of cell division (Qian and Chen, 2013, Sriratanasak et al., 2022). Figure 3-5 reveals Senescence-associated cell growth brought on by an accumulation of proteins is one of the most prominent senescence markers we see in HFF cells after cisplatin therapy (Ksiazek et al., 2007).

According to the mass spectrometry chapter, 366 proteins were either upregulated or

downregulated after cisplatin treatment, leading to the development of robust senescence-associated secretory phenotype (SASP) in all HFF senescent cells (Sun et al., 2018). By changing the protein level, this finding in the figure 4-7 supports the hypothesis that cisplatin has an LIPUS effect on senescent skin fibroblasts.

After determining the impact of cisplatin on HFF cells through the use of several senescence markers. We made a move to examine the impact of LIPUS on these markers. Our findings indicated that LIPU had a beneficial impact on certain senescence markers by reducing their impact. In HFF cells treated with cisplatin, a strong SA β—GAL signal is found associated with cell growth. As shown in figure 3-5, we first see a change in cell shape and a decrease inSA β—galactosidase activity after LIPUS stimulation is applied to treated cells. Positive results indicated that LIPUS stimulation had an impact on the senescent cell itself. Nonetheless, we notice some staining in untreated cells; this may be because our HFF cells are getting older, as SA β—GAL activity rises with aging (de Mera-Rodriguez et al., 2021). As cisplatin is a medication that harms DNA and prevents DNA production. In reaction to DNA double strand breaks (DSBs), γ--H2AX is formed (Basu and Krishnamurthy, 2010). The biomarker phosphorylated histone H2AX has emerged as a potent tool for tracking DNA DSBs. (Ivashkevich et al., 2012). Intriguingly, we discovered that after LIPUS treatment, the γ -H2AX foci either reversed or decreased in cells treated with cisplatin but it is not statistically significant as in figures 3-6 & 3-7. This reduction's mechanism is still unknown. As the number of cells was about the same as in figure 3-8, it was impossible to conclude that the reduction was due to cisplatin killing some of the cells. Another thing we did was calculate the integrated intensity of individual foci, which adds together all the pixels in a location and gives you a total value per cell and clearly shows us that the drop is due to exposure to LIPUS stimulation, which caused the cell cycle halt.

As one of the signs indicating cells are becoming senescent, upregulation of p21$^{WAF1/CIP1}$ is recognised to play a significant role in developmental senescence (Kumari and Jat, 2021). In figure 3-8 applying LIPUS stimulation appears to reduce the protein level in p21$^{WAF1/CIP1}$, which is another sign of the beneficial effects LIPUS has on the amount of HFF senescence.

When conducting this research, it was questioned if cisplatin was permanently halting the cell cycle or if its effects were only temporary. The answer was to wait three days after the cisplatin treatment before initiating the LIPUS stimulation in order to measure the p21$^{WAF1/CIP1}$ protein level. The outcome follows the same pattern as all of the senescent markers we examined. This verified that cisplatin appears to be permanently halting the cell cycle.

Sadly, despite the beneficial effect LIPUS stimulation has on HFF senescent cells. The same impact on proteins released by SASP was not seen (figure 4-6). Our supposition is that either the cisplatin effect was too severe for the cells, or LIPUS is unable to have an impact on SASP. It is necessary to collect further data by experimenting with various LIPUS parameters and observing how they affect SASP secretion.

The use of a single cell line is one of the study's limitations. as organisms are composed of interconnected networks of different cell types and their microenvironments. Important interactions and feedback loops might be missed if only one type is investigated, leaving an incomplete picture and potentially false conclusions. Additionally Many diseases involve abnormalities in different cell types and their interactions. Examining one type may uncover interesting mechanisms, but translating these discoveries into effective therapies often requires an understanding of the bigger picture and how targeting that specific cell type affects the entire system.

5.1.1 p21$^{waf1/cip1}$ and chronic wound

Although p21's role in cellular senescence and wound healing has been thoroughly investigated, its precise function in chronic wounds is still being researched. Here are a few possible roles for p21: p21 functions as a CDK inhibitor, which can cause fibroblasts and other cell types in the wound bed to enter a cell cycle arrest. During the early phases of healing, this arrest can be advantageous because it permits regulated cell proliferation and extracellular matrix deposition(Childs et al., 2015). Senescence is a stress-induced permanent cell cycle arrest state that is facilitated in part by p21. Senescent cells proliferate and release pro-inflammatory factors from chronic wounds, which may impede healing and exacerbate fibrosis. Depending on the situation, p21 can have both pro- and anti-inflammatory effects. It can both encourage the release of pro-inflammatory cytokines and suppress NF-κB signalling, which reduces inflammation (Jun and Lau, 2010).

Research has demonstrated that p21 expression is higher in chronic wounds than in acute wounds, indicating that it may play a role in poor healing. shown that, in comparison to fibroblasts from acute wounds, those from chronic wounds have higher levels of p21 expression and a senescent phenotype. These fibroblasts' ability to migrate and proliferate was partially restored after receiving treatment with a p21 inhibitor(Jiang et al., 2020). On the other hand, research has demonstrated that inhibiting p21 expression has enhanced wound closure and decreased inflammation(Zeng et al., 2020, Manu et al., 2019).

5.1.2 Pathways Regulating Senescence

Different but overlapping pathways control both transient and chronic senescence.

The first pathway for chronic senescence is p53-p21, which is triggered by a number of stressors including oxidative stress and DNA damage. p21 is activated by p53, which results in senescence and cell cycle arrest. The second one, which is p16-INK4a-Rb independent of p53, is frequently connected to telomere shortening-induced replicative senescence. p16 blocks CDK4/6, which causes cell cycle arrest and Rb activation. moreover, the DNA damage response (DDR). Through a variety of DDR

pathways, such as ATM-Chk2 and ATR-Chk1, persistent DNA damage can cause chronic senescence. These pathways ultimately converge on activation of p53 or p16. The last is Epigenetic modifications: Histone modifications and DNA methylation have the ability to activate pro-senescent genes and silence genes that promote proliferation, which can lead to a chronic senescent state(Sacco et al., 2021).

While there are several pathways leading to transient senescence, one of them is p21-DREAM. In this pathway, p21 binds to the DREAM complex, causing cell cycle arrest but not the full senescent phenotype. When the stress stops, cells that have undergone DREAM-mediated senescence can frequently revert to normal cell cycle progression. Moreover, p53-miR-34a: p53 can trigger the expression of miR-34a, which targets genes involved in DNA replication and cell cycle progression, resulting in a brief arrest of the cell cycle. Lastly, inflammatory signals: By activating NF-κB and causing the expression of p21 or p16, pro-inflammatory cytokines such as TNF-α can cause temporary senescence. This may be a defence mechanism to stop the growth of cells in tissues that are inflamed. The reversibility of the senescent state is the primary distinction between the pathways. Transient senescence pathways enable cells to re-enter the cell cycle after the stressor is removed, whereas chronic senescence pathways result in permanent cell cycle arrest (Young et al., 2022, Kumari and Jat, 2021).

5.1.3 LIPUS effect on aged skin fibroblasts

Unexpected results are provided to us by the mass spectrometry results arbitrarily. On untreatedHFF, LIPUS had a discernible effect. Assuming that the HFF used in this experiment was olderfibroblast, replicative senescence of the cells may have occurred.

The stimulation of the LIPUS has been observed to influence the expression of Chloride intracellular channel 4 (CLIC4) as in figure 4-10. Many physiological signals, such as p53, as well as biological stressors like DNA damage and metabolic toxicity cause this protein to be

produced. (Fernandez-Salas et al., 2002). Variations in CLIC4 expression linked to a number of clinical diseases, including cancer (Suh et al., 2007). According to fibroblastsoverexpressing CLIC4, tumour cell motility and invasion are increased in a TGF-dependent manner, and the epithelial to mesenchymal transition is promoted. This suggests that high stromal CLIC4 levels contribute to the growth of the tumour. Hence, through boosting TGF -signaling in a positive feedback loop, CLIC4 plays a crucial role in the formation of a favourable tumour microenvironment. To counteract some of the tumor-enhancing effects of the cancer stroma, targeting CLIC4 in the tumour stroma should be taken into consideration (Shukla et al., 2014).

In a study using CLIC4 knockout mice, it was discovered that up to 40% of null mice experienced spontaneous skin erosions. This suggests that CLIC4 aids in the re-epithelialization of skin and corneal wounds by promoting epithelial migration through a mechanism that may include a damaged TGF- beta pathway (Padmakumar et al., 2012). In anotherstudy, they discovered that endothelial cells with lower levels of CLIC4 expression were less able to promote cell growth and create networks. This method has a good impact when used asa targeting therapy for treating wounds because of the function of senescence in developing chronic wound and the increase in CLIC4 expression in HFF following LIPUS stimulation.

Recent research has identified CLIC4 as a Scleroderma (SSc) and cancer-associated fibroblast activation driver. TGF- signaling controls CLIC4 expression and activity via the transcription factor SMAD3. By controlling the expression of the targetable pathway known as CLIC4, fibroblast activation in SSc and other fibrotic diseases can be prevented. (Wasson et al., 2021).

5.2   Cancer the wound that do not heal

Because the molecular and metabolic processes involved in wound healing and tumour stroma growth and development are comparable, the saying "cancer is a wound that does not heal"

describes how cancer and wounds have similar characteristics (Byun and Gardner, 2013). During

the healing process for wounds, platelet-derived growth factor (PDGF) stimulates fibroblast and

pericyte migration and proliferation, which are subendothelial cells that protect capillary

integrity. Monocytes that are already present start to multiply and develop into macrophages.

What is referred to as granulation tissue is created by this process. Hence, a significant and

widespread phenotypic reprogramming of practically all cellular components can be used to

describe the proliferation phase. Each time, this reprogramming is changed in the tumour

stroma, and these modifications ultimately encourage tumour growth (Dvorak2015). One of

the phenotypically active and perplexing cellular elements of the tumour stromaand wound

healing process is the fibroblast, by far. Fibroblasts play a crucial role in tissue homeostasis and

wound healing. They also govern the form and function of healthy tissues, and they temporarily

take part in tissue repair following acute inflammation. Key participantsin the process of

carcinogenesis are the fibroblasts seen in tumours, which are also known as cancer-associated

fibroblasts (CAFs) (Hanahan and Weinberg, 2011). In the tumour microenvironment, CAFs can

modify it. Changes in miR expression, which have an impact on target genes post-

transcriptionally, are also a part of the reprogramming of cells into CAFs (Mitra et al., 2012).

Moreover, epigenetic alterations have been discovered in CAFs, including global DNA

hypomethylation, which is typically found in cancerous cells (Jiang et al., 2008).When combined,

all of these gene regulation alterations lead to a change in the secretome andmetabolome,

which not only keeps myofibroblasts in their differentiated form in an autocrinemanner but also

stimulates cancerous cells in a paracrine manner (Kojima et al., 2010, Ohlundet al., 2014).

CAFs release soluble substances similar to fibroblast senescent cells. It was again another trait

that CAFs and fibroblast senescence shared. By paracrine interactions involving the productionof

several soluble molecules, CAFs coordinate important pathophysiological events in the

development of cancer. Several cytokines, including CCL7 and CXCL12 (Orimo et al., 2005,Jung et al., 2010). as well as growth factors including hepatocyte growth factor (HGF), connective tissue growth factor (CTGF), epidermal growth factor (EGF), insulin-like growth factor (IGF), nerve growth factor (NGF), and members of the Wnt family (Rasanen and Vaheri,2010, Cirri and Chiarugi, 2011).

Given that as stated above, we hypothesised that LIPUS may benefit CAFs in a manner similarto what we saw with fibroblast senescence. which demand investigation.

5.3   Senescent and aging disease

We can better comprehend how LIPUS might enhance life quality and lengthen human life by knowing the connection between senescent cells and age-related illness. The risk of age-relatedneurodegenerative illnesses is rising with the aging population. Neurodegenerative illnesses like Alzheimer disease age-associated cognitive impairment are characterised by a progressivedecline in the structure and performance of the nervous system. The central nervous system (CNS) changes significantly as people age, including atrophy of the brain and spinal cord, a loss of grey matter, and the buildup of Amyloid beta (A) plaques, neurofibrillary tangles, and senescent cells (Wyss-Coray, 2016). 2021 research on mice that have aged. When LIPUS wasused, the researchers' findings drew our attention because they showed that it improved a number of age-related conditions such bone loss, ovarian structure, immune system regulation, and endurance capacity. which, as a component of an age-related illness, may potentially have an impact on senescent cells(Chen et al., 2022).

Each age-related disease's incidence rate increases nearly exponentially with age. due to immune system deterioration as people age (Palmer et al., 2018). The apparent exponential increase in incidence rate with age has been shown in recent years to be causal for a wide variety of age-related pathologies: the growth of senescent cells (Xu et al., 2018, Baker et al.,

2016). Given that cellular senescence is characterised by essentially irreversible replicative arrest, apoptosis resistance, and frequently increased protein synthesis, metabolic changes with increased glycolysis, decreased fatty acid oxidation, increased generation of reactive oxygen species (ROS), and, occasionally, acquisition of a senescence-associated secretory phenotype (SASP) are also common (Katzir et al., 2021, Wissler Gerdes et al., 2020).Senescence is a factor in age-related disorders, as has been demonstrated in numerous research.Senescent cells begin to amass as tissue ages, and the produced SASP gives cancer cells the ability to multiply and infiltrate nearby tissue (Coppe et al., 2010).

Moreover, the most prevalent neurodegenerative illness is Alzheimer's disease. Older brains definitely contain a vast panel of pro-inflammatory variables, including altered signalling, an accumulation of senescent glia, and a loss in neurons in aged adults (Harry, 2013). Also, as people age, they aremore susceptible to cardiovascular illness, which has been related to telomere shortening, oneof the causes of senescence (Kurz et al., 2006).

Every strategy utilised to combat senescent cells, or their secretion will have a favourable effect on various facets of human existence, extending life expectancy. Delaying the onset of age-related disorders is possible by clearing the senescent. That will relieve the burden of treating age-related illness from the healthcare provider and enhance the social and economic well-being of the aged.

5.4   Future work

It is known that senescent cells behave differently since a study found that the cell of origin, rather than the inducer or type of cellular senescence, is the major contributor to the gene expression profile that results in a senescent cell (Casella et al., 2019). The marker and SASP secretion may be impacted differently by this. As a result, handling senescent cells is challenging because we only evaluated one type of one cell and one kind of senescence

128

inducer. As opposed to the older human foreskin fibroblast we used, which had more passages, we advise using younger cells for better results. The fact that each experiment took a while to complete prevented us from testing every senescent marker. Other LIPUS treatment parameters may have various effects on senescence, but we were unable to evaluatethem. For example, continuous ultrasound may have a better effect than pulsed ultrasound.

Increasing ultrasound amplitude, or treatment duration may produce better results.

This effort therefore does not address the ultrasonic mechanism underlying this effect. Tests on several senescence markers are being done to demonstrate how it is influencing the senescent cells. To better understand how LIPUS works and whether it affects the senescent pathway, more research must be done. Focus should be placed further on how the LIPUS might influence DNA damage and how it was able to lessen DNA damage, which could pave the way for new chemotherapy combination therapies that protect healthy cells from the harm caused by chemotherapy. It is necessary to examine additional LIPUS parameters to determine whether they have an improved or increased capacity for clearing senescent cells.

A new method has also been developed that makes it possible to view senescent cells in alive animals and live cells. This made it possible for us to test the LIPU's potential on living organisms by screening senescence in pertinent physiological and pathological contexts without harming the cells and monitoring them over time to gain further insight into the functions and consequences within the tissue.

To make senescence more strategically targeted and quantifiably characterised, novel senescent markers and detection techniques must be used (Gonzalez-Gualda et al., 2021).

5.4.1   The senescent surfaceome

Well known Age and the senescent phenotype have also been linked to the altered plasma

membrane lipid content, which causes an increase in membrane rigidity (Momchilova et al., 2014, Fulop et al., 2012). Based on their biomechanical characteristics, cells may be identified via tangential flow filtration (Willoughby et al., 2016). concentrating on biochemical changes that can be observed by Raman and infrared (IR) spectroscopy, such as the creation and destruction of chemical bonds in senescent cells. The metabolic makeup of a cell can be mapped using a wide range of wavelengths and analysis of the scattered light profiles, which can be utilised to distinguish between different cell types and cellular states (Eberhardt et al., 2018, Eberhardt et al., 2017).

known The alteration of the plasma membrane lipid composition, which results in increased membrane rigidness, has also been associated with age and the senescent phenotype (Momchilova et al., 2014, Fulop et al., 2012). tangential flow filtration could be used to detect

5.4.2 The lysosomal compartment

By evaluating the SA   —gal, new fluorescent and two-photon probes are being developed for the detection and monitoring of senescence in living animals(Paez-Ribes et al., 2019). Furthermore, intrinsic   -galactosidase have been created with applications in magnetic resonance imaging (MRI, photoacoustic tomography, and fluorescence imaging (Asanuma et al., 2015, Lilley et al., 2020, Yu et al., 2012).

5.4.3 Transcriptional signatures

Senescent programming involves significant changes in gene expression that are tightly regulated and occur as a result of a wide range of signalling pathways being activated and downregulated (Munoz-Espin and Serrano, 2014). Gene signatures for cellular senescence are tissue or organ-specific signatures that are seen in specific physiological or pathological situations. Transcriptional analyses are crucial for identifying senescence and its propensity

to burden tissues, but they can also help identify new, more targetable biomarkers and druggable targets (Wei et al., 2019). Numerous techniques, including RNA sequencing (RNA-Seq), single-cell RNA sequencing (scRNA-Seq), microarrays, and quantitative real-time PCR (qPCR), can be used to accomplish this.

5.5   Conclusion

In conclusion, a promising, less invasive, and economical method appears to have a favorable effect on HFF senescent cells. Many senescent indicators are becoming less prevalent in the LIPUS. In this study LIPU has shown It can decreased lysosomal activity, cisplatin-induced DNA damage, and the p21$^{WAF1/CIP1}$ protein level. Due to the fact that we used older HFF cells with a passage number over 22, a favorable effect is also seen on regular HFF after administering LIPUS stimulation for the same amount of time. This response confirms the pattern we saw in cells treated with cisplatin plus LIPUS. Also, we noticed a change in the proteins that these cells released following the LIPUS stimulation. These are encouraging findings that may aid in the prevention of DNA damage-induced senescence and the elimination or reduction of the senescent impact in normal cells.

CHAPTER 6

Appendices

6 Appendices

Figure 6-1: failed attempt to detect p16^{inka4} protein level using western blot

A) represent P16inka4 B) represent the GAPDH
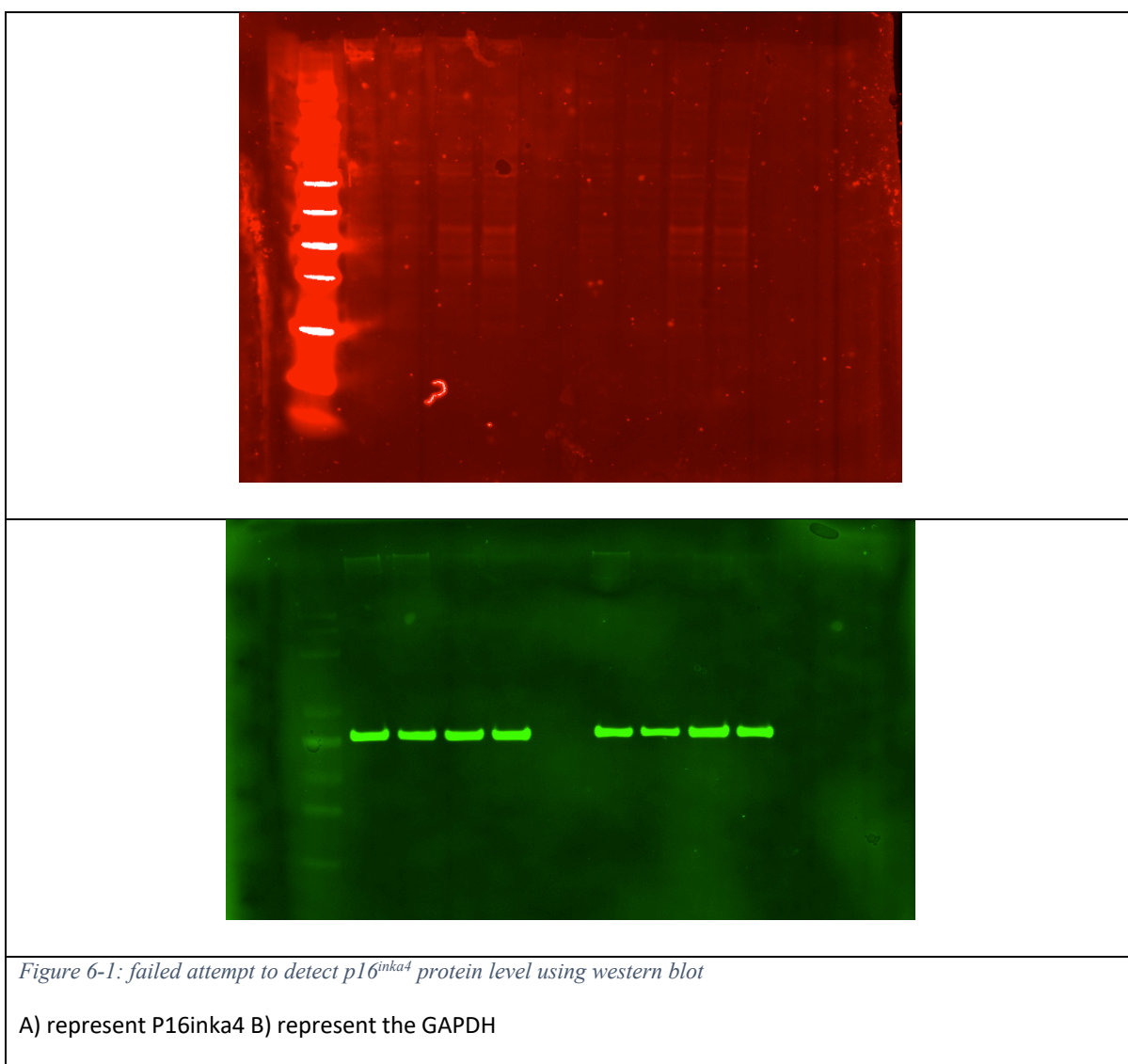
Table 6-1 HFF versus HFF+ LIPUS SASP secretome profile

Protein name	Gene name	LFQ intensity Control	LFQ intensity Ultrasound
Fibronectin	FN1	1379400000	2483700000
Collagen alpha-2(I) chain	COL1A2	1638500000	1124300000
Collagen alpha-1(I) chain	COL1A1	1809600000	909820000
72 kDa type IV collagenase	MMP2	517120000	963690000
Metalloproteinase inhibitor 1	TIMP1	505370000	594580000
Stromelysin-1	MMP3	276950000	460520000
SPARC	SPARC	243880000	497200000
Plasminogen activator inhibitor 1	SERPINE1	95800000	495540000
Lumican	LUM	297950000	404870000
Thrombospondin-1	THBS1	299820000	298080000
Tenascin	TNC	238150000	294110000
Collagen alpha-3(VI) chain	COL6A3	128020000	332580000
Fibulin-1	FBLN1	233920000	261290000
Fibrillin-1	FBN1	255970000	213570000
Insulin-like growth factor-binding protein 4	IGFBP4	442400000	140300000
Collagen alpha-1(VI) chain	COL6A1	78697000	242030000
Cathepsin B	CTSB	171390000	202340000
Insulin-like growth factor-binding protein 7	IGFBP7	279160000	169580000
Procollagen C-endopeptidase enhancer 1	PCOLCE	142070000	157100000
Metalloproteinase inhibitor 2	TIMP2	138200000	141240000
Actin, cytoplasmic 2	ACTG1	55248000	142460000
Beta-2-microglobulin	B2M	203370000	101360000
Glia-derived nexin	SERPINE2	56463000	139940000
Sulfhydryl oxidase 1	QSOX1	68127000	127100000
Laminin subunit gamma-1	LAMC1	87338000	121550000
Follistatin-related protein 1	FSTL1	173840000	72828000
CCN family member 3	CCN3	184280000	100770000
Cathepsin D	CTSD	43877000	91586000
Insulin-like growth factor binding protein 3 isoform b	IGFBP3	138160000	87164000
Interstitial collagenase	MMP1	48131000	81591000
EGF-containing fibulin-like extracellular matrix protein 1	EFEMP1	102600000	82629000
Extracellular matrix protein 1	ECM1	72113000	59651000
Collagen alpha-1(III) chain	COL3A1	45444000	63097000
Complement C1r subcomponent	C1R	59596000	59290000
Insulin-like growth factor-binding protein 6	IGFBP6	237370000	30648000
Collagen alpha-2(VI) chain	COL6A2	22893000	70224000
Cell cycle control protein 50A	TMEM30A	0	53000000
Alpha-enolase	ENO1	23181000	60533000
Cysteine and glycine-rich protein 1	CSRP1	109470000	55192000
Gelsolin	GSN	29480000	56897000

Fibulin-1	FBLN1	92460000	34303000
Tumor necrosis factor receptor superfamily member 11B	TNFRSF11B	28888000	51345000
Laminin subunit beta-1	LAMB1	46268000	48724000
Fibrillin-2	FBN2	53987000	50881000
Progranulin	GRN	140940000	41706000
Profilin-1	PFN1	36886000	51062000

Actin, alpha skeletal muscle	ACTA1	7108000	57458000
Galectin-1	LGALS1	84930000	52770000
Triosephosphate isomerase	TPI1	32091000	50737000
Ectonucleotide pyrophosphatase/phosphodiesterase family member 2	ENPP2	15436000	50050000
Peptidyl-prolyl cis-trans isomerase A	PPIA	37086000	49578000
Stanniocalcin-2	STC2	38681000	34700000
Cathepsin L1	CTSL	28190000	40702000
Nucleobindin-1	NUCB1	34409000	39574000
Plasma protease C1 inhibitor	SERPING1	9528800	37977000
Alpha-actinin-4	ACTN4	10853000	40127000
Calumenin	CALU	17190000	36732000
Filamin-A	FLNA	27710000	33994000
Filamin-C	FLNC	29576000	33311000
Pregnancy-specific beta-1-glycoprotein 4	PSG4	34335000	32406000
Laminin subunit alpha-4	LAMA4	11255000	36261000
Complement C1s subcomponent	C1S	25853000	39878000
NPC intracellular cholesterol transporter 2 (Fragment)	NPC2	44592000	28457000
Superoxide dismutase [Cu-Zn]	SOD1	60581000	28164000
Histone H1.2	H1-2	110850000	14814000
Vimentin	VIM	52487000	22086000
Fructose-bisphosphate aldolase	ALDOA	25346000	30732000
Vinculin	VCL	17902000	24042000
Dickkopf-related protein 3	DKK 3.00	16488000	31268000
Phosphatidylethanolamine-binding protein 1	PEBP1	26352000	25073000
Insulin-like growth factor-binding protein 5	IGFBP5	44321000	26213000
Cathepsin Z	CTSZ	13434000	28583000
Prosaposin	PSAP	10609000	32360000
Transgelin	TAGLN	6581600	25824000
Serpin H1	SERPINH1	13757000	28367000
Mesogenin-1	MSGN1	0	25341000
Pentraxin-related protein PTX3	PTX3	7977400	25037000
Collagen alpha-1(XII) chain	COL12A1	6828300	23733000
Vasorin	VASN	15821000	21001000
Cathepsin K	CTSK	15336000	20782000
Transketolase	TKT	15820000	20928000
Cystatin-C	CST3	43942000	20944000
Thioredoxin	TXN	15216000	15451000
Cofilin-1 (Fragment)	CFL1	13049000	22566000
Phosphoglycerate mutase 1	PGAM1	11927000	23611000
Collagen triple helix repeat-containing protein 1	CTHRC1	7536300	18811000
Peroxiredoxin-1	PRDX1	10236000	17197000
Annexin A2	ANXA2	10328000	19645000
SH3 domain-binding glutamic acid-rich-like protein 3	SH3BGRL3	15682000	21282000
Thymosin beta-4	TMSB4X	76472000	3847800
Spondin-2	SPON2	14860000	24263000
Hemoglobin subunit alpha	HBA1	0	19723000
Putative nucleoside diphosphate kinase	NME2P1	0	15927000
High mobility group protein B1	HMGB1	30504000	19373000
Beta-hexosaminidase subunit beta	HEXB	4635900	17647000
Moesin	MSN	11694000	21653000
Exostosin-1	EXT1	7433100	16148000
L-lactate dehydrogenase A chain	LDHA	21669000	14738000

Pigment epithelium-derived factor	SERPINF1	8227200	18916000
Decorin	DCN	27242000	7915400
Collagen alpha-2(V) chain	COL5A2	15629000	13270000
Thrombospondin-2	THBS2	11952000	14163000
Mannan-binding lectin serine protease 1	MASP1	9908200	13635000
Dystroglycan	DAG1	12432000	12872000
Activated RNA polymerase II transcriptional coactivator p15	SUB1	0	11081000
Peroxiredoxin-6	PRDX6	7332900	9092000
Nidogen-1	NID1	13525000	9784800
Procollagen-lysine,2-oxoglutarate 5-dioxygenase 1	PLOD1	4143800	11732000
N-acetylglucosamine-6-sulfatase	GNS	8521900	11170000
Collagen alpha-2(IV) chain	COL4A2	16037000	8281700
Retinol-binding protein	RBP4	0	11842000
Coiled-coil domain-containing protein 144A	CCDC144A	62076000	0
Transmembrane protease serine	TMPRSS11A	0	8613300
Protein S100-A11	S100A11	7240500	10062000
L-lactate dehydrogenase (Fragment)	LDHB	3457600	11848000
Endosialin	CD248	11760000	11601000
Protein/nucleic acid deglycase DJ-1	PARK7	10267000	9970900
Dickkopf-related protein 1	DKK 1.00	23899000	0
Nidogen-2	NID2	7341700	6722600
Ubiquitin-40S ribosomal protein S27a	RPS27A	11340000	7434900
Rho GDP-dissociation inhibitor 1 (Fragment)	ARHGDIA	7258400	9065400
Pregnancy-specific beta-1-glycoprotein 5	PSG5	3540200	10246000
14-3-3 protein zeta/delta	YWHAZ	2309700	16334000
Peroxidasin homolog	PXDN	4036400	8934600
Fibulin-5	FBLN5	7347900	13341000
Cytochrome c oxidase assembly factor 6 homolog	COA6	0	6624100
Protein S100 (Fragment)	S100A6	0	9703200
Major prion protein	PRNP	4514200	9965000
Glucose-6-phosphate isomerase	GPI	1854400	8550000
Actin, cytoplasmic 1	ACTB	0	7860100
Transforming growth factor-beta-induced protein ig-h3	TGFBI	3050500	9179700
Microfibril-associated glycoprotein 4	MFAP4	0	8769100
Peptidyl-prolyl cis-trans isomerase B	PPIB	8532700	7127000
Out at first protein homolog	OAF	2524800	8737500
Laminin subunit alpha-2	LAMA2	5396100	8817900
Fibrillin-1 (Fragment)	FBN1	0	8205800
Zinc finger protein 577 (Fragment)	ZNF577	0	425450
Peptidyl-prolyl cis-trans isomerase FKBP1A	FKBP1A	16156000	5852200
Brain acid soluble protein 1	BASP1	10310000	6778400
Tripeptidyl-peptidase 1	TPP1	3761800	7591600
CD109 antigen	CD109	1575000	7545800
Glutathione S-transferase P	GSTP1	2992800	8996800
Beta-hexosaminidase	HEXA	2286700	6971200
Exostosin-2	EXT2	0	7841500
Olfactomedin-like protein 3	OLFML3	3910200	6924300
Transgelin-2 (Fragment)	TAGLN2	4559600	8100600
Tropomyosin alpha-4 chain	TPM4	14440000	6746700
Stromelysin-3 (Fragment)	MMP11	0	7508700
Heat shock cognate 71 kDa protein	HSPA8	4419400	6304900
Latent-transforming growth factor beta-binding protein 4	LTBP4	14262000	6496800

Pyruvate kinase	PKM	2996500	6832000
Y-box-binding protein 1 (Fragment)	YBX1	8165300	5518000
Apolipoprotein E	APOE	1868800	6444300
Malate dehydrogenase (Fragment)	MDH1	4894400	6046900
CCN family member 1	CCN1	11800000	5353400
Integrin beta-like protein 1	ITGBL1	8731900	4679200
Insulin-like growth factor II	IGF2	10339000	0
Ubiquitin carboxyl-terminal hydrolase	UCHL1	5102100	0
Alpha-actinin-1	ACTN1	2606100	6210500
Calsyntenin-1	CLSTN1	2950100	5075100
Latent-transforming growth factor beta-binding protein 2	LTBP2	8879600	3470400
Apolipoprotein B-100	APOB	0	6529700
Insulin-like growth factor-binding protein 2	IGFBP2	11223000	6298800
Rab GDP dissociation inhibitor beta	GDI2	2039500	5821200
M-phase inducer phosphatase 3 (Fragment)	CDC25C	0	6203700
Acyl-CoA-binding protein	DBI	8226000	4624300
Dihydropyrimidinase-related protein 2	DPYSL2	4088100	4350200
Elongation factor 1-alpha 1	EEF1A1	0	5350500
SH3 and PX domain-containing protein 2A	SH3PXD2A	0	5380800
Cystatin-B	CSTB	6006000	3912500
Cysteine-rich motor neuron 1 protein	CRIM1	4939000	4698000
Zinc finger protein 106 (Fragment)	ZNF106	0	4770000
Dipeptidyl peptidase 1	CTSC	2061200	4108100
CCN family member 2	CCN2	9126400	2445700
Myristoylated alanine-rich C-kinase substrate	MARCKS	8322800	3781600
Caldesmon (Fragment)	CALD1	9861000	0
Inactive serine protease PAMR1	PAMR1	4170200	3767800
Unconventional myosin-VIIa (Fragment)	MYO7A	25915000	0
Annexin A1	ANXA1	2488900	4669700
Tumor necrosis factor receptor superfamily member 10C	TNFRSF10C	0	4977200
Superoxide dismutase [Mn], mitochondrial	SOD2	1759400	4526300
Metallothionein-2	MT2A	8754600	2659100
Semaphorin-7A	SEMA7A	3477200	4116000
Complement C4-B	C4B	0	4663200
Sushi, von Willebrand factor type A, EGF and pentraxin domain-containing protein 1	SVEP1	4250600	5393900
Growth arrest-specific protein 6	GAS6	2178500	3802400
Endothelial differentiation-related factor 1	EDF1	11818000	0
Carboxypeptidase A4	CPA4	2112600	3524300
Vascular endothelial growth factor C	VEGFC	3844300	4598400
LIM and SH3 domain protein 1	LASP1	0	3221200
Plasminogen activator inhibitor 2	SERPINB2	1720900	4086700
Inactive tyrosine-protein kinase 7	PTK7	4129500	2707700
Gamma-glutamyl hydrolase	GGH	0	4091700
Thioredoxin reductase 1, cytoplasmic	TXNRD1	1990700	4082700
Laminin subunit alpha-1	LAMA1	3279800	3491200
A disintegrin and metalloproteinase with thrombospondin motifs 1	ADAMTS1	0	2886100
Lysosomal Pro-X carboxypeptidase	PRCP	0	4011000
Arylsulfatase A	ARSA	1623800	3329600
Calmodulin-2	CALM2	0	3776900
Reticulocalbin-3	RCN3	3523100	2919600
Alpha-2-macroglobulin	A2M	2098600	2854900

Collagen alpha-1(IV) chain (Fragment)	COL4A1	3160600	3945100
Microtubule-associated protein 4 (Fragment)	MAP4	0	2801100
Deoxyribonuclease-2-alpha	DNASE2	4115700	2710500
14-3-3 protein epsilon	YWHAE	455270	3512200
Aldo-keto reductase family 1 member B1	AKR1B1	0	3313600
Basement membrane-specific heparan sulfate proteoglycan core protein	HSPG2	5100000	2420700
Cadherin-2	CDH2	1153000	3690300
45 kDa calcium-binding protein	SDF4	2021800	0
Sterile alpha motif domain-containing protein 15	SAMD15	0	2886900
Glyceraldehyde-3-phosphate dehydrogenase	GAPDH	2767700	2763300
Serine protease HTRA1	HTRA1	1953500	3125700
Retinoic acid receptor responder protein 2 (Fragment)	RARRES2	0	2403100
Coactosin-like protein	COTL1	0	3082000
C-type lectin domain family 11 member A	CLEC11A	3203600	0
Desmoglein-1	DSG1	4685400	2953200
Lysosomal protective protein	CTSA	0	2856300
Aldo-keto reductase family 1 member A1	AKR1A1	0	2755900
Lysyl oxidase homolog 2	LOXL2	6302400	448120
Septin-14	SEPTIN14	0	2820400
Acid ceramidase	ASAH1	0	2641600
Symplekin	SYMPK	0	2696900
Prostaglandin-H2 D-isomerase	PTGDS	0	2690000
Protein-lysine 6-oxidase	LOX	6076200	673530
Serpin B6	SERPINB6	2197500	2192700
Alpha-N-acetylglucosaminidase	NAGLU	0	2576700
Macrophage migration inhibitory factor	MIF	0	2003100
Proteasome subunit alpha type-7	PSMA7	0	2485500
Golgi membrane protein 1	GOLM1	1444900	2036000
Stromal cell-derived factor 1	CXCL12	0	1545000
Disintegrin and metalloproteinase domain-containing protein 9	ADAM9	5443300	1418000
Cytoplasmic dynein 1 intermediate chain 2 (Fragment)	DYNC1I2	0	1576100
Anthrax toxin receptor 1 (Fragment)	ANTXR1	0	2103500
Lysosome-associated membrane glycoprotein 2	LAMP2	385310	2177500
Protein CREG1	CREG1	0	1948400
Lactadherin	MFGE8	0	1993700
Retinoic acid receptor alpha	RARA	0	1750600
Transitional endoplasmic reticulum ATPase	VCP	0	1999400
Laminin subunit beta-2	LAMB2	2192300	1107000
Gremlin-1	GREM1	5257200	605820
Ribonuclease 4	RNASE4	3122400	782130
Xaa-Pro dipeptidase	PEPD	0	1730100
Myosin light polypeptide 6 (Fragment)	MYL6	1806400	1613100
Cofilin-2	CFL2	0	1711800
Endothelial protein C receptor	PROCR	0	1563500
Prolow-density lipoprotein receptor-related protein 1	LRP1	0	1634300
Tubulin alpha chain	TUBA1C	0	1390300
Peptidyl-glycine alpha-amidating monooxygenase (Fragment)	PAM	0	1609900
Villin-1 (Fragment)	VIL1	0	1602200
Thrombospondin-4	THBS4	0	1695700

Serine/threonine-protein phosphatase CPPED1	CPPED1	0	1635600
Protein disulfide-isomerase A3	PDIA3	0	1310800
Aldo-keto reductase family 1 member C2 (Fragment)	AKR1C2	0	1382400
Septin 11, isoform CRA_b	SEPTIN11	0	1326800
Talin-1	TLN1	0	1588500
Translationally-controlled tumor protein	TPT1	0	1553000
Desmoplakin	DSP	2436700	1614100
Leukotriene A-4 hydrolase	LTA4H	0	1431500
Proteasome subunit beta type-2	PSMB2	0	1396500
Matrix-remodeling-associated protein 5	MXRA5	0	1423700
14-3-3 protein beta/alpha	YWHAB	0	1391000
Vesicular integral-membrane protein VIP36 (Fragment)	LMAN2	0	1385100
EGF-containing fibulin-like extracellular matrix protein 2	EFEMP2	0	1271700
Polypeptide N-acetylgalactosaminyltransferase 2	GALNT2	0	1239300
MRN complex-interacting protein	MRNIP	0	840850
Nuclear pore complex-interacting protein family member A1	NPIPA1	0	1334800
Proteasome subunit beta type-4	PSMB4	0	1316000
Putative phospholipase B-like 2	PLBD2	0	1065900
Ubiquitin-conjugating enzyme E2 L3	UBE2L3	0	1265900
Proteasome subunit beta type-1	PSMB1	0	1290500
Tropomyosin alpha-3 chain	TPM3	0	1097300
Cytosolic phospholipase A2 gamma	PLA2G4C	0	1260000
Neuropilin-1	NRP1	0	1217800
Follistatin-related protein 3	FSTL3	0	1203700
Cadherin-11	CDH11	0	1104400
UPAR/Ly6 domain-containing protein OS=Homo sapiens OX=9606 PE=1 SV=1;tr|A0A2U3TZL5|A0A2U3TZL5	CD59	4717300	0
Probable JmjC domain-containing histone demethylation protein 2C (Fragment)	JMJD1C	0	1193100
Small ubiquitin-related modifier 4	SUMO4	6130700	0
Annexin A5	ANXA5	0	1118300
Ubiquitin-conjugating enzyme E2 variant 1	UBE2V1	1624500	0
Aspartate aminotransferase, cytoplasmic	GOT1	0	1023700
Junction plakoglobin	JUP	2606700	664190
Twisted gastrulation protein homolog 1	TWSG1	1722300	0
Myosin-1	MYH1	0	988680
Reticulocalbin-1	RCN1	0	1096200
Ferritin light chain	FTL	0	983350
Protein disulfide-isomerase A3 (Fragment)	PDIA3	0	615360
Group XV phospholipase A2 (Fragment)	PLA2G15	0	978920
Actin-related protein 2/3 complex subunit 3 (Fragment)	ARPC3	0	810200
Ribonuclease inhibitor (Fragment)	RNH1	0	803660
Transportin-2	TNPO2	0	896430
Poliovirus receptor	PVR	0	743050
10 kDa heat shock protein, mitochondrial	HSPE1	0	487610
N(G),N(G)-dimethylarginine dimethylaminohydrolase 1	DDAH1	0	550200
Actin-related protein 2/3 complex subunit 5	ARPC5	0	704310
Histone H1.5	H1-5	4804600	0
Y-box-binding protein 3 (Fragment)	YBX3	0	567060

Proteasome endopeptidase complex	PSMA2	0	886300
E3 ubiquitin-protein ligase RNF146	RNF146	0	908370
D-dopachrome decarboxylase	DDT	0	904400
Uncharacterized membrane protein C3orf80 (Fragment)	C3orf80	0	870000
Fascin	FSCN1	0	750190
Beta-mannosidase	MANBA	0	849400
Dipeptidyl peptidase 4	DPP4	0	778310
Aminopeptidase N	ANPEP	0	812750
Lysosomal acid lipase/cholesteryl ester hydrolase	LIPA	0	779980
Serpin B7	SERPINB7	0	711890
Voltage-dependent L-type calcium channel subunit alpha	CACNA1D	0	767840
Proteasome subunit alpha type	PSMA4	0	764600
RNA-binding protein FUS	FUS	0	550610
Phosphoglycerate kinase 1	PGK 1.00	0	642470
Fibulin-2	FBLN2	0	730870
Titin	TTN	0	619140
CD166 antigen (Fragment)	ALCAM	0	676030
Paraneoplastic antigen Ma6E	PNMA6E	3749100	0
Actin-related protein 2	ACTR2	0	718050
LIM/homeobox protein Lhx3	LHX3	0	701940
Vascular endothelial growth factor receptor 1	FLT1	758650	0
Tax1-binding protein 3	TAX1BP3	0	616400
Coiled-coil domain-containing protein 80	CCDC80	0	695110
Ig-like domain-containing protein	LOC102723996	0	584250
Plectin	PLEC	0	668290
COL14A1 protein	COL14A1	0	672030
Attractin	ATRN	0	589570
Protein-L-isoaspartate(D-aspartate) O-methyltransferase	PCMT1	0	634810
Retinal dehydrogenase 1	ALDH1A1	0	626490
MORN repeat-containing protein 1 (Fragment)	MORN1	0	258480
Chondroitin sulfate proteoglycan 4	CSPG4	0	529310
Galectin-3-binding protein (Fragment)	LGALS3BP	0	554530
CD81 antigen (Fragment)	CD81	0	579500
Ubiquitin-conjugating enzyme E2 N	UBE2N	0	576070
Zyxin (Fragment)	ZYX	1100800	0
Angiotensinogen	AGT	0	569940
Tetranectin	CLEC3B	0	564120
Fructose-bisphosphate aldolase C	ALDOC	0	557260
Stanniocalcin-1	STC1	0	555460
Cadherin-13	CDH13	702640	0
Plasma alpha-L-fucosidase	FUCA2	0	552330
Syntenin-1	SDCBP	0	542880
Myosin-13	MYH13	0	536810
Tenascin	TNC	0	534220
Protein CDV3 homolog	CDV3	0	389210
Polypeptide N-acetylgalactosaminyltransferase 10	GALNT10	0	476520
Polypeptide N-acetylgalactosaminyltransferase 5	GALNT5	0	505710
Di-N-acetylchitobiase	CTBS	0	487080
Lysosomal alpha-mannosidase	MAN2B1	0	477060
Semaphorin-5A (Fragment)	SEMA5A	0	474380
Methyl-CpG-binding protein 2	MECP2	0	367750
14-3-3 protein theta	YWHAQ	514910	0

Protein	Gene	Value 1	Value 2
Lysozyme	LYZ	2336800	0
Protein ITPRID1 (Fragment)	ITPRID1	2332800	0
Heat shock 70 kDa protein 4	HSPA4	0	446520
Parathymosin (Fragment)	PTMS	0	206630
Tissue alpha-L-fucosidase	FUCA1	0	413540
Calmodulin-like protein 5	CALML5	0	187590
Lymphocyte-specific protein 1 (Fragment)	LSP1	2211900	0
Elongation factor 2	EEF2	0	425670
Thrombospondin-3	THBS3	0	422570
Clathrin light chain (Fragment)	CLTB	2119900	0
Bleomycin hydrolase (Fragment)	BLMH	1347500	0
Glypican-1 (Fragment)	GPC1	0	397110
TPR and ankyrin repeat-containing protein 1 (Fragment)	TRANK1	0	395780
Dipeptidyl peptidase 3	DPP3	0	363030
Plakophilin-1	PKP1	0	259740
Cytoplasmic FMR1-interacting protein 1 (Fragment)	CYFIP1	0	344110
Pappalysin-1	PAPPA	0	343850
Perilipin-3 (Fragment)	PLIN3	0	327660
Zinc finger protein 558	ZNF558	0	324200
Nebulin (Fragment)	NEB	1501900	0
Non-lysosomal glucosylceramidase	GBA2	0	286260
Suprabasin	SBSN	0	233160
Putative sodium-coupled neutral amino acid transporter 10	SLC38A10	1417200	0
Fibrinogen beta chain	FGB	0	262250
SRSF protein kinase 3	SRPK3	0	254820
LIM zinc-binding domain-containing protein OS=Homo sapiens OX=9606 PE=4 SV=1;tr|B3KPU0|B3KPU0	PDZ	0	182990
Synaptotagmin-like protein 2 (Fragment)	SYTL2	1193500	0
14-3-3 protein gamma	YWHAG	1115300	0
Ephrin-B2	EFNB2	0	214680
Serine/threonine-protein kinase Sgk3 (Fragment)	SGK3	0	213620
Protein FAM193A (Fragment)	FAM193A	1090000	0
Trans-Golgi network integral membrane protein 2	TGOLN2	1023600	0
Inositol 1,4,5-trisphosphate receptor type 2	ITPR2	0	201310
Non-histone chromosomal protein HMG-14	HMGN1	0	89621
Gamma-tubulin complex component	TUBGCP3	0	181870
Vascular cell adhesion protein 1	VCAM1	756010	0
40S ribosomal protein S21	RPS21	556250	0
Signal recognition particle subunit SRP72	SRP72	457710	0
Retinal guanylyl cyclase 1	GUCY2D	319370	0
Oxysterol-binding protein-related protein 1 (Fragment)	OSBPL1A	311290	0
NADH dehydrogenase [ubiquinone] flavoprotein 1, mitochondrial (Fragment)	NDUFV1	305810	0
High mobility group protein HMGI-C	HMGA2	259750	0
Disintegrin and metalloproteinase domain-containing protein 23	ADAM23	0	49228
E3 ubiquitin-protein ligase TRIM22	TRIM22	43463	0
Syntaxin-7	STX7	0	0
Small subunit processome component 20 homolog	UTP20	0	0
Protein disulfide-isomerase (Fragment)	P4HB	0	0
Aspartate--tRNA ligase, mitochondrial	DARS2	0	0

DnaJ homolog subfamily C member 14	DNAJC14	0	0
Iporin	RUSC2	0	0
Complement C1q tumor necrosis factor-related protein 3	C1QTNF3	0	0
Uncharacterized protein DKFZp434B061 OS=Homo sapiens OX=9606 PE=2 SV=2		0	0
Vacuolar protein-sorting-associated protein 25 (Fragment)	VPS25	0	0

Table 6-2HFF versus HFF+ Cisplatin SASP secretome profile

Protein name	Gene name	-Log Student's T-test p-value -HFF _HHF+Cisplatin	Student's T-test Difference -HFF _ HFF+ Cisplatin
Pantetheinase	VNN 1.00	1.668282894	3.984273473
Translin	TSN	2.252251679	3.815118551
Myosin regulatory light polypeptide 9	MYL9	1.566433052	3.578861475
Tubulin alpha-1B chain	TUBA1B	4.541350484	3.530382077
Alcohol dehydrogenase class-3	ADH5	3.227160253	3.341021458
6-phosphogluconate dehydrogenase, decarboxylating	PGD	1.609017819	3.317506234
Peroxiredoxin-4	PRDX4	2.060687869	3.233848969
Proteasome subunit beta (Fragment)	PSMA4	1.748996426	3.16816179
Oligoribonuclease, mitochondrial	REXO2	6.042394619	3.058392127
Gamma-enolase	ENO2	2.496702545	2.927528302
Myeloid-derived growth factor (Fragment)	MYDGF	1.161718857	2.828524987
Proteasome subunit beta type-3	PSMB3	1.342873024	2.768097798
14-3-3 protein theta	YWHAQ	3.012498527	2.731779973
Clathrin heavy chain 1	CLTC	2.461788029	2.708042065
14-3-3 protein gamma	YWHAG	1.593956418	2.699018081
Receptor of activated protein C kinase 1	RACK1	1.508804277	2.641978025
Ubiquitin-like modifier-activating enzyme 1	UBA1	2.35272328	2.639869769
T-complex protein 1 subunit epsilon	CCT5	2.688893658	2.627458334
5-nucleotidase	NT5E	2.531798565	2.573488792
Protein CREG1	CREG1	1.706048566	2.549514294
Actin-related protein 2/3 complex subunit 1B	ARPC1B	1.212244587	2.43699797
Apolipoprotein B-100	APOB	1.414588979	2.427228053
Ras GTPase-activating protein-binding protein 1	G3BP1	2.932102603	2.392288605
Putative elongation factor 1-alpha-like 3	EEF1A1P5	2.446509297	2.328970353
Elongation factor 1-beta	EEF1B2	1.22774371	2.315497001
Ubiquitin-conjugating enzyme E2 variant 1	UBE2V1	2.714364143	2.29851981
F-actin-capping protein subunit alpha-1	CAPZA1	4.058963935	2.275290092
Lysosome-associated membrane glycoprotein 2	LAMP2	1.031720385	2.264238914
Collagen alpha-1(VII) chain	COL7A1	1.123642054	2.253711462
MAM domain-containing protein 2	MAMDC2	2.863897973	2.245578686
60S ribosomal protein L5 (Fragment)	RPL5	1.865194755	2.236689965
CXXC motif containing zinc binding protein	CZIB	1.997192358	2.203786612
Extended synaptotagmin-1	ESYT1	3.719693905	2.121606588
N(G),N(G)-dimethylarginine dimethylaminohydrolase 1	DDAH1	5.423727289	2.101363897
Rab GDP dissociation inhibitor alpha	GDI1	2.499582216	2.099007845
ADP-ribosylation factor 1	ARF1	1.751727458	2.092672427

Vesicle-associated membrane protein-associated protein A	VAPA	1.861439235	2.081159393
Twinfilin-1	TWF1	2.564433056	2.065778335
Quinone oxidoreductase PIG3	TP53I3	1.316531574	2.052857161
Chloride intracellular channel protein 4	CLIC4	3.199518487	2.04539005
Cofilin-1	CFL1	3.81754323	2.033172687
14 kDa phosphohistidine phosphatase	PHPT1	2.513585054	2.008646568
Ubiquitin-like protein ISG15 (Fragment)	ISG15	1.70386727	2.000613848
Platelet-activating factor acetylhydrolase IB subunit alpha	PAFAH1B1	1.073529868	1.996134241
Calumenin	CALU	3.541466738	1.955091397
Purine nucleoside phosphorylase	PNP	3.433814728	1.950955153
Elongation factor 1-delta	EEF1D	1.05017468	1.945618272
Stress-induced-phosphoprotein 1	STIP1	1.698877178	1.936811527
Vacuolar protein sorting-associated protein 35	VPS35	2.117072416	1.932843447
Glutathione S-transferase	GSTM2	1.386686285	1.929641088
Septin 11, isoform CRA_b	SEPTIN11	2.815757331	1.909912507
Coronin-1B	CORO1B	2.114088682	1.897441308
Pyruvate kinase PKM	PKM	2.688043645	1.873852173
Proliferation-associated protein 2G4	PA2G4	1.817261079	1.832823912
Glycogenin-1	GYG1	1.179481808	1.812300146
Stromelysin-1	MMP3	3.522645401	1.805720727
Glycogen phosphorylase, brain form	PYGB	2.98645513	1.801081419
Carbonyl reductase [NADPH] 1	CBR1	2.24627543	1.799332698
Phosphoglycerate kinase 1	PGK 1.00	3.218576373	1.792708953
Metallothionein-2	MT2A	1.659312891	1.77044638
Coatomer subunit alpha (Fragment)	COPA	1.41349041	1.768666824
Ubiquitin-conjugating enzyme E2 N	UBE2N	1.341626851	1.760226806
Microtubule-associated protein 1B	MAP1B	2.075723038	1.714044809
Glucosidase 2 subunit beta	PRKCSH	2.610494555	1.703588565
Stress-70 protein, mitochondrial	HSPA9	1.575335872	1.700328668
Prostaglandin reductase 1	PTGR1	1.539173213	1.692549467
40S ribosomal protein SA (Fragment)	RPSA	2.090261952	1.688406229
Peroxiredoxin-5, mitochondrial	PRDX5	3.189843553	1.68658042
Septin-2	SEPTIN2	2.888832936	1.686148405
Ribonuclease inhibitor	RNH1	2.323443191	1.681343794
Periostin	POSTN	3.340023502	1.658221483
Tubulin beta-4B chain	TUBB4B	1.590532944	1.654672384
Thioredoxin-dependent peroxide reductase, mitochondrial	PRDX3	2.081841832	1.644147317
Eukaryotic translation initiation factor 5A-1	EIF5A	1.937194634	1.634700378
Septin-7	SEPTIN7	1.303068653	1.631765207
Transgelin	TAGLN	2.583657889	1.629184643
Peptidyl-prolyl cis-trans isomerase A	PPIA	3.763218619	1.621235609
LIM domain and actin-binding protein 1	LIMA1	1.757278655	1.601178805
WD repeat-containing protein 1	WDR1	2.497427315	1.591236035
Ferritin heavy chain	FTH1	2.243373643	1.570035855
Ubiquitin carboxyl-terminal hydrolase isozyme L1	UCHL1	2.015354993	1.554561218

Filamin-B	FLNB	2.309454676	1.542754253
Chloride intracellular channel protein 1	CLIC1	2.58843974	1.542541265
Actin-related protein 2/3 complex subunit 2	ARPC2	1.540740779	1.507447958
14-3-3 protein beta/alpha	YWHAB	3.161617256	1.506408135
Nuclear transport factor 2	NUTF2	1.56169558	1.476857265
Calpain-1 catalytic subunit	CAPN1	1.644144615	1.473995447
Protein Niban 2	NIBAN2	1.997463572	1.462143819
Actin, alpha cardiac muscle 1	ACTC1	3.299176753	1.457780917
Glyceraldehyde-3-phosphate dehydrogenase	GAPDH	1.973666207	1.457620064
Heat shock cognate 71 kDa protein	HSPA8	2.993093925	1.45371143
Coatomer subunit gamma-1	COPG1	2.438479322	1.438256105
Actin-related protein 2	ACTR2	2.22676492	1.433129549
DNA damage-binding protein 1	DDB1	1.945024874	1.415522973
Eukaryotic translation initiation factor 2 subunit 3	EIF2S3	1.924317619	1.413610379
Thioredoxin reductase 1, cytoplasmic	TXNRD1	2.51483006	1.411765814
Lactoylglutathione lyase	GLO1	1.688573133	1.410896063
F-actin-capping protein subunit beta	CAPZB	4.279201653	1.405105035
L-lactate dehydrogenase B chain	LDHB	2.519893222	1.398455222
Alpha-enolase	ENO1	1.946876385	1.395975033
Malate dehydrogenase, mitochondrial	MDH2	2.654694907	1.389160872
Pappalysin-1	PAPPA	3.598658563	1.389137506
Myosin-9	MYH9	3.474231678	1.384576082
Ferritin light chain	FTL	1.711711957	1.382453998
Elongation factor 2	EEF2	1.915049664	1.374415159
Malate dehydrogenase, cytoplasmic	MDH1	2.614415223	1.36971879
Aldo-keto reductase family 1 member B1	AKR1B1	4.272160758	1.360721668
Fructose-bisphosphate aldolase A	ALDOA	2.150791951	1.358679374
Alpha-soluble NSF attachment protein	NAPA	1.083031732	1.350625197
Plastin-3	PLS3	2.295212192	1.345946709
Calpain-2 catalytic subunit	CAPN2	1.592246451	1.338825941
Heat shock 70 kDa protein 4	HSPA4	2.243771651	1.332213004
Hepatocyte growth factor activator	HGFAC	1.724932078	1.313260476
Nucleotide exchange factor SIL1	SIL1	1.140761117	1.307134549
Eukaryotic translation initiation factor 6	EIF6	1.47745205	1.289973418
Glucose-6-phosphate 1-dehydrogenase	G6PD	1.816637058	1.28573664
Actin-related protein 2/3 complex subunit 4	ARPC4	2.466366316	1.283670187
Phosphatidylinositol-binding clathrin assembly protein (Fragment)	PICALM	1.173804124	1.282360673
Histidine--tRNA ligase, cytoplasmic	HARS1	1.788499422	1.279540777
Fatty acid synthase	FASN	1.189183353	1.271037181
Serine/threonine-protein kinase OSR1	OXSR1	1.892744562	1.269003769
Plasminogen activator inhibitor 2	SERPINB2	2.637648148	1.267392715
Aminopeptidase	NPEPPS	2.673584412	1.262581746
ADP-sugar pyrophosphatase	NUDT5	2.868331144	1.25499781

GTP-binding nuclear protein Ran (Fragment)	RAN	1.959879076	1.254936457
Translationally-controlled tumor protein	TPT1	3.201194227	1.249616702
Coactosin-like protein	COTL1	1.599540133	1.243135691
Transgelin-2	TAGLN2	1.63775124	1.228425582
ADAMTS-like protein 1	ADAMTSL1	1.947853654	1.227348725
Alpha-actinin-1	ACTN1	2.714635986	1.22597607
Plasminogen activator inhibitor 1	SERPINE1	4.269735684	1.225483338
Calpastatin	CAST	1.216791443	1.223063548
Annexin A1	ANXA1	1.330850402	1.217764934
Talin-1	TLN1	2.321965095	1.216322025
Rab GDP dissociation inhibitor beta	GDI2	2.46181693	1.21066006
D-dopachrome decarboxylase	DDT	1.606769305	1.209702571
Synaptic vesicle membrane protein VAT-1 homolog	VAT1	1.94356109	1.197445631
Cysteine and glycine-rich protein 1	CSRP1	3.037636076	1.194711606
Ubiquitin-conjugating enzyme E2 L3	UBE2L3	1.826632634	1.18680946
Filamin-C	FLNC	2.14550177	1.183747689
Heme-binding protein 1	HEBP1	1.338914502	1.181518396
PDZ and LIM domain protein 7	PDLIM7	2.025026213	1.17707936
Src substrate cortactin	CTTN	1.701672372	1.164644957
Rho GDP-dissociation inhibitor 1 (Fragment)	ARHGDIA	1.804612572	1.162687222
Heat shock 70 kDa protein 1B	HSPA1B	2.751645564	1.162087679
Ras-related protein Rab-7a	RAB7A	1.567778952	1.159529448
Erythrocyte band 7 integral membrane protein	STOM	1.123185209	1.135408481
Aspartate aminotransferase, mitochondrial	GOT2	2.07687258	1.132334312
Lysyl oxidase homolog 2	LOXL2	3.041221879	1.129000743
Glutathione S-transferase P	GSTP1	2.871949953	1.120571852
Fibrillin-1	FBN1	2.234873551	1.115126371
Tyrosine-protein phosphatase non-receptor type 11	PTPN11	2.122944983	1.107049306
Adenosylhomocysteinase	AHCY	1.465404221	1.103188117
Elongation factor 1-gamma	EEF1G	2.363388711	1.094078143
AP complex subunit beta	AP2B1	1.930395347	1.090542078
Ubiquitin-fold modifier 1	UFM1	1.197906229	1.088242292
Glucosamine-6-phosphate isomerase 1	GNPDA1	1.572462371	1.082960208
Cytosol aminopeptidase	LAP3	1.196356136	1.08119607
Fascin	FSCN1	1.874362355	1.081179063
Aspartate aminotransferase, cytoplasmic	GOT1	1.507815002	1.07534639
Glutathione synthetase	GSS	1.72631404	1.070843617
Urokinase-type plasminogen activator	PLAU	1.700652658	1.065958897
Protein S100-A4	S100A4	2.062541472	1.062624057
Ras GTPase-activating-like protein IQGAP1	IQGAP1	2.013787555	1.059164286
Proteasome subunit beta type-4	PSMB4	1.808809626	1.057170153
Insulin-like growth factor-binding protein 5	IGFBP5	1.804219217	1.053374211
Leukotriene A-4 hydrolase	LTA4H	1.339829196	1.038998524

Eukaryotic initiation factor 4A-II	EIF4A2	1.342794455	1.037663857
SH3 domain-binding glutamic acid-rich-like protein 3	SH3BGRL3	1.666597541	1.035050154
L-lactate dehydrogenase A chain	LDHA	1.305950794	1.029394229
Alpha-actinin-4	ACTN4	2.01426108	1.025746902
Carboxypeptidase A4	CPA4	2.384005566	1.024316867
Acetyl-CoA acetyltransferase, cytosolic	ACAT2	1.899504663	1.023108562
Staphylococcal nuclease domain-containing protein 1	SND1	1.829974095	1.014042934
Protein disulfide-isomerase A6	PDIA6	1.367826478	1.005396446
Caveolae-associated protein 1	CAVIN1	2.253556127	0.988566637
Dynein light chain roadblock-type 1	DYNLRB1	1.183159579	0.987993042
14-3-3 protein zeta/delta	YWHAZ	2.421521054	0.975981315
Nucleoside diphosphate kinase	NME1-NME2	1.549033756	0.97139128
Actin-related protein 3	ACTR3	1.662959667	0.970356067
Thioredoxin	TXN	1.362670462	0.961741368
1,4-alpha-glucan-branching enzyme	GBE1	1.519233732	0.96158878
Xaa-Pro dipeptidase	PEPD	1.409740716	0.938575506
Glucose-6-phosphate isomerase	GPI	2.233011172	0.936629852
Reticulocalbin-1	RCN1	2.044607354	0.925641616
10 kDa heat shock protein, mitochondrial	HSPE1	1.690164994	0.925576448
Peroxiredoxin-1	PRDX1	1.392168545	0.921243111
Thimet oligopeptidase	THOP1	1.405932032	0.915771246
Peptidyl-prolyl cis-trans isomerase FKBP10	FKBP10	1.737127404	0.91350913
Filamin-A	FLNA	1.775907605	0.903399547
Myosin light polypeptide 6	MYL6	1.277012719	0.899707874
Laminin subunit beta-2	LAMB2	2.37079684	0.884824832
Cystatin-B	CSTB	2.157609562	0.88107578
PDZ and LIM domain protein 1	PDLIM1	1.322207949	0.876016816
Transketolase	TKT	1.972476441	0.875530005
Neutral alpha-glucosidase AB	GANAB	1.924309914	0.874866247
Protein/nucleic acid deglycase DJ-1	PARK7	1.302727336	0.870051463
Superoxide dismutase [Mn], mitochondrial	SOD2	2.514056663	0.852462053
Glia-derived nexin	SERPINE2	3.112090542	0.846344709
Phosphoglycerate mutase 1	PGAM1	2.06540165	0.841613531
Peroxiredoxin-6	PRDX6	1.238716172	0.83525904
Phosphatidylethanolamine-binding protein 1	PEBP1	1.765102514	0.832529624
Plectin	PLEC	1.354111722	0.831125975
Dipeptidyl peptidase 4	DPP4	2.627528207	0.817943176
Glyoxalase domain-containing protein 4	GLOD4	1.877638443	0.8174239
UV excision repair protein RAD23 homolog B	RAD23B	1.311942719	0.813710451
Coronin-1C	CORO1C	1.233393825	0.812747876
Triosephosphate isomerase	TPI1	1.943254005	0.808252732
Catalase	CAT	1.688800207	0.794903318
Aminopeptidase N	ANPEP	2.149556903	0.777899981
Actin, cytoplasmic 2	ACTG1	1.86564059	0.776104371
Reticulocalbin-3	RCN3	1.975139643	0.774582624

Ubiquitin carboxyl-terminal hydrolase	USP14	1.690807314	0.764686584
Endoplasmic reticulum resident protein 29	ERP29	1.420406017	0.764532646
Macrophage-capping protein	CAPG	1.827198175	0.763321956
Heat shock protein beta-1	HSPB1	1.268219889	0.758511782
Moesin	MSN	1.557590982	0.755696058
Protein-L-isoaspartate(D-aspartate) O-methyltransferase	PCMT1	1.482588816	0.735304435
Cytosolic non-specific dipeptidase	CNDP2	1.445030319	0.732365052
Ras suppressor protein 1	RSU1	1.397105202	0.73097078
Platelet-derived growth factor C	PDGFC	1.251757974	0.721753518
NADP-dependent malic enzyme	ME1	1.495155951	0.702733437
Glutathione S-transferase omega-1	GSTO1	1.532732466	0.678772211
Proteasome subunit alpha type-7	PSMA7	1.510832586	0.66792051
Y-box-binding protein 1	YBX1	1.342785751	0.66246438
Brain acid soluble protein 1	BASP1	1.496214159	0.655183713
UTP--glucose-1-phosphate uridylyltransferase	UGP2	1.557010072	0.645210187
Endoplasmic reticulum chaperone BiP	HSPA5	1.84519827	0.615192334
Echinoderm microtubule-associated protein-like 2 (Fragment)	EML2	1.346676984	0.615164042
Prolyl endopeptidase FAP	FAP	2.1415262	0.614759366
C-type mannose receptor 2	MRC2	2.478387558	0.606985013
Leucine-rich repeat-containing protein 15	LRRC15	1.682837048	0.606969118
Tumor necrosis factor receptor superfamily member 11B	TNFRSF11B	1.463804064	0.573033094
Gelsolin	GSN	2.599324575	0.523510536
Polypeptide N-acetylgalactosaminyltransferase 5	GALNT5	3.175383635	0.518176794
Cation-independent mannose-6-phosphate receptor	IGF2R	2.143170207	-0.334080935
Soluble scavenger receptor cysteine-rich domain-containing protein SSC5D	SSC5D	1.83971011	-0.373968999
Semaphorin-7A	SEMA7A	1.88917387	-0.378914913
Extracellular matrix protein 1	ECM1	1.936734286	-0.418185472
Arylsulfatase A	ARSA	1.633886722	-0.434976816
Cathepsin Z	CTSZ	1.80298818	-0.437261661
Beta-galactosidase	GLB1	1.677422419	-0.464292765
Peptidyl-glycine alpha-amidating monooxygenase	PAM	2.082507851	-0.476369619
Epididymis-specific alpha-mannosidase	MAN2B2	3.007291021	-0.503207286
Nidogen-2	NID2	1.99203501	-0.527166446
Cathepsin B	CTSB	3.109493944	-0.547919194
HLA class I histocompatibility antigen, C alpha chain	HLA-C	1.47679021	-0.54924496
N(4)-(beta-N-acetylglucosaminyl)-L-asparaginase	AGA	2.000993889	-0.556050698
Insulin-like growth factor-binding protein 2	IGFBP2	2.460109494	-0.57052954
Prosaposin	PSAP	2.523882266	-0.589289268

EMILIN-1	EMILIN1	1.501755307	-0.59074076
Low-density lipoprotein receptor	LDLR	2.002671921	-0.602883577
Dipeptidyl peptidase 1	CTSC	2.667760193	-0.608767748
Inactive tyrosine-protein kinase 7	PTK7	2.55377704	-0.621681134
Beta-hexosaminidase subunit alpha	HEXA	3.29732132	-0.64792943
EGF-containing fibulin-like extracellular matrix protein 2	EFEMP2	2.396923148	-0.663065513
Beta-hexosaminidase subunit beta	HEXB	2.706062668	-0.670591275
Dystroglycan	DAG1	2.165012242	-0.68160828
Endoglin	ENG	1.529198816	-0.68324844
ADP-ribosyl cyclase/cyclic ADP-ribose hydrolase 2	BST1	1.995359051	-0.687814315
Mannan-binding lectin serine protease 1	MASP1	1.99957814	-0.688429594
Meteorin-like protein	METRNL	1.770093641	-0.697187006
Nucleobindin-1	NUCB1	1.300318862	-0.710095485
Endosialin	CD248	1.411092176	-0.710910082
C-type lectin domain family 11 member A	CLEC11A	2.031804674	-0.739701668
Collagen alpha-1(V) chain	COL5A1	2.348201507	-0.749892473
Serine protease HTRA1	HTRA1	1.829338891	-0.75307854
Thy-1 membrane glycoprotein (Fragment)	THY1	1.319158588	-0.785371542
Alpha-galactosidase A	GLA	1.406136966	-0.789918045
Lysosomal Pro-X carboxypeptidase	PRCP	2.960920504	-0.797686815
Fibulin-2	FBLN2	3.194558183	-0.804758946
Olfactomedin-like protein 3	OLFML3	2.716026207	-0.808616082
Ectonucleotide pyrophosphatase/phosphodiesterase family member 2	ENPP2	4.07237509	-0.808793306
Galectin-3-binding protein	LGALS3BP	2.952356045	-0.813038905
NPC intracellular cholesterol transporter 2	NPC2	1.938774905	-0.814376116
Sphingomyelin phosphodiesterase	SMPD1	1.631891786	-0.816395044
Ribonuclease T2	RNASET2	1.843390962	-0.835504293
Angiopoietin-related protein 2	ANGPTL2	3.146721348	-0.846373002
CD109 antigen	CD109	2.415699211	-0.848838409
Soluble calcium-activated nucleotidase 1	CANT1	3.448695069	-0.851223548
Alpha-N-acetylglucosaminidase	NAGLU	2.663526407	-0.877275705
Cadherin-13	CDH13	2.1522631	-0.87939318
Mannosyl-oligosaccharide 1,2-alpha-mannosidase IA	MAN1A1	3.125921102	-0.879942815
72 kDa type IV collagenase	MMP2	2.510047147	-0.883267641
Group XV phospholipase A2	PLA2G15	4.011000304	-0.890500625
Transcobalamin-2	TCN2	1.455394512	-0.896795352
Legumain	LGMN	1.306291169	-0.899657011
Sialidase-1	NEU1	2.440216245	-0.911350012
Nidogen-1	NID1	1.874880398	-0.925840616
Lysosomal protective protein	CTSA	2.776367162	-0.937858661
Tripeptidyl-peptidase 1	TPP1	3.386242288	-0.941605012
Plasma protease C1 inhibitor	SERPING1	2.684307204	-0.947111209
Decorin	DCN	2.927966737	-0.979318539
Vasorin	VASN	3.88953817	-0.981315692
Palmitoyl-protein thioesterase 1	PPT1	3.228835474	-0.985050917

Interstitial collagenase	MMP1	1.914846048	-0.988228718
Laminin subunit alpha-2	LAMA2	1.413419235	-0.989819129
CD166 antigen	ALCAM	2.869282847	-0.996705612
Insulin-like growth factor-binding protein 4	IGFBP4	2.747510699	-1.006014903
Out at first protein homolog	OAF	3.292369333	-1.010959864
Angiotensinogen	AGT	3.046506871	-1.012792031
Beta-2-microglobulin	B2M	2.118188413	-1.035644134
Cystatin-C	CST3	2.820135329	-1.041520357
Vitamin K-dependent protein S	PROS1	3.167022073	-1.04366231
Ribonuclease 4	RNASE4	2.454235167	-1.054919799
Putative phospholipase B-like 2	PLBD2	4.118318288	-1.056842407
Di-N-acetylchitobiase	CTBS	3.74300535	-1.074478547
Collagen alpha-2(IV) chain	COL4A2	2.458767041	-1.078457594
Deoxyribonuclease-2-alpha	DNASE2	1.169498557	-1.08410128
Insulin-like growth factor-binding protein 6	IGFBP6	2.962140833	-1.105148713
Apolipoprotein E	APOE	3.050180666	-1.108553648
Matrix-remodeling-associated protein 5	MXRA5	4.008704313	-1.127351046
Progranulin	GRN	3.480435351	-1.161289771
Spondin-2	SPON2	3.545301893	-1.166609685
Collagen alpha-2(I) chain	COL1A2	2.982257968	-1.17068092
Cathepsin F	CTSF	3.729397436	-1.183799346
Metalloproteinase inhibitor 2	TIMP2	3.102273153	-1.191121022
Stanniocalcin-1	STC1	1.465564418	-1.252570868
Secreted frizzled-related protein 1	SFRP1	2.191725513	-1.276046991
EGF-containing fibulin-like extracellular matrix protein 1	EFEMP1	4.035398502	-1.29582572
Procollagen C-endopeptidase enhancer 1	PCOLCE	3.360853681	-1.309889078
Clusterin	CLU	3.790159621	-1.345141967
Cathepsin L1	CTSL	4.307720548	-1.35235858
Collagen triple helix repeat-containing protein 1	CTHRC1	2.969999901	-1.365730842
Complement C1s subcomponent	C1S	3.471809563	-1.367104769
Cathepsin D	CTSD	4.255517357	-1.416258732
Tissue factor pathway inhibitor	TFPI	2.984444415	-1.417498032
Carboxypeptidase Q	CPQ	3.73145324	-1.419439554
N-acetylglucosamine-6-sulfatase	GNS	3.323515174	-1.492560148
Proprotein convertase subtilisin/kexin type 9	PCSK9	1.688151205	-1.530788402
Follistatin-related protein 3	FSTL3	1.212386585	-1.605276108
40S ribosomal protein S28	RPS28	1.697174299	-1.63027968
Multiple epidermal growth factor-like domains protein 8	MEGF8	2.025856788	-1.631613334
Acid ceramidase	ASAH1	2.790633159	-1.637872934
Hornerin	HRNR	1.771336803	-1.641937673
Amyloid-beta precursor protein	APP	4.582705506	-1.649942795
Matrix remodeling-associated protein 8	MXRA8	4.109189884	-1.652798414
Latent-transforming growth factor beta-binding protein 4	LTBP4	3.747555529	-1.692041119
Gremlin-1	GREM1	2.420203812	-1.696340322

Multiple epidermal growth factor-like domains protein 6	MEGF6	1.030953355	-1.699915369
Matrix metalloproteinase-14	MMP14	3.781459785	-1.714963039
Complement C1q tumor necrosis factor-related protein 5	C1QTNF5	3.049845934	-1.726441781
Acid sphingomyelinase-like phosphodiesterase 3a	SMPDL3A	4.549576973	-1.851105769
Alpha-N-acetylgalactosaminidase	NAGA	2.909069132	-1.916119814
Ceroid-lipofuscinosis neuronal protein 5 (Fragment)	CLN5	1.250869918	-1.918699781
Receptor-type tyrosine-protein phosphatase S	PTPRS	1.767197764	-1.95966514
Pigment epithelium-derived factor	SERPINF1	2.946425292	-2.040784121
Secreted and transmembrane protein 1 (Fragment)	SECTM1	1.131964229	-2.084770719
Carbonic anhydrase 12	CA12	1.397015538	-2.113438745
Semaphorin-3B	SEMA3B	1.62690144	-2.113555094
Desmoglein-1	DSG1	1.321546062	-2.14633441
Stromelysin-3	MMP11	3.258441533	-2.163607041
Collagen alpha-1(XVIII) chain	COL18A1	4.318022293	-2.216512283
Dipeptidyl peptidase 2	DPP7	1.76436453	-2.257595559
Cadherin-11	CDH11	1.25740922	-2.277912656
Pleiotrophin	PTN	2.860031468	-2.315333307
Complement C1r subcomponent	C1R	4.341140288	-2.335079908
Prostaglandin-H2 D-isomerase	PTGDS	4.392253155	-2.371589263
Retinoic acid receptor responder protein 2	RARRES2	2.447272144	-2.409158309
Microfibrillar-associated protein 2	MFAP2	3.048707111	-2.571843604
Amyloid-like protein 2	APLP2	2.364580699	-2.594886541
Coagulation factor X	F10	1.290852594	-2.871504545
Collagen alpha-1(XVI) chain	COL16A1	2.191419027	-3.267758509
Chitinase-3-like protein 1	CHI3L1	2.619076894	-3.309168994
Extracellular superoxide dismutase [Cu-Zn]	SOD3	1.156404296	-3.669391553
Dermokine	DMKN	2.363315937	-3.785676142
Mesogenin-1	MSGN1	0.639554851	2.66809535
Tetraspanin	CD81	0.955166181	2.527645091
Farnesyl pyrophosphate synthase	FDPS	0.825928569	2.433618625
Leukocyte elastase inhibitor	SERPINB1	0.965753119	2.002376477
Dipeptidyl peptidase 3	DPP3	0.753711846	1.869960864
Tenascin	TNC	0.619322353	1.801878681
Plasminogen activator inhibitor 1 RNA-binding protein	SERBP1	0.987521328	1.758133332
Glutamate dehydrogenase 1, mitochondrial	GLUD1	0.760826462	1.744286537
Endothelial differentiation-related factor 1	EDF1	0.9709638	1.738334656
Calmodulin-3	CALM3	0.360267891	1.710418185
Dickkopf-related protein 1	DKK 1.00	0.551443605	1.682086627
Protein S100-A10	S100A10	0.918383644	1.612988234
Nuclear migration protein nudC	NUDC	0.981999083	1.58617874
60S ribosomal protein L10a	RPL10A	0.772968198	1.579722802
Rho GTPase-activating protein 1	ARHGAP1	0.817963047	1.578868151
Sushi repeat-containing protein SRPX2	SRPX2	0.73388568	1.542654196

Protein	Gene	Value 1	Value 2
Fatty acid-binding protein 5	FABP5	0.778373359	1.446202676
Bone morphogenetic protein 1	BMP1	0.675705021	1.41992116
Proteasome subunit alpha type-3	PSMA3	0.812349569	1.383776983
Copper transport protein ATOX1	ATOX1	0.740664105	1.373387098
Importin-5	IPO5	0.942044991	1.342850765
Mitogen-activated protein kinase 1	MAPK1	0.6057904	1.307312687
Aldo-keto reductase family 1 member C1 (Fragment)	AKR1C1	0.9656138	1.303794841
Tubulin beta chain	TUBB	0.83403071	1.231346051
Early endosome antigen 1	EEA1	0.744327679	1.226502498
Adenylyl cyclase-associated protein 1	CAP1	0.877545829	1.221507629
6-phosphogluconolactonase	PGLS	0.549045125	1.216816823
PDZ and LIM domain protein 5	PDLIM5	0.570099979	1.215338667
Laminin subunit alpha-3	LAMA3	0.541528486	1.215059519
AP-2 complex subunit alpha-1	AP2A1	0.924090139	1.211398999
Protein transport protein SEC23	SEC23A	1.039706798	1.20786341
Glutaredoxin-3	GLRX3	0.741921966	1.203907569
Astrocytic phosphoprotein PEA-15	PEA15	0.805478812	1.190872431
Coatomer subunit delta	ARCN1	0.923570876	1.172869126
Polyadenylate-binding protein 1	PABPC1	0.462479016	1.161211411
Asparagine--tRNA ligase, cytoplasmic	NARS1	0.861969747	1.142909606
Alpha-actinin-1	ACTN1	0.477178662	1.135858297
Septin-9	SEPTIN9	0.88065993	1.134327968
T-complex protein 1 subunit gamma	CCT3	0.447606063	1.132881999
Calponin-3	CNN3	0.403434149	1.132146279
Ran-specific GTPase-activating protein (Fragment)	RANBP1	0.657222357	1.111449639
Basigin (Fragment)	BSG	0.383092914	1.095830162
Cellular retinoic acid-binding protein 2	CRABP2	0.796337176	1.090264241
Coatomer subunit beta	COPB2	0.796817264	1.082842747
Platelet-activating factor acetylhydrolase IB subunit beta	PAFAH1B2	0.748119624	1.050686717
Hsp90 co-chaperone Cdc37	CDC37	0.363825345	1.040936311
Protein S100-A13	S100A13	1.04006381	1.029016256
Ezrin	EZR	0.257219789	1.027226607
Reticulon (Fragment)	RTN4	0.377022563	1.019641638
Vacuolar protein sorting-associated protein 29	VPS29	0.764814309	1.012972315
Heterogeneous nuclear ribonucleoprotein K	HNRNPK	0.962603705	1.003495455
Torsin-1B (Fragment)	TOR1B	0.454439003	0.998319348
Nicotinamide phosphoribosyltransferase	NAMPT	0.578581614	0.988273382
Multifunctional protein ADE2	PAICS	0.625720803	0.974432111
Poly(rC)-binding protein 2 (Fragment)	PCBP2	0.970910443	0.964117606
Nicotinate-nucleotide pyrophosphorylase [carboxylating]	QPRT	1.084287772	0.958269676
Poly(rC)-binding protein 1	PCBP1	0.98317097	0.956842025
Vesicle-trafficking protein SEC22b	SEC22B	1.069917855	0.955706994
Importin subunit beta-1	KPNB1	0.955552676	0.953363498
Phosphoserine aminotransferase	PSAT1	0.777102355	0.952637513
Ubiquitin thioesterase OTUB1	OTUB1	0.95932489	0.941611369

SH3 domain-binding glutamic acid-rich-like protein	SH3BGRL	0.982171114	0.941470702
Proteasome subunit beta type-6	PSMB6	0.585861234	0.94093291
NEDD8	NEDD8	0.784344827	0.938138028
Ras-related protein Rab-11B	RAB11B	1.051352571	0.936566432
Ubiquitin carboxyl-terminal hydrolase 5	USP5	0.956751067	0.936038574
Tubulin alpha-1A chain	TUBA1A	0.78486013	0.930522362
Drebrin	DBN1	0.8315497	0.926125765
Tubulin-specific chaperone A	TBCA	0.86154647	0.918542147
Endoplasmic reticulum mannosyl-oligosaccharide 1,2-alpha-mannosidase	MAN1B1	0.487140044	0.91738836
Ras-related C3 botulinum toxin substrate 1	RAC1	0.449438744	0.915858984
Phosphatidylinositol transfer protein beta isoform	PITPNB	0.638385408	0.915614585
Beta tropomyosin isoform	TPM2	0.179654707	0.912316561
Caldesmon	CALD1	1.085194751	0.903115511
ATP synthase subunit beta, mitochondrial	ATP5F1B	1.131607045	0.892455816
Peroxiredoxin-2	PRDX2	1.107092355	0.892027458
Aminopeptidase B	RNPEP	1.072580627	0.891023715
Protein S100-A11	S100A11	0.493011169	0.883266528
Fumarylacetoacetase	FAH	0.926263978	0.855541309
Peptidyl-prolyl cis-trans isomerase FKBP3	FKBP3	0.417995823	0.841453632
S-phase kinase-associated protein 1	SKP1	0.540025203	0.841420293
Serine--tRNA ligase, cytoplasmic	SARS1	0.77155146	0.838749011
Collagen alpha-3(VI) chain	COL6A3	1.000240203	0.831179698
Heat shock-related 70 kDa protein 2	HSPA2	0.451699296	0.829777241
Heme-binding protein 2	HEBP2	1.058562517	0.815178315
Serpin B6	SERPINB6	0.732058095	0.799505472
Ubiquitin-conjugating enzyme E2 K (Fragment)	UBE2K	0.336384562	0.798599243
Dihydropyrimidinase-related protein 3	DPYSL3	0.596001201	0.796486298
Semaphorin-5A	SEMA5A	0.214263323	0.764399191
LIM and SH3 domain protein 1	LASP1	1.117848228	0.756635269
ATP-citrate synthase	ACLY	0.806440129	0.739698648
Syntaxin-12 (Fragment)	STX12	1.033157683	0.7375923
Thioredoxin domain-containing protein 17	TXNDC17	0.505543101	0.73285985
Proteasome activator complex subunit 1	PSME1	0.655820163	0.73216176
Microtubule-associated protein RP/EB family member 1	MAPRE1	0.46868074	0.730247815
Tryptophan--tRNA ligase, cytoplasmic	WARS1	0.469200793	0.708466272
Tubulin beta-1 chain	TUBB1	0.453300612	0.697334369
Acyl-CoA-binding protein	DBI	1.042509082	0.696588278
Spectrin alpha chain, non-erythrocytic 1	SPTAN1	1.214354965	0.690895796
Cysteinyl-tRNA synthetase 1	CARS1	0.300171894	0.686709126
Calponin (Fragment)	CNN2	0.375672429	0.679778973

Perilipin-3	PLIN3	0.651795762	0.653590759
Protein S100 (Fragment)	S100A6	0.252202306	0.643112421
Fumarate hydratase, mitochondrial	FH	0.912421292	0.63757809
Profilin-1	PFN1	0.843895305	0.635215362
14-3-3 protein epsilon	YWHAE	0.518990213	0.63105003
Spectrin beta chain, non-erythrocytic 1	SPTBN1	0.936081176	0.630083958
Transferrin receptor (P90, CD71), isoform CRA_c	TFRC	0.69704631	0.626204252
Dihydropyrimidinase-related protein 2	DPYSL2	1.142355973	0.61679705
Chitinase domain-containing protein 1	CHID1	0.977772669	0.603016138
Annexin A2	ANXA2	0.81486468	0.594894965
Aldo-keto reductase family 1 member A1	AKR1A1	0.875241011	0.593002558
Proteasome subunit beta type-1	PSMB1	0.800694651	0.587783257
Platelet-activating factor acetylhydrolase IB subunit gamma (Fragment)	PAFAH1B3	0.467112497	0.586437941
Twinfilin-2	TWF2	0.735992228	0.581241687
26S proteasome non-ATPase regulatory subunit 2	PSMD2	0.440323364	0.57870396
Fibrillin-2	FBN2	0.874607143	0.576408784
UMP-CMP kinase	CMPK1	0.158392665	0.57396396
Dynein light chain 2, cytoplasmic	DYNLL2	0.201323133	0.571045895
Vinculin	VCL	1.105006173	0.565798521
Protein SEC13 homolog	SEC13	0.603759614	0.564075947
Vacuolar protein sorting-associated protein 26A	VPS26A	0.684889682	0.561105808
Small nuclear ribonucleoprotein Sm D3	SNRPD3	0.445081966	0.559380829
Glutathione reductase, mitochondrial	GSR	0.380976542	0.553877751
Microtubule-associated protein 1A	MAP1A	0.93307125	0.547966003
Protein FAM3C	FAM3C	0.214756292	0.547220071
Thrombospondin-1	THBS1	1.137393516	0.540014346
Probable ATP-dependent RNA helicase DDX6	DDX6	0.696725548	0.529586395
Transforming growth factor beta receptor type 3	TGFBR3	0.211701286	0.527454217
Cofilin-2	CFL2	0.547072994	0.518479904
Adenylate kinase isoenzyme 1	AK1	0.182168321	0.51840961
Omega-amidase NIT2	NIT2	0.997889166	0.513859034
Sorting nexin-12	SNX12	0.259724666	0.50738887
Tropomyosin 1 (Alpha), isoform CRA_o (Fragment)	TPM1	0.281721221	0.505211671
Ribosome-binding protein 1	RRBP1	0.248243772	0.500103315
Microtubule-associated protein 4	MAP4	0.424121968	0.485429525
Thioredoxin domain-containing protein 5	TXNDC5	0.651505242	0.480779092
Collagen alpha-1(XII) chain	COL12A1	0.582783671	0.47566247
N-acetyl-D-glucosamine kinase	NAGK	0.355821836	0.469865322
Proteasome subunit alpha type	PSMA6	0.935526604	0.469257911

Eukaryotic translation initiation factor 4 gamma 1	EIF4G1	0.388419219	0.466981431
Ras-related protein Rab-1A	RAB1A	1.033644584	0.465621074
Insulin-like growth factor binding protein 3 isoform b	IGFBP3	1.201077849	0.462988774
Transaldolase	TALDO1	0.244304977	0.460857173
DBH-like monooxygenase protein 1	MOXD1	0.790524763	0.4413294
Thrombospondin-2	THBS2	0.664547893	0.440478404
Programmed cell death 6-interacting protein	PDCD6IP	0.758277077	0.433672984
Tropomyosin alpha-3 chain	TPM3	0.956977838	0.431095203
Myoferlin	MYOF	0.128924146	0.429277062
Protein disulfide-isomerase A3	PDIA3	0.77280848	0.428418239
Discoidin, CUB and LCCL domain-containing protein 2	DCBLD2	0.706472022	0.419278224
Four and a half LIM domains protein 2	FHL2	0.319402689	0.413938363
Stanniocalcin-2	STC2	1.495255822	0.406271378
Peptidyl-prolyl cis-trans isomerase FKBP1A	FKBP1A	0.249442696	0.396355073
Vesicular integral-membrane protein VIP36	LMAN2	1.26494854	0.393934647
RGM domain family member B	RGMB	0.774086048	0.391688426
Peptidyl-prolyl cis-trans isomerase B	PPIB	1.224078799	0.390159845
Superoxide dismutase [Cu-Zn]	SOD1	0.656599953	0.389679035
Proteasome subunit alpha type-1	PSMA1	0.530963042	0.387945096
Vasodilator-stimulated phosphoprotein	VASP	0.264939062	0.386965374
40S ribosomal protein S12	RPS12	0.159635379	0.381904483
Insulin-like growth factor-binding protein 7	IGFBP7	0.58764361	0.370351553
Zyxin (Fragment)	ZYX	0.424812472	0.363685846
Myosin light chain kinase, smooth muscle	MYLK	0.283932677	0.36093239
Growth/differentiation factor 15	GDF15	0.341290982	0.359459956
Galectin-1	LGALS1	0.390475872	0.356660287
T-complex protein 1 subunit zeta	CCT6A	0.527812599	0.356265823
Major prion protein	PRNP	1.433755661	0.354911725
Myotrophin	MTPN	0.135201666	0.35161531
Transitional endoplasmic reticulum ATPase	VCP	0.387776297	0.34742252
Proteasome subunit alpha type	PSMA2	0.768999739	0.333800077
Peroxidasin homolog	PXDN	0.934022265	0.324052095
Fibulin-1	FBLN1	2.141638683	0.317128579
Obg-like ATPase 1	OLA1	0.489111731	0.298976143
Gamma-glutamyl hydrolase	GGH	0.783228644	0.294991573
Follistatin	FST	1.30808858	0.294358651
Pregnancy-specific beta-1-glycoprotein 5	PSG5	1.248372103	0.291744788
Thioredoxin-like protein 1	TXNL1	0.355461108	0.291379054
Calcium/calmodulin-dependent protein kinase type II subunit delta	CAMK2D	0.134371495	0.286888619
Isocitrate dehydrogenase [NADP] cytoplasmic	IDH1	0.124484504	0.281799714
Phosphoacetylglucosamine mutase	PGM3	0.188097317	0.276491364

Adenylosuccinate synthetase isozyme 2	ADSS2	0.1292291	0.268136799
Apolipoprotein D	APOD	0.086452391	0.266761184
Alpha-L-iduronidase	IDUA	0.125491648	0.261411945
Protein NOXP20	FAM114A1	0.391999281	0.257456263
Phosphoglucomutase-1	PGM1	0.299564667	0.254699488
Integrin beta-1	ITGB1	0.458078639	0.248000701
Protein disulfide-isomerase	P4HB	0.604342308	0.246497234
Profilin	PFN2	0.089426835	0.24521172
45 kDa calcium-binding protein	SDF4	0.627675779	0.241725842
Prefoldin subunit 3	VBP1	0.423364526	0.24033165
Inactive carboxypeptidase-like protein X2	CPXM2	1.706714177	0.228319883
Laminin subunit alpha-4	LAMA4	0.519354924	0.225649436
Plasma alpha-L-fucosidase	FUCA2	0.402046168	0.222104947
Neuroblast differentiation-associated protein AHNAK	AHNAK	0.208126162	0.209472577
Stathmin (Fragment)	STMN1	0.128709658	0.204058727
Mammalian ependymin-related protein 1	EPDR1	0.490102984	0.202986797
Polypyrimidine tract binding protein 1, isoform CRA_b	PTBP1	0.195290903	0.195099751
Vimentin	VIM	0.148880361	0.192704916
Heterogeneous nuclear ribonucleoprotein D0 (Fragment)	HNRNPD	0.460966291	0.183664083
Neuropilin	NRP1	0.57273392	0.183382273
Dual specificity protein phosphatase 3	DUSP3	0.057112742	0.178610881
Tropomyosin alpha-4 chain	TPM4	0.239583143	0.1775949
40S ribosomal protein S16	RPS16	0.123704952	0.169804653
Tumor protein D54	TPD52L2	0.097520123	0.167672237
Protein-glutamine gamma-glutamyltransferase 2	TGM2	0.064319834	0.167084475
TRIO and F-actin-binding protein (Fragment)	TRIOBP	0.087177816	0.164823691
SPARC	SPARC	0.253343996	0.160933574
Heterogeneous nuclear ribonucleoprotein Q	SYNCRIP	0.092984565	0.14992253
Coiled-coil domain-containing protein 80	CCDC80	0.441305091	0.148980379
Proteasome activator complex subunit 2	PSME2	0.065389929	0.144456665
Phospholipid transfer protein	PLTP	0.280610756	0.127381086
Neural cell adhesion molecule L1	L1CAM	0.312385676	0.117721001
Transforming growth factor-beta-induced protein ig-h3	TGFBI	0.983647637	0.108537118
Pregnancy-specific beta-1-glycoprotein 3	PSG3	0.131720157	0.104186296
Beta-1,4-glucuronyltransferase 1	B4GAT1	0.127055931	0.103849173
Cytochrome c (Fragment)	CYCS	0.073222598	0.100700776
Collagen alpha-2(VI) chain	COL6A2	0.156896555	0.097944975
Polypeptide N-acetylgalactosaminyltransferase 2	GALNT2	0.313473021	0.090163628
Procollagen-lysine,2-oxoglutarate 5-dioxygenase 1	PLOD1	0.238708114	0.086933851

Multiple inositol polyphosphate phosphatase 1	MINPP1	0.022922289	0.083244602
Proteasome subunit alpha type-5	PSMA5	0.081314204	0.08107686
Protein-lysine 6-oxidase	LOX	0.117906508	0.071550131
Galectin-3	LGALS3	0.130783198	0.071405013
Pentraxin-related protein PTX3	PTX3	0.068996618	0.068731546
Nucleobindin-2	NUCB2	0.086641197	0.050719976
Calreticulin	CALR	0.055474369	0.050704718
Complement factor H	CFH	0.108134427	0.048236609
Laminin subunit alpha-1	LAMA1	0.109908546	0.041396538
Nucleophosmin	NPM1	0.014820617	0.033457518
Dickkopf-related protein 3	DKK 3.00	0.065278664	0.028205315
Inactive serine protease PAMR1	PAMR1	0.06287549	0.027279774
Beta-mannosidase	MANBA	0.061064363	0.026618719
Tetraspanin	CD9	0.007461459	0.02566878
Fibulin-1	FBLN1	0.026687736	0.024958849
Anthrax toxin receptor 1	ANTXR1	0.045308139	0.024532715
EH domain-containing protein 2	EHD2	0.011202345	0.022169193
Sulfhydryl oxidase 1	QSOX1	0.068641458	0.02139926
Testican-1	SPOCK1	0.03054329	0.015490452
Multifunctional procollagen lysine hydroxylase and glycosyltransferase LH3	PLOD3	0.017408707	0.014717976
Agrin	AGRN	0.016222198	0.014592727
Microtubule-associated protein 1 light chain 3 beta, isoform CRA_f	MAP1LC3B	0.000636783	0.002199431
Methanethiol oxidase (Fragment)	SELENBP1	0.002018957	0.002117157
Myosin light chain 1/3, skeletal muscle isoform	MYL1	NaN	0
Prolactin-inducible protein	PIP	NaN	0
Aspartyl-tRNA synthetase 1 (Fragment)	DARS1	NaN	0
Glycine--tRNA ligase	GARS1	NaN	0
Tumor necrosis factor-inducible gene 6 protein	TNFAIP6	NaN	0
Tubulin beta-3 chain	TUBB3	NaN	0
AP-2 complex subunit mu	AP2M1	NaN	0
Lysyl oxidase homolog 4	LOXL4	NaN	0
Fibulin-5	FBLN5	0.002218189	-0.002180497
Myosin phosphatase Rho-interacting protein (Fragment)	MPRIP	0.00595644	-0.007666906
Alpha-mannosidase 2	MAN2A1	0.017225143	-0.00972867
HLA class I histocompatibility antigen, A alpha chain	HLA-A	0.013327963	-0.011158864
Basement membrane-specific heparan sulfate proteoglycan core protein	HSPG2	0.04392115	-0.018473546
Thyrotropin-releasing hormone-degrading ectoenzyme	TRHDE	0.04994111	-0.025828123
Cysteine-rich motor neuron 1 protein	CRIM1	0.061213536	-0.035299857
Cadherin-2	CDH2	0.032185103	-0.036393881
Exostosin-1	EXT1	0.100858838	-0.043623368
Protein S100-A16	S100A16	0.032933419	-0.043970545
Polypeptide N-acetylgalactosaminyltransferase 6	GALNT6	0.095427428	-0.046231349

60S acidic ribosomal protein P0 (Fragment)	RPLP0	0.040246189	-0.053255141
Endothelial protein C receptor	PROCR	0.063882028	-0.05603989
Tenascin	TNC	0.041403746	-0.058978001
N-acetylglucosamine-1-phosphotransferase subunit gamma	GNPTG	0.32437905	-0.065951109
Laminin subunit gamma-1	LAMC1	0.125908377	-0.06632638
Neurofascin (Fragment)	NFASC	0.298032912	-0.066758712
Prolow-density lipoprotein receptor-related protein 1	LRP1	0.196370141	-0.069421371
Myristoylated alanine-rich C-kinase substrate	MARCKS	0.017624836	-0.069714586
Latent-transforming growth factor beta-binding protein 2	LTBP2	0.148558075	-0.072689931
CCN family member 1	CCN1	0.089272029	-0.077148835
Tartrate-resistant acid phosphatase type 5	ACP5	0.134229834	-0.077513615
Actin-related protein 2/3 complex subunit 5	ARPC5	0.032125388	-0.077598691
Cathepsin K	CTSK	0.124623232	-0.081551154
Heterogeneous nuclear ribonucleoprotein A1 (Fragment)	HNRNPA1	0.042551733	-0.081837098
Hepatocyte growth factor-like protein (Fragment)	MST1	0.257785199	-0.082461278
Heterogeneous nuclear ribonucleoprotein A/B	HNRNPAB	0.055464081	-0.083924413
Complement C3	C3	0.135212449	-0.084174554
Proteasome subunit beta type-2	PSMB2	0.024661952	-0.086595476
Metalloproteinase inhibitor 1	TIMP1	0.315680241	-0.091641982
Fibronectin	FN1	0.30302166	-0.098887364
Fibroblast growth factor receptor 1	FGFR1	0.03570824	-0.103049477
Lysosomal alpha-mannosidase	MAN2B1	0.335573434	-0.113666455
Carbohydrate sulfotransferase 3	CHST3	0.123764556	-0.127701998
Transmembrane glycoprotein NMB	GPNMB	0.209381831	-0.129987478
Podocan	PODN	0.288685662	-0.13082703
Laminin subunit beta-1	LAMB1	0.30628771	-0.134037574
Pregnancy-specific beta-1-glycoprotein 1	PSG1	0.467785486	-0.134519021
Prelamin-A/C	LMNA	0.100634852	-0.141031663
Serine-threonine kinase receptor-associated protein	STRAP	0.044060553	-0.147514661
Inactive C-alpha-formylglycine-generating enzyme 2 (Fragment)	SUMF2	0.103749072	-0.152743538
Collagen alpha-1(III) chain	COL3A1	0.25860882	-0.153634946
Prolargin	PRELP	0.307148821	-0.159806649
Olfactomedin-like protein 1	OLFML1	0.152815648	-0.163314581
Pregnancy-specific beta-1-glycoprotein 4	PSG4	0.945349255	-0.163491488
Flavin reductase (NADPH)	BLVRB	0.063370223	-0.164509813
Thrombospondin-3	THBS3	0.349634389	-0.170180559
40S ribosomal protein S3	RPS3	0.130241811	-0.172356288
Reversion-inducing cysteine-rich protein with Kazal motifs	RECK	0.364052495	-0.176974376

Sushi, von Willebrand factor type A, EGF and pentraxin domain-containing protein 1	SVEP1	0.687352727	-0.179796616
Sialate O-acetylesterase	SIAE	0.342783271	-0.180612008
Biglycan	BGN	0.79108712	-0.18265446
Endoplasmic reticulum aminopeptidase 1	ERAP1	0.452665433	-0.186700265
Cathepsin S	CTSS	0.8516405	-0.193571329
Cytoplasmic dynein 1 heavy chain 1	DYNC1H1	0.056520088	-0.193644385
Follistatin-related protein 1	FSTL1	0.341220095	-0.204685767
Neprilysin	MME	0.387440123	-0.205853701
Acylamino-acid-releasing enzyme	APEH	0.116683325	-0.215376238
Alpha-1,3-mannosyl-glycoprotein 2-beta-N-acetylglucosaminyltransferase	MGAT1	0.849021718	-0.216223001
Collagen alpha-1(XI) chain	COL11A1	0.527596193	-0.225652138
Target of Nesh-SH3	ABI3BP	0.687645692	-0.226257404
High mobility group protein HMG-I/HMG-Y	HMGA1	0.068235398	-0.229134639
Syntenin-1	SDCBP	0.717715593	-0.23002998
N-acetylgalactosamine-6-sulfatase	GALNS	1.042601439	-0.236880859
60S ribosomal protein L12	RPL12	0.168525472	-0.252744714
Sushi repeat-containing protein SRPX	SRPX	0.49338188	-0.261390448
Serpin H1	SERPINH1	0.345502018	-0.261612495
Chromobox protein homolog 3	CBX3	1.297433903	-0.268467347
Exostosin-2	EXT2	0.762400786	-0.269315163
Glucosylceramidase	GBA	1.916590095	-0.271295945
Biotinidase (Fragment)	BTD	0.105657023	-0.27546831
Lumican	LUM	1.0733711	-0.291396062
Lysosomal alpha-glucosidase	GAA	0.784197673	-0.299209674
Chondroitin sulfate proteoglycan 4	CSPG4	1.611018708	-0.302456299
Growth arrest-specific protein 6	GAS6	0.63621117	-0.303549369
Spliceosome RNA helicase DDX39B	DDX39B	0.209354561	-0.313421885
Pterin-4-alpha-carbinolamine dehydratase	PCBD1	0.278015342	-0.315283
Pro-cathepsin H	CTSH	0.143744012	-0.317852318
Matrix metalloproteinase-19	MMP19	0.13671455	-0.325282971
Proteasome subunit beta type-5	PSMB5	0.367176432	-0.342689435
Dynactin subunit 2 (Fragment)	DCTN2	0.134378304	-0.357490162
Vascular endothelial growth factor C	VEGFC	0.13632951	-0.371932288
Attractin	ATRN	1.586380181	-0.377553542
Cell migration-inducing and hyaluronan-binding protein	CEMIP	0.904941988	-0.377890507
Collagen alpha-2(V) chain	COL5A2	1.13574712	-0.380575895
A disintegrin and metalloproteinase with thrombospondin motifs 5	ADAMTS5	0.352484978	-0.385268927
Disintegrin and metalloproteinase domain-containing protein 10	ADAM10	0.879327091	-0.38582174
Golgi membrane protein 1	GOLM1	0.719961693	-0.386855205
HLA class I histocompatibility antigen, A alpha chain	HLA-A	1.110332351	-0.388292551
Fructose-bisphosphate aldolase C	ALDOC	0.38365371	-0.392734766
Nucleolin	NCL	0.157925955	-0.393222074
Glypican-1	GPC1	0.849691043	-0.39997983
Inhibin beta A chain	INHBA	0.331467569	-0.40601172

Receptor-type tyrosine-protein phosphatase kappa	PTPRK	1.483218073	-0.406799078
Serine/threonine-protein phosphatase CPPED1	CPPED1	0.103623636	-0.407270511
Latent-transforming growth factor beta-binding protein 1	LTBP1	0.351775211	-0.40934668
CCN family member 3	CCN3	0.516737413	-0.41010054
Protein disulfide-isomerase A4	PDIA4	0.401825807	-0.41121761
4F2 cell-surface antigen heavy chain	SLC3A2	0.218012646	-0.412554979
Retinoid-inducible serine carboxypeptidase	SCPEP1	0.515865301	-0.412682136
Collagen alpha-1(VI) chain	COL6A1	0.894288613	-0.416096608
Thymosin beta-4	TMSB4X	0.354125279	-0.418390354
Heat shock 70 kDa protein 13	HSPA13	0.766525575	-0.418607632
RNA-binding motif protein, X chromosome (Fragment)	RBMX	0.182206161	-0.423674027
Twisted gastrulation protein homolog 1	TWSG1	0.431087547	-0.425108989
Collagen alpha-1(I) chain	COL1A1	1.060031607	-0.43995436
Lysosomal acid lipase/cholesteryl ester hydrolase	LIPA	0.51591511	-0.455606222
Neurogenic locus notch homolog protein 2	NOTCH2	0.40052175	-0.457384507
Calsyntenin-1	CLSTN1	1.497120705	-0.467484872
Disintegrin and metalloproteinase domain-containing protein 9	ADAM9	0.773370451	-0.470208248
Poliovirus receptor	PVR	0.345206095	-0.475210706
Beta-1,4-galactosyltransferase 1	B4GALT1	0.484191125	-0.475276391
N-sulphoglucosamine sulphohydrolase	SGSH	1.125398542	-0.477149725
182 kDa tankyrase-1-binding protein	TNKS1BP1	0.39883798	-0.495597045
Glutaminyl-peptide cyclotransferase	QPCT	1.160257378	-0.514094114
Interleukin-6 receptor subunit beta	IL6ST	0.173268398	-0.523417016
Tyrosine-protein kinase receptor UFO	AXL	1.059687661	-0.537263632
Macrophage colony-stimulating factor 1	CSF1	0.665329518	-0.54084293
Adipocyte enhancer-binding protein 1	AEBP1	0.848911667	-0.555448771
Platelet-derived growth factor receptor beta	PDGFRB	0.731621972	-0.557956298
Cellular nucleic acid-binding protein	CNBP	0.720377408	-0.568440755
Lactadherin	MFGE8	0.639139117	-0.570791006
Calpain small subunit 1	CAPNS1	0.259413495	-0.607286692
Heat shock protein HSP 90-beta	HSP90AB1	0.358513812	-0.607802471
Retinol-binding protein	RBP4	0.140792183	-0.611309111
Beta-glucuronidase	GUSB	0.464611918	-0.632908543
Lysyl oxidase homolog 3	LOXL3	0.378420666	-0.638810356
Integrin beta-like protein 1	ITGBL1	0.871762965	-0.644319296
Lymphocyte antigen 96	LY96	0.751433043	-0.697218815
Endoplasmin	HSP90B1	0.48011686	-0.704362313
Galactosylgalactosylxylosylprotein 3-beta-glucuronosyltransferase 3	B3GAT3	1.019696207	-0.710418781
Heterogeneous nuclear ribonucleoproteins A2/B1	HNRNPA2B1	0.904373596	-0.725393375

Cytochrome c oxidase subunit 6B1	COX6B1	0.36445809	-0.728272994
Ganglioside GM2 activator	GM2A	0.754963997	-0.732430538
Interleukin enhancer-binding factor 2	ILF2	0.541438508	-0.740470529
DNA-(apurinic or apyrimidinic site) lyase (Fragment)	APEX1	0.415199756	-0.743161023
High mobility group protein B1	HMGB1	0.455876344	-0.772212923
Disintegrin and metalloproteinase domain-containing protein 17	ADAM17	0.390541718	-0.788431287
Cytoplasmic dynein 1 intermediate chain 2 (Fragment)	DYNC1I2	1.074864952	-0.810199082
Fatty acid-binding protein, heart	FABP3	1.062348557	-0.883185625
Hepatoma-derived growth factor	HDGF	1.09756208	-0.891282876
Neuronal growth regulator 1	NEGR1	0.726543673	-0.911343376
Renin receptor	ATP6AP2	0.512751863	-0.940920194
Thrombospondin-4	THBS4	0.914376566	-0.943706354
Syndecan-4	SDC4	0.347473252	-0.987963319
Platelet-derived growth factor receptor alpha	PDGFRA	0.682508664	-0.993355532
Heat shock protein HSP 90-alpha	HSP90AA1	0.481482445	-1.004070481
Growth-regulated alpha protein	CXCL1	0.35629131	-1.01723516
Formylglycine-generating enzyme	SUMF1	0.585557545	-1.019484599
Destrin	DSTN	1.087238815	-1.034716229
Versican core protein	VCAN	0.552245184	-1.042034686
Receptor-type tyrosine-protein phosphatase gamma	PTPRG	0.634496755	-1.181649089
CD44 antigen	CD44	0.319414494	-1.359974186
Extracellular serine/threonine protein kinase FAM20C	FAM20C	1.053067916	-1.376800617
Iduronate 2-sulfatase	IDS	0.599261384	-1.393489182
Tissue alpha-L-fucosidase	FUCA1	0.378142369	-1.408541421
UPAR/Ly6 domain-containing protein OS=Homo sapiens OX=9606 PE=1 SV=1;tr|A0A2U3TZL5|A0A2U3TZL5	CD59	0.526879673	-1.440245807
Fibromodulin	FMOD	0.667168823	-1.479532878
A-kinase anchor protein 2	AKAP2	0.271417689	-1.683425546
Ubiquitin-40S ribosomal protein S27a	RPS27A	0.749887822	-1.77071929
Microfibril-associated glycoprotein 4	MFAP4	0.775009846	-1.994044224
Stromal cell-derived factor 1	CXCL12	0.786484509	-2.334161003

Table 6-3HFF versus HFF+ LIPUS SASP secretome profile

Protein name	Gene name	Student's T-test Difference - HFF_HFF+LIPUS	-Log Student's T-test p-value -HFF_HFF+LIPUS
Soluble scavenger receptor cysteine-rich domain-containing protein SSC5D	SSC5D	-0.772696336	2.837975814
Multifunctional procollagen lysine hydroxylase and glycosyltransferase LH3	PLOD3	-0.734518687	4.755134873
N(G),N(G)-dimethylarginine dimethylaminohydrolase 1	DDAH1	-0.688067913	3.68911517
Reversion-inducing cysteine-rich protein with Kazal motifs	RECK	-0.536189715	3.279536534
Amyloid-beta precursor protein	APP	0.723594348	3.284839081
Cathepsin B	CTSB	0.414785067	3.327722445
Laminin subunit beta-1	LAMB1	-0.47095267	2.90309079
Collagen alpha-2(VI) chain	COL6A2	-0.905970573	3.308070648
N-acetylglucosamine-6-sulfatase	GNS	1.538537025	3.720740705
Endoglin	ENG	-0.895672639	2.935665601
Pentraxin-related protein PTX3	PTX3	-0.662480354	2.829386082
Fibrillin-1	FBN1	-0.704985142	3.596943754
Fibrillin-2	FBN2	-0.840233485	4.032794965
F-actin-capping protein subunit beta	CAPZB	-0.889746825	2.958296272
Pappalysin-1	PAPPA	-0.538105488	2.999341114
Insulin-like growth factor-binding protein 7	IGFBP7	-0.391960144	2.8437132
Peroxidasin homolog	PXDN	-0.768631458	3.303068676
Collagen alpha-1(XII) chain	COL12A1	-1.424214363	2.932401109
Chloride intracellular channel protein 4	CLIC4	-1.342864196	3.278668256

7 Reference list

ABU-ZIDAN, F. M., HEFNY, A. F. & CORR, P. 2011. Clinical ultrasound physics. *J Emerg Trauma Shock,* 4**,** 501-3.

ACOSTA, J. C., BANITO, A., WUESTEFELD, T., GEORGILIS, A., JANICH, P., MORTON, J. P., ATHINEOS, D., KANG, T. W., LASITSCHKA, F., ANDRULIS, M., PASCUAL, G., MORRIS, K. J., KHAN, S., JIN, H., DHARMALINGAM, G., SNIJDERS, A. P., CARROLL, T., CAPPER, D., PRITCHARD, C., INMAN, G. J., LONGERICH, T., SANSOM, O. J., BENITAH, S. A., ZENDER, L. & GIL, J. 2013. A complex secretory program orchestrated by the inflammasome controls paracrine senescence. *Nat Cell Biol,* 15**,** 978-90.

ACOSTA, J. C., O'LOGHLEN, A., BANITO, A., GUIJARRO, M. V., AUGERT, A., RAGUZ, S., FUMAGALLI, M., DA COSTA, M., BROWN, C., POPOV, N., TAKATSU, Y., MELAMED, J., D'ADDA DI FAGAGNA, F., BERNARD, D., HERNANDO, E. & GIL, J. 2008. Chemokine signaling via the CXCR2 receptor reinforces senescence. *Cell,* 133**,** 1006-18.

AIRD, K. M. & ZHANG, R. 2013. Detection of senescence-associated heterochromatin foci (SAHF). *Methods Mol Biol,* 965**,** 185-96.

ALKAHTANI, S. A., KUNWAR, P. S., JALILIFAR, M., RASHIDI, S. & YADOLLAHPOUR, A. 2017. Ultrasound-based Techniques as Alternative Treatments for Chronic Wounds: A Comprehensive Review of Clinical Applications. *Cureus,* 9**,** e1952.

ALTHUBITI, M., LEZINA, L., CARRERA, S., JUKES-JONES, R., GIBLETT, S. M., ANTONOV, A., BARLEV, N., SALDANHA, G. S., PRITCHARD, C. A.,
N, K. & MACIP, S. 2014.
Characterization of novel markers of senescence and their prognostic potential in cancer. *Cell Death Dis,* 5**,** e1528.

AMAYA, C., LUO, S., BAIGORRI, J., BAUCELLS, R., SMITH, E. R. & XU, X. X. 2021. Exposure to low intensity ultrasound removes paclitaxel cytotoxicity in breast and ovarian cancer cells. *BMC Cancer,* 21**,** 981.

AMOR, C., FEUCHT, J., LEIBOLD, J., HO, Y. J., ZHU, C., ALONSO-CURBELO, D., MANSILLA-SOTO, J., BOYER, J. A., LI, X., GIAVRIDIS, T., KULICK, A., HOULIHAN, S., PEERSCHKE, E., FRIEDMAN, S. L., PONOMAREV, V., PIERSIGILLI, A., SADELAIN, M. & LOWE, S. W. 2020. Senolytic CAR T cells reverse senescence-associated pathologies. *Nature,* 583**,** 127-132.

ASANUMA, D., SAKABE, M., KAMIYA, M., YAMAMOTO, K., HIRATAKE, J., OGAWA, M., KOSAKA, N., CHOYKE, P. L., NAGANO, T., KOBAYASHI, H. & URANO, Y. 2015. Sensitive beta-galactosidase-targeting fluorescence probe for visualizing small peritoneal metastatic tumours in vivo. *Nat Commun,* 6**,** 6463.

ATHERTON, P., LAUSECKER, F., HARRISON, A. & BALLESTREM, C. 2017. Low-intensity pulsed ultrasound promotes cell motility through vinculin-controlled Rac1 GTPase activity. *J Cell Sci,* 130**,** 2277-2291.

AW, D. & PALMER, D. B. 2011. The origin and implication of thymic involution. *Aging Dis,* 2**,** 437-43.

BAINBRIDGE, P. 2013. Wound healing and the role of fibroblasts. *J Wound Care,* 22**,** 407-8, 410-12.

BAKER, D. J., CHILDS, B. G., DURIK, M., WIJERS, M. E., SIEBEN, C. J., ZHONG, J., SALTNESS, R. A., JEGANATHAN, K. B., VERZOSA, G. C., PEZESHKI, A., KHAZAIE, K., MILLER, J. D. & VAN DEURSEN, J. M. 2016. Naturally occurring p16(Ink4a)-positive cells shorten healthy lifespan. *Nature,* 530**,** 184-9.

BAKER, K. G., ROBERTSON, V. J. & DUCK, F. A. 2001. A review of therapeutic ultrasound: biophysical effects. *Phys Ther,* 81**,** 1351-8.

BALAJEE, A. S. & GEARD, C. R. 2004. Replication protein A and gamma-H2AX foci assembly is triggered by cellular response to DNA double-strand breaks. *Exp Cell Res,* 300**,** 320-34.

BASISTY, N., KALE, A., JEON, O. H., KUEHNEMANN, C., PAYNE, T., RAO, C., HOLTZ, A., SHAH, S., SHARMA, V., FERRUCCI, L., CAMPISI, J. & SCHILLING, B. 2020. A proteomic atlas of senescence-associated secretomes for aging biomarker development. *PLoS Biol,* 18**,** e3000599.

BASU, A. & KRISHNAMURTHY, S. 2010. Cellular responses to Cisplatin-induced DNA damage. *J Nucleic Acids,* 2010.

BAVIK, C., COLEMAN, I., DEAN, J. P., KNUDSEN, B., PLYMATE, S. & NELSON, P. S. 2006. The gene expression program of prostate fibroblast senescence modulates neoplastic epithelial cell proliferation through paracrine mechanisms. *Cancer Res,* 66**,** 794-802.

BAZ-MARTINEZ, M., DA SILVA-ALVAREZ, S., RODRIGUEZ, E., GUERRA, J., EL MOTIAM, A., VIDAL, A., GARCIA-CABALLERO, T., GONZALEZ-BARCIA, M., SANCHEZ, L., MUNOZ-FONTELA, C., COLLADO, M. & RIVAS, C. 2016. Cell senescence is an antiviral defense mechanism. *Sci Rep,* 6**,** 37007.

BEAUSEJOUR, C. M., KRTOLICA, A., GALIMI, F., NARITA, M., LOWE, S. W., YASWEN, P. & CAMPISI, J. 2003. Reversal of human cellular senescence: roles of the p53 and p16 pathways. *EMBO J,* 22**,** 4212-22.

BEN-PORATH, I. & WEINBERG, R. A. 2005. The signals and pathways activating cellular senescence. *Int J Biochem Cell Biol,* 37**,** 961-76.

BERNADOTTE, A., MIKHELSON, V. M. & SPIVAK, I. M. 2016. Markers of cellular senescence. Telomere shortening as a marker of cellular senescence. *Aging (Albany NY),* 8**,** 3-11.

BIRCH, J. & GIL, J. 2020. Senescence and the SASP: many therapeutic avenues. *Genes Dev,* 34**,** 1565-1576.

BODE-BOGER, S. M., SCALERA, F. & MARTENS-LOBENHOFFER, J. 2005. Asymmetric dimethylarginine (ADMA) accelerates cell senescence. *Vasc Med,* 10 Suppl 1**,** S65-71.

BONHAM, C. A., KUEHLMANN, B. & GURTNER, G. C. 2020. Impaired Neovascularization in Aging. *Adv Wound Care (New Rochelle),* 9**,** 111-126.

BORODKINA, A. V., DERYABIN, P. I., GIUKOVA, A. A. & NIKOLSKY, N. N. 2018. "Social Life" of Senescent Cells: What Is SASP and Why Study It? *Acta Naturae,* 10**,** 4-14.

BOSANQUET, D. C. & HARDING, K. G. 2014. Wound duration and healing rates: cause or effect? *Wound Repair Regen,* 22**,** 143-50.

BREMNES, R. M., DONNEM, T., AL-SAAD, S., AL-SHIBLI, K., ANDERSEN, S., SIRERA, R., CAMPS, C., MARINEZ, I. & BUSUND, L. T. 2011. The role of tumor stroma in cancer progression and prognosis: emphasis on carcinoma-associated fibroblasts and non-small cell lung cancer. *J Thorac Oncol,* 6**,** 209-17.

BYUN, H. O., LEE, Y. K., KIM, J. M. & YOON, G. 2015. From cell senescence to age-related diseases: differential mechanisms of action of senescence-associated secretory phenotypes. *BMB Rep,* 48**,** 549-58.

BYUN, J. S. & GARDNER, K. 2013. Wounds that will not heal: pervasive cellular reprogramming in cancer. *Am J Pathol,* 182**,** 1055-64.

CAI, Z. J. 2021. Hypothalamic aging and hormones. *Vitam Horm,* 115**,** 15-37.

CAMPISI, J. 1997. The biology of replicative senescence. *Eur J Cancer,* 33**,** 703-9.

CAMPISI, J. 2013. Aging, cellular senescence, and cancer. *Annu Rev Physiol,* 75**,** 685-705.

CAMPISI, J. & D'ADDA DI FAGAGNA, F. 2007. Cellular senescence: when bad things happen to good cells. *Nat Rev Mol Cell Biol,* 8**,** 729-40.

CAPPARELLI, C., CHIAVARINA, B., WHITAKER-MENEZES, D., PESTELL, T. G., PESTELL, R. G., HULIT, J., ANDO, S., HOWELL, A., MARTINEZ-OUTSCHOORN, U. E., SOTGIA, F. & LISANTI, M. P. 2012. CDK inhibitors (p16/p19/p21) induce senescence and autophagy in cancer-associated fibroblasts, "fueling" tumor growth via paracrine interactions, without an increase in neo-angiogenesis. *Cell Cycle,* 11**,** 3599-610.

CASELLA, G., MUNK, R., KIM, K. M., PIAO, Y., DE, S., ABDELMOHSEN, K. & GOROSPE, M. 2019. Transcriptome signature of cellular senescence. *Nucleic Acids Res,* 47**,** 11476.

CAZIN, C., CHICHE, A. & LI, H. 2017. Evaluation of Injury-induced Senescence and In Vivo Reprogramming in the Skeletal Muscle. *J Vis Exp.*

CESARI, M., PAHOR, M. & INCALZI, R. A. 2010. Plasminogen activator inhibitor-1 (PAI-1): a key factor linking fibrinolysis and age-related subclinical and clinical conditions. *Cardiovasc Ther,* 28**,** e72-91.

CHAIB, S., TCHKONIA, T. & KIRKLAND, J. L. 2022. Cellular senescence and senolytics: the path to the clinic. *Nat Med,* 28**,** 1556-1568.

CHANG, B. D., SWIFT, M. E., SHEN, M., FANG, J., BROUDE, E. V. & RONINSON, I. B. 2002. Molecular determinants of terminal growth arrest induced in tumor cells by a chemotherapeutic agent. *Proc Natl Acad Sci U S A,* 99**,** 389-94.

CHANG, Y. R., PERRY, J. & CROSS, K. 2017. Low-Frequency Ultrasound Debridement in Chronic Wound Healing: A Systematic Review of Current Evidence. *Plast Surg (Oakv),* 25**,** 21-26.

CHEN, J., WANG, W., LI, C., XIA, Y., XU, H., CHEN, J., CHEN, W. & WANG, Y. 2022. Potential Application of Low-Intensity Pulsed Ultrasound in Delaying Aging for Mice. *Gerontology,* 68**,** 558-570.

CHEN, J. H., HALES, C. N. & OZANNE, S. E. 2007. DNA damage, cellular senescence and organismal aging: causal or correlative? *Nucleic Acids Res,* 35**,** 7417-28.

CHOU, L. Y., HO, C. T. & HUNG, S. C. 2022. Paracrine Senescence of Mesenchymal Stromal Cells Involves Inflammatory Cytokines and the NF-kappaB Pathway. *Cells,* 11.

CICCIA, A. & ELLEDGE, S. J. 2010. The DNA damage response: making it safe to play with knives. *Mol Cell,* 40**,** 179-204.

CIRRI, P. & CHIARUGI, P. 2011. Cancer associated fibroblasts: the dark side of the coin. *Am J Cancer Res,* 1**,** 482-97.

COLLADO, M., BLASCO, M. A. & SERRANO, M. 2007. Cellular senescence in cancer and aging. *Cell,* 130**,** 223-33.

COLLADO, M., GIL, J., EFEYAN, A., GUERRA, C., SCHUHMACHER, A. J., BARRADAS, M., BENGURIA, A., ZABALLOS, A., FLORES, J. M., BARBACID, M., BEACH, D. & SERRANO, M. 2005. Tumour biology: senescence in premalignant tumours. *Nature,* 436**,** 642.

COMI, P., CHIARAMONTE, R. & MAIER, J. A. 1995. Senescence-dependent regulation of type 1 plasminogen activator inhibitor in human vascular endothelial cells. *Exp Cell Res,* 219**,** 304-8.

COPPE, J. P., DESPREZ, P. Y., KRTOLICA, A. & CAMPISI, J. 2010. The senescence-associated secretory phenotype: the dark side of tumor suppression. *Annu Rev Pathol,* 5**,** 99-118.

COPPE, J. P., PATIL, C. K., RODIER, F., SUN, Y., MUNOZ, D. P., GOLDSTEIN, J., NELSON, P. S., DESPREZ, P. Y. & CAMPISI, J. 2008. Senescence-associated secretory phenotypesreveal cell-nonautonomous functions of oncogenic RAS and the p53 tumor suppressor. *PLoS Biol,* 6**,** 2853-68.

CORREIA-MELO, C. & PASSOS, J. F. 2015. Mitochondria: Are they causal players in cellular senescence? *Biochim Biophys Acta,* 1847**,** 1373-9.

COX, J. & MANN, M. 2008. MaxQuant enables high peptide identification rates, individualized p.p.b.-range mass accuracies and proteome-wide protein quantification. *Nat Biotechnol,* 26**,** 1367-72.

CROCHEMORE, C., FERNANDEZ-MOLINA, C., MONTAGNE, B., SALLES, A. & RICCHETTI, M. 2019. CSB promoter downregulation via histone H3 hypoacetylation is an early determinant of replicative senescence. *Nat Commun,* 10**,** 5576.

CUOLLO, L., ANTONANGELI, F., SANTONI, A. & SORIANI, A. 2020. The Senescence-Associated Secretory Phenotype (SASP) in the Challenging Future of Cancer Therapy and Age-Related Diseases. *Biology (Basel),* 9.

DASARI, S. & TCHOUNWOU, P. B. 2014. Cisplatin in cancer therapy: molecular mechanisms of action. *Eur J Pharmacol,* 740**,** 364-78.

DASGUPTA, J., KAR, S., LIU, R., JOSEPH, J., KALYANARAMAN, B., REMINGTON, S. J., CHEN, C. & MELENDEZ, J. A. 2010. Reactive oxygen species control senescence-associated matrix metalloproteinase-1 through c-Jun-N-terminal kinase. *J Cell Physiol,* 225**,** 52-62.

DE AVILA SANTANA, L., ALVES, J. M., ANDRADE, T. A., KAJIWARA, J. K., GARCIA, S. B., GOMES, F. G. & FRADE, M. A. 2013. Clinical and immunohistopathological aspects of venous ulcers treatment by Low-Intensity Pulsed Ultrasound (LIPUS). *Ultrasonics,* 53**,** 870-9.

DE MAAR, J. S., ROUSOU, C., VAN ELBURG, B., VOS, H. J., LAJOINIE, G. P. R., BOS, C., MOONEN, C. T. W. & DECKERS, R. 2021. Ultrasound-Mediated Drug Delivery With a Clinical Ultrasound System: In Vitro Evaluation. *Front Pharmacol,* 12**,** 768436.

DE MERA-RODRIGUEZ, J. A., ALVAREZ-HERNAN, G., GANAN, Y., MARTIN-PARTIDO, G., RODRIGUEZ-LEON, J. & FRANCISCO-MORCILLO, J. 2021. Is Senescence-Associated beta-Galactosidase a Reliable in vivo Marker of Cellular Senescence During Embryonic Development? *Front Cell Dev Biol,* 9**,** 623175.

DEMARIA, M., O'LEARY, M. N., CHANG, J., SHAO, L., LIU, S., ALIMIRAH, F., KOENIG, K., LE, C., MITIN, N., DEAL, A. M., ALSTON, S., ACADEMIA, E. C., KILMARX, S., VALDOVINOS, A., WANG, B., DE BRUIN, A., KENNEDY, B. K., MELOV, S., ZHOU, D., SHARPLESS, N. E., MUSS, H. & CAMPISI, J. 2017. Cellular Senescence Promotes Adverse Effects of Chemotherapy and Cancer Relapse. *Cancer Discov,* 7**,** 165-176.

DEMARIA, M., OHTANI, N., YOUSSEF, S. A., RODIER, F., TOUSSAINT, W., MITCHELL, J. R., LABERGE, R. M., VIJG, J., VAN STEEG, H., DOLLE, M. E., HOEIJMAKERS, J. H., DE BRUIN, A., HARA, E. & CAMPISI, J. 2014. An essential role for senescent cells in optimal wound healing through secretion of PDGF-AA. *Dev Cell,* 31**,** 722-33.

DEMIDOVA-RICE, T. N., DURHAM, J. T. & HERMAN, I. M. 2012a. Wound Healing Angiogenesis: Innovations and Challenges in Acute and Chronic Wound Healing. *Adv Wound Care (New Rochelle),* 1**,** 17-22.

DEMIDOVA-RICE, T. N., HAMBLIN, M. R. & HERMAN, I. M. 2012b. Acute and impaired wound healing: pathophysiology and current methods for drug delivery, part 1: normal and chronic wounds: biology, causes, and approaches to care. *Adv Skin Wound Care,* 25**,** 304-14.

DHAR, S., KOLISHETTI, N., LIPPARD, S. J. & FAROKHZAD, O. C. 2011. Targeted delivery of a cisplatin prodrug for safer and more effective prostate cancer therapy in vivo. *Proc Natl Acad Sci U S A,* 108**,** 1850-5.

DI MICCO, R., SULLI, G., DOBREVA, M., LIONTOS, M., BOTRUGNO, O. A., GARGIULO, G., DAL ZUFFO, R., MATTI, V., D'ARIO, G., MONTANI, E., MERCURIO, C., HAHN, W. C.,

GORGOULIS, V., MINUCCI, S. & D'ADDA DI FAGAGNA, F. 2011. Interplay between oncogene-induced DNA damage response and heterochromatin in senescence and cancer. *Nat Cell Biol,* 13**,** 292-302.

DIMRI, G. P. 2005. What has senescence got to do with cancer? *Cancer Cell,* 7**,** 505-12.

DIMRI, G. P. & CAMPISI, J. 1994. Molecular and cell biology of replicative senescence. *Cold Spring Harb Symp Quant Biol,* 59**,** 67-73.

DIMRI, G. P., LEE, X., BASILE, G., ACOSTA, M., SCOTT, G., ROSKELLEY, C., MEDRANO, E. E., LINSKENS, M., RUBELJ, I., PEREIRA-SMITH, O. & ET AL. 1995. A biomarker that identifies senescent human cells in culture and in aging skin in vivo. *Proc Natl Acad Sci U S A,* 92**,** 9363-7.

DOAN, N., REHER, P., MEGHJI, S. & HARRIS, M. 1999. In vitro effects of therapeutic ultrasound on cell proliferation, protein synthesis, and cytokine production by human fibroblasts, osteoblasts, and monocytes. *J Oral Maxillofac Surg,* 57**,** 409-19; discussion 420.

DRUELLE, C., DRULLION, C., DESLE, J., MARTIN, N., SAAS, L., CORMENIER, J., MALAQUIN, N., HUOT, L., SLOMIANNY, C., BOUALI, F., VERCAMER, C., HOT, D., POURTIER, A., CHEVET, E., ABBADIE, C. & PLUQUET, O. 2016. ATF6alpha regulates morphological changes associated with senescence in human fibroblasts. *Oncotarget,* 7**,** 67699-67715.

DULIC, V., BENEY, G. E., FREBOURG, G., DRULLINGER, L. F. & STEIN, G. H. 2000. Uncoupling between phenotypic senescence and cell cycle arrest in aging p21-deficient fibroblasts. *Mol Cell Biol,* 20**,** 6741-54.

DVORAK, H. F. 2015. Tumors: wounds that do not heal-redux. *Cancer Immunol Res,* 3**,** 1-11.

EBERHARDT, K., MATTHAUS, C., MARTHANDAN, S., DIEKMANN, S. & POPP, J. 2018. Raman and infrared spectroscopy reveal that proliferating and quiescent human fibroblast cells age by biochemically similar but not identical processes. *PLoS One,* 13**,** e0207380.

EBERHARDT, K., MATTHAUS, C., WINTER, D., WIEGAND, C., HIPLER, U. C., DIEKMANN, S. & POPP, J. 2017. Raman and infrared spectroscopy differentiate senescent from proliferating cells in a human dermal fibroblast 3D skin model. *Analyst,* 142**,** 4405-4414.

ERDOGAN, O., ESEN, E., USTUN, Y., KURKCU, M., AKOVA, T., GONLUSEN, G., UYSAL, H. & CEVLIK, F. 2006. Effects of low-intensity pulsed ultrasound on healing of mandibular fractures: an experimental study in rabbits. *J Oral Maxillofac Surg,* 64**,** 180-8.

FAGET, D. V., REN, Q. & STEWART, S. A. 2019. Unmasking senescence: context-dependent effects of SASP in cancer. *Nat Rev Cancer,* 19**,** 439-453.

FERIL, L. B., JR. 2009. Ultrasound-mediated gene transfection. *Methods Mol Biol,* 542**,** 179-94.

FERNANDEZ-SALAS, E., SUH, K. S., SPERANSKY, V. V., BOWERS, W. L., LEVY, J. M., ADAMS, T., PATHAK, K. R., EDWARDS, L. E., HAYES, D. D., CHENG, C., STEVEN, A. C., WEINBERG, W. C. & YUSPA, S. H. 2002. mtCLIC/CLIC4, an organellular chloride channel protein, is increased by DNA damage and participates in the apoptotic response to p53. *Mol Cell Biol,* 22**,** 3610-20.

FINKEL, T., SERRANO, M. & BLASCO, M. A. 2007. The common biology of cancer and aging. *Nature,* 448**,** 767-74.

FULOP, T., LE PAGE, A., GARNEAU, H., AZIMI, N., BAEHL, S., DUPUIS, G., PAWELEC, G. & LARBI, A. 2012. Aging, immunosenescence and membrane rafts: the lipid connection. *Longev Healthspan,* 1**,** 6.

GASCARD, P. & TLSTY, T. D. 2016. Carcinoma-associated fibroblasts: orchestrating the composition of malignancy. *Genes Dev,* 30**,** 1002-19.

GASEK, N. S., KUCHEL, G. A., KIRKLAND, J. L. & XU, M. 2021. Strategies for Targeting Senescent Cells in Human Disease. *Nat Aging,* 1**,** 870-879.

GEORGILIS, A., KLOTZ, S., HANLEY, C. J., HERRANZ, N., WEIRICH, B., MORANCHO, B., LEOTE, A. C., D'ARTISTA, L., GALLAGE, S., SEEHAWER, M., CARROLL, T., DHARMALINGAM, G., WEE, K. B., MELLONE, M., POMBO, J., HEIDE, D., GUCCIONE, E., ARRIBAS, J., BARBOSA-MORAIS, N. L., HEIKENWALDER, M., THOMAS, G. J., ZENDER, L. & GIL, J. 2018. PTBP1-Mediated Alternative Splicing Regulates the Inflammatory Secretome and the Pro-tumorigenic Effects of Senescent Cells. *Cancer Cell,* 34**,** 85-102 e9.

GERLAND, L. M., PEYROL, S., LALLEMAND, C., BRANCHE, R., MAGAUD, J. P. & FFRENCH, M. 2003. Association of increased autophagic inclusions labeled for beta-galactosidase with fibroblastic aging. *Exp Gerontol,* 38**,** 887-95.

GHOSH, K. & CAPELL, B. C. 2016. The Senescence-Associated Secretory Phenotype: Critical Effector in Skin Cancer and Aging. *J Invest Dermatol,* 136**,** 2133-2139.

GONZALEZ, A. C., COSTA, T. F., ANDRADE, Z. A. & MEDRADO, A. R. 2016. Wound healing - A literature review. *An Bras Dermatol,* 91**,** 614-620.

GONZALEZ-GUALDA, E., BAKER, A. G., FRUK, L. & MUNOZ-ESPIN, D. 2021. A guide to assessing cellular senescence in vitro and in vivo. *FEBS J,* 288**,** 56-80.

GONZALEZ-MELJEM, J. M., APPS, J. R., FRASER, H. C. & MARTINEZ-BARBERA, J. P. 2018. Paracrine roles of cellular senescence in promoting tumourigenesis. *Br J Cancer,* 118**,** 1283-1288.

GOULD, L., ABADIR, P., BREM, H., CARTER, M., CONNER-KERR, T., DAVIDSON, J., DIPIETRO, L., FALANGA, V., FIFE, C., GARDNER, S., GRICE, E., HARMON, J., HAZZARD, W. R., HIGH, K. P., HOUGHTON, P., JACOBSON, N., KIRSNER, R. S., KOVACS, E. J., MARGOLIS, D., MCFARLAND HORNE, F., REED, M. J., SULLIVAN, D. H., THOM, S., TOMIC-CANIC, M., WALSTON, J., WHITNEY, J. A., WILLIAMS, J., ZIEMAN, S. & SCHMADER, K. 2015. Chronic wound repair and healing in older adults: current status and future research. *J Am Geriatr Soc,* 63**,** 427-38.

GUERRERO, F., CARMONA, A., JIMENEZ, M. J., OBRERO, T., PULIDO, V., MORENO, J. A., SORIANO, S., MARTIN-MALO, A. & ALJAMA, P. 2021. Passage Number-Induced Replicative Senescence Modulates the Endothelial Cell Response to Protein-Bound Uremic Toxins. *Toxins (Basel),* 13.

HAFERKAMP, S., TRAN, S. L., BECKER, T. M., SCURR, L. L., KEFFORD, R. F. & RIZOS, H. 2009. The relative contributions of the p53 and pRb pathways in oncogene-induced melanocyte senescence. *Aging (Albany NY),* 1**,** 542-56.

HALL, A. G. & TILBY, M. J. 1992. Mechanisms of action of, and modes of resistance to, alkylating agents used in the treatment of haematological malignancies. *Blood Rev,* 6**,** 163-73.

HANAHAN, D. & WEINBERG, R. A. 2011. Hallmarks of cancer: the next generation. *Cell,* 144**,** 646-74.

HARDING, K. G., MOORE, K. & PHILLIPS, T. J. 2005. Wound chronicity and fibroblast senescence--implications for treatment. *Int Wound J,* 2**,** 364-8.

HARRISON, A., LIN, S., POUNDER, N. & MIKUNI-TAKAGAKI, Y. 2016. Mode & mechanism of low intensity pulsed ultrasound (LIPUS) in fracture repair. *Ultrasonics,* 70**,** 45-52.

HARRY, G. J. 2013. Microglia during development and aging. *Pharmacol Ther,* 139**,** 313-26.

HASSONA, Y., CIRILLO, N., HEESOM, K., PARKINSON, E. K. & PRIME, S. S. 2014. Senescent cancer-associated fibroblasts secrete active MMP-2 that promotes keratinocyte discohesion and invasion. *Br J Cancer,* 111**,** 1230-7.

HAYFLICK, L. & MOORHEAD, P. S. 1961. The serial cultivation of human diploid cell strains. *Exp Cell Res,* 25**,** 585-621.

HAYNES, L. & SWAIN, S. L. 2006. Why aging T cells fail: implications for vaccination. *Immunity,* 24**,** 663-666.

HENDERSON, E. A. 2006. The potential effect of fibroblast senescence on wound healing and the chronic wound environment. *J Wound Care,* 15**,** 315-8.

HERNANDEZ BORRERO, L. J. & EL-DEIRY, W. S. 2021. Tumor suppressor p53: Biology, signaling pathways, and therapeutic targeting. *Biochim Biophys Acta Rev Cancer,* 1876**,** 188556.

HERNANDEZ-SEGURA, A., NEHME, J. & DEMARIA, M. 2018. Hallmarks of Cellular Senescence. *Trends Cell Biol,* 28**,** 436-453.

HINDS, P. & PIETRUSKA, J. 2017. Senescence and tumor suppression. *F1000Res,* 6**,** 2121.

HUANG, Y., DAI, X., GUAN, Z., LIU, D., REN, L., CHEN, M., ZENG, Z., JIANG, J., LUO, Y., HE, Y., HUANG, M. & ZHAO, C. 2022. A DNA damage nanoamplifier for the chemotherapy of triple-negative breast cancer via DNA damage induction and repair blocking. *Int J Pharm,* 622**,** 121897.

HWANG, E. S., YOON, G. & KANG, H. T. 2009. A comparative analysis of the cell biology of senescence and aging. *Cell Mol Life Sci,* 66**,** 2503-24.

IKAI, H., TAMURA, T., WATANABE, T., ITOU, M., SUGAYA, A., IWABUCHI, S., MIKUNI-TAKAGAKI, Y. & DEGUCHI, S. 2008. Low-intensity pulsed ultrasound accelerates periodontal wound healing after flap surgery. *J Periodontal Res,* 43**,** 212-6.

IVASHKEVICH, A., REDON, C. E., NAKAMURA, A. J., MARTIN, R. F. & MARTIN, O. A. 2012. Use of the gamma-H2AX assay to monitor DNA damage and repair in translational cancer research. *Cancer Lett,* 327**,** 123-33.

JANG, K. W., DING, L., SEOL, D., LIM, T. H., BUCKWALTER, J. A. & MARTIN, J. A. 2014. Low-intensity pulsed ultrasound promotes chondrogenic progenitor cell migration via focal adhesion kinase pathway. *Ultrasound Med Biol,* 40**,** 1177-86.

JIANG, L., GONDA, T. A., GAMBLE, M. V., SALAS, M., SESHAN, V., TU, S., TWADDELL, W. S., HEGYI, P., LAZAR, G., STEELE, I., VARRO, A., WANG, T. C. & TYCKO, B. 2008. Global hypomethylation of genomic DNA in cancer-associated myofibroblasts. *Cancer Res,* 68**,** 9900-8.

JOCHEMS, F., THIJSSEN, B., DE CONTI, G., JANSEN, R., POGACAR, Z., GROOT, K., WANG, L., SCHEPERS, A., WANG, C., JIN, H., BEIJERSBERGEN, R. L., LEITE DE OLIVEIRA, R., WESSELS, L. F. A. & BERNARDS, R. 2021. The Cancer SENEScopedia: A delineation of cancer cell senescence. *Cell Rep,* 36**,** 109441.

JOHMURA, Y., YAMANAKA, T., OMORI, S., WANG, T. W., SUGIURA, Y., MATSUMOTO, M., SUZUKI, N., KUMAMOTO, S., YAMAGUCHI, K., HATAKEYAMA, S., TAKAMI, T., YAMAGUCHI, R., SHIMIZU, E., IKEDA, K., OKAHASHI, N., MIKAWA, R., SUEMATSU, M., ARITA, M., SUGIMOTO, M., NAKAYAMA, K. I., FURUKAWA, Y., IMOTO, S. & NAKANISHI, M. 2021. Senolysis by glutaminolysis inhibition ameliorates various age-associated disorders. *Science,* 371**,** 265-270.

JOHNS, L. D. 2002. Nonthermal effects of therapeutic ultrasound: the frequency resonance hypothesis. *J Athl Train,* 37**,** 293-9.

JUN, J. I. & LAU, L. F. 2010. The matricellular protein CCN1 induces fibroblast senescence and restricts fibrosis in cutaneous wound healing. *Nat Cell Biol,* 12**,** 676-85.

JUNG, D. W., CHE, Z. M., KIM, J., KIM, K., KIM, K. Y., WILLIAMS, D. & KIM, J. 2010. Tumor-stromal crosstalk in invasion of oral squamous cell carcinoma: a pivotal role of CCL7. *Int J Cancer,* 127**,** 332-44.

KATANO, M., NARUSE, K., UCHIDA, K., MIKUNI-TAKAGAKI, Y., TAKASO, M., ITOMAN, M. & URABE, K. 2011. Low intensity pulsed ultrasound accelerates delayed healing process by reducing the time required for the completion of endochondral ossification in the aged mouse femur fracture model. *Exp Anim,* 60**,** 385-95.

KATZIR, I., ADLER, M., KARIN, O., MENDELSOHN-COHEN, N., MAYO, A. & ALON, U. 2021. Senescent cells and the incidence of age-related diseases. *Aging Cell,* 20**,** e13314.

KAUL, Z., CESARE, A. J., HUSCHTSCHA, L. I., NEUMANN, A. A. & REDDEL, R. R. 2011. Five dysfunctional telomeres predict onset of senescence in human cells. *EMBO Rep,* 13**,** 52-9.

KEANE, T. J., HOREJS, C. M. & STEVENS, M. M. 2018. Scarring vs. functional healing: Matrix-based strategies to regulate tissue repair. *Adv Drug Deliv Rev,* 129**,** 407-419.

KENNEDY, J. E. 2005. High-intensity focused ultrasound in the treatment of solid tumours. *Nat Rev Cancer,* 5**,** 321-7.

KIM, H. S., HEO, J. I., PARK, S. H., SHIN, J. Y., KANG, H. J., KIM, M. J., KIM, S. C., KIM, J., PARK, J. B. & LEE, J. Y. 2014. Transcriptional activation of p21(WAF(1)/CIP(1)) is mediated by increased DNA binding activity and increased interaction between p53 and Sp1 via phosphorylation during replicative senescence of human embryonic fibroblasts. *Mol Biol Rep,* 41**,** 2397-408.

KIM, K. H., PARK, G. T., LIM, Y. B., RUE, S. W., JUNG, J. C., SONN, J. K., BAE, Y. S., PARK, J. W. & LEE, Y. S. 2004. Expression of connective tissue growth factor, a biomarker in senescence of human diploid fibroblasts, is up-regulated by a transforming growth factor-beta-mediated signaling pathway. *Biochem Biophys Res Commun,* 318**,** 819-25.

KINNER, A., WU, W., STAUDT, C. & ILIAKIS, G. 2008. Gamma-H2AX in recognition and signaling of DNA double-strand breaks in the context of chromatin. *Nucleic Acids Res,* 36**,** 5678-94.

KLEMENT, K. & GOODARZI, A. A. 2014. DNA double strand break responses and chromatin alterations within the aging cell. *Exp Cell Res,* 329**,** 42-52.

KODALI, R., HAJJOU, M., BERMAN, A. B., BANSAL, M. B., ZHANG, S., PAN, J. J. & SCHECTER, A. D. 2006. Chemokines induce matrix metalloproteinase-2 through activation of epidermal growth factor receptor in arterial smooth muscle cells. *Cardiovasc Res,* 69**,** 706-15.

KOJIMA, Y., ACAR, A., EATON, E. N., MELLODY, K. T., SCHEEL, C., BEN-PORATH, I., ONDER, T. T., WANG, Z. C., RICHARDSON, A. L., WEINBERG, R. A. & ORIMO, A. 2010. Autocrine TGF-beta and stromal cell-derived factor-1 (SDF-1) signaling drives the evolution of tumor-promoting mammary stromal myofibroblasts. *Proc Natl Acad Sci U S A,* 107**,** 20009-14.

KORTLEVER, R. M., HIGGINS, P. J. & BERNARDS, R. 2006. Plasminogen activator inhibitor-1 is a critical downstream target of p53 in the induction of replicative senescence. *Nat Cell Biol,* 8**,** 877-84.

KREILING, J. A., TAMAMORI-ADACHI, M., SEXTON, A. N., JEYAPALAN, J. C., MUNOZ-NAJAR, U., PETERSON, A. L., MANIVANNAN, J., ROGERS, E. S., PCHELINTSEV, N. A., ADAMS, P. D. & SEDIVY, J. M. 2011. Age-associated increase in heterochromatic marks in murine and primate tissues. *Aging Cell,* 10**,** 292-304.

KRIZHANOVSKY, V., YON, M., DICKINS, R. A., HEARN, S., SIMON, J., MIETHING, C., YEE, H., ZENDER, L. & LOWE, S. W. 2008. Senescence of activated stellate cells limits liver fibrosis. *Cell,* 134**,** 657-67.

KRTOLICA, A. & CAMPISI, J. 2002. Cancer and aging: a model for the cancer promoting effects of the aging stroma. *Int J Biochem Cell Biol,* 34**,** 1401-14.

KRTOLICA, A., PARRINELLO, S., LOCKETT, S., DESPREZ, P. Y. & CAMPISI, J. 2001. Senescent fibroblasts promote epithelial cell growth and tumorigenesis: a link between cancer and aging. *Proc Natl Acad Sci U S A,* 98**,** 12072-7.

KRUT, Z., GAZIT, D., GAZIT, Z. & PELLED, G. 2022. Applications of Ultrasound-Mediated Gene Delivery in Regenerative Medicine. *Bioengineering (Basel),* 9.

KSIAZEK, K., KORYBALSKA, K., JORRES, A. & WITOWSKI, J. 2007. Accelerated senescence of human peritoneal mesothelial cells exposed to high glucose: the role of TGF-beta1. *Lab Invest,* 87**,** 345-56.

KUILMAN, T., MICHALOGLOU, C., MOOI, W. J. & PEEPER, D. S. 2010. The essence of senescence. *Genes Dev,* 24**,** 2463-79.

KUILMAN, T., MICHALOGLOU, C., VREDEVELD, L. C., DOUMA, S., VAN DOORN, R., DESMET, C. J., AARDEN, L. A., MOOI, W. J. & PEEPER, D. S. 2008. Oncogene-induced senescence relayed by an interleukin-dependent inflammatory network. *Cell,* 133**,** 1019-31.

KUMAR, S., MILLIS, A. J. & BAGLIONI, C. 1992. Expression of interleukin 1-inducible genes and production of interleukin 1 by aging human fibroblasts. *Proc Natl Acad Sci U S A,* 89**,** 4683-7.

KUMARI, R. & JAT, P. 2021. Mechanisms of Cellular Senescence: Cell Cycle Arrest and Senescence Associated Secretory Phenotype. *Front Cell Dev Biol,* 9**,** 645593.

KURZ, D. J., KLOECKENER-GRUISSEM, B., AKHMEDOV, A., EBERLI, F. R., BUHLER, I., BERGER, W., BERTEL, O. & LUSCHER, T. F. 2006. Degenerative aortic valve stenosis, but not coronary disease, is associated with shorter telomere length in the elderly. *Arterioscler Thromb Vasc Biol,* 26**,** e114-7.

LANDEN, N. X., LI, D. & STAHLE, M. 2016. Transition from inflammation to proliferation: a critical step during wound healing. *Cell Mol Life Sci,* 73**,** 3861-85.

LASRY, A. & BEN-NERIAH, Y. 2015. Senescence-associated inflammatory responses: aging and cancer perspectives. *Trends Immunol,* 36**,** 217-28.

LAU, L., PORCIUNCULA, A., YU, A., IWAKURA, Y. & DAVID, G. 2019. Uncoupling the Senescence-Associated Secretory Phenotype from Cell Cycle Exit via Interleukin-1 Inactivation Unveils Its Protumorigenic Role. *Mol Cell Biol,* 39.

LEE, B. Y., HAN, J. A., IM, J. S., MORRONE, A., JOHUNG, K., GOODWIN, E. C., KLEIJER, W. J., DIMAIO, D. & HWANG, E. S. 2006. Senescence-associated beta-galactosidase is lysosomal beta-galactosidase. *Aging Cell,* 5**,** 187-95.

LEE, J. H. & PAULL, T. T. 2005. ATM activation by DNA double-strand breaks through the Mre11-Rad50-Nbs1 complex. *Science,* 308**,** 551-4.

LEE, M. & LEE, J. S. 2014. Exploiting tumor cell senescence in anticancer therapy. *BMB Rep,* 47**,** 51-9.

LEE, Y. H., PARK, J. Y., LEE, H., SONG, E. S., KUK, M. U., JOO, J., OH, S., KWON, H. W., PARK, J. T. & PARK, S. C. 2021. Targeting Mitochondrial Metabolism as a Strategy to Treat Senescence. *Cells,* 10.

LEONTIEVA, O. V. & BLAGOSKLONNY, M. V. 2014. Gerosuppression in confluent cells. *Aging (Albany NY),* 6**,** 1010-8.

LEVI, N., PAPISMADOV, N., SOLOMONOV, I., SAGI, I. & KRIZHANOVSKY, V. 2020. The ECM path of senescence in aging: components and modifiers. *FEBS J,* 287**,** 2636-2646.

LI, M., YOU, L., XUE, J. & LU, Y. 2018. Ionizing Radiation-Induced Cellular Senescence in Normal, Non-transformed Cells and the Involved DNA Damage Response: A Mini Review. *Front Pharmacol,* 9**,** 522.

LI, W., WANG, W., DONG, H., LI, Y., LI, L., HAN, L., HAN, Z., WANG, S., MA, D. & WANG, H. 2014. Cisplatin-induced senescence in ovarian cancer cells is mediated by GRP78. *Oncol Rep,* 31**,** 2525-34.

LILLEY, L. M., KAMPER, S., CALDWELL, M., CHIA, Z. K., BALLWEG, D., VISTAIN, L., KRIMMEL, J., MILLS, T. A., MACRENARIS, K., LEE, P., WATERS, E. A. & MEADE, T. J. 2020. Self-Immolative Activation of beta-Galactosidase-Responsive Probes for In Vivo MR Imaging in Mouse Models. *Angew Chem Int Ed Engl,* 59**,** 388-394.

LIM, H., PARK, H. & KIM, H. P. 2015. Effects of flavonoids on senescence-associated secretory phenotype formation from bleomycin-induced senescence in BJ fibroblasts. *Biochem Pharmacol,* 96**,** 337-48.

LIU, D. & HORNSBY, P. J. 2007. Senescent human fibroblasts increase the early growth of xenograft tumors via matrix metalloproteinase secretion. *Cancer Res,* 67**,** 3117-26.

LIU, J., WANG, L., WANG, Z. & LIU, J. P. 2019. Roles of Telomere Biology in Cell Senescence, Replicative and Chronological Aging. *Cells,* 8.

LU, S. Y., CHANG, K. W., LIU, C. J., TSENG, Y. H., LU, H. H., LEE, S. Y. & LIN, S. C. 2006. Ripe areca nut extract induces G1 phase arrests and senescence-associated phenotypes in normal human oral keratinocyte. *Carcinogenesis,* 27**,** 1273-84.

LUBBERTS, S., MEIJER, C., DEMARIA, M. & GIETEMA, J. A. 2020. Early aging after cytotoxic treatment for testicular cancer and cellular senescence: Time to act. *Crit Rev Oncol Hematol,* 151**,** 102963.

LUJAMBIO, A. 2016. To clear, or not to clear (senescent cells)? That is the question. *Bioessays,* 38 Suppl 1**,** S56-64.

LUJAMBIO, A., AKKARI, L., SIMON, J., GRACE, D., TSCHAHARGANEH, D. F., BOLDEN, J. E., ZHAO, Z., THAPAR, V., JOYCE, J. A., KRIZHANOVSKY, V. & LOWE, S. W. 2013. Non-cell-autonomous tumor suppression by p53. *Cell,* 153**,** 449-60.

LYNCH, H. T., CASEY, M. J., SNYDER, C. L., BEWTRA, C., LYNCH, J. F., BUTTS, M. & GODWIN, A. K. 2009. Hereditary ovarian carcinoma: heterogeneity, molecular genetics, pathology, and management. *Mol Oncol,* 3**,** 97-137.

MAGALHAES, S., ALMEIDA, I., PEREIRA, C. D., REBELO, S., GOODFELLOW, B. J. & NUNES, A. 2022. The Long-Term Culture of Human Fibroblasts Reveals a Spectroscopic Signature of Senescence. *Int J Mol Sci,* 23.

MAIER, J. A., VOULALAS, P., ROEDER, D. & MACIAG, T. 1990. Extension of the life-span of human endothelial cells by an interleukin-1 alpha antisense oligomer. *Science,* 249**,** 1570-4.

MAKRANTONAKI, E., WLASCHEK, M. & SCHARFFETTER-KOCHANEK, K. 2017. Pathogenesis of wound healing disorders in the elderly. *J Dtsch Dermatol Ges,* 15**,** 255-275.

MALAQUIN, N., MARTINEZ, A. & RODIER, F. 2016. Keeping the senescence secretome under control: Molecular reins on the senescence-associated secretory phenotype. *Exp Gerontol,* 82**,** 39-49.

MALONEY, E. & HWANG, J. H. 2015. Emerging HIFU applications in cancer therapy. *Int J Hyperthermia,* 31**,** 302-9.

MANNICK, J. B., MORRIS, M., HOCKEY, H. P., ROMA, G., BEIBEL, M., KULMATYCKI, K., WATKINS, M., SHAVLAKADZE, T., ZHOU, W., QUINN, D., GLASS, D. J. & KLICKSTEIN, L. B. 2018. TORC1 inhibition enhances immune function and reduces infections in the elderly. *Sci Transl Med,* 10.

MANTOVANI, A., LOCATI, M., VECCHI, A., SOZZANI, S. & ALLAVENA, P. 2001. Decoy receptors: a strategy to regulate inflammatory cytokines and chemokines. *Trends Immunol,* 22**,** 328-36.

MAO, Y., KLEINJAN, M. L., JILISHITZ, I., SWAMINATHAN, B., OBINATA, H., KOMAROVA, Y. A., BAYLESS, K. J., HLA, T. & KITAJEWSKI, J. K. 2021. CLIC1 and CLIC4 mediate endothelial S1P receptor signaling to facilitate Rac1 and RhoA activity and function. *Sci Signal,* 14.

MARECHAL, A. & ZOU, L. 2013. DNA damage sensing by the ATM and ATR kinases. *Cold Spring Harb Perspect Biol,* 5.

MARGOLIS, D. J., BILKER, W., SANTANNA, J. & BAUMGARTEN, M. 2002. Venous leg ulcer: incidence and prevalence in the elderly. *J Am Acad Dermatol,* 46**,** 381-6.

MARIA, J. & INGRID, Z. 2017. Effects of bioactive compounds on senescence and components of senescence associated secretory phenotypes in vitro. *Food Funct,* 8**,** 2394-2418.

MARTINEZ, D. E., BORNIEGO, M. L., BATTCHIKOVA, N., ARO, E. M., TYYSTJARVI, E. & GUIAMET, J. J. 2015. SASP, a Senescence-Associated Subtilisin Protease, is involved in reproductive development and determination of silique number in Arabidopsis. *J Exp Bot,* 66**,** 161-74.

MATSUKI, M., TAKAHASHI, A., KATOU, S., TAKAYANAGI, A., TAKAGI, Y. & KAMATA, K. 2013. [Pathological complete response to gemcitabine and cisplatin chemotherapy for advanced upper tract urothelial carcinoma: a case report]. *Nihon Hinyokika Gakkai Zasshi,* 104**,** 33-7.

MATSUMOTO, R., FUKUOKA, H., IGUCHI, G., ODAKE, Y., YOSHIDA, K., BANDO, H., SUDA, K., NISHIZAWA, H., TAKAHASHI, M., YAMADA, S., OGAWA, W. & TAKAHASHI, Y. 2015. Accelerated Telomere Shortening in Acromegaly; IGF-I Induces Telomere Shortening and Cellular Senescence. *PLoS One,* 10**,** e0140189.

MAXWELL, L., COLLECUTT, T., GLEDHILL, M., SHARMA, S., EDGAR, S. & GAVIN, J. B. 1994. The augmentation of leucocyte adhesion to endothelium by therapeutic ultrasound. *Ultrasound Med Biol,* 20**,** 383-90.

MCQUIBBAN, G. A., GONG, J. H., WONG, J. P., WALLACE, J. L., CLARK-LEWIS, I. & OVERALL, C. M. 2002. Matrix metalloproteinase processing of monocyte chemoattractant proteins generates CC chemokine receptor antagonists with anti-inflammatory properties in vivo. *Blood,* 100**,** 1160-7.

MERCURIO, L., LULLI, D., MASCIA, F., DELLAMBRA, E., SCARPONI, C., MORELLI, M., VALENTE, C., CARBONE, M. L., PALLOTTA, S., GIROLOMONI, G., ALBANESI, C., PASTORE, S. & MADONNA, S. 2020. Intracellular Insulin-like growth factor binding protein 2 (IGFBP2) contributes to the senescence of keratinocytes in psoriasis by stabilizing cytoplasmic p21. *Aging (Albany NY),* 12**,** 6823-6851.

MERZ, S. E., KLOPFLEISCH, R., BREITHAUPT, A. & GRUBER, A. D. 2019. Aging and Senescence in Canine Testes. *Vet Pathol,* 56**,** 715-724.

MIJIT, M., CARACCIOLO, V., MELILLO, A., AMICARELLI, F. & GIORDANO, A. 2020. Role of p53 in the Regulation of Cellular Senescence. *Biomolecules,* 10.

MIKULA-PIETRASIK, J., NIKLAS, A., URUSKI, P., TYKARSKI, A. & KSIAZEK, K. 2020. Mechanisms and significance of therapy-induced and spontaneous senescence of cancer cells. *Cell Mol Life Sci,* 77**,** 213-229.

MITRA, A. K., ZILLHARDT, M., HUA, Y., TIWARI, P., MURMANN, A. E., PETER, M. E. & LENGYEL, E. 2012. MicroRNAs reprogram normal fibroblasts into cancer-associated fibroblasts in ovarian cancer. *Cancer Discov,* 2**,** 1100-8.

MITTELDORF, J. 2019. What Is Antagonistic Pleiotropy? *Biochemistry (Mosc),* 84**,** 1458-1468.

MIWA, S., KASHYAP, S., CHINI, E. & VON ZGLINICKI, T. 2022. Mitochondrial dysfunction in cell senescence and aging. *J Clin Invest,* 132.

MOHAMAD KAMAL, N. S., SAFUAN, S., SHAMSUDDIN, S. & FOROOZANDEH, P. 2020. Aging of the cells: Insight into cellular senescence and detection Methods. *Eur J Cell Biol,* 99**,** 151108.

MOISEEVA, O., DESCHENES-SIMARD, X., ST-GERMAIN, E., IGELMANN, S., HUOT, G., CADAR, A. E., BOURDEAU, V., POLLAK, M. N. & FERBEYRE, G. 2013. Metformin inhibits the senescence-associated secretory phenotype by interfering with IKK/NF-kappaB activation. *Aging Cell,* 12**,** 489-98.

MOLDOGAZIEVA, N. T., MOKHOSOEV, I. M., MEL'NIKOVA, T. I., POROZOV, Y. B. & TERENTIEV, A. A. 2019. Oxidative Stress and Advanced Lipoxidation and Glycation End Products (ALEs and AGEs) in Aging and Age-Related Diseases. *Oxid Med Cell Longev,* 2019**,** 3085756.

MOMCHILOVA, A., PETKOVA, D., STANEVA, G., MARKOVSKA, T., PANKOV, R., SKROBANSKA, R., NIKOLOVA-KARAKASHIAN, M. & KOUMANOV, K. 2014. Resveratrol alters the lipid composition, metabolism and peroxide level in senescent rat hepatocytes. *Chem Biol Interact,* 207**,** 74-80.

MORISAKI, H., ANDO, A., NAGATA, Y., PEREIRA-SMITH, O., SMITH, J. R., IKEDA, K. & NAKANISHI, M. 1999. Complex mechanisms underlying impaired activation of Cdk4 and Cdk2 in replicative senescence: roles of p16, p21, and cyclin D1. *Exp Cell Res,* 253**,** 503-10.

MORTIMER, A. J. & DYSON, M. 1988. The effect of therapeutic ultrasound on calcium uptake in fibroblasts. *Ultrasound Med Biol,* 14**,** 499-506.

MOSTEIRO, L., PANTOJA, C., DE MARTINO, A. & SERRANO, M. 2018. Senescence promotes in vivo reprogramming through p16(INK)(4a) and IL-6. *Aging Cell,* 17.

MU, X. C. & HIGGINS, P. J. 1995. Differential growth state-dependent regulation of plasminogen activator inhibitor type-1 expression in senescent IMR-90 human diploid fibroblasts. *J Cell Physiol,* 165**,** 647-57.

MUNOZ-ESPIN, D., CANAMERO, M., MARAVER, A., GOMEZ-LOPEZ, G., CONTRERAS, J., MURILLO-CUESTA, S., RODRIGUEZ-BAEZA, A., VARELA-NIETO, I., RUBERTE, J., COLLADO, M. & SERRANO, M. 2013. Programmed cell senescence during mammalian embryonic development. *Cell,* 155**,** 1104-18.

MUNOZ-ESPIN, D., ROVIRA, M., GALIANA, I., GIMENEZ, C., LOZANO-TORRES, B., PAEZ-RIBES, M., LLANOS, S., CHAIB, S., MUNOZ-MARTIN, M., UCERO, A. C., GARAULET, G., MULERO, F., DANN, S. G., VANARSDALE, T., SHIELDS, D. J., BERNARDOS, A., MURGUIA, J. R., MARTINEZ-MANEZ, R. & SERRANO, M. 2018. A versatile drug delivery system targeting senescent cells. *EMBO Mol Med,* 10.

MUNOZ-ESPIN, D. & SERRANO, M. 2014. Cellular senescence: from physiology to pathology. *Nat Rev Mol Cell Biol,* 15**,** 482-96.

NAKAO, J., FUJII, Y., KUSUYAMA, J., BANDOW, K., KAKIMOTO, K., OHNISHI, T. & MATSUGUCHI, T. 2014. Low-intensity pulsed ultrasound (LIPUS) inhibits LPS-induced inflammatory responses of osteoblasts through TLR4-MyD88 dissociation. *Bone,* 58**,** 17-25.

NARITA, M., NARITA, M., KRIZHANOVSKY, V., NUNEZ, S., CHICAS, A., HEARN, S. A., MYERS, M. P. & LOWE, S. W. 2006. A novel role for high-mobility group a proteins in cellular senescence and heterochromatin formation. *Cell,* 126**,** 503-14.

NARITA, M., NUNEZ, S., HEARD, E., NARITA, M., LIN, A. W., HEARN, S. A., SPECTOR, D. L., HANNON, G. J. & LOWE, S. W. 2003. Rb-mediated heterochromatin formation and silencing of E2F target genes during cellular senescence. *Cell,* 113**,** 703-16.

NELSON, G., WORDSWORTH, J., WANG, C., JURK, D., LAWLESS, C., MARTIN-RUIZ, C. & VON ZGLINICKI, T. 2012. A senescent cell bystander effect: senescence-induced senescence. *Aging Cell,* 11**,** 345-9.

NESS, K. K., KIRKLAND, J. L., GRAMATGES, M. M., WANG, Z., KUNDU, M., MCCASTLAIN, K., LI-HARMS, X., ZHANG, J., TCHKONIA, T., PLUIJM, S. M. F. & ARMSTRONG, G. T. 2018. Premature Physiologic Aging as a Paradigm for Understanding Increased Risk of Adverse Health Across the Lifespan of Survivors of Childhood Cancer. *J Clin Oncol,* 36**,** 2206-2215.

NISHIO, K., INOUE, A., QIAO, S., KONDO, H. & MIMURA, A. 2001. Senescence and cytoskeleton: overproduction of vimentin induces senescent-like morphology in human fibroblasts. *Histochem Cell Biol,* 116**,** 321-7.

NITISS, J. L. 2009. Targeting DNA topoisomerase II in cancer chemotherapy. *Nat Rev Cancer,* 9**,** 338-50.

NYBORG, W. L. 1982. Ultrasonic microstreaming and related phenomena. *Br J Cancer Suppl,* 5**,** 156-60.

OHLUND, D., ELYADA, E. & TUVESON, D. 2014. Fibroblast heterogeneity in the cancer wound. *J Exp Med,* 211**,** 1503-23.

OHTANI, N. 2022. The roles and mechanisms of senescence-associated secretory phenotype (SASP): can it be controlled by senolysis? *Inflamm Regen,* 42**,** 11.

OLOVNIKOV, A. M. 1971. [Principle of marginotomy in template synthesis of polynucleotides]. *Dokl Akad Nauk SSSR,* 201**,** 1496-9.

OLOVNIKOV, A. M. 1973. A theory of marginotomy. The incomplete copying of template margin in enzymic synthesis of polynucleotides and biological significance of the phenomenon. *J Theor Biol,* 41**,** 181-90.

OLSZEWSKA, A., BORKOWSKA, A., GRANICA, M., KAROLCZAK, J., ZGLINICKI, B., KIEDA, C. & WAS, H. 2021. Escape From Cisplatin-Induced Senescence of Hypoxic Lung Cancer Cells Can Be Overcome by Hydroxychloroquine. *Front Oncol,* 11**,** 738385.

ORIMO, A., GUPTA, P. B., SGROI, D. C., ARENZANA-SEISDEDOS, F., DELAUNAY, T., NAEEM, R., CAREY, V. J., RICHARDSON, A. L. & WEINBERG, R. A. 2005. Stromal fibroblasts present in invasive human breast carcinomas promote tumor growth and angiogenesis through elevated SDF-1/CXCL12 secretion. *Cell,* 121**,** 335-48.

ORJALO, A. V., BHAUMIK, D., GENGLER, B. K., SCOTT, G. K. & CAMPISI, J. 2009. Cell surface-bound IL-1alpha is an upstream regulator of the senescence-associated IL-6/IL-8 cytokine network. *Proc Natl Acad Sci U S A,* 106**,** 17031-6.

ORTIZ-MONTERO, P., LONDONO-VALLEJO, A. & VERNOT, J. P. 2017. Senescence-associated IL-6 and IL-8 cytokines induce a self- and cross-reinforced senescence/inflammatory milieu strengthening tumorigenic capabilities in the MCF-7 breast cancer cell line. *Cell Commun Signal,* 15**,** 17.

PADMAKUMAR, V. C., SPEER, K., PAL-GHOSH, S., MASIUK, K. E., RYSCAVAGE, A., DENGLER, S. L., HWANG, S., EDWARDS, J. C., COPPOLA, V., TESSAROLLO, L., STEPP, M. A. & YUSPA,

S. H. 2012. Spontaneous skin erosions and reduced skin and corneal wound healing characterize CLIC4(NULL) mice. *Am J Pathol,* 181**,** 74-84.

PAEZ-RIBES, M., GONZALEZ-GUALDA, E., DOHERTY, G. J. & MUNOZ-ESPIN, D. 2019. Targeting senescent cells in translational medicine. *EMBO Mol Med,* 11**,** e10234.

PALMER, D. B. 2013. The effect of age on thymic function. *Front Immunol,* 4**,** 316.

PALMER, S., ALBERGANTE, L., BLACKBURN, C. C. & NEWMAN, T. J. 2018. Thymic involution and rising disease incidence with age. *Proc Natl Acad Sci U S A,* 115**,** 1883-1888.

PARAMOS-DE-CARVALHO, D., JACINTO, A. & SAUDE, L. 2021. The right time for senescence. *Elife,* 10.

PARIKH, P., WICHER, S., KHANDALAVALA, K., PABELICK, C. M., BRITT, R. D., JR. & PRAKASH, Y. S. 2019. Cellular senescence in the lung across the age spectrum. *Am J Physiol Lung Cell Mol Physiol,* 316**,** L826-L842.

PARRINELLO, S., COPPE, J. P., KRTOLICA, A. & CAMPISI, J. 2005. Stromal-epithelial interactions in aging and cancer: senescent fibroblasts alter epithelial cell differentiation. *J Cell Sci,* 118**,** 485-96.

PATHAK, R., BHANGU, S. K., MARTIN, G. J. O., SEPAROVIC, F. & ASHOKKUMAR, M. 2022. Ultrasound-induced protein restructuring and ordered aggregation to form amyloid crystals. *Eur Biophys J,* 51**,** 335-352.

PEREZ, E. A. 2009. Microtubule inhibitors: Differentiating tubulin-inhibiting agents based on mechanisms of action, clinical activity, and resistance. *Mol Cancer Ther,* 8**,** 2086-95.

PIGNON, J. P., TRIBODET, H., SCAGLIOTTI, G. V., DOUILLARD, J. Y., SHEPHERD, F. A., STEPHENS, R. J., DUNANT, A., TORRI, V., ROSELL, R., SEYMOUR, L., SPIRO, S. G., ROLLAND, E., FOSSATI, R., AUBERT, D., DING, K., WALLER, D., LE CHEVALIER, T. & GROUP, L. C. 2008. Lung adjuvant cisplatin evaluation: a pooled analysis by the LACE Collaborative Group. *J Clin Oncol,* 26**,** 3552-9.

PIZZINO, G., IRRERA, N., CUCINOTTA, M., PALLIO, G., MANNINO, F., ARCORACI, V., SQUADRITO, F., ALTAVILLA, D. & BITTO, A. 2017. Oxidative Stress: Harms and Benefits for Human Health. *Oxid Med Cell Longev,* 2017**,** 8416763.

POUNDER, N. M. & HARRISON, A. J. 2008. Low intensity pulsed ultrasound for fracture healing: a review of the clinical evidence and the associated biological mechanism of action. *Ultrasonics,* 48**,** 330-8.

PRATA, L., OVSYANNIKOVA, I. G., TCHKONIA, T. & KIRKLAND, J. L. 2018. Senescent cell clearance by the immune system: Emerging therapeutic opportunities. *Semin Immunol,* 40**,** 101275.

PRATTICHIZZO, F., DE NIGRIS, V., LA SALA, L., PROCOPIO, A. D., OLIVIERI, F. & CERIELLO, A. 2016. "Inflammaging" as a Druggable Target: A Senescence-Associated Secretory Phenotype-Centered View of Type 2 Diabetes. *Oxid Med Cell Longev,* 2016**,** 1810327.

PRZYSTUPSKI, D. & USSOWICZ, M. 2022. Landscape of Cellular Bioeffects Triggered by Ultrasound-Induced Sonoporation. *Int J Mol Sci,* 23.

QIAN, Y. & CHEN, X. 2013. Senescence regulation by the p53 protein family. *Methods Mol Biol,* 965**,** 37-61.

QU, K., LIN, T., WEI, J., MENG, F., WANG, Z., HUANG, Z., WAN, Y., SONG, S., LIU, S., CHANG, H., DONG, Y. & LIU, C. 2013. Cisplatin induces cell cycle arrest and senescence via upregulating P53 and P21 expression in HepG2 cells. *Nan Fang Yi Ke Da Xue Xue Bao,* 33**,** 1253-9.

QUIJANO, C., CAO, L., FERGUSSON, M. M., ROMERO, H., LIU, J., GUTKIND, S., ROVIRA, II, MOHNEY, R. P., KAROLY, E. D. & FINKEL, T. 2012. Oncogene-induced senescence results in marked metabolic and bioenergetic alterations. *Cell Cycle,* 11**,** 1383-92.

RAJPATHAK, S. N., GUNTER, M. J., WYLIE-ROSETT, J., HO, G. Y., KAPLAN, R. C., MUZUMDAR, R., ROHAN, T. E. & STRICKLER, H. D. 2009. The role of insulin-like growth factor-I and its binding proteins in glucose homeostasis and type 2 diabetes. *Diabetes Metab Res Rev,* 25**,** 3-12.

RASANEN, K. & VAHERI, A. 2010. Activation of fibroblasts in cancer stroma. *Exp Cell Res,* 316**,** 2713-22.

RAYESS, H., WANG, M. B. & SRIVATSAN, E. S. 2012. Cellular senescence and tumor suppressor gene p16. *Int J Cancer,* 130**,** 1715-25.

REDDY, M., GILL, S. S., KALKAR, S. R., WU, W., ANDERSON, P. J. & ROCHON, P. A. 2008. Treatment of pressure ulcers: a systematic review. *JAMA,* 300**,** 2647-62.

REHER, P., DOAN, N., BRADNOCK, B., MEGHJI, S. & HARRIS, M. 1999. Effect of ultrasound on the production of IL-8, basic FGF and VEGF. *Cytokine,* 11**,** 416-23.

REICHENSTEIN, M., REICH, R., LEHOUX, J. G. & HANUKOGLU, I. 2004. ACTH induces TIMP-1 expression and inhibits collagenase in adrenal cortex cells. *Mol Cell Endocrinol,* 215**,** 109-14.

RESNIK, S. R. E., ANDJELA ;ABDO ABUJAMRA, BEATRIZ ;JOZIC, IVAN 2020. Clinical Implications of Cellular Senescence on Wound Healing. *New York: Springer US,* 9**,** 286-297.

ROMANOV, V. S., POSPELOV, V. A. & POSPELOVA, T. V. 2012. Cyclin-dependent kinase inhibitor p21(Waf1): contemporary view on its role in senescence and oncogenesis. *Biochemistry (Mosc),* 77**,** 575-84.

ROPER, J., HARRISON, A. & BASS, M. D. 2012. Induction of adhesion-dependent signals using low-intensity ultrasound. *J Vis Exp***,** e4024.

ROPER, J. A., WILLIAMSON, R. C., BALLY, B., COWELL, C. A. M., BROOKS, R., STEPHENS, P., HARRISON, A. J. & BASS, M. D. 2015. Ultrasonic Stimulation of Mouse Skin Reverses the Healing Delays in Diabetes and Aging by Activation of Rac1. *J Invest Dermatol,* 135**,** 2842-2851.

ROTTENBERG, S., DISLER, C. & PEREGO, P. 2021. The rediscovery of platinum-based cancer therapy. *Nat Rev Cancer,* 21**,** 37-50.

ROZENGURT, E. 1992. Growth factors and cell proliferation. *Curr Opin Cell Biol,* 4**,** 161-5.

SARKAR, D., LEBEDEVA, I. V., EMDAD, L., KANG, D. C., BALDWIN, A. S., JR. & FISHER, P. B. 2004. Human polynucleotide phosphorylase (hPNPaseold-35): a potential link between aging and inflammation. *Cancer Res,* 64**,** 7473-8.

SARKISIAN, C. J., KEISTER, B. A., STAIRS, D. B., BOXER, R. B., MOODY, S. E. & CHODOSH, L. A. 2007. Dose-dependent oncogene-induced senescence in vivo and its evasion during mammary tumorigenesis. *Nat Cell Biol,* 9**,** 493-505.

SCHORTINGHUIS, J., STEGENGA, B., RAGHOEBAR, G. M. & DE BONT, L. G. 2003. Ultrasound stimulation of maxillofacial bone healing. *Crit Rev Oral Biol Med,* 14**,** 63-74.

SCHOSSERER, M., GRILLARI, J. & BREITENBACH, M. 2017. The Dual Role of Cellular Senescence in Developing Tumors and Their Response to Cancer Therapy. *Front Oncol,* 7**,** 278.

SEDELNIKOVA, O. A., HORIKAWA, I., REDON, C., NAKAMURA, A., ZIMONJIC, D. B., POPESCU, N. C. & BONNER, W. M. 2008. Delayed kinetics of DNA double-strand break processing in normal and pathological aging. *Aging Cell,* 7**,** 89-100.

SEDELNIKOVA, O. A., HORIKAWA, I., ZIMONJIC, D. B., POPESCU, N. C., BONNER, W. M. & BARRETT, J. C. 2004. Senescing human cells and aging mice accumulate DNA lesions with unrepairable double-strand breaks. *Nat Cell Biol,* 6**,** 168-70.

SEDLETSKA, Y., GIRAUD-PANIS, M. J. & MALINGE, J. M. 2005. Cisplatin is a DNA-damaging antitumour compound triggering multifactorial biochemical responses in cancer cells: importance of apoptotic pathways. *Curr Med Chem Anticancer Agents,* 5**,** 251-65.

SELUANOV, A., GORBUNOVA, V., FALCOVITZ, A., SIGAL, A., MILYAVSKY, M., ZURER, I., SHOHAT, G., GOLDFINGER, N. & ROTTER, V. 2001. Change of the death pathway in senescent human fibroblasts in response to DNA damage is caused by an inability to stabilize p53. *Mol Cell Biol,* 21**,** 1552-64.

SERGIEV, P. V., DONTSOVA, O. A. & BEREZKIN, G. V. 2015. Theories of aging: an ever-evolving field. *Acta Naturae,* 7**,** 9-18.

SERUP, J., BOVE, T., ZAWADA, T., JESSEN, A. & POLI, M. 2020. High-frequency (20 MHz) high-intensity focused ultrasound: New Treatment of actinic keratosis, basal cellcarcinoma, and Kaposi sarcoma. An open-label exploratory study. *Skin Res Technol,* 26**,** 824-831.

SEVERINO, V., ALESSIO, N., FARINA, A., SANDOMENICO, A., CIPOLLARO, M., PELUSO, G., GALDERISI, U. & CHAMBERY, A. 2013. Insulin-like growth factor binding proteins 4 and 7 released by senescent cells promote premature senescence in mesenchymal stem cells. *Cell Death Dis,* 4**,** e911.

SHANLEY, D. P., AW, D., MANLEY, N. R. & PALMER, D. B. 2009. An evolutionary perspective on the mechanisms of immunosenescence. *Trends Immunol,* 30**,** 374-81.

SHARMA, A., SINGH, K. & ALMASAN, A. 2012. Histone H2AX phosphorylation: a marker for DNA damage. *Methods Mol Biol,* 920**,** 613-26.

SHIBUYA, M. 2011. Vascular Endothelial Growth Factor (VEGF) and Its Receptor (VEGFR) Signaling in Angiogenesis: A Crucial Target for Anti- and Pro-Angiogenic Therapies. *Genes Cancer,* 2**,** 1097-105.

SHIGA, K., HARA, M., NAGASAKI, T., SATO, T., TAKAHASHI, H. & TAKEYAMA, H. 2015. Cancer-Associated Fibroblasts: Their Characteristics and Their Roles in Tumor Growth. *Cancers (Basel),* 7**,** 2443-58.

SHLUSH, L. I., ITZKOVITZ, S., COHEN, A., RUTENBERG, A., BERKOVITZ, R., YEHEZKEL, S., SHAHAR, H., SELIG, S. & SKORECKI, K. 2011. Quantitative digital in situ senescence-associated beta-galactosidase assay. *BMC Cell Biol,* 12**,** 16.

SHUKLA, A., EDWARDS, R., YANG, Y., HAHN, A., FOLKERS, K., DING, J., PADMAKUMAR, V. C., CATAISSON, C., SUH, K. S. & YUSPA, S. H. 2014. CLIC4 regulates TGF-beta-dependent myofibroblast differentiation to produce a cancer stroma. *Oncogene,* 33**,** 842-50.

SIAVOSHIAN, S., BLOTTIERE, H. M., CHERBUT, C. & GALMICHE, J. P. 1997. Butyrate stimulates cyclin D and p21 and inhibits cyclin-dependent kinase 2 expression in HT-29 colonic epithelial cells. *Biochem Biophys Res Commun,* 232**,** 169-72.

SIDDIK, Z. H. 2003. Cisplatin: mode of cytotoxic action and molecular basis of resistance. *Oncogene,* 22**,** 7265-79.

SIDDIQUI, A. R. & BERNSTEIN, J. M. 2010. Chronic wound infection: facts and controversies. *Clin Dermatol,* 28**,** 519-26.

SIDDIQUI, M. S., FRANCOIS, M., FENECH, M. F. & LEIFERT, W. R. 2015. Persistent gammaH2AX: A promising molecular marker of DNA damage and aging. *Mutat Res Rev Mutat Res,* 766**,** 1-19.

SIMONE, T. M., HIGGINS, C. E., CZEKAY, R. P., LAW, B. K., HIGGINS, S. P., ARCHAMBEAULT, J., KUTZ, S. M. & HIGGINS, P. J. 2014. SERPINE1: A Molecular Switch in the Proliferation-Migration Dichotomy in Wound-"Activated" Keratinocytes. *Adv Wound Care (New Rochelle),* 3**,** 281-290.

SINGH, L., ALDOSARY, S., SAEEDAN, A. S., ANSARI, M. N. & KAITHWAS, G. 2018. Prolyl hydroxylase 2: a promising target to inhibit hypoxia-induced cellular metabolism in cancer cells. *Drug Discov Today,* 23**,** 1873-1882.

SMITH, J. S., CHEN, Q., YATSUNYK, L. A., NICOLUDIS, J. M., GARCIA, M. S., KRANASTER, R., BALASUBRAMANIAN, S., MONCHAUD, D., TEULADE-FICHOU, M. P., ABRAMOWITZ, L., SCHULTZ, D. C. & JOHNSON, F. B. 2011. Rudimentary G-quadruplex-based telomere capping in Saccharomyces cerevisiae. *Nat Struct Mol Biol,* 18**,** 478-85.

SON, H. N., CHI, H. N. Q., CHUNG, D. C. & LONG, L. T. 2019. Morphological changes during replicative senescence in bovine ovarian granulosa cells. *Cell Cycle,* 18**,** 1490-1497.

SRIRATANASAK, N., CHUNHACHA, P., EI, Z. Z. & CHANVORACHOTE, P. 2022. Cisplatin Induces Senescent Lung Cancer Cell-Mediated Stemness Induction via GRP78/Akt-Dependent Mechanism. *Biomedicines,* 10.

STOJANOVIC, S. D., FIEDLER, J., BAUERSACHS, J., THUM, T. & SEDDING, D. G. 2020. Senescence-induced inflammation: an important player and key therapeutic target in atherosclerosis. *Eur Heart J,* 41**,** 2983-2996.

SU, J. & CAVACO-PAULO, A. 2021. Effect of ultrasound on protein functionality. *Ultrason Sonochem,* 76**,** 105653.

SUH, K. S., MALIK, M., SHUKLA, A. & YUSPA, S. H. 2007. CLIC4, skin homeostasis and cutaneous cancer: surprising connections. *Mol Carcinog,* 46**,** 599-604.

SUH, K. S., MUTOH, M., GERDES, M., CRUTCHLEY, J. M., MUTOH, T., EDWARDS, L. E., DUMONT, R. A., SODHA, P., CHENG, C., GLICK, A. & YUSPA, S. H. 2005. Antisense suppression of the chloride intracellular channel family induces apoptosis, enhances tumor necrosis factor (Acosta et al.)-induced apoptosis, and inhibits tumor growth. *Cancer Res,* 65**,** 562-71.

SUH, K. S., MUTOH, M., NAGASHIMA, K., FERNANDEZ-SALAS, E., EDWARDS, L. E., HAYES, D. D., CRUTCHLEY, J. M., MARIN, K. G., DUMONT, R. A., LEVY, J. M., CHENG, C., GARFIELD, S. & YUSPA, S. H. 2004. The organellular chloride channel protein CLIC4/mtCLIC translocates to the nucleus in response to cellular stress and accelerates apoptosis. *J Biol Chem,* 279**,** 4632-41.

SUN, X., SHI, B., ZHENG, H., MIN, L., YANG, J., LI, X., LIAO, X., HUANG, W., ZHANG, M., XU, S., ZHU, Z., CUI, H. & LIU, X. 2018. Senescence-associated secretory factors induced by cisplatin in melanoma cells promote non-senescent melanoma cell growth through activation of the ERK1/2-RSK1 pathway. *Cell Death Dis,* 9**,** 260.

TAKAHASHI, A., OHTANI, N. & HARA, E. 2007. Irreversibility of cellular senescence: dual roles of p16INK4a/Rb-pathway in cell cycle control. *Cell Div,* 2**,** 10.

TELGENHOFF, D. & SHROOT, B. 2005. Cellular senescence mechanisms in chronic wound healing. *Cell Death Differ,* 12**,** 695-8.

TER HAAR, G. 1999. Therapeutic ultrasound. *Eur J Ultrasound,* 9**,** 3-9.

TER HAAR, G. 2007. Therapeutic applications of ultrasound. *Prog Biophys Mol Biol,* 93**,** 111-29.

TER RIET, G., KESSELS, A. G. & KNIPSCHILD, P. 1995. Randomised clinical trial of ultrasound treatment for pressure ulcers. *BMJ,* 310**,** 1040-1.

TERAO, R., AHMED, T., SUZUMURA, A. & TERASAKI, H. 2022. Oxidative Stress-Induced Cellular Senescence in Aging Retina and Age-Related Macular Degeneration. *Antioxidants (Basel),* 11.

THOMAS, R., WANG, W. & SU, D. M. 2020. Contributions of Age-Related Thymic Involution to Immunosenescence and Inflammaging. *Immun Aging,* 17**,** 2.

TIAN, Y., LIU, Z., TAN, H., HOU, J., WEN, X., YANG, F. & CHENG, W. 2020. New Aspects of Ultrasound-Mediated Targeted Delivery and Therapy for Cancer. *Int J Nanomedicine,* 15**,** 401-418.

TILSTRA, J. S., ROBINSON, A. R., WANG, J., GREGG, S. Q., CLAUSON, C. L., REAY, D. P., NASTO, L. A., ST CROIX, C. M., USAS, A., VO, N., HUARD, J., CLEMENS, P. R., STOLZ, D. B., GUTTRIDGE, D. C., WATKINS, S. C., GARINIS, G. A., WANG, Y., NIEDERNHOFER, L. J. & ROBBINS, P. D. 2012. NF-kappaB inhibition delays DNA damage-induced senescence and aging in mice. *J Clin Invest,* 122**,** 2601-12.

TONINI, T., ROSSI, F. & CLAUDIO, P. P. 2003. Molecular basis of angiogenesis and cancer. *Oncogene,* 22**,** 6549-56.

TURKE, P. W. 1994. Microbial parasites versus developing T cells: an evolutionary 'arms race' with implications for the timing of thymic involution and HIV pathogenesis. *Thymus,* 24**,** 29-40.

TYANOVA, S., TEMU, T., SINITCYN, P., CARLSON, A., HEIN, M. Y., GEIGER, T., MANN, M. & COX, J. 2016. The Perseus computational platform for comprehensive analysis of (prote)omics data. *Nat Methods,* 13**,** 731-40.

URITA, A., IWASAKI, N., KONDO, M., NISHIO, Y., KAMISHIMA, T. & MINAMI, A. 2013. Effect of low-intensity pulsed ultrasound on bone healing at osteotomy sites after forearm bone shortening. *J Hand Surg Am,* 38**,** 498-503.

VALKENBURG, K. C., DE GROOT, A. E. & PIENTA, K. J. 2018. Targeting the tumour stroma to improve cancer therapy. *Nat Rev Clin Oncol,* 15**,** 366-381.

VAN DEN STEEN, P. E., WUYTS, A., HUSSON, S. J., PROOST, P., VAN DAMME, J. & OPDENAKKER, G. 2003. Gelatinase B/MMP-9 and neutrophil collagenase/MMP-8 process the chemokines human GCP-2/CXCL6, ENA-78/CXCL5 and mouse GCP-2/LIX and modulate their physiological activities. *Eur J Biochem,* 270**,** 3739-49.

VAUGHAN, D. E., RAI, R., KHAN, S. S., EREN, M. & GHOSH, A. K. 2017. Plasminogen Activator Inhibitor-1 Is a Marker and a Mediator of Senescence. *Arterioscler Thromb Vasc Biol,* 37**,** 1446-1452.

VU, R., JIN, S., SUN, P., HAENSEL, D., NGUYEN, Q. H., DRAGAN, M., KESSENBROCK, K., NIE, Q. & DAI, X. 2022. Wound healing in aged skin exhibits systems-level alterations in cellular composition and cell-cell communication. *Cell Rep,* 40**,** 111155.

WAGNER, K. D. & WAGNER, N. 2022. The Senescence Markers p16INK4A, p14ARF/p19ARF, and p21 in Organ Development and Homeostasis. *Cells,* 11.

WAHBA, J., NATOLI, M., WHILDING, L. M., PARENTE-PEREIRA, A. C., JUNG, Y., ZONA, S., LAM, E. W., SMITH, J. R., MAHER, J. & GHAEM-MAGHAMI, S. 2018. Chemotherapy-induced apoptosis, autophagy and cell cycle arrest are key drivers of synergy in chemo-immunotherapy of epithelial ovarian cancer. *Cancer Immunol Immunother,* 67**,** 1753-1765.

WAJAPEYEE, N., SERRA, R. W., ZHU, X., MAHALINGAM, M. & GREEN, M. R. 2008. Oncogenic BRAF induces senescence and apoptosis through pathways mediated by the secreted protein IGFBP7. *Cell,* 132**,** 363-74.

WALL, I. B., MOSELEY, R., BAIRD, D. M., KIPLING, D., GILES, P., LAFFAFIAN, I., PRICE, P. E., THOMAS, D. W. & STEPHENS, P. 2008. Fibroblast dysfunction is a key factor in the non-healing of chronic venous leg ulcers. *J Invest Dermatol,* 128, 2526-40.

WANG, L., LANKHORST, L. & BERNARDS, R. 2022. Exploiting senescence for the treatment of cancer. *Nat Rev Cancer,* 22, 340-355.

WANG, L. Y. & ZHENG, S. S. 2019. Advances in low-frequency ultrasound combined with microbubbles in targeted tumor therapy. *J Zhejiang Univ Sci B,* 20, 291-299.

WANG, S., MOERMAN, E. J., JONES, R. A., THWEATT, R. & GOLDSTEIN, S. 1996. Characterization of IGFBP-3, PAI-1 and SPARC mRNA expression in senescent fibroblasts. *Mech Aging Dev,* 92, 121-32.

WANG, X., WONG, S. C., PAN, J., TSAO, S. W., FUNG, K. H., KWONG, D. L., SHAM, J. S. & NICHOLLS, J. M. 1998. Evidence of cisplatin-induced senescent-like growth arrest in nasopharyngeal carcinoma cells. *Cancer Res,* 58, 5019-22.

WANG, Z., WEI, D. D. & XIAO, H. Y. 2013. Methods of Cellular Senescence Induction Using Oxidative Stress. *Biological Aging: Methods and Protocols, 2nd Edition,* 1048, 135-144.

WASSON, C. W., ROSS, R. L., MORTON, R., MANKOURI, J. & DEL GALDO, F. 2021. The intracellular chloride channel 4 (CLIC4) activates systemic sclerosis fibroblasts. *Rheumatology (Oxford),* 60, 4395-4400.

WATANABE, S., KAWAMOTO, S., OHTANI, N. & HARA, E. 2017. Impact of senescence-associated secretory phenotype and its potential as a therapeutic target for senescence-associated diseases. *Cancer Sci,* 108, 563-569.

WATSON, T. 2008. Ultrasound in contemporary physiotherapy practice. *Ultrasonics,* 48, 321-9.

WEBSTER, D. F., POND, J. B., DYSON, M. & HARVEY, W. 1978. The role of cavitation in the in vitro stimulation of protein synthesis in human fibroblasts by ultrasound. *Ultrasound Med Biol,* 4, 343-51.

WEI, X., LI, M., ZHENG, Z., MA, J., GAO, Y., CHEN, L., PENG, Y., YU, S. & YANG, L. 2022. Senescence in chronic wounds and potential targeted therapies. *Burns Trauma,* 10, tkab045.

WEI, Z., GUO, H., QIN, J., LU, S., LIU, Q., ZHANG, X., ZOU, Y., GONG, Y. & SHAO, C. 2019. Pan-senescence transcriptome analysis identified RRAD as a marker and negative regulator of cellular senescence. *Free Radic Biol Med,* 130, 267-277.

WILEY, C. D. & CAMPISI, J. 2016. From Ancient Pathways to Aging Cells-Connecting Metabolism and Cellular Senescence. *Cell Metab,* 23, 1013-1021.

WILEY, C. D., VELARDE, M. C., LECOT, P., LIU, S., SARNOSKI, E. A., FREUND, A., SHIRAKAWA, K., LIM, H. W., DAVIS, S. S., RAMANATHAN, A., GERENCSER, A. A., VERDIN, E. & CAMPISI, J. 2016. Mitochondrial Dysfunction Induces Senescence with a Distinct Secretory Phenotype. *Cell Metab,* 23, 303-14.

WILKINSON, H. N., CLOWES, C., BANYARD, K. L., MATTEUCI, P., MACE, K. A. & HARDMAN, M. J. 2019. Elevated Local Senescence in Diabetic Wound Healing Is Linked to Pathological Repair via CXCR2. *J Invest Dermatol,* 139, 1171-1181 e6.

WILLOUGHBY, N. A., BOCK, H., HOEVE, M. A., PELLS, S., WILLIAMS, C., MCPHEE, G., FREILE, P., CHOUDHURY, D. & DE SOUSA, P. A. 2016. A scalable label-free approach to separate human pluripotent cells from differentiated derivatives. *Biomicrofluidics,* 10, 014107.

WISSLER GERDES, E. O., ZHU, Y., WEIGAND, B. M., TRIPATHI, U., BURNS, T. C., TCHKONIA, T. & KIRKLAND, J. L. 2020. Cellular senescence in aging and age-related diseases: Implications for neurodegenerative diseases. *Int Rev Neurobiol,* 155, 203-234.

WOOD, A. K. & SEHGAL, C. M. 2015. A review of low-intensity ultrasound for cancer therapy. *Ultrasound Med Biol,* 41**,** 905-28.

WOODS, D. & TURCHI, J. J. 2013. Chemotherapy induced DNA damage response: convergence of drugs and pathways. *Cancer Biol Ther,* 14**,** 379-89.

WU, J. & NYBORG, W. L. 2008. Ultrasound, cavitation bubbles and their interaction with cells. *Adv Drug Deliv Rev,* 60**,** 1103-16.

WYLD, L., BELLANTUONO, I., TCHKONIA, T., MORGAN, J., TURNER, O., FOSS, F., GEORGE, J., DANSON, S. & KIRKLAND, J. L. 2020. Senescence and Cancer: A Review of Clinical Implications of Senescence and Senotherapies. *Cancers (Basel),* 12.

WYSS-CORAY, T. 2016. Aging, neurodegeneration and brain rejuvenation. *Nature,* 539**,** 180-186.

XIN, Z., LIN, G., LEI, H., LUE, T. F. & GUO, Y. 2016. Clinical applications of low-intensity pulsed ultrasound and its potential role in urology. *Transl Androl Urol,* 5**,** 255-66.

XU, M., PIRTSKHALAVA, T., FARR, J. N., WEIGAND, B. M., PALMER, A. K., WEIVODA, M. M., INMAN, C. L., OGRODNIK, M. B., HACHFELD, C. M., FRASER, D. G., ONKEN, J. L., JOHNSON, K. O., VERZOSA, G. C., LANGHI, L. G. P., WEIGL, M., GIORGADZE, N., LEBRASSEUR, N. K., MILLER, J. D., JURK, D., SINGH, R. J., ALLISON, D. B., EJIMA, K., HUBBARD, G. B., IKENO, Y., CUBRO, H., GAROVIC, V. D., HOU, X., WEROHA, S. J., ROBBINS, P. D., NIEDERNHOFER, L. J., KHOSLA, S., TCHKONIA, T. & KIRKLAND, J. L. 2018. Senolytics improve physical function and increase lifespan in old age. *Nat Med,* 24**,** 1246-1256.

YANG, F., TUXHORN, J. A., RESSLER, S. J., MCALHANY, S. J., DANG, T. D. & ROWLEY, D. R. 2005. Stromal expression of connective tissue growth factor promotes angiogenesis and prostate cancer tumorigenesis. *Cancer Res,* 65**,** 8887-95.

YANG, H. & FOGO, A. B. 2010. Cell senescence in the aging kidney. *J Am Soc Nephrol,* 21**,** 1436-9.

YIP, H. T., CHOPRA, R., CHAKRABARTI, R., VEENA, M. S., RAMAMURTHY, B., SRIVATSAN, E. S. & WANG, M. B. 2006. Cisplatin-induced growth arrest of head and neck cancer cells correlates with increased expression of p16 and p53. *Arch Otolaryngol Head Neck Surg,* 132**,** 317-26.

YOSHIDA, S., NAKAGAMI, H., HAYASHI, H., IKEDA, Y., SUN, J., TENMA, A., TOMIOKA, H., KAWANO, T., SHIMAMURA, M., MORISHITA, R. & RAKUGI, H. 2020. The CD153 vaccine is a senotherapeutic option for preventing the accumulation of senescent T cells in mice. *Nat Commun,* 11**,** 2482.

YOSHIMOTO, S., LOO, T. M., ATARASHI, K., KANDA, H., SATO, S., OYADOMARI, S., IWAKURA, Y., OSHIMA, K., MORITA, H., HATTORI, M., HONDA, K., ISHIKAWA, Y., HARA, E. & OHTANI, N. 2013. Obesity-induced gut microbial metabolite promotes liver cancer through senescence secretome. *Nature,* 499**,** 97-101.

YU, J. X., KODIBAGKAR, V. D., HALLAC, R. R., LIU, L. & MASON, R. P. 2012. Dual 19F/1H MR gene reporter molecules for in vivo detection of beta-galactosidase. *Bioconjug Chem,* 23**,** 596-603.

YU, W. K., WANG, Z., FONG, C. C., LIU, D., YIP, T. C., AU, S. K., ZHU, G. & YANG, M. 2017. Chemoresistant lung cancer stem cells display high DNA repair capability to remove cisplatin-induced DNA damage. *Br J Pharmacol,* 174**,** 302-313.

ZENG, S., SHEN, W. H. & LIU, L. 2018. Senescence and Cancer. *Cancer Transl Med,* 4**,** 70-74.

ZHANG, D., TANG, B., XIE, X., XIAO, Y. F., YANG, S. M. & ZHANG, J. W. 2015. The interplay between DNA repair and autophagy in cancer therapy. *Cancer Biol Ther,* 16**,** 1005-13.

ZHAO, R., LIANG, H., CLARKE, E., JACKSON, C. & XUE, M. 2016. Inflammation in Chronic
Wounds. *Int J Mol Sci,* 17.

ZHAO, W., LIN, Z. X. & ZHANG, Z. Q. 2004. Cisplatin-induced premature senescence withconcomitant reduction of gap junctions in human fibroblasts. *Cell Res,* 14**,** 60-6.

ZHOU, S., SCHMELZ, A., SEUFFERLEIN, T., LI, Y., ZHAO, J. & BACHEM, M. G. 2004. Molecular
mechanisms of low intensity pulsed ultrasound in human skin fibroblasts. *J Biol Chem,*
279**,** 54463-9.

ZINGER, A., CHO, W. C. & BEN-YEHUDA, A. 2017. Cancer and Aging - the InflammatoryConnection. *Aging Dis,* 8**,** 611-627.

ASANUMA, D., SAKABE, M., KAMIYA, M., YAMAMOTO, K., HIRATAKE, J., OGAWA, M., KOSAKA, N., CHOYKE, P. L., NAGANO, T., KOBAYASHI, H. & URANO, Y. 2015. Sensitive beta-galactosidase-targeting fluorescence probe for visualizing small peritoneal metastatic tumours in vivo. *Nat Commun,* 6**,** 6463.

BASU, A. & KRISHNAMURTHY, S. 2010. Cellular responses to Cisplatin-induced DNA damage. *J Nucleic Acids,* 2010.

CASELLA, G., MUNK, R., KIM, K. M., PIAO, Y., DE, S., ABDELMOHSEN, K. & GOROSPE, M. 2019. Transcriptome signature of cellular senescence. *Nucleic Acids Res,* 47**,** 11476.

DASARI, S. & TCHOUNWOU, P. B. 2014. Cisplatin in cancer therapy: molecular mechanisms of action. *Eur J Pharmacol,* 740**,** 364-78.

DE MERA-RODRIGUEZ, J. A., ALVAREZ-HERNAN, G., GANAN, Y., MARTIN-PARTIDO, G., RODRIGUEZ-LEON, J. & FRANCISCO-MORCILLO, J. 2021. Is Senescence-Associated beta-Galactosidase a Reliable in vivo Marker of Cellular Senescence During Embryonic Development? *Front Cell Dev Biol,* 9**,** 623175.

DEMARIA, M., O'LEARY, M. N., CHANG, J., SHAO, L., LIU, S., ALIMIRAH, F., KOENIG, K., LE, C., MITIN, N., DEAL, A. M., ALSTON, S., ACADEMIA, E. C., KILMARX, S., VALDOVINOS, A., WANG, B., DE BRUIN, A., KENNEDY, B. K., MELOV, S., ZHOU, D., SHARPLESS, N. E., MUSS, H. & CAMPISI, J. 2017. Cellular Senescence Promotes Adverse Effects of Chemotherapy and Cancer Relapse. *Cancer Discov,* 7**,** 165-176.

DHAR, S., KOLISHETTI, N., LIPPARD, S. J. & FAROKHZAD, O. C. 2011. Targeted delivery of a cisplatin prodrug for safer and more effective prostate cancer therapy in vivo. *Proc Natl Acad Sci U S A,* 108**,** 1850-5.

EBERHARDT, K., MATTHAUS, C., MARTHANDAN, S., DIEKMANN, S. & POPP, J. 2018. Raman and infrared spectroscopy reveal that proliferating and quiescent human fibroblast cells age by biochemically similar but not identical processes. *PLoS One,* 13**,** e0207380.

EBERHARDT, K., MATTHAUS, C., WINTER, D., WIEGAND, C., HIPLER, U. C., DIEKMANN, S. & POPP, J. 2017. Raman and infrared spectroscopy differentiate senescent from proliferating cells in a human dermal fibroblast 3D skin model. *Analyst,* 142**,** 4405-4414.

FERNANDEZ-SALAS, E., SUH, K. S., SPERANSKY, V. V., BOWERS, W. L., LEVY, J. M., ADAMS, T., PATHAK, K. R., EDWARDS, L. E., HAYES, D. D., CHENG, C., STEVEN, A. C., WEINBERG, W. C. & YUSPA, S. H. 2002. mtCLIC/CLIC4, an organellular chloride channel protein, is

increased by DNA damage and participates in the apoptotic response to p53. *Mol Cell Biol,* 22**,** 3610-20.

FULOP, T., LE PAGE, A., GARNEAU, H., AZIMI, N., BAEHL, S., DUPUIS, G., PAWELEC, G. & LARBI, A. 2012. Aging, immunosenescence and membrane rafts: the lipid connection. *Longev Healthspan,* 1**,** 6.

GONZALEZ-GUALDA, E., BAKER, A. G., FRUK, L. & MUNOZ-ESPIN, D. 2021. A guide to assessing cellular senescence in vitro and in vivo. *FEBS J,* 288**,** 56-80.

IVASHKEVICH, A., REDON, C. E., NAKAMURA, A. J., MARTIN, R. F. & MARTIN, O. A. 2012. Use of the gamma-H2AX assay to monitor DNA damage and repair in translational cancer research. *Cancer Lett,* 327**,** 123-33.

KSIAZEK, K., KORYBALSKA, K., JORRES, A. & WITOWSKI, J. 2007. Accelerated senescence of human peritoneal mesothelial cells exposed to high glucose: the role of TGF-beta1. *Lab Invest,* 87**,** 345-56.

KUMARI, R. & JAT, P. 2021. Mechanisms of Cellular Senescence: Cell Cycle Arrest and Senescence Associated Secretory Phenotype. *Front Cell Dev Biol,* 9**,** 645593.

LILLEY, L. M., KAMPER, S., CALDWELL, M., CHIA, Z. K., BALLWEG, D., VISTAIN, L., KRIMMEL, J., MILLS, T. A., MACRENARIS, K., LEE, P., WATERS, E. A. & MEADE, T. J. 2020. Self-Immolative Activation of beta-Galactosidase-Responsive Probes for In Vivo MR Imaging in Mouse Models. *Angew Chem Int Ed Engl,* 59**,** 388-394.

LUBBERTS, S., MEIJER, C., DEMARIA, M. & GIETEMA, J. A. 2020. Early aging after cytotoxic treatment for testicular cancer and cellular senescence: Time to act. *Crit Rev Oncol Hematol,* 151**,** 102963.

LYNCH, H. T., CASEY, M. J., SNYDER, C. L., BEWTRA, C., LYNCH, J. F., BUTTS, M. & GODWIN, A. K. 2009. Hereditary ovarian carcinoma: heterogeneity, molecular genetics, pathology, and management. *Mol Oncol,* 3**,** 97-137.

MATSUKI, M., TAKAHASHI, A., KATOU, S., TAKAYANAGI, A., TAKAGI, Y. & KAMATA, K. 2013. [Pathological complete response to gemcitabine and cisplatin chemotherapy for advanced upper tract urothelial carcinoma: a case report]. *Nihon Hinyokika Gakkai Zasshi,* 104**,** 33-7.

MIKULA-PIETRASIK, J., NIKLAS, A., URUSKI, P., TYKARSKI, A. & KSIAZEK, K. 2020. Mechanisms and significance of therapy-induced and spontaneous senescence of cancer cells. *Cell Mol Life Sci,* 77**,** 213-229.

MOMCHILOVA, A., PETKOVA, D., STANEVA, G., MARKOVSKA, T., PANKOV, R., SKROBANSKA, R., NIKOLOVA-KARAKASHIAN, M. & KOUMANOV, K. 2014. Resveratrol alters the lipid composition, metabolism and peroxide level in senescent rat hepatocytes. *Chem Biol Interact,* 207**,** 74-80.

MUNOZ-ESPIN, D. & SERRANO, M. 2014. Cellular senescence: from physiology to pathology. *Nat Rev Mol Cell Biol,* 15**,** 482-96.

NESS, K. K., KIRKLAND, J. L., GRAMATGES, M. M., WANG, Z., KUNDU, M., MCCASTLAIN, K., LI-HARMS, X., ZHANG, J., TCHKONIA, T., PLUIJM, S. M. F. & ARMSTRONG, G. T. 2018. Premature Physiologic Aging as a Paradigm for Understanding Increased Risk of Adverse Health Across the Lifespan of Survivors of Childhood Cancer. *J Clin Oncol,* 36**,** 2206-2215.

PADMAKUMAR, V. C., SPEER, K., PAL-GHOSH, S., MASIUK, K. E., RYSCAVAGE, A., DENGLER, S. L., HWANG, S., EDWARDS, J. C., COPPOLA, V., TESSAROLLO, L., STEPP, M. A. & YUSPA, S. H. 2012. Spontaneous skin erosions and reduced skin and corneal wound healing characterize CLIC4(NULL) mice. *Am J Pathol,* 181**,** 74-84.

PAEZ-RIBES, M., GONZALEZ-GUALDA, E., DOHERTY, G. J. & MUNOZ-ESPIN, D. 2019. Targeting senescent cells in translational medicine. *EMBO Mol Med,* 11**,** e10234.

PIGNON, J. P., TRIBODET, H., SCAGLIOTTI, G. V., DOUILLARD, J. Y., SHEPHERD, F. A., STEPHENS, R. J., DUNANT, A., TORRI, V., ROSELL, R., SEYMOUR, L., SPIRO, S. G., ROLLAND, E., FOSSATI, R., AUBERT, D., DING, K., WALLER, D., LE CHEVALIER, T. & GROUP, L. C. 2008. Lung adjuvant cisplatin evaluation: a pooled analysis by the LACE Collaborative Group. *J Clin Oncol,* 26**,** 3552-9.

QIAN, Y. & CHEN, X. 2013. Senescence regulation by the p53 protein family. *Methods Mol Biol,* 965**,** 37-61.

SEDLETSKA, Y., GIRAUD-PANIS, M. J. & MALINGE, J. M. 2005. Cisplatin is a DNA-damaging antitumour compound triggering multifactorial biochemical responses in cancer cells: importance of apoptotic pathways. *Curr Med Chem Anticancer Agents,* 5**,** 251-65.

SELUANOV, A., GORBUNOVA, V., FALCOVITZ, A., SIGAL, A., MILYAVSKY, M., ZURER, I., SHOHAT, G., GOLDFINGER, N. & ROTTER, V. 2001. Change of the death pathway in senescent human fibroblasts in response to DNA damage is caused by an inability to stabilize p53. *Mol Cell Biol,* 21**,** 1552-64.

SHUKLA, A., EDWARDS, R., YANG, Y., HAHN, A., FOLKERS, K., DING, J., PADMAKUMAR, V. C., CATAISSON, C., SUH, K. S. & YUSPA, S. H. 2014. CLIC4 regulates TGF-beta-dependent myofibroblast differentiation to produce a cancer stroma. *Oncogene,* 33**,** 842-50.

SIDDIK, Z. H. 2003. Cisplatin: mode of cytotoxic action and molecular basis of resistance. *Oncogene,* 22**,** 7265-79.

SINGH, L., ALDOSARY, S., SAEEDAN, A. S., ANSARI, M. N. & KAITHWAS, G. 2018. Prolyl hydroxylase 2: a promising target to inhibit hypoxia-induced cellular metabolism in cancer cells. *Drug Discov Today,* 23**,** 1873-1882.

SRIRATANASAK, N., CHUNHACHA, P., EI, Z. Z. & CHANVORACHOTE, P. 2022. Cisplatin Induces Senescent Lung Cancer Cell-Mediated Stemness Induction via GRP78/Akt-Dependent Mechanism. *Biomedicines,* 10.

SUH, K. S., MALIK, M., SHUKLA, A. & YUSPA, S. H. 2007. CLIC4, skin homeostasis and cutaneous cancer: surprising connections. *Mol Carcinog,* 46**,** 599-604.

SUN, X., SHI, B., ZHENG, H., MIN, L., YANG, J., LI, X., LIAO, X., HUANG, W., ZHANG, M., XU, S., ZHU, Z., CUI, H. & LIU, X. 2018. Senescence-associated secretory factors induced by cisplatin in melanoma cells promote non-senescent melanoma cell growth through activation of the ERK1/2-RSK1 pathway. *Cell Death Dis,* 9**,** 260.

WANG, X., WONG, S. C., PAN, J., TSAO, S. W., FUNG, K. H., KWONG, D. L., SHAM, J. S. & NICHOLLS, J. M. 1998. Evidence of cisplatin-induced senescent-like growth arrest in nasopharyngeal carcinoma cells. *Cancer Res,* 58**,** 5019-22.

WASSON, C. W., ROSS, R. L., MORTON, R., MANKOURI, J. & DEL GALDO, F. 2021. The intracellular chloride channel 4 (CLIC4) activates systemic sclerosis fibroblasts. *Rheumatology (Oxford),* 60**,** 4395-4400.

WEI, Z., GUO, H., QIN, J., LU, S., LIU, Q., ZHANG, X., ZOU, Y., GONG, Y. & SHAO, C. 2019. Pan-senescence transcriptome analysis identified RRAD as a marker and negative regulator of cellular senescence. *Free Radic Biol Med,* 130**,** 267-277.

WILLOUGHBY, N. A., BOCK, H., HOEVE, M. A., PELLS, S., WILLIAMS, C., MCPHEE, G., FREILE, P., CHOUDHURY, D. & DE SOUSA, P. A. 2016. A scalable label-free approach to separate human pluripotent cells from differentiated derivatives. *Biomicrofluidics,* 10**,** 014107.

YU, J. X., KODIBAGKAR, V. D., HALLAC, R. R., LIU, L. & MASON, R. P. 2012. Dual 19F/1H MR gene reporter molecules for in vivo detection of beta-galactosidase. *Bioconjug Chem,* 23**,** 596-603.

ACOSTA, J. C., BANITO, A., WUESTEFELD, T., GEORGILIS, A., JANICH, P., MORTON, J. P., ATHINEOS, D., KANG, T. W., LASITSCHKA, F., ANDRULIS, M., PASCUAL, G., MORRIS, K. J., KHAN, S., JIN, H., DHARMALINGAM, G., SNIJDERS, A. P., CARROLL, T., CAPPER, D., PRITCHARD, C., INMAN, G. J., LONGERICH, T., SANSOM, O. J., BENITAH, S. A., ZENDER, L. & GIL, J. 2013. A complex secretory program orchestrated by the inflammasome controls paracrine senescence. *Nat Cell Biol,* 15**,** 978-90.

ALEXIUS-LINDGREN, M., ANDERSSON, E., LINDSTEDT, I. & ENGSTROM, W. 2014. The RECK gene and biological malignancy--its significance in angiogenesis and inhibition of matrix metalloproteinases. *Anticancer Res,* 34**,** 3867-73.

BASISTY, N., KALE, A., JEON, O. H., KUEHNEMANN, C., PAYNE, T., RAO, C., HOLTZ, A., SHAH, S., SHARMA, V., FERRUCCI, L., CAMPISI, J. & SCHILLING, B. 2020. A proteomic atlas of senescence-associated secretomes for aging biomarker development. *PLoS Biol,* 18**,** e3000599.

CAPPARELLI, C., CHIAVARINA, B., WHITAKER-MENEZES, D., PESTELL, T. G., PESTELL, R. G., HULIT, J., ANDO, S., HOWELL, A., MARTINEZ-OUTSCHOORN, U. E., SOTGIA, F. & LISANTI, M. P. 2012. CDK inhibitors (p16/p19/p21) induce senescence and autophagy in cancer-associated fibroblasts, "fueling" tumor growth via paracrine interactions, without an increase in neo-angiogenesis. *Cell Cycle,* 11**,** 3599-610.

COLLADO, M., BLASCO, M. A. & SERRANO, M. 2007. Cellular senescence in cancer and aging. *Cell,* 130**,** 223-33.

COPPE, J. P., DESPREZ, P. Y., KRTOLICA, A. & CAMPISI, J. 2010. The senescence-associated secretory phenotype: the dark side of tumor suppression. *Annu Rev Pathol,* 5**,** 99-118.

COX, J. & MANN, M. 2008. MaxQuant enables high peptide identification rates, individualized p.p.b.-range mass accuracies and proteome-wide protein quantification. *Nat Biotechnol,* 26**,** 1367-72.

CROCHEMORE, C., FERNANDEZ-MOLINA, C., MONTAGNE, B., SALLES, A. & RICCHETTI, M. 2019. CSB promoter downregulation via histone H3 hypoacetylation is an early determinant of replicative senescence. *Nat Commun,* 10**,** 5576.

EDWARDS, J. C., BRUNO, J., KEY, P. & CHENG, Y. W. 2014. Absence of chloride intracellular channel 4 (CLIC4) predisposes to acute kidney injury but has minimal impact on recovery. *BMC Nephrol,* 15**,** 54.

HERNANDEZ-SEGURA, A., NEHME, J. & DEMARIA, M. 2018. Hallmarks of Cellular Senescence. *Trends Cell Biol,* 28**,** 436-453.

KIM, H. S., HEO, J. I., PARK, S. H., SHIN, J. Y., KANG, H. J., KIM, M. J., KIM, S. C., KIM, J., PARK, J. B. & LEE, J. Y. 2014. Transcriptional activation of p21(WAF(1)/CIP(1)) is mediated by increased DNA binding activity and increased interaction between p53 and Sp1 via phosphorylation during replicative senescence of human embryonic fibroblasts. *Mol Biol Rep,* 41**,** 2397-408.

KUROSAKI, Y., IMOTO, A., KAWAKAMI, F., OUCHI, M., MORITA, A., YOKOBA, M., TAKENAKA, T., ICHIKAWA, T., KATAGIRI, M., NIELSEN, R. & ISHII, N. 2022. In vitro study on effect of bardoxolone methyl on cisplatin-induced cellular senescence in human proximal tubular cells. *Mol Cell Biochem*.

MALAQUIN, N., MARTINEZ, A. & RODIER, F. 2016. Keeping the senescence secretome under control: Molecular reins on the senescence-associated secretory phenotype. *Exp Gerontol,* 82**,** 39-49.

MORISAKI, H., ANDO, A., NAGATA, Y., PEREIRA-SMITH, O., SMITH, J. R., IKEDA, K. & NAKANISHI, M. 1999. Complex mechanisms underlying impaired activation of Cdk4 and Cdk2 in replicative senescence: roles of p16, p21, and cyclin D1. *Exp Cell Res,* 253**,** 503-10.

MOSTEIRO, L., PANTOJA, C., DE MARTINO, A. & SERRANO, M. 2018. Senescence promotes in vivo reprogramming through p16(INK)(4a) and IL-6. *Aging Cell,* 17.

NELSON, G., WORDSWORTH, J., WANG, C., JURK, D., LAWLESS, C., MARTIN-RUIZ, C. & VON ZGLINICKI, T. 2012. A senescent cell bystander effect: senescence-induced senescence. *Aging Cell,* 11**,** 345-9.

ORTIZ-MONTERO, P., LONDONO-VALLEJO, A. & VERNOT, J. P. 2017. Senescence-associated IL-6 and IL-8 cytokines induce a self- and cross-reinforced senescence/inflammatory milieu strengthening tumorigenic capabilities in the MCF-7 breast cancer cell line. *Cell Commun Signal,* 15**,** 17.

PADMAKUMAR, V. C., SPEER, K., PAL-GHOSH, S., MASIUK, K. E., RYSCAVAGE, A., DENGLER, S. L., HWANG, S., EDWARDS, J. C., COPPOLA, V., TESSAROLLO, L., STEPP, M. A. & YUSPA, S. H. 2012. Spontaneous skin erosions and reduced skin and corneal wound healing characterize CLIC4(NULL) mice. *Am J Pathol,* 181**,** 74-84.

PARIKH, P., WICHER, S., KHANDALAVALA, K., PABELICK, C. M., BRITT, R. D., JR. & PRAKASH, Y. S. 2019. Cellular senescence in the lung across the age spectrum. *Am J Physiol Lung Cell Mol Physiol,* 316**,** L826-L842.

SUH, K. S., MALIK, M., SHUKLA, A. & YUSPA, S. H. 2007. CLIC4, skin homeostasis and cutaneous cancer: surprising connections. *Mol Carcinog,* 46**,** 599-604.

SUH, K. S., MUTOH, M., GERDES, M., CRUTCHLEY, J. M., MUTOH, T., EDWARDS, L. E., DUMONT, R. A., SODHA, P., CHENG, C., GLICK, A. & YUSPA, S. H. 2005. Antisense suppression of the chloride intracellular channel family induces apoptosis, enhances tumor necrosis factor {alpha}-induced apoptosis, and inhibits tumor growth. *Cancer Res,* 65**,** 562-71.

THOMAS, P. D., CAMPBELL, M. J., KEJARIWAL, A., MI, H., KARLAK, B., DAVERMAN, R., DIEMER, K., MURUGANUJAN, A. & NARECHANIA, A. 2003. PANTHER: a library of protein families and subfamilies indexed by function. *Genome Res,* 13**,** 2129-41.

TYANOVA, S., TEMU, T., SINITCYN, P., CARLSON, A., HEIN, M. Y., GEIGER, T., MANN, M. & COX, J. 2016. The Perseus computational platform for comprehensive analysis of (prote)omics data. *Nat Methods,* 13**,** 731-40.

ULMASOV, B., BRUNO, J., GORDON, N., HARTNETT, M. E. & EDWARDS, J. C. 2009. Chloride intracellular channel protein-4 functions in angiogenesis by supporting acidification of vacuoles along the intracellular tubulogenic pathway. *Am J Pathol,* 174**,** 1084-96.

WANG, J., VASAIKAR, S., SHI, Z., GREER, M. & ZHANG, B. 2017. WebGestalt 2017: a more comprehensive, powerful, flexible and interactive gene set enrichment analysis toolkit. *Nucleic Acids Res,* 45**,** W130-W137.

ZHAO, W., LIN, Z. X. & ZHANG, Z. Q. 2004. Cisplatin-induced premature senescence with concomitant reduction of gap junctions in human fibroblasts. *Cell Res,* 14**,** 60-6.

ALKAHTANI, S. A., KUNWAR, P. S., JALILIFAR, M., RASHIDI, S. & YADOLLAHPOUR, A. 2017. Ultrasound-based Techniques as Alternative Treatments for Chronic Wounds: A Comprehensive Review of Clinical Applications. *Cureus,* 9**,** e1952.

AMAYA, C., LUO, S., BAIGORRI, J., BAUCELLS, R., SMITH, E. R. & XU, X. X. 2021. Exposure to low intensity ultrasound removes paclitaxel cytotoxicity in breast and ovarian cancer cells. *BMC Cancer,* 21**,** 981.

ATHERTON, P., LAUSECKER, F., HARRISON, A. & BALLESTREM, C. 2017. Low-intensity pulsed ultrasound promotes cell motility through vinculin-controlled Rac1 GTPase activity. *J Cell Sci,* 130**,** 2277-2291.

BONHAM, C. A., KUEHLMANN, B. & GURTNER, G. C. 2020. Impaired Neovascularization in Aging. *Adv Wound Care (New Rochelle),* 9**,** 111-126.

CAZIN, C., CHICHE, A. & LI, H. 2017. Evaluation of Injury-induced Senescence and In Vivo Reprogramming in the Skeletal Muscle. *J Vis Exp.*

DE AVILA SANTANA, L., ALVES, J. M., ANDRADE, T. A., KAJIWARA, J. K., GARCIA, S. B., GOMES, F. G. & FRADE, M. A. 2013. Clinical and immunohistopathological aspects of venous ulcers treatment by Low-Intensity Pulsed Ultrasound (LIPUS). *Ultrasonics,* 53**,** 870-9.

DE MERA-RODRIGUEZ, J. A., ALVAREZ-HERNAN, G., GANAN, Y., MARTIN-PARTIDO, G., RODRIGUEZ-LEON, J. & FRANCISCO-MORCILLO, J. 2021. Is Senescence-Associated beta-Galactosidase a Reliable in vivo Marker of Cellular Senescence During Embryonic Development? *Front Cell Dev Biol,* 9**,** 623175.

GUERRERO, F., CARMONA, A., JIMENEZ, M. J., OBRERO, T., PULIDO, V., MORENO, J. A., SORIANO, S., MARTIN-MALO, A. & ALJAMA, P. 2021. Passage Number-Induced Replicative Senescence Modulates the Endothelial Cell Response to Protein-Bound Uremic Toxins. *Toxins (Basel),* 13.

HARDING, K. G., MOORE, K. & PHILLIPS, T. J. 2005. Wound chronicity and fibroblast senescence--implications for treatment. *Int Wound J,* 2**,** 364-8.

HUANG, Y., DAI, X., GUAN, Z., LIU, D., REN, L., CHEN, M., ZENG, Z., JIANG, J., LUO, Y., HE, Y., HUANG, M. & ZHAO, C. 2022. A DNA damage nanoamplifier for the chemotherapy of triple-negative breast cancer via DNA damage induction and repair blocking. *Int J Pharm,* 622**,** 121897.

JANG, K. W., DING, L., SEOL, D., LIM, T. H., BUCKWALTER, J. A. & MARTIN, J. A. 2014. Low-intensity pulsed ultrasound promotes chondrogenic progenitor cell migration via focal adhesion kinase pathway. *Ultrasound Med Biol,* 40**,** 1177-86.

KATANO, M., NARUSE, K., UCHIDA, K., MIKUNI-TAKAGAKI, Y., TAKASO, M., ITOMAN, M. & URABE, K. 2011. Low intensity pulsed ultrasound accelerates delayed healing process by reducing the time required for the completion of endochondral ossification in the aged mouse femur fracture model. *Exp Anim,* 60**,** 385-95.

KINNER, A., WU, W., STAUDT, C. & ILIAKIS, G. 2008. Gamma-H2AX in recognition and signaling of DNA double-strand breaks in the context of chromatin. *Nucleic Acids Res,* 36**,** 5678-94.

KLEMENT, K. & GOODARZI, A. A. 2014. DNA double strand break responses and chromatin alterations within the aging cell. *Exp Cell Res,* 329**,** 42-52.

LEE, B. Y., HAN, J. A., IM, J. S., MORRONE, A., JOHUNG, K., GOODWIN, E. C., KLEIJER, W. J., DIMAIO, D. & HWANG, E. S. 2006. Senescence-associated beta-galactosidase is lysosomal beta-galactosidase. *Aging Cell,* 5**,** 187-95.

LEE, J. H. & PAULL, T. T. 2005. ATM activation by DNA double-strand breaks through the Mre11-Rad50-Nbs1 complex. *Science,* 308**,** 551-4.

LEONTIEVA, O. V. & BLAGOSKLONNY, M. V. 2014. Gerosuppression in confluent cells. *Aging (Albany NY),* 6**,** 1010-8.

LI, W., WANG, W., DONG, H., LI, Y., LI, L., HAN, L., HAN, Z., WANG, S., MA, D. & WANG, H. 2014. Cisplatin-induced senescence in ovarian cancer cells is mediated by GRP78. *Oncol Rep,* 31**,** 2525-34.

MAGALHAES, S., ALMEIDA, I., PEREIRA, C. D., REBELO, S., GOODFELLOW, B. J. & NUNES, A. 2022. The Long-Term Culture of Human Fibroblasts Reveals a Spectroscopic Signature of Senescence. *Int J Mol Sci,* 23.

MERZ, S. E., KLOPFLEISCH, R., BREITHAUPT, A. & GRUBER, A. D. 2019. Aging and Senescence in Canine Testes. *Vet Pathol,* 56**,** 715-724.

MEUTER, A., ROGMANN, L. M., WINTERHOFF, B. J., TCHKONIA, T., KIRKLAND, J. L. & MORBECK, D. E. 2014. Markers of cellular senescence are elevated in murine blastocysts cultured in vitro: molecular consequences of culture in atmospheric oxygen. *J Assist Reprod Genet,* 31**,** 1259-67.

OLSZEWSKA, A., BORKOWSKA, A., GRANICA, M., KAROLCZAK, J., ZGLINICKI, B., KIEDA, C. & WAS, H. 2021. Escape From Cisplatin-Induced Senescence of Hypoxic Lung Cancer Cells Can Be Overcome by Hydroxychloroquine. *Front Oncol,* 11**,** 738385.

PRZYSTUPSKI, D. & USSOWICZ, M. 2022. Landscape of Cellular Bioeffects Triggered by Ultrasound-Induced Sonoporation. *Int J Mol Sci,* 23.

QU, K., LIN, T., WEI, J., MENG, F., WANG, Z., HUANG, Z., WAN, Y., SONG, S., LIU, S., CHANG, H., DONG, Y. & LIU, C. 2013. Cisplatin induces cell cycle arrest and senescence via upregulating P53 and P21 expression in HepG2 cells. *Nan Fang Yi Ke Da Xue Xue Bao,* 33**,** 1253-9.

RESNIK, S. R. E., ANDJELA ;ABDO ABUJAMRA, BEATRIZ ;JOZIC, IVAN 2020. Clinical Implications of Cellular Senescence on Wound Healing. *New York: Springer US,* 9**,** 286-297.

ROMANOV, V. S., POSPELOV, V. A. & POSPELOVA, T. V. 2012. Cyclin-dependent kinase inhibitor p21(Waf1): contemporary view on its role in senescence and oncogenesis. *Biochemistry (Mosc),* 77**,** 575-84.

ROPER, J., HARRISON, A. & BASS, M. D. 2012. Induction of adhesion-dependent signals using low-intensity ultrasound. *J Vis Exp***,** e4024.

ROPER, J. A., WILLIAMSON, R. C., BALLY, B., COWELL, C. A. M., BROOKS, R., STEPHENS, P., HARRISON, A. J. & BASS, M. D. 2015. Ultrasonic Stimulation of Mouse Skin Reverses the Healing Delays in Diabetes and Aging by Activation of Rac1. *J Invest Dermatol,* 135**,** 2842-2851.

SIAVOSHIAN, S., BLOTTIERE, H. M., CHERBUT, C. & GALMICHE, J. P. 1997. Butyrate stimulates cyclin D and p21 and inhibits cyclin-dependent kinase 2 expression in HT-29 colonic epithelial cells. *Biochem Biophys Res Commun,* 232**,** 169-72.

SIDDIQUI, M. S., FRANCOIS, M., FENECH, M. F. & LEIFERT, W. R. 2015. Persistent gammaH2AX: A promising molecular marker of DNA damage and aging. *Mutat Res Rev Mutat Res,* 766**,** 1-19.

VU, R., JIN, S., SUN, P., HAENSEL, D., NGUYEN, Q. H., DRAGAN, M., KESSENBROCK, K., NIE, Q. & DAI, X. 2022. Wound healing in aged skin exhibits systems-level alterations in cellular composition and cell-cell communication. *Cell Rep,* 40**,** 111155.

WAGNER, K. D. & WAGNER, N. 2022. The Senescence Markers p16INK4A, p14ARF/p19ARF, and p21 in Organ Development and Homeostasis. *Cells,* 11.

WAHBA, J., NATOLI, M., WHILDING, L. M., PARENTE-PEREIRA, A. C., JUNG, Y., ZONA, S., LAM, E. W., SMITH, J. R., MAHER, J. & GHAEM-MAGHAMI, S. 2018. Chemotherapy-induced

apoptosis, autophagy and cell cycle arrest are key drivers of synergy in chemo-immunotherapy of epithelial ovarian cancer. *Cancer Immunol Immunother,* 67**,** 1753-1765.

WANG, Z., WEI, D. D. & XIAO, H. Y. 2013. Methods of Cellular Senescence Induction Using Oxidative Stress. *Biological Aging: Methods and Protocols, 2nd Edition,* 1048**,** 135-144.

WEI, X., LI, M., ZHENG, Z., MA, J., GAO, Y., CHEN, L., PENG, Y., YU, S. & YANG, L. 2022. Senescence in chronic wounds and potential targeted therapies. *Burns Trauma,* 10**,** tkab045.

WOODS, D. & TURCHI, J. J. 2013. Chemotherapy induced DNA damage response: convergence of drugs and pathways. *Cancer Biol Ther,* 14**,** 379-89.

YU, W. K., WANG, Z., FONG, C. C., LIU, D., YIP, T. C., AU, S. K., ZHU, G. & YANG, M. 2017. Chemoresistant lung cancer stem cells display high DNA repair capability to remove cisplatin-induced DNA damage. *Br J Pharmacol,* 174**,** 302-313.

ZHANG, D., TANG, B., XIE, X., XIAO, Y. F., YANG, S. M. & ZHANG, J. W. 2015. The interplay between DNA repair and autophagy in cancer therapy. *Cancer Biol Ther,* 16**,** 1005-13.

ZHAO, W., LIN, Z. X. & ZHANG, Z. Q. 2004. Cisplatin-induced premature senescence with concomitant reduction of gap junctions in human fibroblasts. *Cell Res,* 14**,** 60-6.

ROPER, J. A., WILLIAMSON, R. C., BALLY, B., COWELL, C. A. M., BROOKS, R., STEPHENS, P., HARRISON, A. J. & BASS, M. D. 2015. Ultrasonic Stimulation of Mouse Skin Reverses the Healing Delays in Diabetes and Aging by Activation of Rac1. *J Invest Dermatol,* 135**,** 2842-2851.

WANG, Z., WEI, D. D. & XIAO, H. Y. 2013. Methods of Cellular Senescence Induction Using Oxidative Stress. *Biological Aging: Methods and Protocols, 2nd Edition,* 1048**,** 135-144.

Reference list

ABU-ZIDAN, F. M., HEFNY, A. F. & CORR, P. 2011. Clinical ultrasound physics. *J Emerg Trauma Shock,* 4**,** 501-3.

ACOSTA, J. C., BANITO, A., WUESTEFELD, T., GEORGILIS, A., JANICH, P., MORTON, J. P., ATHINEOS, D., KANG, T. W., LASITSCHKA, F., ANDRULIS, M., PASCUAL, G., MORRIS, K. J., KHAN, S., JIN, H., DHARMALINGAM, G., SNIJDERS, A. P., CARROLL, T., CAPPER, D., PRITCHARD, C., INMAN, G. J., LONGERICH, T., SANSOM, O. J., BENITAH, S. A., ZENDER, L. & GIL, J. 2013. A complex secretory program orchestrated by the inflammasome controls paracrine senescence. *Nat Cell Biol,* 15**,** 978-90.

ACOSTA, J. C., O'LOGHLEN, A., BANITO, A., GUIJARRO, M. V., AUGERT, A., RAGUZ, S., FUMAGALLI, M., DA COSTA, M., BROWN, C., POPOV, N., TAKATSU, Y., MELAMED, J., D'ADDA DI FAGAGNA, F., BERNARD, D., HERNANDO, E. & GIL, J. 2008. Chemokine signaling via the CXCR2 receptor reinforces senescence. *Cell,* 133**,** 1006-18.

AIRD, K. M. & ZHANG, R. 2013. Detection of senescence-associated heterochromatin foci (SAHF). *Methods Mol Biol,* 965**,** 185-96.

ALKAHTANI, S. A., KUNWAR, P. S., JALILIFAR, M., RASHIDI, S. & YADOLLAHPOUR, A. 2017. Ultrasound-based Techniques as Alternative Treatments for Chronic Wounds: A Comprehensive Review of Clinical Applications. *Cureus,* 9**,** e1952.

ALTHUBITI, M., LEZINA, L., CARRERA, S., JUKES-JONES, R., GIBLETT, S. M., ANTONOV, A., BARLEV, N., SALDANHA, G. S., PRITCHARD, C. A., CAIN, K. & MACIP, S. 2014.

Characterization of novel markers of senescence and their prognostic potential in cancer. *Cell Death Dis,* 5**,** e1528.

AMAYA, C., LUO, S., BAIGORRI, J., BAUCELLS, R., SMITH, E. R. & XU, X. X. 2021. Exposure to low intensity ultrasound removes paclitaxel cytotoxicity in breast and ovarian cancer cells. *BMC Cancer,* 21**,** 981.

AMIT, M., MARGULETS, V., SEGEV, H., SHARIKI, K., LAEVSKY, I., COLEMAN, R. & ITSKOVITZ-ELDOR, J. 2003. Human feeder layers for human embryonic stem cells. *Biol Reprod,* 68**,** 2150-6.

AMOR, C., FEUCHT, J., LEIBOLD, J., HO, Y. J., ZHU, C., ALONSO-CURBELO, D., MANSILLA-SOTO, J., BOYER, J. A., LI, X., GIAVRIDIS, T., KULICK, A., HOULIHAN, S., PEERSCHKE, E., FRIEDMAN, S. L., PONOMAREV, V., PIERSIGILLI, A., SADELAIN, M. & LOWE, S. W. 2020. Senolytic CAR T cells reverse senescence-associated pathologies. *Nature,* 583**,** 127-132.

ANTON, B., VITETTA, L., CORTIZO, F. & SALI, A. 2005. Can we delay aging? The biology and science of aging. *Ann N Y Acad Sci,* 1057**,** 525-35.

ARCHER, C. R., SAKALUK, S. K., SELMAN, C., ROYLE, N. J. & HUNT, J. 2013. Oxidative stress and the evolution of sex differences in life span and ageing in the decorated cricket, Gryllodes sigillatus. *Evolution,* 67**,** 620-34.

ATHERTON, P., LAUSECKER, F., HARRISON, A. & BALLESTREM, C. 2017. Low-intensity pulsed ultrasound promotes cell motility through vinculin-controlled Rac1 GTPase activity. *J Cell Sci,* 130**,** 2277-2291.

BAI, M., DENG, J., DAI, C., PFEUFFER, J., SACHSENBERG, T. & PEREZ-RIVEROL, Y. 2023. LFQ-Based Peptide and Protein Intensity Differential Expression Analysis. *J Proteome Res,* 22**,** 2114-2123.

BAINBRIDGE, P. 2013. Wound healing and the role of fibroblasts. *J Wound Care,* 22**,** 407-8, 410-12.

BAKER, K. G., ROBERTSON, V. J. & DUCK, F. A. 2001. A review of therapeutic ultrasound: biophysical effects. *Phys Ther,* 81**,** 1351-8.

BALAJEE, A. S. & GEARD, C. R. 2004. Replication protein A and gamma-H2AX foci assembly is triggered by cellular response to DNA double-strand breaks. *Exp Cell Res,* 300**,** 320-34.

BASISTY, N., KALE, A., JEON, O. H., KUEHNEMANN, C., PAYNE, T., RAO, C., HOLTZ, A., SHAH, S., SHARMA, V., FERRUCCI, L., CAMPISI, J. & SCHILLING, B. 2020. A proteomic atlas of senescence-associated secretomes for aging biomarker development. *PLoS Biol,* 18**,** e3000599.

BASU, A. & KRISHNAMURTHY, S. 2010. Cellular responses to Cisplatin-induced DNA damage. *J Nucleic Acids,* 2010.

BAVIK, C., COLEMAN, I., DEAN, J. P., KNUDSEN, B., PLYMATE, S. & NELSON, P. S. 2006. The gene expression program of prostate fibroblast senescence modulates neoplastic epithelial cell proliferation through paracrine mechanisms. *Cancer Res,* 66**,** 794-802.

BAZ-MARTINEZ, M., DA SILVA-ALVAREZ, S., RODRIGUEZ, E., GUERRA, J., EL MOTIAM, A., VIDAL, A., GARCIA-CABALLERO, T., GONZALEZ-BARCIA, M., SANCHEZ, L., MUNOZ-FONTELA, C., COLLADO, M. & RIVAS, C. 2016. Cell senescence is an antiviral defense mechanism. *Sci Rep,* 6**,** 37007.

BEAUSEJOUR, C. M., KRTOLICA, A., GALIMI, F., NARITA, M., LOWE, S. W., YASWEN, P. & CAMPISI, J. 2003. Reversal of human cellular senescence: roles of the p53 and p16 pathways. *EMBO J,* 22**,** 4212-22.

BEN-PORATH, I. & WEINBERG, R. A. 2005. The signals and pathways activating cellular senescence. *Int J Biochem Cell Biol,* 37**,** 961-76.

BERNADOTTE, A., MIKHELSON, V. M. & SPIVAK, I. M. 2016. Markers of cellular senescence. Telomere shortening as a marker of cellular senescence. *Aging (Albany NY),* 8**,** 3-11.

BIRCH, J. & GIL, J. 2020. Senescence and the SASP: many therapeutic avenues. *Genes Dev,* 34**,** 1565-1576.

BJORKSTEN, J. 1968. The crosslinkage theory of aging. *J Am Geriatr Soc,* 16**,** 408-27.

BODE-BOGER, S. M., SCALERA, F. & MARTENS-LOBENHOFFER, J. 2005. Asymmetric dimethylarginine (ADMA) accelerates cell senescence. *Vasc Med,* 10 Suppl 1**,** S65-71.

BONHAM, C. A., KUEHLMANN, B. & GURTNER, G. C. 2020. Impaired Neovascularization in Aging. *Adv Wound Care (New Rochelle),* 9**,** 111-126.

BORODKINA, A. V., DERYABIN, P. I., GIUKOVA, A. A. & NIKOLSKY, N. N. 2018. "Social Life" of Senescent Cells: What Is SASP and Why Study It? *Acta Naturae,* 10**,** 4-14.

BOSANQUET, D. C. & HARDING, K. G. 2014. Wound duration and healing rates: cause or effect? *Wound Repair Regen,* 22**,** 143-50.

BREMNES, R. M., DONNEM, T., AL-SAAD, S., AL-SHIBLI, K., ANDERSEN, S., SIRERA, R., CAMPS, C., MARINEZ, I. & BUSUND, L. T. 2011. The role of tumor stroma in cancer progression and prognosis: emphasis on carcinoma-associated fibroblasts and non-small cell lung cancer. *J Thorac Oncol,* 6**,** 209-17.

BROUGHTON, G., 2ND, JANIS, J. E. & ATTINGER, C. E. 2006. The basic science of wound healing. *Plast Reconstr Surg,* 117**,** 12S-34S.

BYUN, H. O., LEE, Y. K., KIM, J. M. & YOON, G. 2015. From cell senescence to age-related diseases: differential mechanisms of action of senescence-associated secretory phenotypes. *BMB Rep,* 48**,** 549-58.

CAI, Z. J. 2021. Hypothalamic aging and hormones. *Vitam Horm,* 115**,** 15-37.

CAMPISI, J. 2013. Aging, cellular senescence, and cancer. *Annu Rev Physiol,* 75**,** 685-705.

CAMPISI, J. 2016. Cellular Senescence and Lung Function during Aging. Yin and Yang. *Ann Am Thorac Soc,* 13 Suppl 5**,** S402-S406.

CAMPISI, J. & D'ADDA DI FAGAGNA, F. 2007. Cellular senescence: when bad things happen to good cells. *Nat Rev Mol Cell Biol,* 8**,** 729-40.

CAZIN, C., CHICHE, A. & LI, H. 2017. Evaluation of Injury-induced Senescence and In Vivo Reprogramming in the Skeletal Muscle. *J Vis Exp*.

CESARI, M., PAHOR, M. & INCALZI, R. A. 2010. Plasminogen activator inhibitor-1 (PAI-1): a key factor linking fibrinolysis and age-related subclinical and clinical conditions. *Cardiovasc Ther,* 28**,** e72-91.

CHAIB, S., TCHKONIA, T. & KIRKLAND, J. L. 2022. Cellular senescence and senolytics: the path to the clinic. *Nat Med,* 28**,** 1556-1568.

CHANG, B. D., SWIFT, M. E., SHEN, M., FANG, J., BROUDE, E. V. & RONINSON, I. B. 2002. Molecular determinants of terminal growth arrest induced in tumor cells by a chemotherapeutic agent. *Proc Natl Acad Sci U S A,* 99**,** 389-94.

CHEN, J. H., HALES, C. N. & OZANNE, S. E. 2007. DNA damage, cellular senescence and organismal ageing: causal or correlative? *Nucleic Acids Res,* 35**,** 7417-28.

CHILDS, B. G., DURIK, M., BAKER, D. J. & VAN DEURSEN, J. M. 2015. Cellular senescence in aging and age-related disease: from mechanisms to therapy. *Nat Med,* 21**,** 1424-35.

CHOU, L. Y., HO, C. T. & HUNG, S. C. 2022. Paracrine Senescence of Mesenchymal Stromal Cells Involves Inflammatory Cytokines and the NF-kappaB Pathway. *Cells,* 11.

CICCIA, A. & ELLEDGE, S. J. 2010. The DNA damage response: making it safe to play with knives. *Mol Cell,* 40**,** 179-204.

COLLADO, M., GIL, J., EFEYAN, A., GUERRA, C., SCHUHMACHER, A. J., BARRADAS, M., BENGURIA, A., ZABALLOS, A., FLORES, J. M., BARBACID, M., BEACH, D. & SERRANO, M. 2005. Tumour biology: senescence in premalignant tumours. *Nature,* 436**,** 642.

COMI, P., CHIARAMONTE, R. & MAIER, J. A. 1995. Senescence-dependent regulation of type 1 plasminogen activator inhibitor in human vascular endothelial cells. *Exp Cell Res,* 219**,** 304-8.

COPPE, J. P., DESPREZ, P. Y., KRTOLICA, A. & CAMPISI, J. 2010. The senescence-associated secretory phenotype: the dark side of tumor suppression. *Annu Rev Pathol,* 5**,** 99-118.

COPPE, J. P., PATIL, C. K., RODIER, F., SUN, Y., MUNOZ, D. P., GOLDSTEIN, J., NELSON, P. S., DESPREZ, P. Y. & CAMPISI, J. 2008. Senescence-associated secretory phenotypes reveal cell-nonautonomous functions of oncogenic RAS and the p53 tumor suppressor. *PLoS Biol,* 6**,** 2853-68.

CORREIA-MELO, C. & PASSOS, J. F. 2015. Mitochondria: Are they causal players in cellular senescence? *Biochim Biophys Acta,* 1847**,** 1373-9.

COX, J. & MANN, M. 2008. MaxQuant enables high peptide identification rates, individualized p.p.b.-range mass accuracies and proteome-wide protein quantification. *Nat Biotechnol,* 26**,** 1367-72.

CUOLLO, L., ANTONANGELI, F., SANTONI, A. & SORIANI, A. 2020. The Senescence-Associated Secretory Phenotype (SASP) in the Challenging Future of Cancer Therapy and Age-Related Diseases. *Biology (Basel),* 9.

DA COSTA, J. P., VITORINO, R., SILVA, G. M., VOGEL, C., DUARTE, A. C. & ROCHA-SANTOS, T. 2016. A synopsis on aging-Theories, mechanisms and future prospects. *Ageing Res Rev,* 29**,** 90-112.

DASARI, S. & TCHOUNWOU, P. B. 2014. Cisplatin in cancer therapy: molecular mechanisms of action. *Eur J Pharmacol,* 740**,** 364-78.

DASGUPTA, J., KAR, S., LIU, R., JOSEPH, J., KALYANARAMAN, B., REMINGTON, S. J., CHEN, C. & MELENDEZ, J. A. 2010. Reactive oxygen species control senescence-associated matrix metalloproteinase-1 through c-Jun-N-terminal kinase. *J Cell Physiol,* 225**,** 52-62.

DE AVILA SANTANA, L., ALVES, J. M., ANDRADE, T. A., KAJIWARA, J. K., GARCIA, S. B., GOMES, F. G. & FRADE, M. A. 2013. Clinical and immunohistopathological aspects of venous ulcers treatment by Low-Intensity Pulsed Ultrasound (LIPUS). *Ultrasonics,* 53**,** 870-9.

DE MAAR, J. S., ROUSOU, C., VAN ELBURG, B., VOS, H. J., LAJOINIE, G. P. R., BOS, C., MOONEN, C. T. W. & DECKERS, R. 2021. Ultrasound-Mediated Drug Delivery With a Clinical Ultrasound System: In Vitro Evaluation. *Front Pharmacol,* 12**,** 768436.

DE MERA-RODRIGUEZ, J. A., ALVAREZ-HERNAN, G., GANAN, Y., MARTIN-PARTIDO, G., RODRIGUEZ-LEON, J. & FRANCISCO-MORCILLO, J. 2021. Is Senescence-Associated beta-Galactosidase a Reliable in vivo Marker of Cellular Senescence During Embryonic Development? *Front Cell Dev Biol,* 9**,** 623175.

DEMARIA, M., OHTANI, N., YOUSSEF, S. A., RODIER, F., TOUSSAINT, W., MITCHELL, J. R., LABERGE, R. M., VIJG, J., VAN STEEG, H., DOLLE, M. E., HOEIJMAKERS, J. H., DE BRUIN, A., HARA, E. & CAMPISI, J. 2014. An essential role for senescent cells in optimal wound healing through secretion of PDGF-AA. *Dev Cell,* 31**,** 722-33.

DEMIDOVA-RICE, T. N., DURHAM, J. T. & HERMAN, I. M. 2012a. Wound Healing Angiogenesis: Innovations and Challenges in Acute and Chronic Wound Healing. *Adv Wound Care (New Rochelle),* 1**,** 17-22.

DEMIDOVA-RICE, T. N., HAMBLIN, M. R. & HERMAN, I. M. 2012b. Acute and impaired wound healing: pathophysiology and current methods for drug delivery, part 1: normal and chronic wounds: biology, causes, and approaches to care. *Adv Skin Wound Care,* 25**,** 304-14.

DHAR, S., KOLISHETTI, N., LIPPARD, S. J. & FAROKHZAD, O. C. 2011. Targeted delivery of a cisplatin prodrug for safer and more effective prostate cancer therapy in vivo. *Proc Natl Acad Sci U S A,* 108**,** 1850-5.

DI MICCO, R., SULLI, G., DOBREVA, M., LIONTOS, M., BOTRUGNO, O. A., GARGIULO, G., DAL ZUFFO, R., MATTI, V., D'ARIO, G., MONTANI, E., MERCURIO, C., HAHN, W. C., GORGOULIS, V., MINUCCI, S. & D'ADDA DI FAGAGNA, F. 2011. Interplay between oncogene-induced DNA damage response and heterochromatin in senescence and cancer. *Nat Cell Biol,* 13**,** 292-302.

DIMRI, G. P. 2005. What has senescence got to do with cancer? *Cancer Cell,* 7**,** 505-12.

DIMRI, G. P., LEE, X., BASILE, G., ACOSTA, M., SCOTT, G., ROSKELLEY, C., MEDRANO, E. E., LINSKENS, M., RUBELJ, I., PEREIRA-SMITH, O. & ET AL. 1995. A biomarker that identifies senescent human cells in culture and in aging skin in vivo. *Proc Natl Acad Sci U S A,* 92**,** 9363-7.

DOAN, N., REHER, P., MEGHJI, S. & HARRIS, M. 1999. In vitro effects of therapeutic ultrasound on cell proliferation, protein synthesis, and cytokine production by human fibroblasts, osteoblasts, and monocytes. *J Oral Maxillofac Surg,* 57**,** 409-19; discussion 420.

DRUELLE, C., DRULLION, C., DESLE, J., MARTIN, N., SAAS, L., CORMENIER, J., MALAQUIN, N., HUOT, L., SLOMIANNY, C., BOUALI, F., VERCAMER, C., HOT, D., POURTIER, A., CHEVET, E., ABBADIE, C. & PLUQUET, O. 2016. ATF6alpha regulates morphological changes associated with senescence in human fibroblasts. *Oncotarget,* 7**,** 67699-67715.

DULIC, V., BENEY, G. E., FREBOURG, G., DRULLINGER, L. F. & STEIN, G. H. 2000. Uncoupling between phenotypic senescence and cell cycle arrest in aging p21-deficient fibroblasts. *Mol Cell Biol,* 20**,** 6741-54.

DUVAL, K., GROVER, H., HAN, L. H., MOU, Y., PEGORARO, A. F., FREDBERG, J. & CHEN, Z. 2017. Modeling Physiological Events in 2D vs. 3D Cell Culture. *Physiology (Bethesda),* 32**,** 266-277.

DVORAK, H. F. 2015. Tumors: wounds that do not heal-redux. *Cancer Immunol Res,* 3**,** 1-11.

EFFROS, R. B. 2005. Roy Walford and the immunologic theory of aging. *Immun Ageing,* 2**,** 7.

ERDOGAN, O., ESEN, E., USTUN, Y., KURKCU, M., AKOVA, T., GONLUSEN, G., UYSAL, H. & CEVLIK, F. 2006. Effects of low-intensity pulsed ultrasound on healing of mandibular fractures: an experimental study in rabbits. *J Oral Maxillofac Surg,* 64**,** 180-8.

FAGET, D. V., REN, Q. & STEWART, S. A. 2019. Unmasking senescence: context-dependent effects of SASP in cancer. *Nat Rev Cancer,* 19**,** 439-453.

FALCONE, M., DE ANGELIS, B., PEA, F., SCALISE, A., STEFANI, S., TASINATO, R., ZANETTI, O. & DALLA PAOLA, L. 2021. Challenges in the management of chronic wound infections. *J Glob Antimicrob Resist,* 26**,** 140-147.

FERIL, L. B., JR. 2009. Ultrasound-mediated gene transfection. *Methods Mol Biol,* 542**,** 179-94.

FINKEL, T., SERRANO, M. & BLASCO, M. A. 2007. The common biology of cancer and ageing. *Nature,* 448**,** 767-74.

GASCARD, P. & TLSTY, T. D. 2016. Carcinoma-associated fibroblasts: orchestrating the composition of malignancy. *Genes Dev,* 30**,** 1002-19.

GASEK, N. S., KUCHEL, G. A., KIRKLAND, J. L. & XU, M. 2021. Strategies for Targeting Senescent Cells in Human Disease. *Nat Aging,* 1**,** 870-879.

GEORGILIS, A., KLOTZ, S., HANLEY, C. J., HERRANZ, N., WEIRICH, B., MORANCHO, B., LEOTE, A. C., D'ARTISTA, L., GALLAGE, S., SEEHAWER, M., CARROLL, T., DHARMALINGAM, G., WEE, K. B., MELLONE, M., POMBO, J., HEIDE, D., GUCCIONE, E., ARRIBAS, J., BARBOSA-MORAIS, N. L., HEIKENWALDER, M., THOMAS, G. J., ZENDER, L. & GIL, J. 2018. PTBP1-Mediated Alternative Splicing Regulates the Inflammatory Secretome and the Pro-tumorigenic Effects of Senescent Cells. *Cancer Cell,* 34**,** 85-102 e9.

GERLAND, L. M., PEYROL, S., LALLEMAND, C., BRANCHE, R., MAGAUD, J. P. & FFRENCH, M. 2003. Association of increased autophagic inclusions labeled for beta-galactosidase with fibroblastic aging. *Exp Gerontol,* 38**,** 887-95.

GHOSH, K. & CAPELL, B. C. 2016. The Senescence-Associated Secretory Phenotype: Critical Effector in Skin Cancer and Aging. *J Invest Dermatol,* 136**,** 2133-2139.

GOLDBERGER, A. L., PENG, C. K. & LIPSITZ, L. A. 2002. What is physiologic complexity and how does it change with aging and disease? *Neurobiol Aging,* 23**,** 23-6.

GONZALEZ, A. C., COSTA, T. F., ANDRADE, Z. A. & MEDRADO, A. R. 2016. Wound healing - A literature review. *An Bras Dermatol,* 91**,** 614-620.

GONZALEZ-GUALDA, E., BAKER, A. G., FRUK, L. & MUNOZ-ESPIN, D. 2021. A guide to assessing cellular senescence in vitro and in vivo. *FEBS J,* 288**,** 56-80.

GONZALEZ-MELJEM, J. M., APPS, J. R., FRASER, H. C. & MARTINEZ-BARBERA, J. P. 2018. Paracrine roles of cellular senescence in promoting tumourigenesis. *Br J Cancer,* 118**,** 1283-1288.

GUARENTE, L. 2014. Aging research-where do we stand and where are we going? *Cell,* 159**,** 15-19.

GUERRERO, F., CARMONA, A., JIMENEZ, M. J., OBRERO, T., PULIDO, V., MORENO, J. A., SORIANO, S., MARTIN-MALO, A. & ALJAMA, P. 2021. Passage Number-Induced Replicative Senescence Modulates the Endothelial Cell Response to Protein-Bound Uremic Toxins. *Toxins (Basel),* 13.

GURTNER, G. C., WERNER, S., BARRANDON, Y. & LONGAKER, M. T. 2008. Wound repair and regeneration. *Nature,* 453**,** 314-21.

HAFERKAMP, S., TRAN, S. L., BECKER, T. M., SCURR, L. L., KEFFORD, R. F. & RIZOS, H. 2009. The relative contributions of the p53 and pRb pathways in oncogene-induced melanocyte senescence. *Aging (Albany NY),* 1**,** 542-56.

HALL, A. G. & TILBY, M. J. 1992. Mechanisms of action of, and modes of resistance to, alkylating agents used in the treatment of haematological malignancies. *Blood Rev,* 6**,** 163-73.

HARDING, K. G., MOORE, K. & PHILLIPS, T. J. 2005. Wound chronicity and fibroblast senescence--implications for treatment. *Int Wound J,* 2**,** 364-8.

HARMAN, D. 1992. Free radical theory of aging. *Mutat Res,* 275**,** 257-66.

HARRISON, A., LIN, S., POUNDER, N. & MIKUNI-TAKAGAKI, Y. 2016. Mode & mechanism of low intensity pulsed ultrasound (LIPUS) in fracture repair. *Ultrasonics,* 70**,** 45-52.

HASSONA, Y., CIRILLO, N., HEESOM, K., PARKINSON, E. K. & PRIME, S. S. 2014. Senescent cancer-associated fibroblasts secrete active MMP-2 that promotes keratinocyte dis-cohesion and invasion. *Br J Cancer,* 111**,** 1230-7.

HAYFLICK, L. & MOORHEAD, P. S. 1961. The serial cultivation of human diploid cell strains. *Exp Cell Res,* 25**,** 585-621.

HENDERSON, E. A. 2006. The potential effect of fibroblast senescence on wound healing and the chronic wound environment. *J Wound Care,* 15**,** 315-8.

HERNANDEZ BORRERO, L. J. & EL-DEIRY, W. S. 2021. Tumor suppressor p53: Biology, signaling pathways, and therapeutic targeting. *Biochim Biophys Acta Rev Cancer,* 1876**,** 188556.

HERNANDEZ-SEGURA, A., NEHME, J. & DEMARIA, M. 2018. Hallmarks of Cellular Senescence. *Trends Cell Biol,* 28**,** 436-453.

HIEBERT, P., WIETECHA, M. S., CANGKRAMA, M., HAERTEL, E., MAVROGONATOU, E., STUMPE, M., STEENBOCK, H., GROSSI, S., BEER, H. D., ANGEL, P., BRINCKMANN, J., KLETSAS, D., DENGJEL, J. & WERNER, S. 2018. Nrf2-Mediated Fibroblast Reprogramming Drives Cellular Senescence by Targeting the Matrisome. *Dev Cell,* 46**,** 145-161 e10.

HINDS, P. & PIETRUSKA, J. 2017. Senescence and tumor suppression. *F1000Res,* 6**,** 2121.

HUANG, Y., DAI, X., GUAN, Z., LIU, D., REN, L., CHEN, M., ZENG, Z., JIANG, J., LUO, Y., HE, Y., HUANG, M. & ZHAO, C. 2022. A DNA damage nanoamplifier for the chemotherapy of triple-negative breast cancer via DNA damage induction and repair blocking. *Int J Pharm,* 622**,** 121897.

HWANG, E. S., YOON, G. & KANG, H. T. 2009. A comparative analysis of the cell biology of senescence and aging. *Cell Mol Life Sci,* 66**,** 2503-24.

IKAI, H., TAMURA, T., WATANABE, T., ITOU, M., SUGAYA, A., IWABUCHI, S., MIKUNI-TAKAGAKI, Y. & DEGUCHI, S. 2008. Low-intensity pulsed ultrasound accelerates periodontal wound healing after flap surgery. *J Periodontal Res,* 43**,** 212-6.

JANG, K. W., DING, L., SEOL, D., LIM, T. H., BUCKWALTER, J. A. & MARTIN, J. A. 2014. Low-intensity pulsed ultrasound promotes chondrogenic progenitor cell migration via focal adhesion kinase pathway. *Ultrasound Med Biol,* 40**,** 1177-86.

JIANG, D., DE VRIES, J. C., MUSCHHAMMER, J., SCHATZ, S., YE, H., HEIN, T., FIDAN, M., ROMANOV, V. S., RINKEVICH, Y. & SCHARFFETTER-KOCHANEK, K. 2020. Local and transient inhibition of p21 expression ameliorates age-related delayed wound healing. *Wound Repair Regen,* 28**,** 49-60.

JOCHEMS, F., THIJSSEN, B., DE CONTI, G., JANSEN, R., POGACAR, Z., GROOT, K., WANG, L., SCHEPERS, A., WANG, C., JIN, H., BEIJERSBERGEN, R. L., LEITE DE OLIVEIRA, R., WESSELS, L. F. A. & BERNARDS, R. 2021. The Cancer SENESCopedia: A delineation of cancer cell senescence. *Cell Rep,* 36**,** 109441.

JOHMURA, Y., YAMANAKA, T., OMORI, S., WANG, T. W., SUGIURA, Y., MATSUMOTO, M., SUZUKI, N., KUMAMOTO, S., YAMAGUCHI, K., HATAKEYAMA, S., TAKAMI, T., YAMAGUCHI, R., SHIMIZU, E., IKEDA, K., OKAHASHI, N., MIKAWA, R., SUEMATSU, M., ARITA, M., SUGIMOTO, M., NAKAYAMA, K. I., FURUKAWA, Y., IMOTO, S. & NAKANISHI, M. 2021. Senolysis by glutaminolysis inhibition ameliorates various age-associated disorders. *Science,* 371**,** 265-270.

JOHNS, L. D. 2002. Nonthermal effects of therapeutic ultrasound: the frequency resonance hypothesis. *J Athl Train,* 37**,** 293-9.

JUN, J. I., KIM, K. H. & LAU, L. F. 2015. The matricellular protein CCN1 mediates neutrophil efferocytosis in cutaneous wound healing. *Nat Commun,* 6**,** 7386.

JUN, J. I. & LAU, L. F. 2010. The matricellular protein CCN1 induces fibroblast senescence and restricts fibrosis in cutaneous wound healing. *Nat Cell Biol,* 12**,** 676-85.

KATANO, M., NARUSE, K., UCHIDA, K., MIKUNI-TAKAGAKI, Y., TAKASO, M., ITOMAN, M. & URABE, K. 2011. Low intensity pulsed ultrasound accelerates delayed healing process by reducing the time required for the completion of endochondral ossification in the aged mouse femur fracture model. *Exp Anim,* 60**,** 385-95.

KAUL, Z., CESARE, A. J., HUSCHTSCHA, L. I., NEUMANN, A. A. & REDDEL, R. R. 2011. Five dysfunctional telomeres predict onset of senescence in human cells. *EMBO Rep,* 13**,** 52-9.

KEANE, T. J., HOREJS, C. M. & STEVENS, M. M. 2018. Scarring vs. functional healing: Matrix-based strategies to regulate tissue repair. *Adv Drug Deliv Rev,* 129**,** 407-419.

KENNEDY, J. E. 2005. High-intensity focused ultrasound in the treatment of solid tumours. *Nat Rev Cancer,* 5**,** 321-7.

KIM, K. H., PARK, G. T., LIM, Y. B., RUE, S. W., JUNG, J. C., SONN, J. K., BAE, Y. S., PARK, J. W. & LEE, Y. S. 2004. Expression of connective tissue growth factor, a biomarker in senescence of human diploid fibroblasts, is up-regulated by a transforming growth factor-beta-mediated signaling pathway. *Biochem Biophys Res Commun,* 318**,** 819-25.

KINNER, A., WU, W., STAUDT, C. & ILIAKIS, G. 2008. Gamma-H2AX in recognition and signaling of DNA double-strand breaks in the context of chromatin. *Nucleic Acids Res,* 36**,** 5678-94.

KLEMENT, K. & GOODARZI, A. A. 2014. DNA double strand break responses and chromatin alterations within the aging cell. *Exp Cell Res,* 329**,** 42-52.

KLINGBERG, F., HINZ, B. & WHITE, E. S. 2013. The myofibroblast matrix: implications for tissue repair and fibrosis. *J Pathol,* 229**,** 298-309.

KODALI, R., HAJJOU, M., BERMAN, A. B., BANSAL, M. B., ZHANG, S., PAN, J. J. & SCHECTER, A. D. 2006. Chemokines induce matrix metalloproteinase-2 through activation of epidermal growth factor receptor in arterial smooth muscle cells. *Cardiovasc Res,* 69**,** 706-15.

KORTLEVER, R. M., HIGGINS, P. J. & BERNARDS, R. 2006. Plasminogen activator inhibitor-1 is a critical downstream target of p53 in the induction of replicative senescence. *Nat Cell Biol,* 8**,** 877-84.

KREILING, J. A., TAMAMORI-ADACHI, M., SEXTON, A. N., JEYAPALAN, J. C., MUNOZ-NAJAR, U., PETERSON, A. L., MANIVANNAN, J., ROGERS, E. S., PCHELINTSEV, N. A., ADAMS, P. D. & SEDIVY, J. M. 2011. Age-associated increase in heterochromatic marks in murine and primate tissues. *Aging Cell,* 10**,** 292-304.

KRIZHANOVSKY, V., YON, M., DICKINS, R. A., HEARN, S., SIMON, J., MIETHING, C., YEE, H., ZENDER, L. & LOWE, S. W. 2008. Senescence of activated stellate cells limits liver fibrosis. *Cell,* 134**,** 657-67.

KRTOLICA, A. & CAMPISI, J. 2002. Cancer and aging: a model for the cancer promoting effects of the aging stroma. *Int J Biochem Cell Biol,* 34**,** 1401-14.

KRTOLICA, A., PARRINELLO, S., LOCKETT, S., DESPREZ, P. Y. & CAMPISI, J. 2001. Senescent fibroblasts promote epithelial cell growth and tumorigenesis: a link between cancer and aging. *Proc Natl Acad Sci U S A,* 98**,** 12072-7.

KRUK, P. A., RAMPINO, N. J. & BOHR, V. A. 1995. DNA damage and repair in telomeres: relation to aging. *Proc Natl Acad Sci U S A,* 92**,** 258-62.

KRUT, Z., GAZIT, D., GAZIT, Z. & PELLED, G. 2022. Applications of Ultrasound-Mediated Gene Delivery in Regenerative Medicine. *Bioengineering (Basel),* 9.

KUILMAN, T., MICHALOGLOU, C., MOOI, W. J. & PEEPER, D. S. 2010. The essence of senescence. *Genes Dev,* 24**,** 2463-79.

KUILMAN, T., MICHALOGLOU, C., VREDEVELD, L. C., DOUMA, S., VAN DOORN, R., DESMET, C. J., AARDEN, L. A., MOOI, W. J. & PEEPER, D. S. 2008. Oncogene-induced senescence relayed by an interleukin-dependent inflammatory network. *Cell,* 133**,** 1019-31.

KUMAR, S., MILLIS, A. J. & BAGLIONI, C. 1992. Expression of interleukin 1-inducible genes and production of interleukin 1 by aging human fibroblasts. *Proc Natl Acad Sci U S A,* 89**,** 4683-7.

KUMARI, R. & JAT, P. 2021. Mechanisms of Cellular Senescence: Cell Cycle Arrest and Senescence Associated Secretory Phenotype. *Front Cell Dev Biol,* 9**,** 645593.

KURZ, D. J., DECARY, S., HONG, Y. & ERUSALIMSKY, J. D. 2000. Senescence-associated (beta)-galactosidase reflects an increase in lysosomal mass during replicative ageing of human endothelial cells. *J Cell Sci,* 113 (Pt 20)**,** 3613-22.

LANDEN, N. X., LI, D. & STAHLE, M. 2016. Transition from inflammation to proliferation: a critical step during wound healing. *Cell Mol Life Sci,* 73**,** 3861-85.

LAU, L., PORCIUNCULA, A., YU, A., IWAKURA, Y. & DAVID, G. 2019. Uncoupling the Senescence-Associated Secretory Phenotype from Cell Cycle Exit via Interleukin-1 Inactivation Unveils Its Protumorigenic Role. *Mol Cell Biol,* 39.

LEE, B. Y., HAN, J. A., IM, J. S., MORRONE, A., JOHUNG, K., GOODWIN, E. C., KLEIJER, W. J., DIMAIO, D. & HWANG, E. S. 2006. Senescence-associated beta-galactosidase is lysosomal beta-galactosidase. *Aging Cell,* 5**,** 187-95.

LEE, J. H. & PAULL, T. T. 2005. ATM activation by DNA double-strand breaks through the Mre11-Rad50-Nbs1 complex. *Science,* 308**,** 551-4.

LEE, M. & LEE, J. S. 2014. Exploiting tumor cell senescence in anticancer therapy. *BMB Rep,* 47**,** 51-9.

LEE, Y. H., PARK, J. Y., LEE, H., SONG, E. S., KUK, M. U., JOO, J., OH, S., KWON, H. W., PARK, J. T. & PARK, S. C. 2021. Targeting Mitochondrial Metabolism as a Strategy to Treat Senescence. *Cells,* 10.

LEONTIEVA, O. V. & BLAGOSKLONNY, M. V. 2014. Gerosuppression in confluent cells. *Aging (Albany NY),* 6**,** 1010-8.

LEVI, N., PAPISMADOV, N., SOLOMONOV, I., SAGI, I. & KRIZHANOVSKY, V. 2020. The ECM path of senescence in aging: components and modifiers. *FEBS J,* 287**,** 2636-2646.

LI, M., YOU, L., XUE, J. & LU, Y. 2018. Ionizing Radiation-Induced Cellular Senescence in Normal, Non-transformed Cells and the Involved DNA Damage Response: A Mini Review. *Front Pharmacol,* 9**,** 522.

LI, W., WANG, W., DONG, H., LI, Y., LI, L., HAN, L., HAN, Z., WANG, S., MA, D. & WANG, H. 2014. Cisplatin-induced senescence in ovarian cancer cells is mediated by GRP78. *Oncol Rep,* 31**,** 2525-34.

LIM, H., PARK, H. & KIM, H. P. 2015. Effects of flavonoids on senescence-associated secretory phenotype formation from bleomycin-induced senescence in BJ fibroblasts. *Biochem Pharmacol,* 96**,** 337-48.

LIU, D. & HORNSBY, P. J. 2007. Senescent human fibroblasts increase the early growth of xenograft tumors via matrix metalloproteinase secretion. *Cancer Res,* 67**,** 3117-26.

LOPEZ-OTIN, C., BLASCO, M. A., PARTRIDGE, L., SERRANO, M. & KROEMER, G. 2013. The hallmarks of aging. *Cell,* 153**,** 1194-217.

LOPEZ-OTIN, C., BLASCO, M. A., PARTRIDGE, L., SERRANO, M. & KROEMER, G. 2023. Hallmarks of aging: An expanding universe. *Cell,* 186**,** 243-278.

LU, S. Y., CHANG, K. W., LIU, C. J., TSENG, Y. H., LU, H. H., LEE, S. Y. & LIN, S. C. 2006. Ripe areca nut extract induces G1 phase arrests and senescence-associated phenotypes in normal human oral keratinocyte. *Carcinogenesis,* 27**,** 1273-84.

LUJAMBIO, A. 2016. To clear, or not to clear (senescent cells)? That is the question. *Bioessays,* 38 Suppl 1**,** S56-64.

LUJAMBIO, A., AKKARI, L., SIMON, J., GRACE, D., TSCHAHARGANEH, D. F., BOLDEN, J. E., ZHAO, Z., THAPAR, V., JOYCE, J. A., KRIZHANOVSKY, V. & LOWE, S. W. 2013. Non-cell-autonomous tumor suppression by p53. *Cell,* 153**,** 449-60.

LYNCH, H. T., CASEY, M. J., SNYDER, C. L., BEWTRA, C., LYNCH, J. F., BUTTS, M. & GODWIN, A. K. 2009. Hereditary ovarian carcinoma: heterogeneity, molecular genetics, pathology, and management. *Mol Oncol,* 3**,** 97-137.

MAGALHAES, S., ALMEIDA, I., PEREIRA, C. D., REBELO, S., GOODFELLOW, B. J. & NUNES, A. 2022. The Long-Term Culture of Human Fibroblasts Reveals a Spectroscopic Signature of Senescence. *Int J Mol Sci,* 23.

MAIER, J. A., VOULALAS, P., ROEDER, D. & MACIAG, T. 1990. Extension of the life-span of human endothelial cells by an interleukin-1 alpha antisense oligomer. *Science,* 249**,** 1570-4.

MAKRANTONAKI, E., WLASCHEK, M. & SCHARFFETTER-KOCHANEK, K. 2017. Pathogenesis of wound healing disorders in the elderly. *J Dtsch Dermatol Ges,* 15**,** 255-275.

MALAQUIN, N., MARTINEZ, A. & RODIER, F. 2016. Keeping the senescence secretome under control: Molecular reins on the senescence-associated secretory phenotype. *Exp Gerontol,* 82**,** 39-49.

MALONEY, E. & HWANG, J. H. 2015. Emerging HIFU applications in cancer therapy. *Int J Hyperthermia,* 31**,** 302-9.

MANNICK, J. B., MORRIS, M., HOCKEY, H. P., ROMA, G., BEIBEL, M., KULMATYCKI, K., WATKINS, M., SHAVLAKADZE, T., ZHOU, W., QUINN, D., GLASS, D. J. & KLICKSTEIN, L. B. 2018. TORC1 inhibition enhances immune function and reduces infections in the elderly. *Sci Transl Med,* 10.

MANTOVANI, A., LOCATI, M., VECCHI, A., SOZZANI, S. & ALLAVENA, P. 2001. Decoy receptors: a strategy to regulate inflammatory cytokines and chemokines. *Trends Immunol,* 22**,** 328-36.

MANU, K. A., CAO, P. H. A., CHAI, T. F., CASEY, P. J. & WANG, M. 2019. p21cip1/waf1 Coordinate Autophagy, Proliferation and Apoptosis in Response to Metabolic Stress. *Cancers (Basel),* 11.

MARECHAL, A. & ZOU, L. 2013. DNA damage sensing by the ATM and ATR kinases. *Cold Spring Harb Perspect Biol,* 5.

MARIA, J. & INGRID, Z. 2017. Effects of bioactive compounds on senescence and components of senescence associated secretory phenotypes in vitro. *Food Funct,* 8**,** 2394-2418.

MARTINEZ, D. E., BORNIEGO, M. L., BATTCHIKOVA, N., ARO, E. M., TYYSTJARVI, E. & GUIAMET, J. J. 2015. SASP, a Senescence-Associated Subtilisin Protease, is involved in reproductive development and determination of silique number in Arabidopsis. *J Exp Bot,* 66**,** 161-74.

MATSUKI, M., TAKAHASHI, A., KATOU, S., TAKAYANAGI, A., TAKAGI, Y. & KAMATA, K. 2013. [Pathological complete response to gemcitabine and cisplatin chemotherapy for advanced upper tract urothelial carcinoma: a case report]. *Nihon Hinyokika Gakkai Zasshi,* 104**,** 33-7.

MATSUMOTO, R., FUKUOKA, H., IGUCHI, G., ODAKE, Y., YOSHIDA, K., BANDO, H., SUDA, K., NISHIZAWA, H., TAKAHASHI, M., YAMADA, S., OGAWA, W. & TAKAHASHI, Y. 2015. Accelerated Telomere Shortening in Acromegaly; IGF-I Induces Telomere Shortening and Cellular Senescence. *PLoS One,* 10**,** e0140189.

MAXWELL, L., COLLECUTT, T., GLEDHILL, M., SHARMA, S., EDGAR, S. & GAVIN, J. B. 1994. The augmentation of leucocyte adhesion to endothelium by therapeutic ultrasound. *Ultrasound Med Biol,* 20**,** 383-90.

MCQUIBBAN, G. A., GONG, J. H., WONG, J. P., WALLACE, J. L., CLARK-LEWIS, I. & OVERALL, C. M. 2002. Matrix metalloproteinase processing of monocyte chemoattractant proteins generates CC chemokine receptor antagonists with anti-inflammatory properties in vivo. *Blood,* 100**,** 1160-7.

MERCURIO, L., LULLI, D., MASCIA, F., DELLAMBRA, E., SCARPONI, C., MORELLI, M., VALENTE, C., CARBONE, M. L., PALLOTTA, S., GIROLOMONI, G., ALBANESI, C., PASTORE, S. & MADONNA, S. 2020. Intracellular Insulin-like growth factor binding protein 2 (IGFBP2) contributes to the senescence of keratinocytes in psoriasis by stabilizing cytoplasmic p21. *Aging (Albany NY),* 12**,** 6823-6851.

MERZ, S. E., KLOPFLEISCH, R., BREITHAUPT, A. & GRUBER, A. D. 2019. Aging and Senescence in Canine Testes. *Vet Pathol,* 56**,** 715-724.

MIJIT, M., CARACCIOLO, V., MELILLO, A., AMICARELLI, F. & GIORDANO, A. 2020. Role of p53 in the Regulation of Cellular Senescence. *Biomolecules,* 10.

MIWA, S., KASHYAP, S., CHINI, E. & VON ZGLINICKI, T. 2022. Mitochondrial dysfunction in cell senescence and aging. *J Clin Invest,* 132.

MOHAMAD KAMAL, N. S., SAFUAN, S., SHAMSUDDIN, S. & FOROOZANDEH, P. 2020. Aging of the cells: Insight into cellular senescence and detection Methods. *Eur J Cell Biol,* 99**,** 151108.

MOISEEVA, O., DESCHENES-SIMARD, X., ST-GERMAIN, E., IGELMANN, S., HUOT, G., CADAR, A. E., BOURDEAU, V., POLLAK, M. N. & FERBEYRE, G. 2013. Metformin inhibits the senescence-associated secretory phenotype by interfering with IKK/NF-kappaB activation. *Aging Cell,* 12**,** 489-98.

MOLDOGAZIEVA, N. T., MOKHOSOEV, I. M., MEL'NIKOVA, T. I., POROZOV, Y. B. & TERENTIEV, A. A. 2019. Oxidative Stress and Advanced Lipoxidation and Glycation End Products (ALEs and AGEs) in Aging and Age-Related Diseases. *Oxid Med Cell Longev,* 2019**,** 3085756.

MORTIMER, A. J. & DYSON, M. 1988. The effect of therapeutic ultrasound on calcium uptake in fibroblasts. *Ultrasound Med Biol,* 14**,** 499-506.

MU, X. C. & HIGGINS, P. J. 1995. Differential growth state-dependent regulation of plasminogen activator inhibitor type-1 expression in senescent IMR-90 human diploid fibroblasts. *J Cell Physiol,* 165**,** 647-57.

MUNOZ-ESPIN, D., CANAMERO, M., MARAVER, A., GOMEZ-LOPEZ, G., CONTRERAS, J., MURILLO-CUESTA, S., RODRIGUEZ-BAEZA, A., VARELA-NIETO, I., RUBERTE, J., COLLADO, M. & SERRANO, M. 2013. Programmed cell senescence during mammalian embryonic development. *Cell,* 155**,** 1104-18.

MUNOZ-ESPIN, D., ROVIRA, M., GALIANA, I., GIMENEZ, C., LOZANO-TORRES, B., PAEZ-RIBES, M., LLANOS, S., CHAIB, S., MUNOZ-MARTIN, M., UCERO, A. C., GARAULET, G., MULERO, F., DANN, S. G., VANARSDALE, T., SHIELDS, D. J., BERNARDOS, A., MURGUIA, J. R., MARTINEZ-MANEZ, R. & SERRANO, M. 2018. A versatile drug delivery system targeting senescent cells. *EMBO Mol Med,* 10.

NAKAO, J., FUJII, Y., KUSUYAMA, J., BANDOW, K., KAKIMOTO, K., OHNISHI, T. & MATSUGUCHI, T. 2014. Low-intensity pulsed ultrasound (LIPUS) inhibits LPS-induced inflammatory responses of osteoblasts through TLR4-MyD88 dissociation. *Bone,* 58**,** 17-25.

NARITA, M., NARITA, M., KRIZHANOVSKY, V., NUNEZ, S., CHICAS, A., HEARN, S. A., MYERS, M. P. & LOWE, S. W. 2006. A novel role for high-mobility group a proteins in cellular senescence and heterochromatin formation. *Cell,* 126**,** 503-14.

NARITA, M., NUNEZ, S., HEARD, E., NARITA, M., LIN, A. W., HEARN, S. A., SPECTOR, D. L., HANNON, G. J. & LOWE, S. W. 2003. Rb-mediated heterochromatin formation and silencing of E2F target genes during cellular senescence. *Cell,* 113**,** 703-16.

NELSON, G., WORDSWORTH, J., WANG, C., JURK, D., LAWLESS, C., MARTIN-RUIZ, C. & VON ZGLINICKI, T. 2012. A senescent cell bystander effect: senescence-induced senescence. *Aging Cell,* 11**,** 345-9.

NISHIO, K., INOUE, A., QIAO, S., KONDO, H. & MIMURA, A. 2001. Senescence and cytoskeleton: overproduction of vimentin induces senescent-like morphology in human fibroblasts. *Histochem Cell Biol,* 116**,** 321-7.

NITISS, J. L. 2009. Targeting DNA topoisomerase II in cancer chemotherapy. *Nat Rev Cancer,* 9**,** 338-50.

NYBORG, W. L. 1982. Ultrasonic microstreaming and related phenomena. *Br J Cancer Suppl,* 5**,** 156-60.

OHTANI, N. 2022. The roles and mechanisms of senescence-associated secretory phenotype (SASP): can it be controlled by senolysis? *Inflamm Regen,* 42**,** 11.

OLOVNIKOV, A. M. 1971. [Principle of marginotomy in template synthesis of polynucleotides]. *Dokl Akad Nauk SSSR,* 201**,** 1496-9.

OLOVNIKOV, A. M. 1973. A theory of marginotomy. The incomplete copying of template margin in enzymic synthesis of polynucleotides and biological significance of the phenomenon. *J Theor Biol,* 41**,** 181-90.

OLSZEWSKA, A., BORKOWSKA, A., GRANICA, M., KAROLCZAK, J., ZGLINICKI, B., KIEDA, C. & WAS, H. 2021. Escape From Cisplatin-Induced Senescence of Hypoxic Lung Cancer Cells Can Be Overcome by Hydroxychloroquine. *Front Oncol,* 11**,** 738385.

ORJALO, A. V., BHAUMIK, D., GENGLER, B. K., SCOTT, G. K. & CAMPISI, J. 2009. Cell surface-bound IL-1alpha is an upstream regulator of the senescence-associated IL-6/IL-8 cytokine network. *Proc Natl Acad Sci U S A,* 106**,** 17031-6.

PARAMOS-DE-CARVALHO, D., JACINTO, A. & SAUDE, L. 2021. The right time for senescence. *Elife,* 10.

PARIKH, P., WICHER, S., KHANDALAVALA, K., PABELICK, C. M., BRITT, R. D., JR. & PRAKASH, Y. S. 2019. Cellular senescence in the lung across the age spectrum. *Am J Physiol Lung Cell Mol Physiol,* 316**,** L826-L842.

PARRINELLO, S., COPPE, J. P., KRTOLICA, A. & CAMPISI, J. 2005. Stromal-epithelial interactions in aging and cancer: senescent fibroblasts alter epithelial cell differentiation. *J Cell Sci,* 118**,** 485-96.

PATHAK, R., BHANGU, S. K., MARTIN, G. J. O., SEPAROVIC, F. & ASHOKKUMAR, M. 2022. Ultrasound-induced protein restructuring and ordered aggregation to form amyloid crystals. *Eur Biophys J,* 51**,** 335-352.

PEREZ, E. A. 2009. Microtubule inhibitors: Differentiating tubulin-inhibiting agents based on mechanisms of action, clinical activity, and resistance. *Mol Cancer Ther,* 8**,** 2086-95.

PIGNON, J. P., TRIBODET, H., SCAGLIOTTI, G. V., DOUILLARD, J. Y., SHEPHERD, F. A., STEPHENS, R. J., DUNANT, A., TORRI, V., ROSELL, R., SEYMOUR, L., SPIRO, S. G., ROLLAND, E., FOSSATI, R., AUBERT, D., DING, K., WALLER, D., LE CHEVALIER, T. & GROUP, L. C. 2008. Lung adjuvant cisplatin evaluation: a pooled analysis by the LACE Collaborative Group. *J Clin Oncol,* 26**,** 3552-9.

PIZZINO, G., IRRERA, N., CUCINOTTA, M., PALLIO, G., MANNINO, F., ARCORACI, V., SQUADRITO, F., ALTAVILLA, D. & BITTO, A. 2017. Oxidative Stress: Harms and Benefits for Human Health. *Oxid Med Cell Longev,* 2017**,** 8416763.

POUNDER, N. M. & HARRISON, A. J. 2008. Low intensity pulsed ultrasound for fracture healing: a review of the clinical evidence and the associated biological mechanism of action. *Ultrasonics,* 48**,** 330-8.

PRATA, L., OVSYANNIKOVA, I. G., TCHKONIA, T. & KIRKLAND, J. L. 2018. Senescent cell clearance by the immune system: Emerging therapeutic opportunities. *Semin Immunol,* 40**,** 101275.

PRATTICHIZZO, F., DE NIGRIS, V., LA SALA, L., PROCOPIO, A. D., OLIVIERI, F. & CERIELLO, A. 2016. "Inflammaging" as a Druggable Target: A Senescence-Associated Secretory Phenotype-Centered View of Type 2 Diabetes. *Oxid Med Cell Longev,* 2016**,** 1810327.

PRZYSTUPSKI, D. & USSOWICZ, M. 2022. Landscape of Cellular Bioeffects Triggered by Ultrasound-Induced Sonoporation. *Int J Mol Sci,* 23.

QIAN, Y. & CHEN, X. 2013. Senescence regulation by the p53 protein family. *Methods Mol Biol,* 965**,** 37-61.

QU, K., LIN, T., WEI, J., MENG, F., WANG, Z., HUANG, Z., WAN, Y., SONG, S., LIU, S., CHANG, H., DONG, Y. & LIU, C. 2013. Cisplatin induces cell cycle arrest and senescence via upregulating P53 and P21 expression in HepG2 cells. *Nan Fang Yi Ke Da Xue Xue Bao,* 33**,** 1253-9.

RAJPATHAK, S. N., GUNTER, M. J., WYLIE-ROSETT, J., HO, G. Y., KAPLAN, R. C., MUZUMDAR, R., ROHAN, T. E. & STRICKLER, H. D. 2009. The role of insulin-like growth factor-I and its binding proteins in glucose homeostasis and type 2 diabetes. *Diabetes Metab Res Rev,* 25**,** 3-12.

RAYESS, H., WANG, M. B. & SRIVATSAN, E. S. 2012. Cellular senescence and tumor suppressor gene p16. *Int J Cancer,* 130**,** 1715-25.

REDDY, M., GILL, S. S., KALKAR, S. R., WU, W., ANDERSON, P. J. & ROCHON, P. A. 2008. Treatment of pressure ulcers: a systematic review. *JAMA,* 300**,** 2647-62.

REHER, P., DOAN, N., BRADNOCK, B., MEGHJI, S. & HARRIS, M. 1999. Effect of ultrasound on the production of IL-8, basic FGF and VEGF. *Cytokine,* 11**,** 416-23.

REICHENSTEIN, M., REICH, R., LEHOUX, J. G. & HANUKOGLU, I. 2004. ACTH induces TIMP-1 expression and inhibits collagenase in adrenal cortex cells. *Mol Cell Endocrinol,* 215**,** 109-14.

RESNIK, S. R. E., ANDJELA ;ABDO ABUJAMRA, BEATRIZ ;JOZIC, IVAN 2020. Clinical Implications of Cellular Senescence on Wound Healing. *New York: Springer US,* 9**,** 286-297.

ROMANOV, V. S., POSPELOV, V. A. & POSPELOVA, T. V. 2012. Cyclin-dependent kinase inhibitor p21(Waf1): contemporary view on its role in senescence and oncogenesis. *Biochemistry (Mosc),* 77**,** 575-84.

ROPER, J., HARRISON, A. & BASS, M. D. 2012. Induction of adhesion-dependent signals using low-intensity ultrasound. *J Vis Exp**,*** e4024.

ROPER, J. A., WILLIAMSON, R. C., BALLY, B., COWELL, C. A. M., BROOKS, R., STEPHENS, P., HARRISON, A. J. & BASS, M. D. 2015. Ultrasonic Stimulation of Mouse Skin Reverses the Healing Delays in Diabetes and Aging by Activation of Rac1. *J Invest Dermatol,* 135**,** 2842-2851.

ROTTENBERG, S., DISLER, C. & PEREGO, P. 2021. The rediscovery of platinum-based cancer therapy. *Nat Rev Cancer,* 21**,** 37-50.

SACCO, A., BELLONI, L. & LATELLA, L. 2021. From Development to Aging: The Path to Cellular Senescence. *Antioxid Redox Signal,* 34**,** 294-307.

SARKAR, D., LEBEDEVA, I. V., EMDAD, L., KANG, D. C., BALDWIN, A. S., JR. & FISHER, P. B. 2004. Human polynucleotide phosphorylase (hPNPaseold-35): a potential link between aging and inflammation. *Cancer Res,* 64**,** 7473-8.

SARKISIAN, C. J., KEISTER, B. A., STAIRS, D. B., BOXER, R. B., MOODY, S. E. & CHODOSH, L. A. 2007. Dose-dependent oncogene-induced senescence in vivo and its evasion during mammary tumorigenesis. *Nat Cell Biol,* 9**,** 493-505.

SCHORTINGHUIS, J., STEGENGA, B., RAGHOEBAR, G. M. & DE BONT, L. G. 2003. Ultrasound stimulation of maxillofacial bone healing. *Crit Rev Oral Biol Med,* 14**,** 63-74.

SCHOSSERER, M., GRILLARI, J. & BREITENBACH, M. 2017. The Dual Role of Cellular Senescence in Developing Tumors and Their Response to Cancer Therapy. *Front Oncol,* 7**,** 278.

SEDELNIKOVA, O. A., HORIKAWA, I., REDON, C., NAKAMURA, A., ZIMONJIC, D. B., POPESCU, N. C. & BONNER, W. M. 2008. Delayed kinetics of DNA double-strand break processing in normal and pathological aging. *Aging Cell,* 7**,** 89-100.

SEDELNIKOVA, O. A., HORIKAWA, I., ZIMONJIC, D. B., POPESCU, N. C., BONNER, W. M. & BARRETT, J. C. 2004. Senescing human cells and ageing mice accumulate DNA lesions with unrepairable double-strand breaks. *Nat Cell Biol,* 6**,** 168-70.

SEDLETSKA, Y., GIRAUD-PANIS, M. J. & MALINGE, J. M. 2005. Cisplatin is a DNA-damaging antitumour compound triggering multifactorial biochemical responses in cancer cells: importance of apoptotic pathways. *Curr Med Chem Anticancer Agents,* 5**,** 251-65.

SERGIEV, P. V., DONTSOVA, O. A. & BEREZKIN, G. V. 2015. Theories of aging: an ever-evolving field. *Acta Naturae,* 7**,** 9-18.

SERUP, J., BOVE, T., ZAWADA, T., JESSEN, A. & POLI, M. 2020. High-frequency (20 MHz) high-intensity focused ultrasound: New Treatment of actinic keratosis, basal cell carcinoma, and Kaposi sarcoma. An open-label exploratory study. *Skin Res Technol,* 26**,** 824-831.

SEVERINO, V., ALESSIO, N., FARINA, A., SANDOMENICO, A., CIPOLLARO, M., PELUSO, G., GALDERISI, U. & CHAMBERY, A. 2013. Insulin-like growth factor binding proteins 4 and 7 released by senescent cells promote premature senescence in mesenchymal stem cells. *Cell Death Dis,* 4**,** e911.

SHARMA, A., SINGH, K. & ALMASAN, A. 2012. Histone H2AX phosphorylation: a marker for DNA damage. *Methods Mol Biol,* 920**,** 613-26.

SHIBUYA, M. 2011. Vascular Endothelial Growth Factor (VEGF) and Its Receptor (VEGFR) Signaling in Angiogenesis: A Crucial Target for Anti- and Pro-Angiogenic Therapies. *Genes Cancer,* 2**,** 1097-105.

SHIGA, K., HARA, M., NAGASAKI, T., SATO, T., TAKAHASHI, H. & TAKEYAMA, H. 2015. Cancer-Associated Fibroblasts: Their Characteristics and Their Roles in Tumor Growth. *Cancers (Basel),* 7**,** 2443-58.

SHLUSH, L. I., ITZKOVITZ, S., COHEN, A., RUTENBERG, A., BERKOVITZ, R., YEHEZKEL, S., SHAHAR, H., SELIG, S. & SKORECKI, K. 2011. Quantitative digital in situ senescence-associated beta-galactosidase assay. *BMC Cell Biol,* 12**,** 16.

SIAVOSHIAN, S., BLOTTIERE, H. M., CHERBUT, C. & GALMICHE, J. P. 1997. Butyrate stimulates cyclin D and p21 and inhibits cyclin-dependent kinase 2 expression in HT-29 colonic epithelial cells. *Biochem Biophys Res Commun,* 232**,** 169-72.

SIDDIK, Z. H. 2003. Cisplatin: mode of cytotoxic action and molecular basis of resistance. *Oncogene,* 22**,** 7265-79.

SIDDIQUI, A. R. & BERNSTEIN, J. M. 2010. Chronic wound infection: facts and controversies. *Clin Dermatol,* 28**,** 519-26.

SIDDIQUI, M. S., FRANCOIS, M., FENECH, M. F. & LEIFERT, W. R. 2015. Persistent gammaH2AX: A promising molecular marker of DNA damage and aging. *Mutat Res Rev Mutat Res,* 766**,** 1-19.

SIMONE, T. M., HIGGINS, C. E., CZEKAY, R. P., LAW, B. K., HIGGINS, S. P., ARCHAMBEAULT, J., KUTZ, S. M. & HIGGINS, P. J. 2014. SERPINE1: A Molecular Switch in the Proliferation-Migration Dichotomy in Wound-"Activated" Keratinocytes. *Adv Wound Care (New Rochelle),* 3**,** 281-290.

SINGH, L., ALDOSARY, S., SAEEDAN, A. S., ANSARI, M. N. & KAITHWAS, G. 2018. Prolyl hydroxylase 2: a promising target to inhibit hypoxia-induced cellular metabolism in cancer cells. *Drug Discov Today,* 23**,** 1873-1882.

SIVAGNANAM, V. & GIJS, M. A. 2013. Exploring living multicellular organisms, organs, and tissues using microfluidic systems. *Chem Rev,* 113**,** 3214-47.

SMITH, J. S., CHEN, Q., YATSUNYK, L. A., NICOLUDIS, J. M., GARCIA, M. S., KRANASTER, R., BALASUBRAMANIAN, S., MONCHAUD, D., TEULADE-FICHOU, M. P., ABRAMOWITZ, L., SCHULTZ, D. C. & JOHNSON, F. B. 2011. Rudimentary G-quadruplex-based telomere capping in Saccharomyces cerevisiae. *Nat Struct Mol Biol,* 18**,** 478-85.

SON, H. N., CHI, H. N. Q., CHUNG, D. C. & LONG, L. T. 2019. Morphological changes during replicative senescence in bovine ovarian granulosa cells. *Cell Cycle,* 18**,** 1490-1497.

SORG, H., TILKORN, D. J., HAGER, S., HAUSER, J. & MIRASTSCHIJSKI, U. 2017. Skin Wound Healing: An Update on the Current Knowledge and Concepts. *Eur Surg Res,* 58**,** 81-94.

STOJANOVIC, S. D., FIEDLER, J., BAUERSACHS, J., THUM, T. & SEDDING, D. G. 2020. Senescence-induced inflammation: an important player and key therapeutic target in atherosclerosis. *Eur Heart J,* 41**,** 2983-2996.

SU, J. & CAVACO-PAULO, A. 2021. Effect of ultrasound on protein functionality. *Ultrason Sonochem,* 76**,** 105653.

TAKAHASHI, A., OHTANI, N. & HARA, E. 2007. Irreversibility of cellular senescence: dual roles of p16INK4a/Rb-pathway in cell cycle control. *Cell Div,* 2**,** 10.

TELGENHOFF, D. & SHROOT, B. 2005. Cellular senescence mechanisms in chronic wound healing. *Cell Death Differ,* 12**,** 695-8.

TER HAAR, G. 1999. Therapeutic ultrasound. *Eur J Ultrasound,* 9**,** 3-9.

TER HAAR, G. 2007. Therapeutic applications of ultrasound. *Prog Biophys Mol Biol,* 93**,** 111-29.

TER RIET, G., KESSELS, A. G. & KNIPSCHILD, P. 1995. Randomised clinical trial of ultrasound treatment for pressure ulcers. *BMJ,* 310**,** 1040-1.

TERAO, R., AHMED, T., SUZUMURA, A. & TERASAKI, H. 2022. Oxidative Stress-Induced Cellular Senescence in Aging Retina and Age-Related Macular Degeneration. *Antioxidants (Basel),* 11.

TIAN, Y., LIU, Z., TAN, H., HOU, J., WEN, X., YANG, F. & CHENG, W. 2020. New Aspects of Ultrasound-Mediated Targeted Delivery and Therapy for Cancer. *Int J Nanomedicine,* 15**,** 401-418.

TILSTRA, J. S., ROBINSON, A. R., WANG, J., GREGG, S. Q., CLAUSON, C. L., REAY, D. P., NASTO, L. A., ST CROIX, C. M., USAS, A., VO, N., HUARD, J., CLEMENS, P. R., STOLZ, D. B., GUTTRIDGE, D. C., WATKINS, S. C., GARINIS, G. A., WANG, Y., NIEDERNHOFER, L. J. & ROBBINS, P. D. 2012. NF-kappaB inhibition delays DNA damage-induced senescence and aging in mice. *J Clin Invest,* 122**,** 2601-12.

TONINI, T., ROSSI, F. & CLAUDIO, P. P. 2003. Molecular basis of angiogenesis and cancer. *Oncogene,* 22**,** 6549-56.

TRACY, L. E., MINASIAN, R. A. & CATERSON, E. J. 2016. Extracellular Matrix and Dermal Fibroblast Function in the Healing Wound. *Adv Wound Care (New Rochelle),* 5**,** 119-136.

TYANOVA, S., TEMU, T., SINITCYN, P., CARLSON, A., HEIN, M. Y., GEIGER, T., MANN, M. & COX, J. 2016. The Perseus computational platform for comprehensive analysis of (prote)omics data. *Nat Methods,* 13**,** 731-40.

UDDIN, A., RUSSELL, D., GAME, F., SANTOS, D. & SIDDLE, H. J. 2022. The effectiveness of systemic antibiotics for osteomyelitis of the foot in adults with diabetes mellitus: a systematic review protocol. *J Foot Ankle Res,* 15**,** 48.

URITA, A., IWASAKI, N., KONDO, M., NISHIO, Y., KAMISHIMA, T. & MINAMI, A. 2013. Effect of low-intensity pulsed ultrasound on bone healing at osteotomy sites after forearm bone shortening. *J Hand Surg Am,* 38**,** 498-503.

VALKENBURG, K. C., DE GROOT, A. E. & PIENTA, K. J. 2018. Targeting the tumour stroma to improve cancer therapy. *Nat Rev Clin Oncol,* 15**,** 366-381.

VAN DEN STEEN, P. E., WUYTS, A., HUSSON, S. J., PROOST, P., VAN DAMME, J. & OPDENAKKER, G. 2003. Gelatinase B/MMP-9 and neutrophil collagenase/MMP-8 process the chemokines human GCP-2/CXCL6, ENA-78/CXCL5 and mouse GCP-2/LIX and modulate their physiological activities. *Eur J Biochem,* 270**,** 3739-49.

VAUGHAN, D. E., RAI, R., KHAN, S. S., EREN, M. & GHOSH, A. K. 2017. Plasminogen Activator Inhibitor-1 Is a Marker and a Mediator of Senescence. *Arterioscler Thromb Vasc Biol,* 37**,** 1446-1452.

VON JOEST, M., CHEN, C., DOUCHE, T., CHANTREL, J., CHICHE, A., GIANETTO, Q. G., MATONDO, M. & LI, H. 2022. Amphiregulin mediates non-cell-autonomous effect of senescence on reprogramming. *Cell Rep,* 40**,** 111074.

VU, R., JIN, S., SUN, P., HAENSEL, D., NGUYEN, Q. H., DRAGAN, M., KESSENBROCK, K., NIE, Q. & DAI, X. 2022. Wound healing in aged skin exhibits systems-level alterations in cellular composition and cell-cell communication. *Cell Rep,* 40**,** 111155.

WAGNER, K. D. & WAGNER, N. 2022. The Senescence Markers p16INK4A, p14ARF/p19ARF, and p21 in Organ Development and Homeostasis. *Cells,* 11.

WAHBA, J., NATOLI, M., WHILDING, L. M., PARENTE-PEREIRA, A. C., JUNG, Y., ZONA, S., LAM, E. W., SMITH, J. R., MAHER, J. & GHAEM-MAGHAMI, S. 2018. Chemotherapy-induced apoptosis, autophagy and cell cycle arrest are key drivers of synergy in chemo-immunotherapy of epithelial ovarian cancer. *Cancer Immunol Immunother,* 67**,** 1753-1765.

WAJAPEYEE, N., SERRA, R. W., ZHU, X., MAHALINGAM, M. & GREEN, M. R. 2008. Oncogenic BRAF induces senescence and apoptosis through pathways mediated by the secreted protein IGFBP7. *Cell,* 132**,** 363-74.

WALL, I. B., MOSELEY, R., BAIRD, D. M., KIPLING, D., GILES, P., LAFFAFIAN, I., PRICE, P. E., THOMAS, D. W. & STEPHENS, P. 2008. Fibroblast dysfunction is a key factor in the non-healing of chronic venous leg ulcers. *J Invest Dermatol,* 128**,** 2526-40.

WANG, L., LANKHORST, L. & BERNARDS, R. 2022a. Exploiting senescence for the treatment of cancer. *Nat Rev Cancer,* 22**,** 340-355.

WANG, L. Y. & ZHENG, S. S. 2019. Advances in low-frequency ultrasound combined with microbubbles in targeted tumor therapy. *J Zhejiang Univ Sci B,* 20**,** 291-299.

WANG, S., MOERMAN, E. J., JONES, R. A., THWEATT, R. & GOLDSTEIN, S. 1996. Characterization of IGFBP-3, PAI-1 and SPARC mRNA expression in senescent fibroblasts. *Mech Ageing Dev,* 92**,** 121-32.

WANG, Z., QI, F., LUO, H., XU, G. & WANG, D. 2022b. Inflammatory Microenvironment of Skin Wounds. *Front Immunol,* 13**,** 789274.

WANG, Z., WEI, D. D. & XIAO, H. Y. 2013. Methods of Cellular Senescence Induction Using Oxidative Stress. *Biological Aging: Methods and Protocols, 2nd Edition,* 1048**,** 135-144.

WATSON, T. 2008. Ultrasound in contemporary physiotherapy practice. *Ultrasonics,* 48**,** 321-9.

WEBSTER, D. F., POND, J. B., DYSON, M. & HARVEY, W. 1978. The role of cavitation in the in vitro stimulation of protein synthesis in human fibroblasts by ultrasound. *Ultrasound Med Biol,* 4**,** 343-51.

WEI, X., LI, M., ZHENG, Z., MA, J., GAO, Y., CHEN, L., PENG, Y., YU, S. & YANG, L. 2022. Senescence in chronic wounds and potential targeted therapies. *Burns Trauma,* 10**,** tkab045.

WILEY, C. D. & CAMPISI, J. 2016. From Ancient Pathways to Aging Cells-Connecting Metabolism and Cellular Senescence. *Cell Metab,* 23**,** 1013-1021.

WILEY, C. D., VELARDE, M. C., LECOT, P., LIU, S., SARNOSKI, E. A., FREUND, A., SHIRAKAWA, K., LIM, H. W., DAVIS, S. S., RAMANATHAN, A., GERENCSER, A. A., VERDIN, E. & CAMPISI, J. 2016. Mitochondrial Dysfunction Induces Senescence with a Distinct Secretory Phenotype. *Cell Metab,* 23**,** 303-14.

WILKINSON, H. N., CLOWES, C., BANYARD, K. L., MATTEUCI, P., MACE, K. A. & HARDMAN, M. J. 2019. Elevated Local Senescence in Diabetic Wound Healing Is Linked to Pathological Repair via CXCR2. *J Invest Dermatol,* 139**,** 1171-1181 e6.

WOOD, A. K. & SEHGAL, C. M. 2015. A review of low-intensity ultrasound for cancer therapy. *Ultrasound Med Biol,* 41**,** 905-28.

WOODS, D. & TURCHI, J. J. 2013. Chemotherapy induced DNA damage response: convergence of drugs and pathways. *Cancer Biol Ther,* 14**,** 379-89.

WU, J. & NYBORG, W. L. 2008. Ultrasound, cavitation bubbles and their interaction with cells. *Adv Drug Deliv Rev,* 60**,** 1103-16.

WYLD, L., BELLANTUONO, I., TCHKONIA, T., MORGAN, J., TURNER, O., FOSS, F., GEORGE, J., DANSON, S. & KIRKLAND, J. L. 2020. Senescence and Cancer: A Review of Clinical Implications of Senescence and Senotherapies. *Cancers (Basel),* 12.

XI, C., SUN, J., XU, X., WU, Y., KOU, X., ZHAO, Y., SHEN, J., DONG, Y., CHEN, K., SU, Z., LIU, D., YE, W., LIU, Y., ZHANG, R., XU, Y., WANG, H., HAO, L., WU, L. & GAO, S. 2022. Mettl14-driven senescence-associated secretory phenotype facilitates somatic cell reprogramming. *Stem Cell Reports,* 17**,** 1799-1809.

XIN, Z., LIN, G., LEI, H., LUE, T. F. & GUO, Y. 2016. Clinical applications of low-intensity pulsed ultrasound and its potential role in urology. *Transl Androl Urol,* 5**,** 255-66.

YANG, F., TUXHORN, J. A., RESSLER, S. J., MCALHANY, S. J., DANG, T. D. & ROWLEY, D. R. 2005. Stromal expression of connective tissue growth factor promotes angiogenesis and prostate cancer tumorigenesis. *Cancer Res,* 65**,** 8887-95.

YOSHIDA, S., NAKAGAMI, H., HAYASHI, H., IKEDA, Y., SUN, J., TENMA, A., TOMIOKA, H., KAWANO, T., SHIMAMURA, M., MORISHITA, R. & RAKUGI, H. 2020. The CD153 vaccine is a senotherapeutic option for preventing the accumulation of senescent T cells in mice. *Nat Commun,* 11**,** 2482.

YOSHIMOTO, S., LOO, T. M., ATARASHI, K., KANDA, H., SATO, S., OYADOMARI, S., IWAKURA, Y., OSHIMA, K., MORITA, H., HATTORI, M., HONDA, K., ISHIKAWA, Y., HARA, E. & OHTANI, N. 2013. Obesity-induced gut microbial metabolite promotes liver cancer through senescence secretome. *Nature,* 499**,** 97-101.

YOUNG, L. V., WAKELIN, G., CAMERON, A. W. R., SPRINGER, S. A., ROSS, J. P., WOLTERS, G., MURPHY, J. P., ARSENAULT, M. G., NG, S., COLLAO, N., DE LISIO, M., LJUBICIC, V. & JOHNSTON, A. P. W. 2022. Muscle injury induces a transient senescence-like state that is required for myofiber growth during muscle regeneration. *FASEB J,* 36**,** e22587.

YU, W. K., WANG, Z., FONG, C. C., LIU, D., YIP, T. C., AU, S. K., ZHU, G. & YANG, M. 2017. Chemoresistant lung cancer stem cells display high DNA repair capability to remove cisplatin-induced DNA damage. *Br J Pharmacol,* 174**,** 302-313.

ZENG, S., SHEN, W. H. & LIU, L. 2018. Senescence and Cancer. *Cancer Transl Med,* 4**,** 70-74.

ZENG, Z. M., DU, H. Y., XIONG, L., ZENG, X. L., ZHANG, P., CAI, J., HUANG, L. & LIU, A. W. 2020. BRCA1 protects cardiac microvascular endothelial cells against irradiation by regulating p21-mediated cell cycle arrest. *Life Sci,* 244**,** 117342.

ZHANG, D., TANG, B., XIE, X., XIAO, Y. F., YANG, S. M. & ZHANG, J. W. 2015. The interplay between DNA repair and autophagy in cancer therapy. *Cancer Biol Ther,* 16**,** 1005-13.

ZHAO, R., LIANG, H., CLARKE, E., JACKSON, C. & XUE, M. 2016. Inflammation in Chronic Wounds. *Int J Mol Sci,* 17.

ZHAO, W., LIN, Z. X. & ZHANG, Z. Q. 2004. Cisplatin-induced premature senescence with concomitant reduction of gap junctions in human fibroblasts. *Cell Res,* 14**,** 60-6.

ZHOU, S., SCHMELZ, A., SEUFFERLEIN, T., LI, Y., ZHAO, J. & BACHEM, M. G. 2004. Molecular mechanisms of low intensity pulsed ultrasound in human skin fibroblasts. *J Biol Chem,* 279**,** 54463-9.